Advanced Analytical Methods for Assessing Biological Nutrient Removal in Membrane Wastewater Treatment Systems

by

Avery Lachlann Carlson

A dissertation submitted in partial fulfillment
of the requirements for the degree of
Doctor of Philosophy
(Environmental Engineering)
in the University of Michigan
2023

Doctoral Committee:

Professor Glen T. Daigger, Co-Chair
Professor Nancy G. Love, Co-Chair
Professor Greg Dick
Dr. Dwight Houweling, Dynamita

Avery L. Carlson

averyca@umich.edu

ORCID iD: 0000-0001-5408-827X

Dedication

This dissertation is dedicated to my parents, Gary, and Mary; to my brother Zach; and my mentor and friend, Patty. All I have learned; I have learned from you.

Proverbs 4:5-9

Acknowledgements

A portion of this dissertation research is funded by Dajiang Environment. I am grateful to Chunyan "Cathy" Chai for her (and Dajiang's) support of my work. I also want to acknowledge funding support from Jacobs O&M, operating the Traverse City Regional Wastewater Treatment Plant for the other half of this dissertation. In particular, I want to thank the TCRWWTP staff, Elizabeth Hart, Mark Huggard, Josh Lycka, and Justin Straub, for allowing me to visit their beautiful city and conduct experiments from their lab.

I would like to thank my advisors Dr. Nancy Love and Dr. Glen Daigger. From the beginning, they pushed me to reach my full potential as a scientist, an engineer, and a thinker. In particular, I would like to thank Dr. Love for her role in helping me become a clearer, more coherent writer. My deepest gratitude to Glen for taking a chance on me, and encouraging me long ago to pursue my career as an engineer. I wouldn't be where I am without your mentorship, friendship, and guidance.

I would like to thank all the staff at Ann Arbor Wastewater Treatment Plant for being such hospitable hosts of various University of Michigan research projects over the years. A huge thank you to Keith Sanders, Kyle Weinman, and Nick Jaworski for all their help in keeping my reactors running smoothly and my bugs alive. For their mentorship in the early years of graduate school, I want to thank Drs. Nicole Rockey and Jeseth Delgado Vela. I would also like to thank Dr. Alex Rosenthal for graciously spending his time teaching me the FISH protocol. I want to commend and thank my research partner Huanqi He, and former research assistants Tong Yu, Yi Cao, and Jiawei Liu. A huge thank you also goes to the Civil and Environmental Engineering Staff, Tom

Yavaraski, Steve Donajkowski, and Ethan Kennedy. Their expertise in chemical analysis, fabrication, and all things electrical was an invaluable help. Also, a thank you to Mike Lazarz, and the CEE financial team (Amy Shepherd and Ingra Stimach) for helping make my research run smoothly.

To the incredibly smart scientists and engineers that worked beside me in the Environmental Engineering program—Dr. Brett Wagner, Dr. Enrique Rodriguez, Tim Fairley-Wax, and Maddy Fairley-Wax—I'm honored to have been part of your incoming cohort, and lucky to be considered your friend. What a long, strange trip it's been.

Finally, to Madeline, my mom, dad, and brother for endless support. Thank you is hard to say, because the words wouldn't quite do it justice.

Table of Contents

List of Tables

List of Figures

List of Appendices

Abstract

Biological nutrient removal (BNR) wastewater treatment processes are an established field of research in environmental engineering. Harnessing knowledge on carbon, nitrogen, and phosphorus removal pathways has been effective in remediating water bodies around the world. Membrane treatment technologies are an evolving subsection of BNR wastewater treatment, including membrane bioreactors (MBRs) and membrane aerated biofilm reactors (MABRs). The former configuration processes wastewater through conventional suspended growth, but performs liquid-solid separation on mixed liquor biomass. The latter directs aerates a nitrifying biofilm through a gas-permeable membrane. Advanced chemical and biomolecular methods, beyond what is standard at wastewater plant laboratories, can be used to trouble-shoot existing plant issues, provide feasibility for technologies in the development stage, or to provide more insight on fundamental biological metabolisms driving BNR at membrane wastewater plants.

In this dissertation, chemical and biomolecular tools were used to uncover drivers of sudden onset fouling preventing permeability at the Traverse City Regional Wastewater Treatment Plant MBR. Early observations hypothesized fouling occurred due to a gram-positive bacterium captured on microscopic evaluations of mixed liquor. Illumina 16s rRNA sequencing of laboratory isolates, and fluorescent *in situ* hybridization were used to identify the organisms as *Staphylococcus*; however relative abundance in mixed liquor samples from normal and disrupted operation were statistically insignificant. Constrained ordination plotting of sequence variance with plant metadata suggested fouling correlated with calcium concentrations in the plants mixed liquor. It was hypothesized and supported through multivariate statistical analysis, and estimation

of specific resistance to filtration values, that a calcium-intermediated polymer bridging mechanism is one major contributor to fouling and permeability disruptions in the plant's MBR.

Computer simulation was later used to assess the feasibility of BNR in a proposed hybrid MABR design. A highly-efficient nitrifying biofilm coupled with a large anoxic suspended growth zone demonstrated strategic advantages over conventional activated sludge configurations. Results show successful removal of total inorganic nitrogen and orthophosphate below common permit limits, and carbon capture at solids retention times (SRTs) of 4.0 days or lower. To assess the veracity of process models, a series of batch reactors were constructed to treat domestic wastewater. Experimental measurements calculated oxidized carbon of side-by-side aerobic and anoxic treatment systems. At longer SRTs, a divergent response pattern was observed for anoxic hydrolysis compared to aerobic. Results suggest that a fraction of influent particulate and/or colloidal organic matter was hydrolyzed in the aerobic culture, but not in the anoxic culture with nitrate as the terminal electron acceptor.

Anoxic hydrolysis reduced volatile fatty acid (VFA) production, and ultimately the orthophosphate release rate of denitrifying phosphorus-accumulating organisms. Stoichiometric evaluation suggested a lower anoxic P/O ratio (0.90 versus 1.7 for the aerobic reactor) suggesting less efficient oxidation of anaerobically-stored polyhydroxybutyrate. Furthermore, metagenomic sequencing revealed the presence of respiratory (*nar*) and periplasmic (*nap*) nitrate reductase in the anoxic bacterial population. Periplasmic nitrate reductase is considered thermodynamically unfavorable, which may factor into less efficient intracellular energy generation.

The results of this dissertation show how interactions between nutrients and biology can impact wastewater treatment performance in various designed environments. Ultimately, this research serves to provide vital information on how to analyze designed membrane treatment

plants in operation, how to optimize resources, and further reduce nutrients beyond what is available with conventional activated sludge treatment systems.

Chapter 1 Introduction

Biological nutrient removal (BNR) wastewater treatment processes have been part of an established field of research for over six decades and are well-documented in academic canon. A range of treatment technologies and design configurations have come about as various research paths were explored, and many are implemented in treatment plants around the world. Prior to the mid-20th century, municipal treatment plants were focused on removing biodegradable organic matter that was suspended in wastewater streams (Tchobanoglous et al., 2003). Suspended growth treatment designs, e.g. activated sludge (AS) configurations, were upgraded by environmental engineers and practitioners in the 1970's, after the passing of the Clean Water Act, as they were found most effective for removing inorganic wastewater contaminants (nitrogenous species, such as nitrate, and phosphorus) prior to their outfall into natural water bodies (Randall et al., 1992; Tchobanoglous et al., 2003; Grady Jr. et al., 2011). At the forefront of these environmental engineering and wastewater treatment objectives is BNR to prevent harmful bacterial and algal growth caused by eutrophication. Reducing these bacterial and algal bloom events has been transformational in terms of improving a vast range of water bodies –some examples include the Great lakes, Chesapeake Bay, Long Island Sound, and the Florida coasts in the US, and locations around the world, such as the river systems of Calgary (Alberta, Canada) and Okanagan Lake (British Columbia, Canada), and the North and Baltic Seas in Europe (Carpenter et al., 1998; Sayler et al., 2012; Smol et al., 2020). Some of these regions still face severe issues with hypoxic ecosystems and dead zones linked to eutrophication, but specific policies and regulations have been established to address effects of eutrophication to coastal areas (Bricker et al., 1999).

BNR has been an effective tool in wastewater treatment practice over the last several decades to curb point-source pollution to receiving water bodies, and now the field faces the challenge of optimizing these technologies for contemporary policy demands, maximize efficiency of spent non-renewable materials, and generate products for the circular economy. Traditional BNR suspended growth configurations include a large aerobic zone to allow growth of the nitrifying organisms, which are responsible for the oxidation of ammonia-nitrogen to nitrite- and nitrate-nitrogen (Bellucci & Curtis, 2011; Grady Jr. et al., 2011). BNR systems designed for biological nitrogen removal typically incorporate an initial anoxic zone followed by an aerobic zone, with recirculation of mixed liquor (MLR) from the downstream aerobic to the upstream anoxic zone as a way of transporting oxidized nitrogen (nitrite and nitrate) produced in the aerobic zone to heterotrophic denitrifiers growing in the anoxic zone (Randall et al., 1992). Systems designed for combined biological nitrogen and phosphorus removal often include these anoxic and aerobic zones with MLR, but also typically include an anaerobic zone that receives only influent wastewater and return activated sludge (RAS) from the downstream secondary clarifiers for production of fermented products upstream of the anoxic zone (Randall et al., 1992).

There are several reasons to rethink and expand upon the traditional AS paradigm from the 1970's through the 1990's, despite being a well-established process in terms of theory development and implementation in practice around the world with sophisticated configurations designed for BNR. First of all, BNR plants inherently have a large plant volume, and therefore high capital investment. Because of the various operational and chemical requirements of a metabolically diverse bacterial population, consisting of nitrifiers, denitrifiers, and phosphorus-accumulating organisms (PAOs), many stages of treatment are necessary for BNR removal. In particular, the aerobic zone is the largest percentage of a plant's footprint because of the slow

growth rate of nitrifiers relative to the other bacteria (Grady Jr. et al., 2011). Therefore, the inventory of nitrifying biomass must be retained in the suspension via long solid retention times (SRT), which—all other things being equal—directly translates to higher volume. Furthermore, overall energy costs are high to provide oxygen to aerobic biomass in a conventional AS treatment plant; roughly 30% of a plants overall operational budget (Carns, 2005; EPA Office of Water, 2006). On a basis of treated volume, this demand is estimated to be around 0.35-0.60 kWh/m3 and 0.40 in North American wastewater treatment plants, most of which is expended through aeration (50%), pumping (16%), thickeners (12%), mixing (3.0%), and other necessary operations (McCarty et al., 2011; Liu et al., 2019). In the United States this translates to roughly 3% of the total energy load (McCarty et al., 2011). As geographical demography changes from rural to urban and sub-urban, total flow is expected to increase and therefore so is energy demand (EPA Office of Water, 2006). Moreover, the oxygenation efficiency is governed by gas transfer, which can be quite low in these conventional systems—standard oxygen transfer efficiency in process wastewater is around 5-15% (Tchobanoglous et al., 2003). Additional energy costs could come in the form of MLR from aerobic zone to anoxic zone, discussed above. Throughout the conventional AS process, excess energy from raw wastewater is “burned” with aeration rather than captured in a regenerative anaerobic process. All traditional suspended growth configurations take advantage of available carbon (measured as chemical oxygen demand or COD) as it is processed in upstream anaerobic and anoxic zones, but the addition of a downstream aeration zone results in heterotrophic oxidation of biodegradable organic matter, present through the hydrolysis of particulate and leftover colloidal matter. This has negative effects on the net energy balance, simultaneously increasing process oxygen requirements and reducing the mass of biodegradable organic matter available for other purposes (such as conversion to biogas in an anaerobic digester) (McCarty et

al., 2011). The benefits to conventional AS treatment processes can be realized, and the downsides minimized, through the use of various types of membrane technologies for BNR.

Membrane treatment technologies are an evolving subsection of wastewater treatment processes, and specific effort is being made to understand how to operate membranes in practice to optimize nutrient removal. The cutting-edge of engineering practice involves membrane systems treating domestic wastewater at full-scale for either filtration or aeration. Commercialized filtration membranes are typically employed at wastewater plants for a specialized function: chiefly, liquid-solid separation of suspended biomass from secondary treatment, or absorption and extraction of selected target pollutants (Visvanathan et al., 2000; T. Li et al., 2008). This type of membrane treatment system is known as a membrane bioreactor (MBR). An extension of conventional AS systems, MBR systems apply biological treatment of organic and inorganic pollutants. One major difference is rather than secondary clarification for biomass retention, membrane treatment uses size exclusionary pores to physically separate biomass, particulate matter, and microbial products to generate an excellent-quality treated effluent (Lin et al., 2012). A fundamentally different application of membrane technology utilizing a gas-permeable pore instead of separating liquids and solids, a membrane aerated biofilm reactors (MABR), is also becoming increasingly implemented in wastewater treatment plants as a means of enhancing nitrification, removal of organic matter, or simultaneous nitrification and denitrification (SND) (T. Li et al., 2008; Lu et al., 2021). These two unit processes provide systematic advantages over conventional treatment systems and configurations, e.g., suspended growth AS, when utilized in BNR treatment designs.

1.1 Overview of the Dissertation

The objective of this dissertation is to understand the fundamental chemical and biological drivers affecting two different applications of membrane treatment technologies treating domestic sewage in practice. Because of the complex biological and chemical nature of constituents in domestic sewage—as opposed to synthetic wastewater—this dissertation seeks to find solutions to existing research gaps surrounding MBRs and MABRs in real-life field scenarios. Chapter 2 describes the existing state of knowledge on membrane fouling, including common fouling mechanisms that remain a pervasive hinderance to the reliable operation in MBR treatment systems completing BNR. Chapter 3 is the complementary case study that troubleshoots long-term membrane fouling at one of North America's largest full-scale MBRs.

Additionally, Chapter 2 provides background on the fundamental difference between MBR and MABR treatment systems, the current emphasis on process intensification, and the decoupling of aerated growth to complete BNR. To explore the feasibility of decoupling traditional aeration from a BNR suspended growth design, and the utilization of MABR for nitrification, Chapter 4 investigates this with full-scale treatment simulation using SUMO20 software. Various scenarios are simulated in the chapter to evaluate process design implications and outcomes for a hybrid MABR/anoxic suspended growth system servicing a domestic wastewater load for 100,000 people. The overall idea of a fully anoxic suspended growth treating domestic wastewater is further explored in Chapters 4 and 5. A series of sequencing batch reactors (SBRs) were operated at the Ann Arbor Wastewater Treatment Plant (AAWWTP) to first analyze the extent of carbon oxidation in conventional aerobic and fully anoxic suspended growth. Next, the SBRs were reconfigured to undergo biological phosphorus removal (Chapter 5) with conventional anaerobic/aerobic (AO) and anaerobic/anoxic designs, respectively. For both sets of

experimentation, standard wet chemistry methods were used to monitor the major organic and inorganic constituents of the influent waste (i.e., primary effluent from AAWWTP clarifiers), mixed liquor during the reaction cycle, waste activated sludge (WAS), and final treated effluent, similar to the analyses performed at wastewater treatment plant laboratory. However, beyond these standard techniques, advanced microscopic methods were used to visualize and identify individual bacteria *in situ*, and biomolecular methods were used to extract and consolidate genomic information from the broader biological community. Overall, this analysis goes through in detail how advanced techniques can help solve complex issues facing membrane treatment technologies in practice.

1.2 References

Bellucci, M., & Curtis, T. P. (2011). Chapter Eleven - Ammonia-Oxidizing Bacteria in Wastewater. In M. G. Klotz & L. Y. Stein (Eds.), *Research on Nitrification and Related Processes, Part B* (Vol. 496, pp. 269–286). Academic Press. https://doi.org/https://doi.org/10.1016/B978-0-12-386489-5.00011-7

Bricker, S. B., Clement, C. G., Pirhalla, D. E., Orland, S. P., & Farrow, D. R. G. (1999). *National Estuarine Eutrophication Assessment: Effects of Nutrient Enrichment in the Nation's Estuaries*.

Carns, K. (2005). Bringing Energy Efficiency to Water & Wastewater Industry: How do we get there? *Water Environment Federation Technical Conference*.

Carpenter, S. R., Caraco, N. F., Correll, D. L., Howarth, R. W., Sharpley, A. N., & Smith, V. H. (1998). Nonpoint pollution of surface waters with phosphorus and nitrogen. In *Ecological Applications* (Vol. 8, Issue 3). https://doi.org/10.1890/1051-0761(1998)008[0559:NPOSWW]2.0.CO;2

EPA Office of Water. (2006). *Wastewater Management Fact Sheet: Energy Conservation*. https://doi.org/doi:10.7499/j.issn.1008-8830.2013.11.011.

Grady Jr., L., Daigger, G. T., Love, N. G., & Filipe, C. D. M. (2011). *Biological Wastewater Treatment* (Third). CRC Press.

Li, T., Liu, J., & Bai, R. (2008). Membrane Aerated Biofilm Reactors: A Brief Current Review. *Recent Patent on Biotechnology*, *2*(February 2008), 88–93. https://doi.org/10.2174/187220808784619739

Lin, H., Gao, W., Meng, F., Liao, B. Q., Leung, K. T., Zhao, L., Chen, J., & Hong, H. (2012). Membrane bioreactors for industrial wastewater treatment: A critical review. *Critical Reviews in Environmental Science and Technology*, *42*(7), 677–740. https://doi.org/10.1080/10643389.2010.526494

Liu, Y., Gu, J., & Zhang, M. (2019). *A-B Processes: Towards Energy Self-Sufficient Municipal Wastewater Treatment*. IWA Publishing.

Lu, D., Bai, H., Kong, F., Liss, S. N., & Liao, B. (2021). Recent advances in membrane aerated biofilm reactors. *Critical Reviews in Environmental Science and Technology*, *51*(7), 649–703. https://doi.org/10.1080/10643389.2020.1734432

McCarty, P. L., Bae, J., & Kim, J. (2011). Domestic wastewater treatment as a net energy producer-can this be achieved? *Environmental Science and Technology*, *45*(17), 7100–7106. https://doi.org/10.1021/es2014264

Randall, C., Barnard, J. L., & Stensel, H. D. (1992). *Design and Retrofit of Wastewater Treatment Plants for Biological Nutrient Removal* (Vol. 5). Technomic Publishing Compnay, Inc.

Sayler, G. S., Sanseverino, J., & Davis, K. L. (2012). *Biotechnology in the Sustainable Environment*. Springer US. https://books.google.com/books?id=4zTjBwAAQBAJ

Smol, M., Preisner, M., Bianchini, A., Rossi, J., Hermann, L., Schaaf, T., & Kruopien, J. (2020). Strategies for Sustainable and Circular Management of Phosphorus in the Baltic Sea Region: The Holistic Approach of the InPhos Project. *Sustainability*, *12*, 2567.

Tchobanoglous, G., Burton, F. L., & Stensel, D. H. (2003). *Wastewater Engineering: Treatment and Reuse* (4th Editio). Metcalf & Eddy, Inc.

Visvanathan, C., Ben Aim, R., & Parameshwaran, K. (2000). Membrane separation bioreactors for wastewater treatment. *Critical Reviews in Environmental Science and Technology*, *30*(1), 1–48. https://doi.org/10.1080/10643380091184165

Chapter 2 Background

2.1 Introduction

Wastewater treatment technology is currently in an inflection point; the adoption of membrane technologies over conventional systems is becoming more mainstream, but significant challenges still exist. A common phrase in the technology management space states that technological change is exponential, while organizational change is logarithmic (Brinker 2016). In this case, the practical challenges that exist with highly functional membrane treatment systems are still influencing their widespread adoption at wastewater plants, despite process advantages over conventional AS systems. Two types of membrane technologies treating domestic wastewater will be studied in this dissertation, the first being a membrane bioreactor (MBR). MBRs can be utilized at the end stage of a conventional AS treatment system in any configuration that is necessary for BNR. Mixed liquor suspended growth provides the biological treatment in this type of system, while the MBR cassette provides separation of the biomass in a pressure-driven environment that forces liquid permeate out into a secondary effluent stream (Radjenović et al., 2008; Hamedi et al., 2019). It is estimated that over 5,000 wastewater treatment plants all over the world are adopting MBRs, from municipal to industrial applications (Lin et al., 2012; Vaccari et al., 2022). A portion of this dissertation is dedicated to diagnosing an existing MBR fouling problem in the field. The other type, membrane aerated biofilm reactors (MABRs), employ a semi-permeable membrane in a fundamentally different way than MBRs, but are also starting to become implemented in wastewater treatment plants as a means of enhancing nitrification, removal of organic matter, or a combination of ammonia and nitrate removal, called simultaneous nitrification

and denitrification (SND) (T. Li et al., 2008; Lu et al., 2021). MABR shows promise, but is still relatively young on the technological S-curve compared to other treatment systems. In either case, whether it is troubleshooting an existing issue or charting a course for future performance upgrades, membrane treatment systems need more advanced analytics beyond the standard chemical methods to evaluate equipment performance, measure hydraulic parameters, and identify issues as they arise in the mixed liquor biology.

2.2 Current Practices at BNR Wastewater Treatment Facilities

At a fundamental level, all treatment system design and operation sit at the intersection of biology and chemistry such that biological and chemical methods are needed to evaluate performance during the short and long term. Required measurements at wastewater plants are dictated at the state and federal level, which typically include only chemical measurements of effluent discharges through the NPDES permit program (USEPA, 2010). The typical wastewater treatment process consists of four major steps: preliminary screening/grit removal, primary clarification, secondary treatment (including biological processes and secondary clarification), and advanced/tertiary treatment (Randall et al., 2010). Over the last six decades, various activated sludge configurations were designed to remove organic (carbon-based) and inorganic wastewater contaminants (nitrogen and phosphorus) that fuel bacterial and algal growth in our planet's natural water bodies, leading to eutrophication (Carpenter et al., 1998; Tchobanoglous et al., 2003). These configurations can include separate stages or zones, each operated to facilitate a particular biological metabolism, such as ammonia oxidizing bacteria (AOBs) and nitrite oxidizing bacteria (NOBs), ordinary heterotrophs (OHOs) for carbon oxidation or anoxic denitrification, or phosphorus accumulating organisms (PAOs) (Yeoman et al., 1988; Tchobanoglous et al., 2003; Komorowska-Kaufman et al., 2006). Among the most common configurations are activated sludge

(AS) designs that include a mixed liquor recycle (MLR) from the downstream aerobic zone to an upstream anoxic zone. Aeration is provided via blowers that pump air into the secondary treatment process from a fine-bubble diffuser. As the bubbles rise to the surface, oxygen is transferred to the liquid governed by the principles of mass transfer, which is often inefficient and dependent on how long the bubble stays beneath the water (Tchobanoglous et al., 2003).

Examples of single-sludge nitrogen removal included the Ludzack-Ettinger design (1961), the Wuhrman design (1964), and later the Modified Ludzack-Ettinger (MLE) (1973), and the four-stage Bardenpho Process (1978). Biological phosphorus removal research started in 1965 with the PhoStrip, then later anaerobic/aerobic (AO/Phoredox), anaerobic/anoxic/oxic (A2O), and University of Cape Town (UCT) processes for combined nitrogen and phosphorus removal (Randall et al., 2010; Grady Jr. et al., 2011). These designs eventually spread to full-scale systems around North America and Europe by the mid-1980's. However, recent reflection on these systems illustrate an inflection point in technology advances to biological fixed film and membrane systems, reordering treatment systems to avoid costly energy intensive practices, and scaling down the inherently large footprint required for nutrient-removing organisms to proliferate (McCarty et al., 2011).

Wastewater treatment plant operators utilize the design criteria of their outflow permits and their individual strategic plan to modify the performance of individual pieces of equipment. Considerable effort goes into monitoring plant dynamic wastewater flow rates, hydraulic retention time (HRT), and solids retention time (SRT), which effect the biology growing within the plant (Grady Jr. et al., 2011). Plants will often utilize online instrumentation, daily composite, or grab samples to monitor influent, mixed liquor, or effluent constituents via laboratory methods: biological oxygen demand (BOD), total suspended solids (TSS), mixed liquor suspended solids

(MLSS), organically available nitrogen or total Kjeldahl nitrogen (TKN), inorganic nitrogen (nitrate and nitrite), and total and dissolved phosphorus, are commonly measured (Randall et al., 2010). Also typically measured are pH, temperature, dissolved oxygen (DO), and alkalinity as these will directly affect biological performance. Plant operators will sometimes conduct special analytical campaigns to provide additional data about the inner-workings of the wastewater treatment process, or to feed predictive models for optimization purposes or operational flexibility (Randall et al., 2010). However, many of the special campaigns and advanced analyses plant operation would need to employ to understand the complex biological and chemical interactions occurring in their secondary treatment processes are extremely cost-prohibitive (Randall et al., 2010). Advanced nutrient analyses, such as micronutrients, on influent, effluent, and mixed liquor flows; fluorescent microscopic analysis of mixed liquor floc particles; and community characterization using advanced biomolecular techniques are not typically performed.

2.3 Membrane Technologies for Advanced Wastewater Treatment

The objective in all wastewater treatment design and operation—regardless of treatment method—is to maximize biological metabolism of nutrient substrates. For example, biological nitrogen removal in conventional AS is completed via an initial anoxic zone followed by an aerobic zone, with recirculation of mixed liquor (MLR) from the downstream aerobic to the upstream anoxic zone as a way of transporting oxidized nitrogen (nitrite and nitrate) produced in the aerobic zone to heterotrophic denitrifiers growing in the anoxic zone. BNR systems designed for combined biological nitrogen and phosphorus removal include these anoxic and aerobic zones with mixed liquor recirculation, but also typically include an anaerobic zone upstream of the anoxic zone that receives only influent wastewater and return activated sludge (RAS) from the downstream secondary clarifiers (Randall et al., 1992). Similar configurations exist in MBR treatment systems

(Randall et al., 2010). There are reported instances of combined nitrogen and phosphorus removal in MABR configurations, however, the underlying biological mechanisms behind these occurrences are still unknown (Underwood et al., 2018; Q. Li, 2018).

2.3.1 Membrane Bioreactor

Membrane bioreactors (MBRs) have become increasingly popular in wastewater treatment practice since the end of the 20th century. In contrast to conventional activated sludge (CAS) systems, which rely on sedimentation and flocculation to control organic material degradation and nutrient collection, MBRs combine the biological processes of activated sludge and liquid-solid separation through size exclusion by a membrane to remove wastewater pollutants and produce a high-quality effluent (Meng et al., 2017). MBR technology has been increasingly implemented in wastewater treatment plants throughout China, Europe, and the United States because of its inherent benefits, such as an easily controllable solids retention time (SRT), ammonia reduction capacity, and enhanced biological phosphorus removal (EBPR) potential (Lesjean et al., 2002; Meng et al., 2017).

The principal benefit of MBR treatment processes over AS systems is the ability to operate with highly concentrated biomass through physical retention or selection of an attached growth biofilm. As discussed previously, conventional AS requires a large aerobic zone to allow growth of slow-growing nitrifying organisms to provide sufficient capacity for the oxidation of ammonia-nitrogen to nitrite- and nitrate-nitrogen (Grady Jr. et al., 2011). BNR plants inherently have a large plant volume, and therefore high capital investment. In particular, the aerobic zone is the largest percentage of a plant's footprint because of the slow growth rate of nitrifiers relative to the other bacteria. Therefore, the inventory of nitrifying biomass must be retained in the suspension via long solid retention times (SRT), which—all other things being equal—directly translates to higher

volume. MBRs have been shown to have biomass concentrations 5-7 times higher than conventional systems, leading to increased uptake and metabolization of substrate, a high-quality effluent, and decreased sludge production (van Dijk & Roncken, 1997). Furthermore, secondary clarification is eliminated because MBRs operate by separating biomass and other suspended solids from the treated permeate via size-excluding, semi-permeable pores. Despite the numerous advantages over conventional AS, however, MBR treatment systems in wastewater are subject to regular fouling, i.e., detrimental blockage to the filtration capacity of the membrane pores (see Appendix A, Figure A-1).

MBRs are susceptible to different types of fouling and scaling, which can lead to loss of flux, and increases to transmembrane pressure that can cause serious damage if left unchecked (Meng et al., 2017; Hamedi et al., 2019). Fouling often displays several characteristic symptoms, such as permeability loss, TMP increase, increased TTF, and higher specific resistance to filtration (SRF), but the degree to which fouling is reversible or irreversible can determine the course of action for plant personnel (Kimura et al., 2005). Membranes are inherently fouled during the course of treatment; the build-up of solids on the surface or within the pores of the membrane can sometimes be abated through permeation cycles. Reversible fouling describes this build up over the course of normal cycling. Some physical operational options to mitigate the effect of reversible fouling include relax time, backpulse, or air scouring. Various other types of fouling mechanisms are known that decrease membrane permeability, both on the surface and in the pores of the membrane, and include: cake layer and gel layer build-up; inorganic scaling; surface charge adsorption; and pore obstruction (Lin et al., 2014). These types of irreversible fouling require chemical cleaning with sodium hypochlorite, sodium hydroxide, disinfectants or oxidants, or hydrochloric acid.

The causes of MBR fouling in wastewater treatment are often complex. All suspended solids, colloidal material, organic substances, salts, and soluble microbial products have potential to contribute to fouling. Particular focus in MBR fouling research is focused on extracellular polymeric substances (EPS), which are macromolecules produced by organisms in wastewater for many different reasons, including bacterial signaling, biofilm creation, and nutrient accumulation (Lin et al., 2014; Meng et al., 2017). There is strong evidence to suggest that EPS is significantly linked to physical-chemical membrane fouling mechanisms (Lin et al., 2014; Jørgensen et al., 2017). EPS is mainly composed of biopolymeric chains, which can include carbohydrates and proteins, with hydrophilic and hydrophobic sites (Radjenović et al., 2008; Lin et al., 2014). These groups have adhesive properties to the membrane surface through hydrogen bonding, but have also been shown to interact with monovalent or multivalent cations to form polymer bridges (Kara et al., 2008; Tang et al., 2009). Sludge deflocculation could also become an issue as the porous space between flocculating particles becomes susceptible to colloidal matter, creating a thick cake layer that prevents the passage of permeate (T. Nguyen et al., 2012; Meng et al., 2017; Hamedi et al., 2019). Innumerable combinations can exist. The key to understanding membrane biofouling in the field is to aggregate knowledge on operation measurements, qualitative observations, and mixed liquor characteristics to provide a semblance of what is occurring in the MBR. Sometimes, however, this complexity is too much for traditional measurements of daily operations, and advanced methods are required to understand more about the chemical and biological environment of the reactor. This dissertation will demonstrate the usefulness of advanced methods to examine the drivers of fouling at a MBR in northern Michigan.

2.3.2 Membrane Aerated Biofilm Reactors

Membrane aerated biofilm reactors (MABRs) are a recently commercialized process that has been implemented at BNR treatment plants, mainly as a means of enhancing nitrification (Heffernan et al., 2017; Houweling et al., 2017a; Jeff Peeters et al., 2017). In an MABR treatment system, low-pressure air is provide to the inner portion of a gas-permeable membrane, and supplies an attached aerobic biofilm growing on its surface Appendix A, Figure A-2. As the oxygen diffuses into the biofilm from the inside, ammonia and other substrates diffuse into the biofilm from the bulk liquid (the surrounding wastewater). Thus, the process is counter-diffusional, and two different concentration profiles can be found as the nitrifiers growing in the biofilm consume both electron donor (ammonia) and electron acceptor (O_2) (Downing & Nerenberg, 2008c; Martin & Nerenberg, 2012; Gilmore et al., 2013). MABRs deployed in practice have been shown to provide robust nitrification and COD removal, resulting in a high-quality effluent, and increasing the capacity of BNR treatment plants (Terada et al., 2003; Houweling & Daigger, 2019; Mehrabi et al., 2020). A benefit of MABRs is that, unlike MBRs, the issues related to fouling are not present, although they do require sophisticated levels of biofilm thickness control, management of ammonia and nitrate mass transport, and population stabilization and cohesion within the various biofilm layers (Lu et al., 2021).

The method of supplying aeration, i.e., bubble-less diffusion from inside the membrane, presents a significant advantage over fine bubble diffusers utilized in conventional systems. The theoretical oxygen transfer efficiency (OTE) for MABRs reaches near 100% (Ahmed & Semmens, 1992; Pankhania et al., 1994), whereas most field measurements are in the range of 30-40%, which constitutes more than three- to five-fold increase over a traditional aeration basin (Heffernan et al., 2017; Gilmore et al., 2009; Bicudo et al., 2019). Nitrification decoupled from a large aerobic zone

in this manner generates nitrate that can diffuse into the anoxic bulk liquid, which presents the opportunity for further BNR when combined with influent readily biodegradable carbon and a suspended heterotrophic biomass—denitrification for total nitrogen reduction would occur in such a case, or provided other factors, a combination of nitrogen and phosphorus removal (Sunner et al., 2018; Downing & Nerenberg, 2008a; Houweling et al., 2017b). The level of treatment is dependent on a couple of key factors, such as the biofilm surface area in the MABR zone, and the influent COD to nitrogen ratio (C:N), but typical nitrification rates achieved in practice range from 1.0-3.0 g-N/m^2-day (Koch et al., 2019; Côté et al., 2015; T. Kunetz et al., 2016; J Peeters et al., 2017; Jeff Peeters et al., 2017; Houweling et al., 2017b). Furthermore, because air diffuses directly into the biofilm at the point of greatest consumption, the calculated oxygen transfer rate (OTR) is much higher than a conventional system, drastically decreasing energy demand (Lu et al., 2021). Competition between heterotrophs and nitrifiers for resources within the biofilm can occur, depending on the diffusion of soluble carbon dictated by influent wastewater characteristics, although small-scale demonstrations have shown reliable nitrification performance. Past research has shown an influent COD/N ratio of around 4 to be optimal and impaired lower than 2; however, real domestic sewage influent component ratios can vary widely depending on population dynamics, pollution, or water quality from drinking water treatment systems (LaPara et al., 2006; Landes et al., 2011).

Placing a MABR in the same zone as suspended growth AS is shown to be a viable alternative to conventional AS alone, considered here as a hybrid MABR/anoxic suspended growth configuration. SND has already been established as a BNR pathway in pilot and full-scale builds, with up to 90% ammonia removal, and up to 70-85% TN removal reported in multiple process intensification projects (Heffernan et al., 2017; Augusto et al., 2018; Shechter et al., 2020). A

hybrid MABR operated as a side-stream treatment process to a full-scale wastewater plant in Northern Europe (Ejby Mølle WRRF, Odense, Denmark) achieved volumetric NR of 175-364 g-N/m^3/day and NO_3 concentrations below 1 g-N/m^3 (Uri-Carreño et al., 2021). High-rate MABR treatment systems with suspended growth SRT around 1.5 days, operating conditions below what could be realized with conventional AS, were also able to achieve TN removal (25-30%) (Sathyamoorthy et al., 2019). Another hybrid system study at SRT less than 5.0 days and dynamic influent loading demonstrated reliable ammonia removal, with effluent ammonia concentrations below 1.0-2.0 mg-N/L (ammonia removal rate = 1.0-3.0 g NH_3-N/m^2/day) (Houweling et al., 2017a).

Combined nitrogen and phosphorus removal in hybrid MABR systems has been achieved in past research, but there is still more to understand about how phosphorus removal would occur in a multi-variable attached growth/suspended growth system with a required alternating metabolism, and what mechanisms are involved to influence effective hybrid MABR performance. In one particular pilot study, effluent total phosphorus (TP) concentrations were consistently below 1.0 mg-P/L, which is considered high-quality by most treatment standards (T. Kunetz et al., 2016). But in the vast majority of hybrid MABRs, the treatment system is a "black box", where inputs and outputs can be measured, but the manner in which certain metabolic activities occur is speculative. Enhanced biological phosphorus removal (EBPR) in a hybrid MABR treatment system would necessitate the addition of an anaerobic zone at the beginning of secondary treatment before the MABR zone, similar to a conventional system (Sathyamoorthy et al., 2019; Q. Li, 2018). However, one study reported biological phosphorus removal (more than 65% total phosphorus reduction) without added chemical treatment. The system was not designed for bio-P and did not include an anaerobic zone (Q. Li, 2018). Other studies with chemical addition, such as the EBPR

operation at Ejby Mølle during primary treatment, benefitted the already existent bio-P process, but it is not clear to what extent the MABR played a role in that treatment (Uri-Carreño et al., 2021). A hybrid treatment system in Yorkville, IL achieved exceptional effluent TP concentrations (0.5 mg-P/L), however in this study it was again unclear how and why the bio-P removal was occurring (Underwood et al., 2018). Bio-P removal in a hybrid MABR system with anoxic mixed liquor is poorly characterized at this point. Research is needed in this area to provide detailed results on anoxic bio-P removal mechanisms using nitrate supplied from an MABR, as well as process conditions that would allow denitrifying PAO growth.

2.3.3 Gaps in Research

Biological methods, i.e., the methods of experimentation focused on identifying the living organisms and microbial products within the system, are not as common but can provide a wealth of information about the health of BNR systems. Standard wet chemistry has been applied to most of the examples detailed in this introduction, i.e., chemical methods to measure influent, mixed liquor, and effluent concentrations, or to further calculate removal rates. Techniques such as plate counting, visual light microscopy, and staining (Gram stain, Neisser stain, Indica stain, etc.) are also sometimes completed (Jenkins et al., 2004). Far less common are biomolecular techniques looking at genetic identity, metabolic activity, or genetic potential of the biomass population growing in the system. A couple of recent examples utilizing combined chemical and biomolecular analysis have impacted the engineering community's knowledge of antibiotic resistance genes in anaerobic/aerobic MBR systems (P. Wang et al., 2022), and developing the effect of sulfide interference on the nitrogen processing (ammonia oxidation and denitrification populations) of a MABR biofilm (Delgado Vela et al., 2021). This research similarly seeks to demonstrate the effectiveness of combining chemical, biological, and biomolecular methods in evaluation of

membrane systems treating domestic wastewater. This will include physical and modeling applications: deployed methods at a significant full-scale MBR system in practice at Traverse City Regional Wastewater Treatment Plant (TCRWWTP), proof-of-concept modeling of nitrogen and phosphorus removal in MABR units, and deployment of pilot-scale units performing BNR treatment of Ann Arbor's domestic sewage.

2.4 References

Ahmed, T., & Semmens, M. J. (1992). The use of independently sealed microporous hollow fiber membranes for oxygenation of water: model development. *Journal of Membrane Science*, *69*(1), 11–20. https://doi.org/https://doi.org/10.1016/0376-7388(92)80163-E

Augusto, M. R., Camiloti, P. R., & de Souza, T. S. O. (2018). Fast start-up of the single-stage nitrogen removal using anammox and partial nitritation (SNAP) from conventional activated sludge in a membrane-aerated biofilm reactor. *Bioresource Technology*, *266*, 151–157.

Bicudo, J., Heffernan, B., Klassen, A., Rao, M., McConomy, J., Syron, E., & McDermott, L. (2019). A one year demonstration of nutrient removal with Membrane Aerated Biofilm Reactor (MABR). *Nutrient Removal and Recovery Symposium 2019*.

Carpenter, S. R., Caraco, N. F., Correll, D. L., Howarth, R. W., Sharpley, A. N., & Smith, V. H. (1998). Nonpoint pollution of surface waters with phosphorus and nitrogen. In *Ecological Applications* (Vol. 8, Issue 3). https://doi.org/10.1890/1051-0761(1998)008[0559:NPOSWW]2.0.CO;2

Côté, P., Peeters, J., Adams, N., Hong, Y., Long, Z., & Ireland, J. (2015). *A New Membrane-Aerated Biofilm Reactor for Low Energy Wastewater Treatment: Pilot Results*.

Delgado Vela, J., Bristow, L. A., Marchant, H. K., Love, N. G., & Dick, G. J. (2021). Sulfide alters microbial functional potential in a methane and nitrogen cycling biofilm reactor. *Environmental Microbiology*, *23*(3), 1481–1495. https://doi.org/https://doi.org/10.1111/1462-2920.15352

Downing, L. S., & Nerenberg, R. (2008a). Effect of bulk liquid BOD concentration on activity and microbial community structure of a nitrifying, membrane-aerated biofilm. *Applied Microbiology Biotechnology*, *81*, 153–162. https://doi.org/10.1007/s00253-008-1705-x

Downing, & Nerenberg, R. (2008b). Total nitrogen removal in a hybrid, membrane-aerated activated sludge process. *Water Research*, *42*(14), 3697–3708. https://doi.org/10.1016/j.watres.2008.06.006

Gilmore, K. R., Little, J. C., Smets, B. F., & Love, N. G. (2009). Oxygen transfer model for a flow-through hollow-fiber membrane biofilm reactor. *Journal of Environmental Engineering*, *135*(9), 806–814.

Gilmore, K. R., Terada, A., Smets, B. F., Love, N. G., & Garland, J. L. (2013). Autotrophic nitrogen removal in a membrane-aerated biofilm reactor under continuous aeration: a demonstration. *Environmental Engineering Science*, *30*(1), 38–45.

Grady Jr., L., Daigger, G. T., Love, N. G., & Filipe, C. D. M. (2011). *Biological Wastewater Treatment* (Third). CRC Press.

Hamedi, H., Ehteshami, M., Mirbagheri, S. A., Rasouli, S. A., & Zendehboudi, S. (2019). Current Status and Future Prospects of Membrane Bioreactors (MBRs) and Fouling Phenomena: A Systematic Review. *The Canadian Journal of Chemical Engineering*, *97*, 32–58. https://doi.org/10.1002/cjce.23345

Heffernan, A. B., Shrivastava, A., Toniolo, D., Semmens, M., & Syron, E. (2017). Operation of a Large-Scale Membrane Aerated Biofilm Reactor for the treatment of Municipal Wastewater. *Proceedings of the Water Environment Federation*, 285–297.

Houweling, D., & Daigger, G. T. (2019). *Intensification of the Activated Sludge Process Using Media Supported Biofilms*. IWA Publishing.

Houweling, D., Peeters, J., Cote, P., Long, Z., & Adams, N. (2017a). Proving membrane aerated biofilm reactor (MABR) performance and reliability: Results from four pilots and a full-scale plant. *Proceedings of the Water Environment Federation*, *2017*(16), 272–284.

Houweling, D., Peeters, J., Cote, P., Long, Z., & Adams, N. (2017b). Proving Membrane Aerated Biofilm Reactor (MABR) Performance and Reliability: Results from Four Pilots and a Full-Scale Plant. *Proceedings of the Water Environment Federation*, *2017*(16), 272–284. https://doi.org/10.2175/193864717822155786

Jenkins, D., Richard, M. G., & Daigger, G. T. (2004). *Manual of the Causes and Cotrol of Activated Sludge Bulking, Foaming, and Other Solids Separation Problems* (3rd edn). CRC Press.

Jørgensen, M. K., Nierychlo, M., Nielsen, A. H., Larsen, P., Christensen, M. L., & Nielsen, P. H. (2017). Unified understanding of physico-chemical properties of activated sludge and fouling propensity. *Water Research*, *120*, 117–132. https://doi.org/10.1016/j.watres.2017.04.056

Kara, F., Gurakan, G. C., & Sanin, F. D. (2008). Monovalent cations and their influence on activated sludge floc chemistry, structure, and physical characteristics. *Biotechnology and Bioengineering*, *100*(2), 231–239. https://doi.org/10.1002/bit.21755

Kimura, K., Yamato, N., Yamamura, H., & Watanabe, Y. (2005). Membrane fouling in pilot-scale membrane bioreactors (MBRs) treating municipal wastewater. *Environmental Science and Technology*, *39*(16), 6293–6299. https://doi.org/10.1021/es0502425

Koch, J., Gehring, M., Oriol, G. G., Massons, G., Wang, C. F., Heffernan, B., & Nemeth, A. (2019). Optimized substrate removal and energy consumption in membrane aerated biofilm reactor with intelligent biofilm thickness measurement and control. WEFTEC 2019-92nd Annu. *Water Environ. Fed. Tech. Exhib. Conf*, 3773–3783.

Komorowska-Kaufman, M., Majcherek, H., & Klaczyński, E. (2006). Factors affecting the biological nitrogen removal from wastewater. *Process Biochemistry*, *41*(5), 1015–1021. https://doi.org/https://doi.org/10.1016/j.procbio.2005.11.001

Kunetz, T., Oskouie, A., Poonsapaya, A., Peeters, J., Adams, N., Long, Z., & Côté, P. (2016). *Innovative Membrane-Aerated Biofilm Reactor Pilot Test to Achieve Low- energy Nutrient Removal at the Chicago MWRD Innovative Membrane-Aerated Biofilm Reactor Pilot Test to Achieve Low-energy Nutrient Removal at the Chicago MWRD*. https://doi.org/10.2175/193864716819713006

Landes, N. C., Jackson, W. A., & Morse, A. N. (2011). Limitations Encountered for the Treatment of a Low C:N Waste Using a Modified Membrane-Aerated Biofilm Reactor. *Water Environment Research*, *83*(2), 128–139. https://doi.org/10.2175/106143010x12780288628138

LaPara, T. M., Cole, A. C., Shanahan, J. W., & Semmens, M. J. (2006). The effects of organic carbon, ammoniacal-nitrogen, and oxygen partial pressure on the stratification of membrane-aerated biofilms. *Journal of Industrial Microbiology and Biotechnology*, *33*(4), 315–323.

Lesjean, B., Gnirss, R., & Adam, C. (2002). Process configurations adapted to membrane bioreactors for enhanced biological phosphorous and nitrogen removal. *Desalination*, *149*(1–3), 217–224. https://doi.org/10.1016/S0011-9164(02)00762-2

Li, Q. (2018). *Pilot-scale Plant Applicatio of Membrane Aerated Biofilm Reactor (MABR) Technology in Wastewater Treatment*. KTH Royal Institute of Technology.

Li, T., Liu, J., & Bai, R. (2008). Membrane Aerated Biofilm Reactors: A Brief Current Review. *Recent Patent on Biotechnology*, *2*(February 2008), 88–93. https://doi.org/10.2174/187220808784619739

Lin, H., Gao, W., Meng, F., Liao, B. Q., Leung, K. T., Zhao, L., Chen, J., & Hong, H. (2012). Membrane bioreactors for industrial wastewater treatment: A critical review. *Critical Reviews in Environmental Science and Technology*, *42*(7), 677–740. https://doi.org/10.1080/10643389.2010.526494

Lin, H., Zhang, M., Wang, F., Meng, F., Liao, B., Hong, H., Chen, J., & Gao, W. (2014). *A critical review of extracellular polymeric substances (EPSs) in membrane bioreactors : Characteristics , roles in membrane fouling and control strategies*. *460*, 110–125. https://doi.org/10.1016/j.memsci.2014.02.034

Lu, D., Bai, H., Kong, F., Liss, S. N., & Liao, B. (2021). Recent advances in membrane aerated biofilm reactors. *Critical Reviews in Environmental Science and Technology*, *51*(7), 649–703. https://doi.org/10.1080/10643389.2020.1734432

Management, O. of W. (2010). *NPDES Permit Writers' Manual*. https://www.epa.gov/npdes/npdes-permit-writers-manual

Martin, K. J., & Nerenberg, R. (2012). The membrane biofilm reactor (MBfR) for water and wastewater treatment: principles, applications, and recent developments. *Bioresource Technology*, *122*, 83–94.

McCarty, P. L., Bae, J., & Kim, J. (2011). Domestic wastewater treatment as a net energy producer-can this be achieved? *Environmental Science and Technology*, *45*(17), 7100–7106. https://doi.org/10.1021/es2014264

Mehrabi, S., Houweling, D., & Dagnew, M. (2020). Establishing mainstream nitrite shunt

process in membrane aerated biofilm reactors: Impact of organic carbon and biofilm scouring intensity. *Journal of Water Process Engineering*, *37*, 101460.

Meng, F., Zhang, S., Oh, Y., Zhou, Z., Shin, H. S., & Chae, S. R. (2017). Fouling in membrane bioreactors: An updated review. *Water Research*, *114*, 151–180. https://doi.org/10.1016/j.watres.2017.02.006

Nguyen, T., Roddick, F. A., & Fan, L. (2012). *Biofouling of Water Treatment Membranes: A Review of the Underlying Causes, Monitoring Techniques and Control Measures*. 804–840. https://doi.org/10.3390/membranes2040804

Pankhania, M., Stephenson, T., & Semmens, M. J. (1994). Hollow fibre bioreactor for wastewater treatment using bubbleless membrane aeration. *Water Research*, *28*(10), 2233–2236. https://doi.org/https://doi.org/10.1016/0043-1354(94)90037-X

Peeters, J, Adams, N., Long, Z., Côté, P., & Kunetz, T. (2017). Demonstration of innovative MABR low-energy nutrient removal technology at Chicago MWRD. *Water Practice & Technology*, *12*(4), 927–936.

Peeters, Jeff, Long, Z., Houweling, D., Côté, P., Daigger, G. T., & Snowling, S. (2017). Nutrient removal intensification with MABR–developing a process model supported by piloting. *Proceedings of the Water Environment Federation*, *2017*(3), 657–669.

Radjenović, J., Matošić, M., Mijatović, I., Petrović, M., & Barcelo, D. (2008). *Erratum to Membrane Bioreactor (MBR) as an Advanced Wastewater Treatment Technology*. *5*(January), 275–280. https://doi.org/10.1007/698

Randall, C., Barnard, J. L., & Stensel, H. D. (1992). *Design and Retrofit of Wastewater Treatment Plants for Biological Nutrient Removal* (Vol. 5). Technomic Publishing Compnay, Inc.

Randall, C., James, B., Stensel, H. D., & Defresne, L. (2010). *Nutrient Control Design Manual*. www.epa.gov/nrmrl

Sathyamoorthy, S., Tse, Y., Gordon, K., Houwelling, D., & Coutts, D. (2019). BNR Process Intensification using Membrane Aerated Biofilm Reactors. *WEF Nutrient Removal and Recovery Symposium*, 527–535.

Shechter, R., Downing, L., Gordon, K., Nathan, N., Shefer, I., & Ben-Yosef, C. (2020). First Full-Scale Activated Sludge Retrofit Using a Spirally-Would MABR: Results and Model Evaluation. *Proceedings of the Water Environment Federation*.

Sunner, N., Long, Z., Houweling, D., Monti, A., & Peeters, J. (2018). MABR as a low-energy compact solution for nutrient removal upgrades—results from a demonstration in the UK. *WEFTEC 2018*, 1264–1281.

Tang, C. Y., Kwon, Y.-N., & Leckie, J. O. (2009). The role of foulant–foulant electrostatic interaction on limiting flux for RO and NF membranes during humic acid fouling—Theoretical basis, experimental evidence, and AFM interaction force measurement. *Journal of Membrane Science*, *326*(2), 526–532. https://doi.org/https://doi.org/10.1016/j.memsci.2008.10.043

Tchobanoglous, G., Burton, F. L., & Stensel, D. H. (2003). *Wastewater Engineering: Treatment and Reuse* (4th Editio). Metcalf & Eddy, Inc.

Terada, A., Hibiya, K., Nagai, J., Tsuneda, S., & Hirata, A. (2003). Nitrogen removal characteristics and biofilm analysis of a membrane-aerated biofilm reactor applicable to high-strength nitrogenous wastewater treatment. *Journal of Bioscience and Bioengineering*, *95*(2), 170–178.

Underwood, A., McMains, C., Coutts, D., Peeters, J., Ireland, J., & Houweling, D. (2018). Design and startup of the first full-scale membrane aerated biofilm reactor in the United States. *Proceedings of the Water Environment Federation*, 1282–1296.

Uri-Carreño, N., Nielsen, P. H., Gernaey, K. V, & Flores-Alsina, X. (2021). Long-term operation assessment of a full-scale membrane-aerated biofilm reactor under Nordic conditions. *Science of The Total Environment*, *779*, 146366. https://doi.org/https://doi.org/10.1016/j.scitotenv.2021.146366

Vaccari, M., Abbà, A., Bertanza, G., & Collivignarelli, C. (2022). An Evidence-Based Survey on Full-Scale Membrane Biological Reactors: Main Technical Features and Operational Aspects. *Applied Sciences (Switzerland)*, *12*(13), 0–11. https://doi.org/10.3390/app12136559

van Dijk, L., & Roncken, G. C. G. (1997). Membrane Bioreactors for Wastewater Treatment: The State of the Art and New Developments. *Water Science and Technology*, *35*(10), 35–41. https://doi.org/https://doi.org/10.2166/wst.1997.0353

Wang, P., Zarei-Baygi, A., Delgado Vela, J., & Smith, A. L. (2022). Metagenomic Analysis of the Antibiotic Resistance Risk between an Aerobic and Anaerobic Membrane Bioreactor. *ACS ES&T Water*. https://doi.org/10.1021/acsestwater.2c00383

Yeoman, S., Stephenson, T., Lester, J. N., & Perry, R. (1988). The removal of phosphorus during wastewater treatment: A review. *Environmental Pollution*, *49*(3), 183–233. https://doi.org/https://doi.org/10.1016/0269-7491(88)90209-6

Chapter 3 Multi-Year Diagnosis of Unpredictable Fouling Occurrences in a Full-Scale Membrane Bioreactor

Analysis reprinted with permission from: Avery L. Carlson, Glen T. Daigger, Nancy G. Love, Elizabeth Hart. Multi-year diagnosis of unpredictable fouling occurrences in a full-scale membrane bioreactor. *Water Science and Technology*, 2020. https://doi.org/10.2166/wst.2020.354

3.1 Abstract

The membrane bioreactor (MBR) at the Traverse City Regional Wastewater Treatment Plant has experienced sudden and unpredictable periods of substantial permeability decline since 2011. Early observations detected irregularly-shaped gram-positive bacteria that correlated with plant upsets. Use of biomolecular techniques, such as DNA sequencing of laboratory isolates and the mixed liquor microbial community, and fluorescent *in situ* hybridization, identified the dispersed organisms as members of the genus *Staphylococcus*. However, *Staphylococcus* members were consistently present during normal operation and therefore more likely an indicator of the upset, not the cause. The results suggest that these microorganisms are responding to specific influent wastewater constituents. We chemically analyzed seven mixed liquor samples from periods of permeability decline in 2017 and 2018, and four samples from a period of normal operation. During upset conditions, the total carbohydrate content exceeded that of normal operation by 40%. Additionally, mixed liquor calcium concentrations were 65% above normal during the upset in 2017. It is hypothesized and supported through multivariate statistical analysis and estimation of specific resistance to filtration (SRF) values, that a calcium-intermediated

polymer bridging mechanism with EPS constituents is one major contributor to fouling and permeability disruptions in the Traverse City MBR.

3.2 Introduction and Problem Description

The Traverse City Regional Wastewater Treatment Plant (TCRWWTP) (Traverse City, MI, USA) is an 8.5 million gallon per day (MGD) average flow capacity facility serving the community of Traverse City in northern Michigan with a wide array of customers, from municipal (90-95%) to industrial (5-10%). With original construction in 1932, the facility has been upgraded and expanded several times to increase treatment capacity and performance. The most recent upgrade and expansion was completed in 2004, when the plant was converted to a membrane bioreactor (MBR) process, representing one of the first facilities of its kind at that time to use the MBR process at significant scale in North America. The TCRWWTP also consists of screening/grit removal, primary clarification, and UV disinfection following the MBR activated sludge process. Mean cell residence time (MCRT) is seasonally varied to promote nitrification (5-15 days), and the mixed liquor suspended solids (MLSS) inventory ranges from 1.50-8.50 g/L. Secondary effluent is discharged to Boardman Lake, which ultimately drains into the Grand Traverse Bay on northern Lake Michigan. Waste activated sludge (WAS) is thickened in a gravity belt concentrator, and combined with primary sludge prior to anaerobic digestion. Digested sludge thickening and storage facilities are provided, and digested sludge is land applied.

The TCRWWTP MBR process has performed quite well historically, consistently complying with, and in many cases exceeding, not only plant discharge standards but also with significantly more stringent operational performance targets. Plant operational characteristics were also generally quite acceptable, and operational issues which did arise were successfully addressed. Prior to 2011, marking nearly eight years of operation, MBR operational parameters,

permeability and transmembrane pressure, had a standard and reproducible differential throughout 12-minute permeation cycles (Blair, 2012). In 2011, however, the treatment plant experienced a sudden and substantial membrane fouling event; unexpected, rapid decline in membrane permeability (Appendix B, Figure B-1), transmembrane pressure (TMP) that increased throughout the permeation cycle (Figure B-2), and an exponential increase in time-to-filter (TTF) (Figure B-3). Permeability is the hydraulic loading rate on the membranes per unit of membrane surface area, also known as the flux, divided by TMP (Hudkins et al., 2012). Permeability is expressed here in units of gallons per square foot of membrane surface area per day (GFD) per pounds per square inch (PSI) of pressure, and increases normally occur over time as a result of membrane fouling, resulting in the periodic need to clean the membranes using chemicals, such as sodium hypochlorite and citric acid (Judd, 2011). The much more rapid TMP increase, and subsequent permeability decrease, during the events of 2011 and beyond were so severe that filtering capability was threatened. Increased TTF which is used as an indicator of the effects of changing biological characteristics on the MBR process, suggested that dynamics to mixed liquor biology may be related to the increased membrane fouling rate (Blair, 2012). Plant operators observed a characteristic “slimy” coating on the membrane surfaces, as well as increased counts of globular zoogloeal organisms during and after the plant upset. A third-party review of sludge samples in 2011 revealed substantially increased amounts of dispersed bacteria (Blair, 2012).

Early investigation by WWTP personnel lead to a proposal that membrane fouling was due to high numbers of dispersed bacteria or dispersed colonies growing in the mixed liquor (see Appendix Section B-2). Gram staining and light microscopy indicated that these observed bacteria were gram positive, an unusual characteristic for municipal mixed liquors, which normally contain much higher gram-negative populations (Jenkins et al., 2004). Moreover, the bacteria have an

irregular bent rod morphology that plant operators coined “comma shaped” (Blair, 2012). Obvious dispersed bacteria growth in mixed liquor is unusual because it signifies disruption in the normal physiochemical process of bioflocculation (Jenkins et al., 2004). The dispersed bacteria phenomenon is poorly understood, but some research has pointed to biological factors, such as selection of fast-growing, non-flocculating bacteria (Bisogni & Lawrence, 1971). Other research shows displacement caused by an imbalance in the concentrations of monovalent and divalent cations (Higgins & Novak, 1997a, 1997b), or non-biodegradable organic surfactants (Bott & Love, 2002). Further complicating the matter was also the appearance of viscous slime on the MBR cassette during periods of declining filterability, where exceedingly high concentrations of exocellular biopolymers surrounded the observed dispersed bacteria, suggesting micronutrient imbalance (Jenkins et al., 2004).

While this operating condition had not been continuously present since 2011, similar events have reoccurred periodically since, occurring once or twice a year at random times (see Appendix Table B-1 for full timeline of events). TCRWWTP has been able to manage these events with increased ferric dosing, recovery cleans, air scouring, and relaxation or backpulsing of the membrane, although the duration and magnitude of upsets continues to be difficult to predict and makes preparation unrealistic. Efforts were made to limit the effects of periodic declines in permeability, and identify if they are related to CSGPB appearance, but no causal factors have been clearly identified. Plant staff initially hypothesized that permeability decline was directly related to the dispersed bacteria population that appeared based on observations of mixed liquor microbiology and measurement of biocake resistance on the membrane surface (Blair, 2012). This research relays the experimental and evaluative process that ensued to evaluate their assertion.

3.2.1 Membrane Fouling Symptoms Seen in Practice

Membrane bioreactors (MBRs) have become increasingly popular in wastewater treatment practice since the end of the 20th century. They combine the biological processes of activated sludge and liquid-solid separation through size exclusion by a membrane to remove wastewater pollutants and produce a high-quality effluent (Meng et al., 2017). MBR technology has been increasingly implemented in wastewater treatment plants throughout China, Europe, and the United States because of its inherent benefits, such as an easily controllable solids retention time (SRT), ammonia reduction capacity, and enhanced biological phosphorus removal (EBPR) potential (Lesjean et al., 2002; Meng et al., 2017). MBR fouling is one of the largest studied areas in practice, as it often displays several characteristic symptoms that can destroy the equipment and ruin performance, such as permeability loss, TMP increase, increased TTF, and higher specific resistance to filtration (SRF), all of which were witnessed at the TCRWWTP (Kimura et al., 2005). Each of these perpetuate loss to filtering and treatment capacity in the plant. Researchers will often categorize MBR disfunction according to the major factors that drive an event; including inorganics (scaling), organics, particulate or colloidal material, or biologics (microbial or microbial material); then by the mechanism driving the fouling, such as cake layer and gel layer build-up, surface charge adsorption, or pore obstruction (T. Nguyen et al., 2012; Meng et al., 2017; Hamedi et al., 2019). These mechanisms can involve a vast multitude of chemical or biological constituents, which are dynamically available in a complex environment like domestic wastewater (Lin et al., 2014). Polysaccharides are pointed out as one of the most common foulants, more so than other material common in wastewater, i.e., proteins or humic substances, because of their large structure, degree of rejection by the membrane, and ability to form cross-linking bridges with cations (Meng et al., 2017). Extracellular polymeric substances (EPS), another complex form of

organic material that could include polysaccharides, proteins, humic acids, and lipids present in and around microbial flocs, are considered common biofoulants as part of a larger formation, known as the "biocake", on the membrane surface (Lin et al., 2014; Meng et al., 2017). The contribution of individual components, the interaction of multiple components, or the degradation of the biocake can lead to a less porous filtering layer and higher adhesion, which in turn results in inferior membrane performance characteristics (Hamedi et al., 2019). The difficulty in starting the investigation at TCRWWTP was a lack of compelling evidence identifying a clear fouling mechanism to implicate for the reduced permeability events.

3.3 Hypothesis Development Process

Plant personnel had qualitative evidence, photographs of a seemingly novel gram-positive organism that appeared, and also observed slime formation; nevertheless, it was unclear to what extent specific microbiological and chemical factors were driving the observed effects. They were unable to narrow down the cause employing traditional tools at the plant laboratory in practice. Before any conclusions were drawn, we initially explored the hypothesis that first required identification of the irregularly-shaped gram-positive microorganisms found in the plant's mixed liquor. The investigation began in 2016 with a review of historical operational data to establish baseline mass loadings and seasonal trends for commonly monitored wastewater constituents. This was used as a starting point for research conducted at the University of Michigan labs where we employed advanced chemical analysis, culture-dependent and *in situ* genomic methods, and fluorescent microscopy techniques to identify the unknown organisms and assess its effect on mixed liquor quality.

This case study is organized to convey both experimental evidence and the thought process that led to identifying the cause of MBR upset. The first section of this paper is dedicated to

establishing why the initial hypothesis was unsupported, and the rationale for a secondary hypothesis. A March 2017 permeability and subsequent dispersed bacterial growth event allowed concurrent experimental testing on the MBR mixed liquor. Four rounds of sampling occurred: two characterized by MBR permeability decline, and two during normal operation. Once experimental data were analyzed, evidence supported shifting the hypothesis away from a microbiological cause for MBR upsets to chemical and physical mechanisms that involve components previously unmeasured at the full plant scale. The second section then explains the experimental outcomes and analyses used to evaluate the second hypothesis. A roadmap detailing the transition between the unsupported initial hypothesis to an alternative hypothesis that led to the conclusions of this study is shown in Figure 3-1. The hypothesis development process was used to unravel a challenge occurring to a significant North American MBR system. For use in MBR assessments, it provides a framework to assist current and future MBR plant operations. We applied a combination of chemical and biomolecular techniques to investigate the nature of the dispersed organisms relative to permeability upsets, and developed a hypothesis regarding the actual drivers of permeability disruptions in this full-scale wastewater treatment MBR. The outcomes of this study provide useful methodological and analytical information.

Throughout the course of experimentation, little evidence was found to directly implicate the microbial population with reduced permeability, but rather the novel organisms were an excellent indicator of changing mixed liquor chemistry brought on by influent organics and inorganics. An alternative hypothesis was then developed postulating that complex interactions between the influent organic components and inorganic cations were leading to deteriorating sludge flocculation and polymer bridging to form a surface gel on the MBR surface.

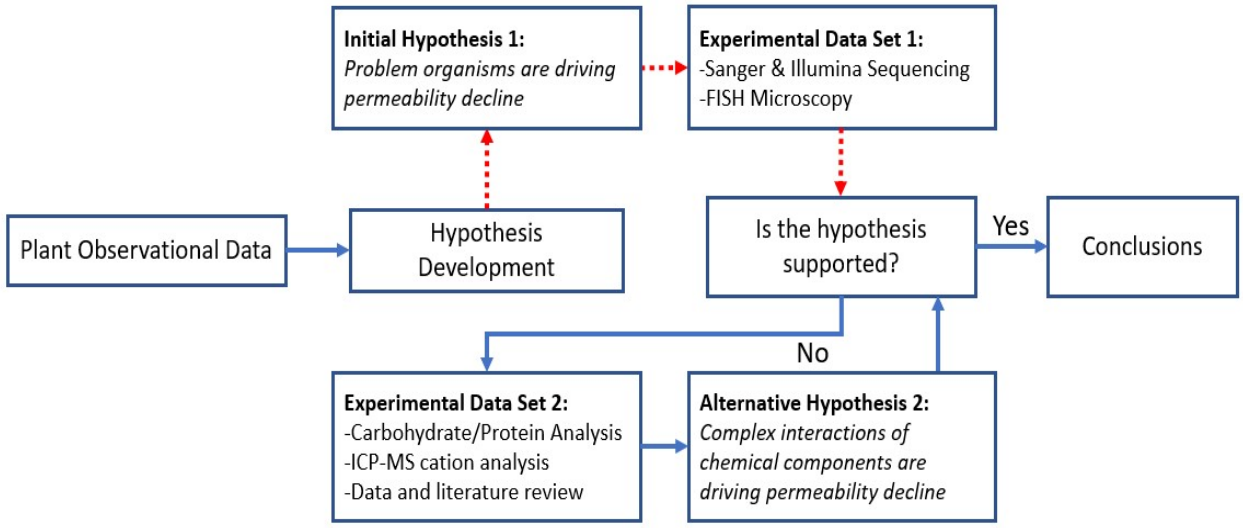

Figure 3–1 Project roadmap detailing the hypothesis development process from initial to alternative hypothesis Initial hypothesis based on personnel observations, alternative hypothesis after exploratory data collection. Dotted lines indicate direction of initial experimentation, solid line indicates ultimate concluding path.

3.4 Materials and Methods

3.4.1 Plant Data, Activated Sludge Samples, Enrichments and Culture Isolation

Activated sludge samples were collected during periods when the TCRWWTP was performing normally, and also when it was experiencing reduced membrane permeability. Sampling occurred in August and September 2017 (baseline operation without permeability issues, sample IDs designated C for control), and during upset events that occurred in March/April 2017 and January/March 2018 (sample IDs designated RP for Reduced Permeability). A summary of these sampling events along with sample identifying codes is given in Appendix Table B-1. Furthermore, historical data performed by TCRWWTP staff using *Standard Methods for the Examination of Water and Wastewater* (2017), including five-day biochemical oxygen demand (BOD_5), total suspended solids (TSS), total ammonia-nitrogen, and total phosphorus, were

collected and reviewed for the plant's influent, primary effluent, and secondary effluent for each outbreak from 2011 through the end of 2018.

Activated sludge samples (RP-TC-ML 1-5) were enriched by exploiting the dispersed nature of the problem bacteria. Several two-liter samples were taken from the TCRWWTP aeration basin. A portion of the original sample was separated and allowed to gravity settle for several hours. The supernatant after the settling phase was presumed to have a higher abundance of the problem organisms based on their observed preference for the planktonic state. The selected dispersed biomass was further concentrated from the supernatant by centrifugation for 10 min at low speed to avoid cell destruction (4,000xg), transferred to a 50% v/v glycerol solution, and frozen at -20°C. Bacterial colonies were cultured from these enriched samples (sample IDs: RP-TC-ML E1-E5) on Reasoner's 2A (R2A, Teknova, Hollister, CA, USA) media using a sterile T-streaking technique. Each individual enriched sample was then re-streaked 3 times to capture isolates (n=13). The less concentrated micronutrient profile of the R2A media was selected to decrease bias towards fast-growing heterotrophs and provide an opportunity for slower-growing microorganisms to grow.

3.4.2 Biomolecular Analyses

DNA was extracted from the isolated colonies using a "crude" extraction technique of extreme cyclical heating (five minutes at 95°C) and freezing (-80°C) in a Mastercycler Thermocycler (Eppendorf AG, Hamburg, Germany), according to Miller et al. (1999). The nearly full-length 16S rRNA gene was amplified by polymerase chain reaction (PCR) using forward primer 8F and reverse primer 1387R (Chiao et al., 2014). The PCR conditions were: 10 s at 98 °C followed by 30 cycles of 98 °C for 1 s, 62 °C for 5 s, 72 °C for 21 s, followed by 72 °C for 1 min and held at 4 °C until sample retrieval. PCR products were pre-processed through gel

electrophoresis, and fully cleaned using the Qiaquick Gel Extraction Kit (Qiagen, Hilden, Germany) before submission to the University of Michigan Advanced Genomics Sequencing Core (Ann Arbor, MI, USA) for Sanger Sequencing. Forward and reverse sequence reads were entered into BLAST (NCBI) for species identification with near 100% sequence alignment.

Mixed liquor samples collected during periods of stable plant operation and an upset period (sample IDs: C-TC-FISH 1-2, RP-TC-ML-FISH 3-6) were analyzed by fluorescent *in situ* hybridization (FISH). Mixed liquor (10 mL) from the aerobic zone of TCRWWTP's aeration basin was centrifuged for 10 min at 4,000xg, washed twice in 5 mL phosphate buffer solution, and fixed with 2.5 mL of absolute ethanol. Fixed samples were stored in a -20°C freezer. FISH DNA probes were designed for each of the three gram-positive bacterial genera found during the previous Sanger Sequencing process (*Microbacterium, Micrococcus,* and *Staphylococcus*) using DECIPHER (Wright et al., 2014); the probe sequences are provided in Appendix Table B-2. Interference for each individual probe was checked using the Ribosomal Database Project (RDP) (Cole et al., 2014). A probe was considered viable: if it had a 100% sequence match with the genera in DECIPHER; high specificity; and the lowest potential cross reaction according to RDP. These sequences were then tested for mismatches against our known Sanger sequences, and were found to have none. At this point, the three probes have highly specific and identifiable sequences. Finally, the laboratory isolates were used as a positive control for FISH to confirm that the probe was fluorescing with the desired bacterial target.

Fixation, permeabilization, and hybridization were completed according to the FISH Handbook for Biological Wastewater Treatment (Nielsen et al., 2009). An optimal formamide concentration was needed to first ensure adequate specificity with positive controls and *in situ* samples. We estimated the workable concentration of formamide for each probe using DECIPHER

(30% for *Microbacterium* and *Staphylococcus probes*, and 15% for the *Micrococcus* probe). The final hybridization buffer solution was determined using the recipe in Nielsen et al., 2009. The correct formamide concentration was estimated on a trial-and-error basis using the above process with a universal bacteria probe, Bact-338, prior to the higher specificity designed probes. The entire pre-processing, hybridization, and microscopy of TCRWWTP mixed liquor samples were verified with a universal bacteria probe, Bact-338, and a negative control (nonsense) probe, Non-EUB338.

DNA was extracted from unaltered mixed liquor samples collected during the permeability declines of 2017 and 2018 (sample IDs: RP-TC-ML Weeks 1-4, RP-TC-ML Weeks 9-10) and a period of normal operation (sample ID: C-TC-ML Weeks 5-8). Mixed liquor was vacuum filtered through a 0.2 μm polycarbonate filter (GTTP, MilliporeSigma, Burlington, MA, USA) and digested in a phenol-chloroform-isoamyl alcohol (25:24:1) solution according to the protocol by Hill et al. (2015). The mixture underwent bead beating for two minutes at room temperature, followed by centrifugation at 12,500xg three times where the DNA-rich aqueous phase was captured and purified using the Maxwell® LEV Blood DNA kit (Promega, Madison, WI, USA). The extracted DNA was sequenced using the Illumina MiSeq 16S rRNA gene platform to reveal relative changes to the entire microbial community in the MBR during plant upsets. PCR conditions and barcoded dual-index paired-end primers targeting a 250 base pair hypervariable segment of the V4 region of the 16s rRNA gene were used to amplify the DNA, according to the procedure detailed in Kozich et al., 2013. Sequencing results of the larger microbial community from March and April 2017, August and September 2017, and January 2018 samples were processed, aligned to a reference database (SILVA Release 132) (Pruesse et al., 2007) and analyzed using mothur (version 1.42.0). Erroneous sequence fragments and chimeras were

removed with mothur quality control algorithms (Schloss et al., 2009; Kozich et al., 2013) and the remaining sequences were annotated and clustered into operational taxonomic units (OTUs). Relative abundance was determined as the number of individual OTUs divided by the total number of community OTUs.

3.4.3 Mixed Liquor Chemical and Physical Analysis

Mixed liquor samples from the plant's aeration basin were analyzed to determine the biochemical constituents of observed slime that formed during a permeability upset in March/April 2017 (sample IDs: RP-TC-ML Weeks 1-4), as well as a period of normal operation in August/September 2017 (sample IDs: C-TC-ML Weeks 5-8). Total carbohydrates and total protein concentrations were analyzed in triplicate using the DuBois and the Thermo Fischer micro-Bicinchoninic Acid (micro BCA) methods, respectively (Dubois et al., 1951; Item #23235, Thermo Scientific). The DuBois method was slightly altered to include additional digestion with sulfuric acid and 80% phenol at 90°C for five minutes. Colorimetric measurements were taken on a spectrophotometric plate reader at 490 nm, and concentration was calculated from an acid/phenol-digested dextrose standard curve. Total protein content was solubilized through base digestion with 1 N sodium hydroxide at 100°C, according to Lowry et al., 1951, diluted by a factor of 20 and measured at 562 nm using a microplate reader. Total protein concentration was calculated from correlation to a base-digested bovine serum albumin (BSA) standard curve.

Additionally, mixed liquor (RP-TC-ML Weeks 1-4, C-TC-ML Weeks 5-8, RP-TC-ML Weeks 9-12, C-TC-ML Week 13), and primary effluent (RP-TC-PE Weeks 11-13) samples were subjected to micronutrient analysis. All samples were digested with nitric acid and hydrogen peroxide to dissolve suspended solids, per U.S. EPA (1996). Micronutrients, as defined by Jenkins et al. (2004), were analyzed using Inductively Coupled Plasma Mass Spectroscopy (ICP-MS) and

included calcium (Ca^{2+}), magnesium (Mg^{2+}), potassium (K^{+}), sodium (Na^{+}), manganese, iron, and zinc.

Routine TTF measurements by plant staff were supplemented with measurement of specific resistance to filtration (SRF), a filtering procedure that quantifies the resistance of filtrate passing through a biocake (Scholes et al., 2016). The mechanical setup consisted of a glass vacuum filter holder attached to a graduated cylinder. Polycarbonate filters (MilliporeSigma, Burlington, MA, USA) with a 0.8 μm pore size were used to retain as much flocculated and dispersed biomass as possible (Ng & Hermanowicz, 2005). The polycarbonate filter was chosen to best match the hydrophilic properties of the ZeeWeed membrane fibers. The filtering arrangement was attached to a vacuum pump with a constant operating pressure of 10 inches Hg (33.9 kPa). Baseline measurements were taken using unaltered TCRWWTP primary effluent and mixed liquor from the aerobic zone (SRF-TC-PE 1-5, SRF-TC-ML 1-5). SRF was also measured on MBR mixed liquor samples (SRF-DUN-ML 1-2) from the Dundee Wastewater Plant (Dundee, MI, USA), a plant not experiencing the difficulties occurring the TCRWWTP. Biocake SRF values were calculated for both plants using the equation derived in Christensen & Dick (1985) for mixed liquor solutions spiked with Na^{+} and Ca^{2+} (23, 46, 115, 230, and 460 mg/L Na^{+}, and 40, 80, 200, 400, and 800 mg/L Ca^{2+}, respectively), similar to the experimental framework of Novak et al. (1998). Finally, a time-dependent SRF study was completed using a mixture of 200 mL mixed liquor and 50 mL primary effluent from the TCRWWTP. After three hours, 0.5 mL of a 20 g/L Ca^{2+} solution was added and SRF was tested intermittently and over an 18-hour timespan.

3.5 Evaluating Preliminary Hypothesis 1

MBR fouling often displays several characteristic symptoms, such as permeability loss, TMP increase, increased TTF, and higher SRF, all of which were witnessed at the TCRWWTP

(Kimura et al., 2005). Each of these perpetuate loss to filtering and treatment capacity in the plant. The known physiochemical mechanisms of MBR fouling can occur both on the surface and in the pores of the membrane. Researchers will often categorize MBR disfunction according to the mechanism driving the fouling; cake layer and gel layer build-up; surface charge adsorption; and pore obstruction are common mechanisms that involve various chemical or biological constituents (Lin et al., 2014). The difficulty in starting the investigation at TCRWWTP was a lack of compelling evidence identifying a clear fouling mechanism to implicate for the reduced permeability events. Plant personnel had qualitative evidence, photographs of a seemingly novel gram-positive organism that appeared, and also observed slime formation; nevertheless, it was unclear to what extent specific microbiological and chemical factors were driving the observed effects. Therefore, we initially explored a hypothesis that involved identifying the gram-positive microorganisms.

3.5.1 Historical Data Review

Most treatment plants in practice utilize chemical analyzers strategically positioned to continuously measure online data and plant performance, gathered into interfaces, e.g., OP10 or SCADA, to allow real-time feedback to plant operators. In Appendix B there is a comprehensive set of figures illustrating the historical patterns of influent and primary effluent characteristics measured by these online analyzers between November 2010 and March 2017. The influent flow and temperature are shown in Figures B-6 and B-7, respectively. These curves follow typical seasonal patterns for a treatment plant, i.e., high influent flow during warmer summer months, eventually leading to lower influent flow during colder winter months. Northern Michigan's "temperate" climate is subject to highs in the summer and lows in the winter, which accounts for an oscillating curve throughout the year. Plant influent flow gradually increased between 2011 to

2016 as seen in Figure B-6, while influent concentrations of BOD, TSS, ammonia and phosphorus remained stable or moderately decreased. The chemical components of the influent, measured as total phosphorous (TP), five-day biochemical oxygen demand (BOD_5), total suspended solids (TSS), and total ammonia, are typically stable throughout the seasons (see Appendix Figures B-8 through B-12). TP concentration is stable in the range of 3 to 5 mg/L, while the typical range for ammonia concentration is around 20 to 30 mg/L. BOD_5 and TSS concentrations are much more variable, but do not exhibit discernible pattern between seasons.

During normal operation, primary effluent ammonia levels remain between 25 and 35 mg/L throughout the year. Primary effluent TSS and TP do not fluctuate with any noticeable magnitude. BOD_5, however, experiences a pattern of slight decrease in the spring months (March through May), eventually increasing back to previous levels in late summer. The average pollutant mass loadings for the past six years are consolidated in Appendix Table B-3. Since the initial outbreak in 2011, TCRWWTP has experienced events with varying degrees of magnitude; however, despite the severity, the plant has remained in full compliance with its permit. In the same time period, average mass pollutant loadings in the influent and primary effluent have remained fairly consistent or slightly decreased.

Plant operators followed traditional control strategies in the North and South Aeration Basins, decreasing the MLSS concentration gradually in the summer months and eventually returning to higher values during the winter months. The mean cell retention time (MCRT) follows the same pattern as the wastewater temperature, indicating that the MCRT is regularly adjusted in proportion to the seasonal temperature change (Appendix Figure B-13). Cell yield, the amount of new cell mass per amount of substrate removal, was calculated to determine the effect of MCRT on MLSS changes within the activated sludge process. Observed cell yield (Y_{OBS}) is found by

dividing TSS in the waste activated sludge (WAS) by the amount of BOD_5 in the primary effluent. According to Sherrard and Schroeder (1972), typical sludge processes will have a "linear and exponential" relationship between observed cell yield and MCRT. In other words, at large MCRTs, cell yield should approach a linear asymptote and become constant. Indeed, the seasonal MLSS changes in TCRWWTP follow a typical process with a constant cell yield; the observed cell yield curve is nearly linear. Thus, any variation of MLSS has a rational basis, and is a direct result of operational changes in MCRT to ensure nitrification will occur (Appendix Figure B-14). Nitrifiers are one of the more sensitive and slow growing organisms in the system, and operational change in MCRT is to ensure growth of nitrifying biomass within the system (Grady Jr. et al., 2011).

TCRWWTP has historically produced high quality and stable effluent, even throughout the presence of CSGPB. A distinct pattern, however, in seasonal water quality arises around the middle of March into the middle of April. Brief, and sometimes significant, spikes in effluent ammonia concentrations can be seen in this small window of time, regardless of CSGPB presence. A 2014 example of spring ammonia spike is shown in Figure B-15. In periods with CSGPB outbreaks, effluent ammonia spikes are often coupled with, or followed by, spikes in effluent TSS concentration, as depicted in Figure B-16. Normal seasonal operation in the plant produces effluent with TSS at the minimum detection limit (MDL) of 1 mg/L, and $cBOD_5$ of 2 mg/L that does not vary. Similarly, phosphorus levels fluctuate slightly throughout the year, but do not exhibit a noticable pattern.

3.5.2 Gram-positive Organism Identification

Culture-dependent Biomolecular Methods

Activated sludge samples were enriched with the observed "comma-shaped" organism by exploiting their dispersed nature and isolated cultures were grown in the lab on media. Full-length

16s rRNA Sanger sequences of these isolates were entered into the BLAST algorithm (NCBI) for species identification with 100% sequence alignment. Among the fourteen isolates submitted for sequencing, there were ten unique genera of organisms identified, but only three were gram-positive genera identified most frequently in NCBI BLAST with the highest percent identity (>97%) and no random database matches (E-Value = 0): *Staphylococcus, Microbacterium, and Micrococcus.* Multiple rounds of culturing and sequencing efforts were completed to minimize bias and to ensure consideration of all relevant organisms. All three of these organisms are ubiquitous in the environment, particularly sewage (Götz et al., 2006; Kim et al., 2011). Culturing techniques completed *in vitro* were not sufficient to induce the bent rod morphology from any of the suspect species, presumably due to the distinct environment in the plant's aeration basin. Therefore, *in situ* experimentation was necessary to capture the organism of interest.

Fluorescent Microscopy morphology matching

Mixed liquor samples were additionally fixed for fluorescent in situ hybridization (FISH) to visualize the organisms identified by the above steps using fluorescent microscopy. FISH technique is an advanced microscopic technique to visualize the selected isolates in the TCRWWTP mixed liquor samples to determine if they had the comma-shaped morphology under *in situ* growth conditions. FISH images with *Staphylococcus*-specific probes show a comma-shaped morphology that matched what was seen and documented by TCRWWTP staff during periods of permeability decline (Figure 3-2). *Staphylococcus* is a genus of facultative anaerobes whose members are known to contour into irregular morphologies based on environmental stressors, and whose genomes encode for capsular polysaccharide production (Stingele et al., 1996; García-Lara et al., 2015). With this evidence, we initially concluded that a species in the

Staphylococcus genera most likely represents the "comma-shaped" problem-indicating organisms, and more information was needed on its role in conjunction with permeability upsets.

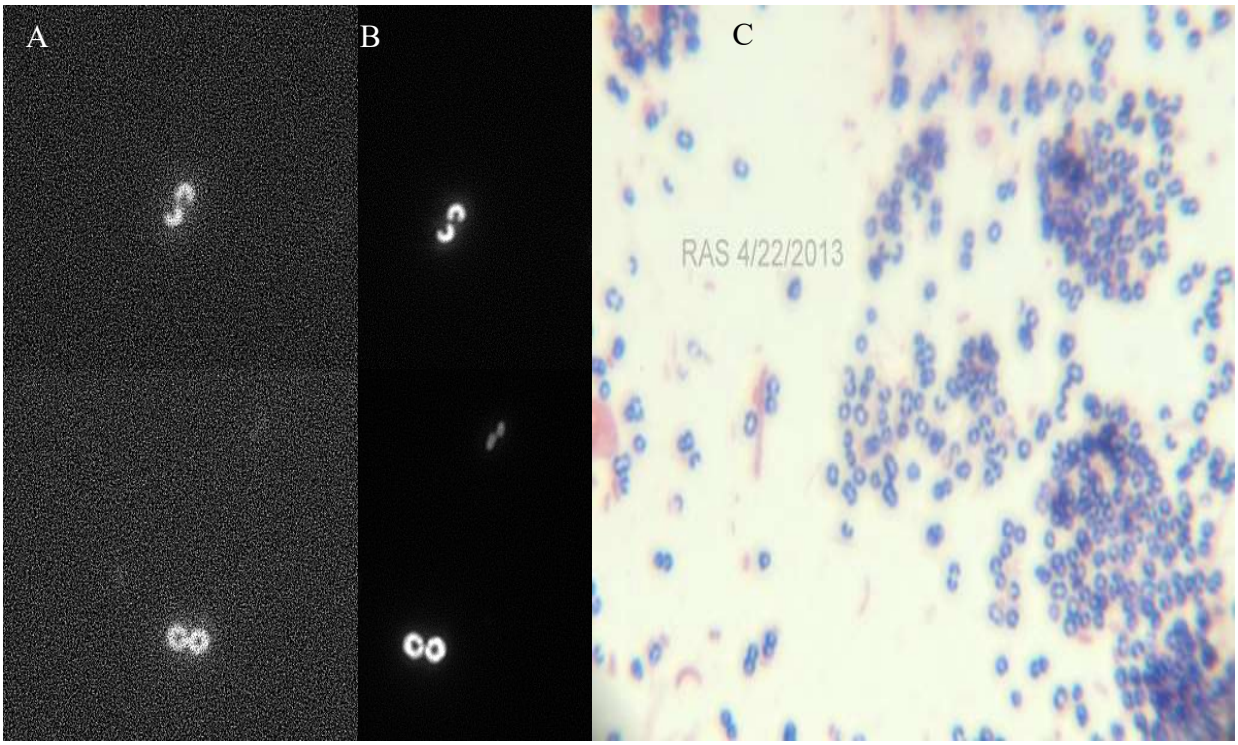

Figure 3–2 Fluorescent microscopy (FISH) of MBR mixed liquor sample using (A) Staphylococcus-specific FISH probe (100x magnification) and (B) universal DAPI stain.
Comparison of the two abundant morphologies shows match to sludge samples taken from permeability decline in 2013 (C).

Community 16s rRNA Amplicon Sequencing

Subsequent to the cell isolation techniques above, DNA extracted from unaltered mixed liquor samples was sequenced using the Illumina MiSeq 16s rRNA platform (Illumina Inc., San Diego, CA, USA) to reveal changes to the entire microbial community in the MBR during plant upsets. Annotated Illumina MiSeq 16S rRNA gene analysis (see Appendix Table B-4) revealed the presence and relative abundance of *Staphylococcus* within the larger activated sludge community. OTU 0910 matched the sequence of the *Staphylococcus* isolate (100% similarity, see Figure B-17). Other OTUs from the *Staphylococcaceae* family found in the mixed liquor

(specifically, those annotated as genera *Macrococcus* and *Jeotgalicoccus*) did not align with the *Staphylococcus* isolate Sanger sequences. When evaluating samples RP-TC-ML Weeks 1-4 and C-TC-ML Weeks 5-8, the relative abundance of OTU 0910 *Staphylococcus* was very low (ranging between 0% and 0.012%) for all samples and was not different between upset and control conditions after evaluation with a non-parametric Wilcoxon signed rank test (p-value = 0.77). Therefore, we could not discern a correlation between the suspected problematic comma-shaped *Staphylococcus* and permeability decline.

Whole community 16S rRNA gene sequencing analysis revealed the extent to which declining permeability events are unique. At the phylum-level, the relative abundance of *Firmicutes* (the phylum containing the genus *Staphylococcus)* decreased from an average of 31% during the permeability decline in Spring 2017 (sample IDs RP-TC-ML-Weeks 1-4) to 11% for the control event (samples C-TC-ML-Weeks 5-8) (see Figure B-18 and B-19). When looking at the overall bacterial community, this decrease in *Firmicutes* equates to higher diversity in the control samples (Shannon Index = 0.68-0.71), whereas samples RP-TC-ML-Weeks 1-4 are less diverse (Shannon Index = 0.54-0.6) with *Firmicutes* being one of the most dominant Phyla in the community. It is also interesting that samples from January 2018 (RP-TC-ML-Weeks 9-12) have a low relative abundance of *Firmicutes* (5.5%) and a similar diversity index as the control (0.69-0.71). Nevertheless, both samples from reduced permeability events deviate widely in community composition from the control sample and each other (PERMANOVA = 0.001). This result seems to not only reinforce the idea that treatment plant conditions are different between periods of stable operation and upset, which manifests into unique bacterial community composition, but also that the conditions between individual permeability events could also be different. Since the microbial community structure during each of the declining permeability events was also different, this

challenges the initial expectation that a particular microbiological composition would correlate with episodes of permeability decline.

Although we cannot conclude that bacterial composition plays a role in indicating permeability decline, our inability to detect a change in OTU 0910 across upset and control periods weakens the hypothesis that comma-shaped *Staphylococcus* is directly causing the treatment plant upsets. Low relative abundance does not immediately translate to low impact on the system, however, the biological analysis showing a consistently low abundance even during normal operation weakens the hypothesis that the gram positive, comma-shaped organisms were the direct cause of plant upsets. Classic biofouling mechanisms of dispersed bacteria, pore blockage for example, is considered unlikely. Rather, our data suggests that: (1) the *Staphylococcus* organisms stably exist in the mixed liquor, and (2) growth of comma-shaped bacteria as observed by the operational staff during upset events is an indicator of upset events, either due to changes in the influent or within the bioreactor. This is consistent with plant personnel observations that the comma-shaped bacteria formed clusters in the plant's return activated sludge (RAS), and at the climax of upset events those clusters released planktonic cells into the bulk liquid. Because of this apparent change, it is emphasized that *Staphylococcus* and their gram-positive relatives are helpful early warning indicators for plant operators of impending upsets. This conclusion led us to acquire new data to support the development of a revised hypothesis concerning factors driving the upsets.

3.6 Development of Hypothesis 2

Carbohydrate:Protein Characterization of Mixed Liquor

Based on the inconclusive biomolecular investigation, chemical investigations were initiated. Additional emphasis was placed on unmeasured aspects of TCRWWTP that could elucidate the basis for permeability decline. Because the treatment plant operators observed slime

formation during upset events, experiments were initiated to characterize the carbohydrate and protein concentrations of TCRWWTP's mixed liquor. Traditional knowledge of activated sludge systems states that viscous bulking conditions can occur when carbohydrates are overproduced (Jenkins et al., 2004). An average total carbohydrate concentration of around 255 mg/L was seen during the permeability decline in March and April 2017 (RP-TC-ML Weeks 1-4), over 40% higher (p-value = 4.9×10^{-13}, see Table 3-1) than the average measured from unstressed control samples during normal operation in August and September 2017 (C-TC-ML Weeks 5-8). Protein content was also measured as a representative indicator of biomass and intercellular carbohydrates, and was relatively stable between 1300-1800 mg/L with a coefficient of variation between all sample reads of 9.6%. This suggests a changing EPS composition relative to the amount of cellular biomass in the system.

Ratios of total carbohydrates to total protein during the period of permeability decline in Spring 2017 were found to be slightly higher on average (0.16), compared to the control (0.12) (p-value = 7.60×10^{-3}), implying the majority of change to mixed liquor carbohydrates was extracellular. Peak concentration of this carbohydrate content occurred in the third week after the observed start of the permeability decline, which may indicate EPS mechanisms were still adjusting to a rapid physical-chemical shift in the MBR that presumably triggered the event. Complex carbohydrates (polysaccharides) have been known to negatively affect activated sludge systems through slime formation, or zoogleal or nonfilamentous bulking (Jenkins et al., 2004); these conditions can cause fouling and decreased permeability in MBR systems (Hamedi et al., 2019). Starting in 2011 and onward, TCRWWTP personnel observed that the membrane surfaces were "slimy" during critical permeability upsets. The reduced permeability mixed liquor samples also appeared to be more uniformly viscous, and had small, dense floc particles compared to larger,

easily settleable particles from the control samples. From a functional standpoint, it is logical that a sticky, carbohydrate-rich mixed liquor environment could create or facilitate a more impermeable biocake on the membrane surface.

Table 3-1 Mixed liquor assessment of carbohydrate:protein ratio during a reduced permeability period (March/April 2017) and during normal operation (August/September 2017).

Sample ID	Total Carbohydrate Conc. (mg/L)	Total Protein Conc. (mg/L)	Ratio (Carb/Protein)	Avg.
RP-TC-ML-Week 1	234	1,510	0.16	0.16
RP-TC-ML-Week 2	248	1,510	0.16	
RP-TC-ML-Week 3	285	1,750	0.16	
RP-TC-ML-Week 4	252	1,790	0.14	
C-TC-ML-Week 5	216	1,480	0.15	0.12
C-TC-ML-Week 6	139	1,580	0.09	
C-TC-ML-Week 7	175	1,330	0.13	
C-TC-ML-Week 8	190	1,420	0.13	

Carbohydrate concentrations in MBR mixed liquor are often attributed to mixed liquor extracellular polymeric substances (EPS), which is a well-researched component of membrane fouling. EPS production is known to be stimulated for many different reasons, including bacterial signaling, biofilm creation, and nutrient accumulation, among others (Lin et al., 2014; Meng et al., 2017). Microbial secretions of extracellular polymeric substances (EPS) are a response to the surrounding chemical environment, and are a fundamental element of biofilm creation, floc structure, and nutrient accumulation. Strong evidence exists to suggest that EPS is significantly linked to physical-chemical membrane fouling mechanisms (Lin et al., 2014; Jørgensen et al., 2017); however, the relationship of EPS and the changing nature of the TCRWWTP mixed liquor in this study was not fully understood. Unlike conventional AS systems, the relationship between

organic and inorganic concentrations as a causative agent for full-scale plant upsets is under-studied, and more characterization is needed to establish how these parameters exist in conjunction with microbial EPS production, and accumulate in MBRs to induce fouling (Lin et al., 2014; Meng et al., 2017). Furthermore, there is limited knowledge about the role dispersed (non-floc-forming) bacteria play within this context, and its influence or response to these fouling conditions (Ng & Hermanowicz, 2005).

Carbon:Nitrogen Ratio.

The carbon to nitrogen (C:N) ratio is another important parameter impacting wastewater treatment systems. Wastewater streams contain dissolved, colloidal and particulate matter, including both organics and inorganics, which can blend together to create unfavorable environments that drive fouling mechanisms (Meng et al., 2017). As with all wastewater technologies, a proper balance of the ever-changing mass loads to an MBR system is required to stimulate microbial metabolism and growth, and satisfy treatment objectives. For MBR mixed liquor, this ratio becomes even more critical to keep EPS production at healthy levels. C:N imbalances or shock loads to a system have been shown to correlate with membrane fouling events (Wu et al., 2012).

The historical plant data review was revisited after the Spring sampling, and we found valuable underlying patterns when the ratios of influent constituents were calculated and plotted, versus plotting the constituents individually. For instance, the BOD_5 to ammonia mass ratio entering the aeration basins through the primary effluent (summarized in Appendix Table B-5) modestly increased after September 2017 in the lead-up to the permeability event in January 2018, from 5.38 to 6.68 mg BOD_5/mg NH_3-N. The primary effluent BOD_5 to TSS ratio noticeably dropped just before the upset in December/January 2018 from 1.62 to 1.09 mg BOD_5/mg TSS

(Figure B-20). Analysis of operational data from separate events in 2011, 2012, and 2013 also revealed a variable BOD_5 to ammonia ratio relative to the amount of suspended solids in the system. Data from a particularly troublesome upset in 2013 was reviewed, and a sustained elevated BOD_5 to ammonia ratio (8.11 mg BOD_5/mg TSS on average) in the primary effluent was noticed two weeks before the beginning of the observed permeability decline (see Figures B-21 and B-22). The same ratio for August 2018 would seem to negate the previous pattern, but this appears to be an outlier when viewed with the full data set for the rest of the year (Table B-5).

It is possible that a shock load of organic matter could be continuously disrupting the MBR. A sudden change in the food to microorganism ratio (F/M) causes rapid metabolism and production of bound EPS constituents in the mixed liquor (Hamedi et al., 2019). Results from Xin et al. (2015) validate the idea of increased cake layer resistance after feeding long chain polysaccharides, specifically alginate, to a membrane system. The higher BOD_5 to ammonia and BOD_5 to TSS ratios suggest that the industrial fraction of the influent may be changing just before a plant disruption. Samples were not collected that could be used to identify the form of organic entering the plant during disruptive periods. Nevertheless, revisiting the influent data allowed us to characterize the baseline within which individual constituents were changing relative to each other. The outcome of this modified analysis, compared to solely viewing changes to individual mass loadings, implies that permeability issues at TCRWWTP are not attributed to a single influent constituent; rather, a confluence of different constituents perhaps industrial or non-domestic in nature, could be driving mixed liquor quality deterioration.

Monovalent:Divalent Cationic Ratios

The connection between the utility's observation of slime production and the measured increase in the carbohydrate:protein ratio during and after permeability events offered a possible

hint about the mechanism of membrane permeability reduction. Slime is often tied to micronutrient deficiencies caused by insufficient cationic inorganic salts, such as Na^+, K^+, Ca^{2+}, and Mg^{2+} (Jenkins et al., 2004). We measured high baseline average total sodium and calcium concentrations (106 and 129 mg/L, respectively), and adequate average total magnesium and potassium concentrations (33.3 and 51.9 mg/L, respectively) in the treatment plant's aeration basin during normal operation (samples C-TC-ML-Weeks 5-8, C-TC-ML Week 13, C-TC-ML Weeks 22-23). The required total concentration of these salts for bacterial growth were calculated to be 12.5 mg/L Na^+, 41.6 mg/L Ca^{2+}, 29.1 mg/L Mg^{2+}, and 41.6 mg/L K^+ based on the MLSS and stoichiometric parameters in Grady et al. (2014). Concentrations of manganese, iron, and zinc were also above the threshold for bacterial growth, which ultimately dismissed micronutrient deficiency as a prevailing factor. In fact, ICP-MS data from mixed liquor samples in 2017 showed that perhaps the opposite was occurring. For the first period of permeability decline (RP-TC-ML Weeks 1-4), high levels of total calcium (between 175 and 278 mg/L) were detected in the mixed liquor (Table B-5 for full detail). During the same time period, Traverse City's drinking water treatment had less than 34 mg/L Ca^{2+}, on average, suggesting the remaining mass fraction came from external industrial or domestic sources. The concentrations of total calcium during the March/April 2017 TCRWWTP reduced permeability period were found to be significantly higher ($p=0.045$) than the control samples taken several months later in August/September 2017.

Inorganics are known to have a direct effect on biocake permeability, specifically manifested in deteriorating sludge dewatering quality (Novak et al., 1998). According to Higgins & Novak (1997a, 1997b), elevated monovalent cations (Na^+ and K^+) in activated sludge wastewater treatment systems result in deflocculation, interfering with liquid-solids separation. In contrast, they showed that divalent cations help consolidate flocs and improve liquid-solids

separation. Activated sludge dewatering characteristics are frequently measured by resistance to water passage through an activated sludge cake, which serves as a surrogate for resistance to permeability through an MBR biocake. The work by Higgins and Novak (1997a) formed the basis for today's standard recommendation to keep the monovalent-to-divalent cation ratio (milliequivalent-to-milliequivalent, designated M:D ratio) below 1:1 to achieve adequate activated sludge dewaterability. At TCRWWTP, the M:D ratio of the mixed liquor averages 0.83:1, less than the 1:1 recommended by Higgins & Novak, regardless of permeability issues. The high Ca^{2+} levels experienced during the first week of the permeability upset drove the ratio down to 0.45:1, and then modestly increased over the remaining three weeks, but remained far less than the control period and the other periods of reduced permeability in January 2018. In contrast, several studies concerning calcium fouling mechanisms show increased resistance to filtration coinciding with calcium bridging to different types of polysaccharides at total calcium concentrations ranging from 13.3-133 mg/L indicating polymer deposition, up to 240 mg/L indicating gel-layer formation (Xin et al., 2015; Miao et al., 2018). The concentrations for March 2017 are most similar to the latter; however, over the January 2018 (RP-TC-ML Weeks 9-12) period of permeability decline total calcium concentrations were indistinguishable from the control (128 versus 130 mg/L, respectively) ($p=0.75$). This would seem to contradict the notion that calcium-induced gel formation caused the treatment plant's permeability problems under all conditions. These observations, together with changing mixed liquor and influent characteristics, again imply that the permeability stress experienced by the TCRWWTP MBR cannot be consistently attributed to a single factor, but may be related to a combination of inorganic and organic constituents. An alternative line of reasoning was developed that involved high organic and inorganic loading: sludge deflocculation and polymer bridging.

3.7 Results and Discussion of Alternative Hypothesis 2

3.7.1 Complex Interactions of Chemical Components

Consideration of the above led to a general hypothesis involving both high inorganic and organic constituents causing sludge deflocculation and polymer bridging. The question remained whether the permeability upsets at TCRWTTP were the result of two different mechanisms: one due solely to high calcium concentration inducing gel formation with organics found native to the mixed liquor; the other relating to external organic loads and subsequent calcium polymer bridging. On this basis, we evaluated whether our data supported calcium as the primary cation causing polymer bridging in the MBR system at TCRWWTP, or if another pattern of fouling emerged that included an organic component.

Support of the hypothesis that organic loading and calcium-mediated bridging was dependent on the coordination of data from biological and chemical data sets. A constrained ordination plot (Figure 3-3) of the OTU variance from the MiSeq Illumina reads show three clusters of communities from the three sampling periods in 2017 and 2018. The variance calculation is developed from the PERMANOVA statistical analysis described previously, but visually shows just how distinct the biological variance is within these three sample groups. Overlapped with the biological variance are chemical concentrations from ICP-MS and TCRWWTP operational metadata from the same time. The direction and magnitude of the arrows point towards objects with similar variance and are considered closely correlated. What is apparent is the correlation of variance between total mixed liquor calcium concentrations and the mixed liquor microbiology from March and April 2017. In January, the community variance appears to be related to high levels of primary effluent suspended solids that is reinforced by the operational data at that time. This strengthens the proposition that a unique set of carbonaceous and inorganic

nutrient concentrations in the system mixed liquor has been dictating microbiological response, likely causing irregularities in morphology, dispersal of organisms, and production of carbohydrate-rich EPS.

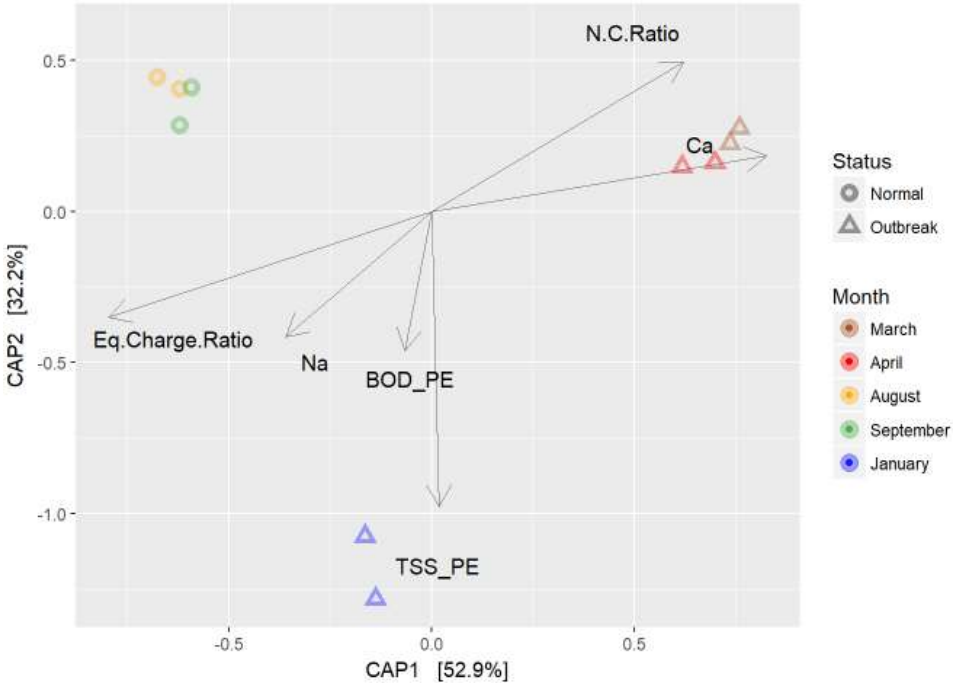

Figure 3–3 Constrained ordination plot of TCRWWTP mixed liquor OTU variance and statistical variance of operational metadata
Primary effluent nitrogen:carbon ratio (N.C.Ratio), primary effluent BOD (BOD_PE), primary effluent suspended solids (TSS_PE), mixed liquor total calcium concentration (Ca), mixed liquor sodium concentration (Na), mixed liquor equivalence charge ratio (Eq.Charge.Ratio).

3.7.2 Membrane resistance

The hypothesis that increased calcium resulted in adverse changes to mixed liquor filtration characteristics was tested by controlled addition of Ca^{2+} to TCRWWTP mixed liquor, followed by SRF measurement (samples SRF-TC-ML 6-8). Regular mixed liquor from TCRWWTP filtered well (Figure 3-4), with an average SRF value of 1.3 x 10^{12} m/kg, but increased steadily with increasing calcium ion addition.

After addition of 800 mg/L Ca^{2+}, SRF values increased nearly 25% over the ML baseline. Na^{+} additions to the mixed liquor had variable impact to biocake SRF, but with a general positive correlation with slightly higher resistance values. These results demonstrate a negative effect on biocake permeability relative to the cation concentration in the mixed liquor, but the magnitude of the changes to SRF was lower than expected. This could explain why plant personnel noted in March 2017, when mixed liquor total calcium concentrations were 278 mg/L, that permeability was not impacted as greatly as other upsets seen in the past, or the upset experienced in January 2018.

In comparison (Figure 3-4), the exact same filterability experiment using mixed liquor from Dundee Wastewater Plant had opposite results. The Dundee mixed liquor resistance to filtrations decreased with the same spiked additions of calcium. Sodium addition caused a minor deterioration in filterability, which agrees with the results from Higgins & Novak (1997). However, in direct contrast to TCRWWTP measurements, Dundee's baseline mixed liquor total calcium concentration was higher than TCRWWTP at 281 mg/L. As the polymer bridging studies in Xin et al. (2015) demonstrate, total calcium concentrations exceeding 280 mg/L have dramatic decreases in cake resistance, solution viscosity, and filtration times due to the formation of porous aggregates. This likely explains the high mixed liquor baseline SRF value of 1.94×10^{12} and subsequent decline with additional calcium. It would appear that TCRWWTP mixed liquor has a unique quality, where it exists normally at Ca^{2+} concentrations near the threshold for cationic saturation of polymer binding sites to induce a gel formation, and diverges from literature expectations where any additional Ca^{2+} loads past this threshold continue to be detrimental to biocake permeability.

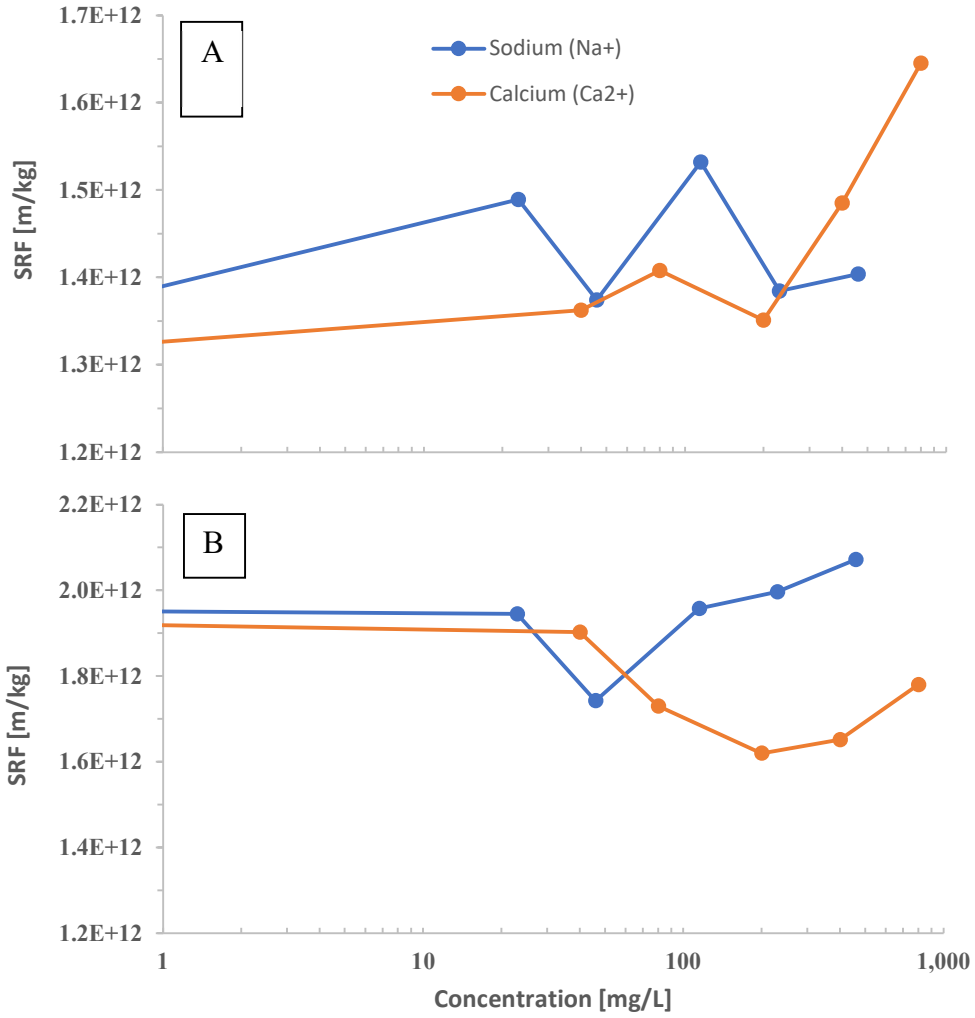

Figure 3–4 Comparison of TCRWWTP (A) and Dundee Wastewater Plant (B) SRF values with increasing sodium and calcium concentrations.

Preliminary SRF tests were conducted to uncover the extreme permeability events of January 2018 by taking SRF values after additions of both organic matter from the primary effluent and inorganics through spiked additions of Ca^{2+}. Ultimately, SRF values were found to substantially increase over time: a resistance measurement over 10X that of a fresh mixed liquor sample was seen after 18 hours of mixing. This also marked a considerable increase over the calcium spiked addition values discussed above (see Appendix Section B-7 and Figure B-21 for

details and results), but more testing is required with samples from known locations to establish a connection to the source of problem organic matter.

3.8 Recommendations and Future Work

Subsequent to the experimental laboratory investigation, TCRWWTP began routine sampling in July 2018 of influent wastewater (C-TC-INF Weeks 14-23) to analyze total and filtered chemical oxygen demand (COD) and total and filtered carbohydrates (Standard Methods; DuBois Method, described previously). In April 2019, this sample regimen was extended to significant industrial customers (SIUs) that are known to contribute higher strength wastewater to the plant collection system (C-SIU-EFF Weeks 22-23). Knowledge of what to look for in terms of carbon and macronutrient inconsistencies, previously unmeasured, gives plant personnel a better understanding of external effects on the plant influent and mixed liquor quality. Samples from targeted collection system outfalls, plant influent, and plant mixed liquor will be compiled into one mass balance with the goal of understanding sources of organic and inorganic sources. As a practical step towards day-to-day monitoring of influent cations, a conductance probe was installed at the headworks to the plant, and routine samples are collected for ICP-MS quantification.

3.9 Conclusions

This study investigated the contribution of chemical and biological factors at a full-scale MBR plant experiencing periods of sudden permeability decline using advanced chemical and biomolecular analyses beyond what was employed at the plant laboratory. At the onset of experimentation, it was believed that dispersed organisms were the root cause from simple microscopic analysis. The organisms were the most apparent visual link to permeability decline because of their unmistakable growth pattern, but were ultimately not found to be a principal cause

of permeability decline at TCRWWTP. However, increased *Staphylococcus* appearance in mixed liquor samples will continue to be a useful tool for indicating an impending upset. Chemical analysis and filtration characteristics showed the mixed liquor response to calcium and sodium additions was different from normal operations, and opposite the response from another MBR wastewater treatment plant treating largely municipal wastewater.

A compliment of data and analysis suggests that permeability decreases at the TCRWWTP occur when a combination of inorganic (principally calcium) and organic constituents are present in the plant influent wastewater. There is evidence to suggest that the organics are from non-domestic sources. The exact makeup of these flows is unknown; however, plant staff are using the techniques identified through this study to identify potential sources of the constituents that cause periodic permeability upsets.

3.10 References

Bisogni, J. J., & Lawrence, W. M. A. (1971). Relationships betweeen biological solids rentention time and settling characteristics of activated sludge. *Water Research*, *5*, 753–763.

Blair, S. (2012). Investigation into causes of a permeability crisis at large membrane bioreactor. *Proceedings of the Water Environment Federation*.

Bott, C. B., & Love, N. G. (2002). Investigating a Mechanistic Cause for Activated-Sludge Deflocculation in Response to Shock Loads of Toxic Electrophilic Chemicals. *Water Environment Research*, *74*(3), 306–315. https://doi.org/10.2175/106143002x140044

Chiao, T., Clancy, T. M., Pinto, A., Xi, C., & Raskin, L. (2014). Differential Resistance of Drinking Water Bacterial Populations to Monochloramine Disinfection. *Environmental Science & Technology*, *48*, 4038–4047. https://doi.org/10.1021/es4055725

Christensen, B. G. L., & Dick, R. I. (1985). Specific resistance measurements: methods and procedures. *J. Environ. Eng.*, *111*(3), 258–271.

Cole, J. R., Wang, Q., Fish, J. A., Chai, B., McGarrell, D. M., Sun, Y., Brown, C. T., Porras-Alfaro, A., Kuske, C. R., & Tiedje, J. M. (2014). Ribosomal Database Project: data and tools for high throughput rRNA analysis. *Nucleic Acids Research*, *42*(D1), D633–D642. https://doi.org/10.1093/nar/gkt1244

Dubois, M., Gilles, K., Hamilton, J. K., Rebers, P. A., & Smith, F. (1951). A colorimetric method for the determination of sugars. *Nature*, *168*(4265), 167.

https://doi.org/10.1038/168167a0

García-Lara, J., Weihs, F., Ma, X., Walker, L., Chaudhuri, R. R., Kasturiarachchi, J., Crossley, H., Golestanian, R., & Foster, S. J. (2015). Supramolecular structure in the membrane of *Staphylococcus aureus*. *Proceedings of the National Academy of Sciences*, 201509557. https://doi.org/10.1073/pnas.1509557112

Götz, F., Bannerman, T., & Schleifer, K. (2006). The Genera *Staphylococcus* and *Macrococcus*. In *The Prokayotes* (Vol. 4). https://doi.org/10.1007/0-387-30744.3_1

Grady Jr., L., Daigger, G. T., Love, N. G., & Filipe, C. D. M. (2011). *Biological Wastewater Treatment* (Third). CRC Press.

Hamedi, H., Ehteshami, M., Mirbagheri, S. A., Rasouli, S. A., & Zendehboudi, S. (2019). Current Status and Future Prospects of Membrane Bioreactors (MBRs) and Fouling Phenomena: A Systematic Review. *The Canadian Journal of Chemical Engineering*, *97*, 32–58. https://doi.org/10.1002/cjce.23345

Higgins, M. J., & Novak, J. T. (1997a). *Dewatering and settling of sludges: the case for using cation analysis*. *69*(2), 225–232.

Higgins, M. J., & Novak, J. T. (1997b). The effect of cations on the settling and dewatering of activated sludges: Laboratory results. *Water Environment Research*, *69*(2), 215–224. https://doi.org/10.2175/106143097X125371

Hill, V. R., Narayanan, J., Gallen, R. R., Ferdinand, K. L., Cromeans, T., & Vinjé, J. (2015). Development of a nucleic acid extraction procedure for simultaneous recovery of DNA and RNA from diverse microbes in water. *Pathogens*, *4*(2), 335–354. https://doi.org/10.3390/pathogens4020335

Hudkins, J. M., Aerts, P., Bundy, J. C., Schmidt, M., & Wilf, M. (2012). Membrane Fundamentals. In W. E. Federation (Ed.), *Membrane Bioreactors: WEF Manual of Practice No. 36* (First edit). McGraw-Hill Education. https://www.accessengineeringlibrary.com/content/book/9780071753661/chapter/chapter2

Jenkins, D., Richard, M. G., & Daigger, G. T. (2004). *Manual of the Causes and Cotrol of Activated Sludge Bulking, Foaming, and Other Solids Separation Problems* (3rd edn). CRC Press.

Jørgensen, M. K., Nierychlo, M., Nielsen, A. H., Larsen, P., Christensen, M. L., & Nielsen, P. H. (2017). Unified understanding of physico-chemical properties of activated sludge and fouling propensity. *Water Research*, *120*, 117–132. https://doi.org/10.1016/j.watres.2017.04.056

Judd, S. (2011). *The MBR book: principles and applications of membrane bioreactors for water and wastewater treatment* (S. Judd & C. Judd (Eds.); Second). Elsevier.

Kim, D. W., Heinze, T. M., Kim, B. S., Schnackenberg, L. K., Woodling, K. A., & Sutherland, J. B. (2011). Modification of norfloxacin by a Microbacterium sp. strain isolated from a wastewater treatment plant. *Applied and Environmental Microbiology*, *77*(17), 6100–6108. https://doi.org/10.1128/AEM.00545-11

Kimura, K., Yamato, N., Yamamura, H., & Watanabe, Y. (2005). Membrane fouling in pilot-scale membrane bioreactors (MBRs) treating municipal wastewater. *Environmental Science*

and Technology, *39*(16), 6293–6299. https://doi.org/10.1021/es0502425

Kozich, J. J., Westcott, S. L., Baxter, N. T., Highlander, S. K., & Schloss, P. D. (2013). Development of a Dual-Index Sequencing Strategy and Curation Pipeline for Analyzing Amplicon Sequence Data on the MiSeq Illumina Sequencing Platform. *Applied and Environmental Microbiology*, *79*(17), 5112 LP – 5120. https://doi.org/10.1128/AEM.01043-13

Lesjean, B., Gnirss, R., & Adam, C. (2002). Process configurations adapted to membrane bioreactors for enhanced biological phosphorous and nitrogen removal. *Desalination*, *149*(1–3), 217–224. https://doi.org/10.1016/S0011-9164(02)00762-2

Lin, H., Zhang, M., Wang, F., Meng, F., Liao, B., Hong, H., Chen, J., & Gao, W. (2014). *A critical review of extracellular polymeric substances (EPSs) in membrane bioreactors : Characteristics , roles in membrane fouling and control strategies*. *460*, 110–125. https://doi.org/10.1016/j.memsci.2014.02.034

Lowry, O. H., Rosebrough, N. J., Farr, A. L., & Randall, R. J. (1951). Protein measurement with the Folin phenol reagent. *The Journal of Biological Chemistry*, *193*(1), 265–275. https://doi.org/10.1016/s0021-9258(19)52451-6

Meng, F., Zhang, S., Oh, Y., Zhou, Z., Shin, H. S., & Chae, S. R. (2017). Fouling in membrane bioreactors: An updated review. *Water Research*, *114*, 151–180. https://doi.org/10.1016/j.watres.2017.02.006

Miao, R., Wu, Y., Wang, P., Wu, G., Wang, L., Li, X., Wang, J., Lv, Y., & Liu, T. (2018). New insights into the humic acid fouling mechanism of ultrafiltration membranes for different Ca^{2+} dosage ranges: results from micro- and macro-level analyses. *Water Science and Technology*, *77*(9), 2265–2273. https://doi.org/10.2166/wst.2018.141

Miller, D. N., Bryant, J. E., Madsen, E. L., & Ghiorse, W. C. (1999). Evaluation and optimization of DNA extraction and purification procedures for soil and sediment samples. *Applied and Environmental Microbiology*, *65*(11), 4715–4724.

Ng, H. Y., & Hermanowicz, S. W. (2005). Specific Resistance to Filtration of Biomass from Membrane Bioreactor Reactor and Activated Sludge: Effects of exocellular polymeric substances and dispersed microorganisms. *Water Environment Research*, *77*(2), 187–192.

Nguyen, T., Roddick, F. A., & Fan, L. (2012). *Biofouling of Water Treatment Membranes: A Review of the Underlying Causes, Monitoring Techniques and Control Measures*. 804–840. https://doi.org/10.3390/membranes2040804

Nielsen, P. H., Daims, H., Lemmer, H., Arslan-Alaton, I., & Olmez-Hanci, T. (2009). *FISH Handbook for Biological Wastewater Treatment*. IWA Publishing.

Novak, J. T., Love, N. G., Smith, M. L., & Wheeler, E. R. (1998). The effect of cationic salt addition on the settling and dewatering properties of an industrial activated sludge. *Water Environment Research*, *70*(5), 984–996.

Pruesse, E., Quast, C., Knittel, K., Fuchs, B. M., Ludwig, W., Peplies, J., & Glöckner, F. O. (2007). SILVA: a comprehensive online resource for quality checked and aligned ribosomal RNA sequence data compatible with ARB. *Nucleic Acids Research*, *35*(21), 7188–7196. https://doi.org/10.1093/nar/gkm864

Schloss, P. D., Westcott, S. L., Ryabin, T., Hall, J. R., Hartmann, M., Hollister, E. B., Lesniewski, R. A., Oakley, B. B., Parks, D. H., Robinson, C. J., Sahl, J. W., Stres, B., Thallinger, G. G., Van Horn, D. J., & Weber, C. F. (2009). Introducing mothur: Open-Source, Platform-Independent, Community-Supported Software for Describing and Comparing Microbial Communities. *Applied and Environmental Microbiology*, *75*(23), 7537 LP – 7541. https://doi.org/10.1128/AEM.01541-09

Scholes, E., Verheyen, V., & Brook-Carter, P. (2016). A review of practical tools for rapid monitoring of membrane bioreactors. *Water Research*, *102*, 252–262. https://doi.org/10.1016/j.watres.2016.06.031

Sherrard, J. H., & Scmtoeder, E. D. (1972). *Relationship between the observed cell activated sludge process*. *6*(1), 1039–1049.

Standard Methods for the Examination of Water and Wastewater (3rd ed.). (2017). American Public Health Association/American Water works Association/WAter Environment Federation.

Stingele, F., & Neeser, J. (1996). *Identification and Characterization of the eps (Exopolysaccharide) Gene Cluster from Streptococcus thermophilus Sfi6*. *178*(6), 1680–1690.

U.S. EPA. (1996). *Method 3050B: Acid Digestion of Sediments, Sludges, and Soils*.

Wright, E. S., Safak Yilmaz, L., Corcoran, A. M., Ökten, H. E., & Noguera, D. R. (2014). Automated design of probes for rRNA-targeted fluorescence in situ hybridization reveals the advantages of using dual probes for accurate identification. *Applied and Environmental Microbiology*, *80*(16), 5124–5133. https://doi.org/10.1128/AEM.01685-14

Wu, B., Yi, S., & Fane, A. G. (2012). Effect of substrate composition (C/N/P ratio) on microbial community and membrane fouling tendency of biomass in membrane bioreactors. *Separation Science and Technology*, *47*(3), 440–445. https://doi.org/10.1080/01496395.2011.621503

Xin, Y., Bligh, M. W., Kinsela, A. S., Wang, Y., & Waite, T. D. (2015). *Calcium-mediated polysaccharide gel formation and breakage : Impact on membrane foulant hydraulic properties*. *475*, 395–405.

Chapter 4 Comparison of Hybrid Membrane Aerated Biofilm Reactor (MABR) with Anoxic Suspended Growth with Conventional Biological Nutrient Removal Processes

Analysis of computer model reprinted with permission from: Avery L. Carlson, Huanqi He, Cheng Yang, and Glen T. Daigger. Comparison of hybrid membrane aerated biofilm reactor (MABR/suspended growth and conventional biological nutrient removal processes. *Water Science and Technology*, 2021, https://doi.org/10.2166/wst.2021.062.

4.1 Abstract

Mathematical modeling was used to investigate the possibility to use membrane aerated biofilm reactors (MABRs) in a largely anoxic suspended growth bioreactor to produce the nitrate-nitrogen required for heterotrophic denitrification. The results indicate such a process can be used to achieve a variety of process objectives. The capture of influent biodegradable organic matter while also achieving significant total inorganic nitrogen (TIN) removal can be achieved with or without use of primary treatment by operation at a relatively short suspended growth solids residence time (SRT). Low effluent TIN concentrations were achieved, irrespective of the influent wastewater COD/TN ratio, with somewhat larger suspended growth SRT. Further experimental work validated these modeling results in a physical system treating domestic wastewater. Denitrification occurred as expected utilizing mostly soluble COD, and less anoxic hydrolysis of colloidal organic matter was seen than the aerobic reactor. A fraction (roughly 25%) of the particulate and colloidal organic matter was not hydrolyzed in the anoxic reactors versus the aerobic reactors. This was demonstrated with theoretical carbon oxidation via calculation of the observed yield (a function of the true growth yield and the system SRT) compared to measured carbon mass balances over several SRTs sampling periods at steady-state.

4.2 Introduction

Membrane aerated biofilm reactors (MABRs) are a recently commercialized biological wastewater treatment process where air or pure oxygen is supplied to a biofilm from a gas permeable membrane (Downing & Nerenberg, 2008c). As the dissolved oxygen diffuses through the inner-most lumen of the membrane, carbon and ammonia-nitrogen diffuse from the bulk liquid, thereby creating a counter-diffusional flow of oxidizing and reducing agents allowing the aerobic growth of nitrifiers on the surface of the biofilm. MABR technology has been through various stages of development, but particularly over the past two decades has made significant leaps and is now coming into commercial applications. The unit process offers the opportunity to supplement or replace the aerobic zone in conventional activated sludge (AS) facilities (the largest portion of the bioreactor) with MABR units, which provides advantages over conventional treatment systems and configurations.

The objective in all wastewater treatment design and operation, regardless of treatment method, is to maximize biological metabolism of nutrient substrates. However, the use of MABRs in treatment processes have demonstrated improvements over the conventional AS systems, particularly the oxygen transfer from membrane into the nitrifying biofilm that allows decoupling of the ammonia removal pathway from the large aeration zones (Lu et al., 2021). Traditional AS systems are treatment processes utilizing suspended growth to perform biological nutrient removal (BNR), nitrogen and phosphorus being the most common nutrients designated for removal. These AS configurations are often designed with a large aerobic zone to allow growth of nitrifying organisms, which are responsible for the oxidation of ammonia-nitrogen to nitrite- and nitrate-nitrogen (Grady Jr. et al., 2011). A biological nitrogen removal configuration typically incorporates an initial anoxic zone followed by this large aerobic zone, with recirculation of mixed

liquor (MLR) from the downstream aerobic to the upstream anoxic zone as a way of transporting oxidized nitrogen (nitrite and nitrate) produced in the aerobic zone to heterotrophic denitrifiers growing in the anoxic zone. BNR systems designed for combined biological nitrogen and phosphorus removal include these anoxic and aerobic zones with mixed liquor recirculation, but require an anaerobic zone upstream of the anoxic zone that receives only influent wastewater and return activated sludge (RAS) from the downstream secondary clarifiers.

The topic of this chapter will focus on biological nitrogen removal; a discussion of combined nitrogen and phosphorus removal will continue in Chapter 5. In particular, we will assess in this chapter the feasibility of a designed hybrid MABR system with fully anoxic suspended growth to achieve nitrogen removal, which marks a significant paradigm shift in the treatment of domestic wastewater.

4.2.1 State of Knowledge Supporting MABR Research

The MABR treatment process operates via oxygen diffusion through the membrane and into the attached biofilm, thereby allowing the aerobic growth of heterotrophs and nitrifiers. Substrates in the bulk liquid diffuse into the biofilm from the opposite direction, consequently creating a counter-diffusional process with distinct concentration profiles over other widespread biofilm technologies. Practically speaking, these types of attached growth systems have little reliance on the system solids retention time (SRT), and, provided enough surface area, an MABR can promote a dense nitrifying biofilm layer and an anoxic outer layer (Li et al., 2008). The biofilm reduces an influent load of ammonia-nitrogen that would otherwise need to be oxidized in the downstream aerobic zone, and denitrification is now limited solely by diffusion without any needed recirculation. More recently, researchers have incorporated MABR units into the anoxic zone of conventional suspended growth biological nutrient removal (BNR) processes, allowing

the nitrate produced by nitrification in the MABR biofilm to serve as electron acceptor for heterotrophs in the suspended growth while reducing or eliminating needing mixed liquor recirculation for total nitrogen removal (Downing & Nerenberg, 2008c; Houweling & Daigger, 2019; Sathyamoorthy et al., 2019). This is considered as a "process intensification" step, meaning that it is an improvement or modification to a traditional AS system, but still relies on a large aerobic zone (Guglielmi et al., 2020). To date, the MABR component of the system has been sized to accomplish only a portion of the needed nitrification (often about 30 percent and less than 50 percent) (Houweling et al. 2017), and this has allowed a modest reduction in the size of the downstream aerobic suspended growth zone needed to complete the bulk of nitrification required for effluent permits. Some side-stream applications with various configurations also exist, but still either rely on chemical precipitation of nutrients or large aerobic AS zones (Q. Li, 2018; Uri-Carreño et al., 2021). Overall, these processes benefit from the much higher oxygen transfer efficiency (OTE) achieved with MABR units, compared to the oxygen transfer systems available for suspended growth bioreactors (T. Li et al., 2008; Côté et al., 2015).

MABR technology has been through various stages of development, but particularly over the past two decades has made significant leaps and is now coming into commercial applications. Slight rethinking of the design use could lead us to replace the aerobic zone in conventional activated sludge BNR facilities (the largest portion of the bioreactor) with MABR units. In theory, this would shrink the size of suspended growth zones, thus reducing total bioreactor size (by perhaps a factor of 3 or more); reduce energy requirements (perhaps by a factor of 3 or more) due to the much higher oxygen transfer efficient of MABRs compared to conventional oxygen transfer technologies and reduced pumping; and facilitates anoxic growth instead of aerobic growth so that carbon is more efficiently used in the nutrient removal process

(Downing & Nerenberg, 2008a; Houweling et al., 2017; Houweling & Daigger, 2019). Process energy requirements would be reduced because an increased proportion of the oxygen demand for nitrification is satisfied by the more energy efficient MABR units. Nitrogen removal would also no longer be limited by mixed liquor recirculation, potentially allowing for increased nitrogen removal. Reduction or elimination of the suspended growth aerobic zone could also result in a significant reduction in the suspended growth solids residence time (SRT), thereby reducing the fraction of influent biodegradable organic matter oxidized, thereby allowing more of the influent carbon to be captured for other purposes. This last prediction would also make more carbon available for other purposes, such as biogas generation in an anaerobic digester. This proposal has a foundational basis in past research with commercial applications, but evaluation is needed to evaluate specific benefits over traditional aerated suspended growth and determine where more investment in development of this technology is warranted.

Despite past research on commercialized MABR units demonstrating functional benefits, implementation of the next component of a hybrid system—a fully anoxic activated sludge zone—is extremely rare and many challenges exist, particularly with influent C/N limitations and sludge settling. Previous work by this group using a simplified modeling approach demonstrated these benefits could be realized. At that time, MABR modules had not yet been developed in any established biological process simulation software that we were aware of. With specific respect to the MABR portion of a proposed hybrid treatment train, the objectives in this chapter are to: (1) further quantify differences between hybrid MABR process options, compared to conventional suspended growth process configurations and (2) identify hybrid MABR process operating conditions that may be interesting to pursue experimentally in a physical system. A proof-of-concept evaluation using computer simulation is used in the first half of the chapter to evaluate

specific benefits over traditional aerated suspended growth and determine the extent to which investment in developing a hybrid anoxic suspended growth with a MABR process is warranted.

4.2.2 Proposed Hybrid MABR/Anoxic Suspended Growth Process

It is envisioned that a MABR/anoxic suspended growth design process would utilize nitrate as the main terminal electron acceptor for metabolism of biodegradable organic matter and denitrification. Recently, researchers have shown MABR units incorporated into the anoxic zone of conventional suspended growth processes develop a nitrifying biofilm that results in the production of nitrate (Houweling & Daigger, 2019). The MABR already has shown potential for significant improved nitrification at full-scale and can be integrated with existing enhanced phosphorus removal processes (Kunetz et al., 2016). In terms of energy demand and generation, the direct aeration strategy of an MABR increases OTE as much as five times, which dramatically reduces energy needed for treatment (Côté et al., 2015). Moreover, the OTE is governed by gas transfer, which can be quite low in these conventional systems—conservative estimates of oxygen transfer are around 10-15%. Coupled with a high-rate denitrifying suspended growth system, e.g., a process for metabolizing readily biodegradable COD (rbCOD) at SRTs < 3.0 days and a low rate of hydrolysis, it is proposed that an MABR could achieve BNR capacity at or exceeding traditional systems. The total nitrogen (TN) and inorganic nitrogen (ammonia, nitrate, and nitrate-nitrogen) removal performance of such a system will be studied extensively with sequencing batch reactors (SBRs), while simultaneously measuring particulate (pCOD) and colloidal COD (cCOD) capture in secondary sludge for biogas production. It is unclear what tradeoffs or limitations exist with bioflocculation; particularly, filaments that serve an essential function as “backbone” to settleable flocs may be inhibited in low DO environments (Chudoba, 1985; Gabb et al., 1991). Furthermore, known issues with floating solids (also known as “rising sludge”) in anoxic treatment

configurations, where nitrogen gas remains trapped in flocs causing them to float to the surface, will have to be addressed (Ekama et al., 1997).

This novel approach serves two academic functions in addressing existing knowledge gaps: it continues to evaluate BNR capacity in a relatively new wastewater treatment technology; and examines the technology under a new set of design conditions, previously unstudied. The purpose of this examination was to start from fundamental science, utilize various tools, and envision how an MABR performing BNR could be integrated with a large anoxic suspended growth zone—otherwise known as a hybrid MABR system.

4.3 Material and Methods

We used a computer simulation software (SUMO, Dynamita) which implements fundamental mass balance, mass transfer, and kinetic equations to estimate the fate of solids, nitrogenous species, phosphorus, and chemical oxygen demand (COD) in a full-scale configuration. The main criteria we used for comparison to a conventional BNR configuration were total inorganic nitrogen (TIN) in the effluent; design parameters, such as SRT; and process energy demand or energy generation potential through conversion to biogas. TIN was the metric of effluent total nitrogen performance considered in this study instead of total nitrogen (TN) because the former captures the components of nitrification and denitrification, whereas the organic nitrogen components of the latter are wastewater-specific and dynamic. Capture of influent COD for productive purposes was assessed by the fraction of influent COD converted to biogas when primary sludge (when primary clarifiers were included) and waste activated sludge (WAS) is subjected to anaerobic digestion. Scenarios were also conducted with and without primary clarification.

We are attempting to find the limits of our proposed MABR system through computer simulation to facilitate later development of a pilot-scale system. This computer process modeling discussed below was built piece-wise from the simplest design possible to a more advanced model using MABR cassettes. The modeling was then followed by design and operation of a series of bench-scale reactors in the field treating domestic sewage from the Ann Arbor Wastewater Treatment Plant (AAWWTP). This study evaluated suspended growth under separate anoxic and aerobic growth conditions to evaluate the conclusions found in computer simulations. Standard wet chemistry methods used to measure a complete system mass balance, to measure effluent quality, the extent of carbon oxidation, and calculate BNR treatment capacity, specially nitrogen removal performance.

4.3.1 Proof-of-concept Model

A proof-of-concept process model was developed to provide preliminary results regarding the feasibility of decoupling nitrification from a BNR treatment system. The logic was that an envisioned full-scale system that features MABR would separate nitrification from the rest of the treatment train, i.e., a conventional suspended growth AS system. The expectation with this step would reaffirm what we already know regarding SND, cement the results in fundamental theory, and build upon prior research (Côté et al., 2015; Kunetz et al., 2016; Houweling et al., 2017; Houweling & Daigger, 2019) demonstrating sufficient removal of TIN and COD. The added value of this phase is it allows side-by-side evaluation based on identical simulated inputs, and provides high-level evaluation of effluent quality and nutrient processing of anoxic suspended growth treatment of raw sewage without heavy reliance on traditional aeration schemes, as well as estimate baseline design parameters to serve as a "sanity check". Modeling tools are helpful in developing proof of concept, and have been used in the past to successfully develop new BNR treatment

processes: an example being the historically important iterations of the Activated Sludge Models (Henze et al., 2000).

To simulate treatment of domestic wastewater, an influent formula was created in SUMO 2016 (Dynamita, France) characterized by typical COD, ammonia, and phosphorus values for a population of 100,000 (see Table 4-1). For this portion of the modeling, however, the main influent stream was divided into two: one containing the entire influent mass flow of ammonia-nitrogen, and the other containing organic nitrogen and COD. The proof-of-concept model configuration was made up of a completely stirred tank reactor (CSTR) instead of an MABR cassette, and it was designed to perform complete nitrification on the influent stream of ammonia only. The assumption made at this phase of modeling is that a "surrogate" MABR (i.e., this first aerobic CSTR) could process nearly all the ammonia-nitrogen, or complete nitrification. Then, the nitrified effluent was sent downstream and blended with the remaining constituents of the influent stream, mainly carbonaceous COD, in a subsequent anoxic suspended growth zone of two CSTRs in series to simulate denitrification (see Figure C-1 in the appendix). A wide range of operating conditions were also simulated, including with and without primary treatment, in this initial assessment to provide a general understanding on process options and trade-offs (Daigger et al., 2019). This computer model was expanded upon in more detailed fashion in the advanced model, discussed below. Table 4-1 summarizes the influent wastewater flows and constituent mass loadings used, along with the per-capita values used to calculate them for a service population of 100,000 people. The relatively low water use used (0.25 m^3/cap-day) results in a relatively strong wastewater (680 mg/L COD, 60 mg-N/L TKN, 10 mg-P/L TP). Since biological nitrogen removal via heterotrophic metabolism depends on the availability of sufficient organic matter, a sensitivity analysis was conducted to assess the impact of a lower wastewater COD/TN ratio on the effluent TIN. For this

analysis, the per-capita COD loading was reduced from 170 to 100 g-COD/cap-day, resulting in a reduction in the influent wastewater COD/TN ratio from 11 to 6.7 mg-COD/mg-N. Table 4-1 presents the revised influent wastewater flows and constituent loadings used for both scenarios in this analysis.

Table 4-1 Wastewater Flow and Constituent Loadings Used in Simulations (100,000 Population).

High COD/TN Simulations				
Item	**Value**	**Units**	**Value**	**Units**
Flow	0.25	m^3/cap-day	25,000	m^3/day
COD	170	g/cap-day	17,000	kg/day
TKN	15	g-N/cap-day	1,500	kg-N/day
NH_3-N	65	% of TKN	980	kg-N/day
TP	2.5	g-P/cap-day	250	kg-P/day
COD/N	11	mg-COD/mg-N		
Low COD/TN Simulations				
Item	**Value**	**Units**	**Value**	**Units**
Flow	0.25	m^3/cap-day	25,000	m^3/day
COD	100.	g/cap-day	10,000	kg/day
TKN	15	g-N/cap-day	1,500	kg-N/day
NH_3-N	75%	% of TKN	1,100	kg-N/day
TP	2.5	g-P/cap-day	250	kg-P/day
COD/TN	6.7	mg-COD/mg-N		

4.3.2 Advanced MABR Model

Upgrades to the 2020-version of SUMO (Dynamita, France) simulation software included MABR unit processes allowing additional important design parameters, and includes the prerequisite diffusional mass transfer and reaction equations of a MABR biofilm. With SUMO20, we built upon the previous modeling results to assess the growth characteristics of key bacterial populations existing in our system under certain selective pressures. The model developed in

SUMO20 extends the previous work by incorporating MABR unit processes directly into a hybrid suspended growth design, and compares results to the modified Ludzak-Ettinger (MLE) suspended growth process—conventional configuration often used in practice for their simplicity in performing nitrogen removal (Grady Jr. et al., 2011; Water Environment Federation, 2020).

The first major design consideration for the proposed hybrid MABR treatment process was the process flow (shown in Figure 4-1); nitrification occurs in the MABR zone and is preceded by a large anoxic suspended growth (ANX) zone and a small aerated (AER) zone. The bioreactor may be viewed as a rectangular unit with MABR units located at the inlet end, followed by a zone with mechanical mixing for suspended solids suspension, and finally a moderate level of diffused aeration adjacent to the outlet. The suspended growth process SRT is controlled by adjusting the bioreactor effluent waste flowrate, with a secondary clarifier effluent total suspended solids (TSS) concentration set to zero mg/L to simplify use of the model. Sludge from the secondary clarifier was recycled back to the head of secondary treatment. Waste sludge from the primary clarifier (when included) and suspended growth process were combined, thickened such that no solids (100 percent solids removal) were returned to the primary effluent stream, and directed to a single-stage anaerobic digester. Capture of influent COD for productive purposes was assessed by the fraction of influent COD converted to biogas when primary sludge (when primary clarifiers were included) and waste activated sludge (WAS) is subjected to anaerobic digestion. Simulations incorporating primary treatment were conducted using a primary treatment TSS removal efficiency of 60 percent, while simulations with no primary treatment were conducted by lowering the removal efficiency to zero percent.

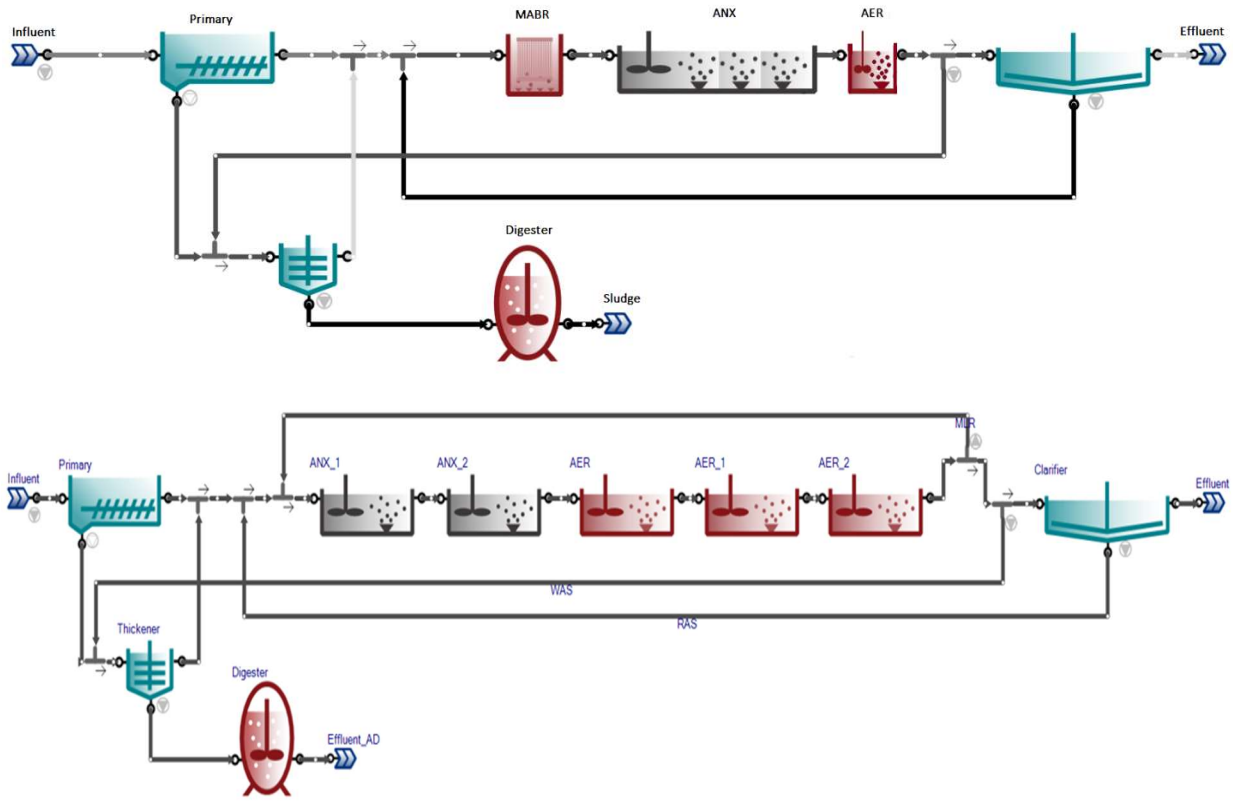

Figure 4-1 Schematic of SUMO20 process flow diagrams.
Top: Hybrid MABR/anoxic suspended growth system. Bottom: Conventional MLE Nitrogen removal process.

A suspended growth mixed liquor suspended solids (MLSS) concentration of 3,000 mg/L was maintained for both the hybrid MABR and conventional processes so that the same size secondary clarifier would be required, allowing the suspended growth SRT to fully characterize the difference in required bioreactor volume for all process options. This required varying the suspended growth bioreactor volume. Sufficient bioreactor volume was provided by the MABR volume for the lowest SRT investigated, but volume for the downstream anoxic and aerobic zone was required to maintain the target 3,000 mg/L MLSS concentration as the suspended growth SRT increased. Total system SRTs were varied between 0.50 to 5.0 days. When these zones were added, the relative volumes for the system were maintained at 90 percent anoxic and 10 percent aerobic. The terminal aerobic zone was found to be necessary to oxidize residual ammonia, and a dissolved oxygen (DO) concentration of 1.0 mg/L was maintained for all simulations where this zone was

included. Overall process performance was also found to be optimized if a minimal DO concentration of 0.10 mg/L was maintained in the anoxic zone. A small amount of residual oxygen decreased ammonia release downstream of the MABR from anoxic hydrolysis of organic nitrogen and decay products. The settleability of anoxic suspended growth was predicted likely to be poor, and rising sludge a pertinent issue to full-scale systems (Ekama et al., 1997). Thus, it seemed logical that a modest amount of aeration would be necessary in any bioreactor configuration in a full-scale facility.

Other design considerations were specific to the MABR biofilm, such as biofilm thickness, biofilm density, membrane packing density, and oxygen mass flow rate. For this work, we defined the system ammonia loading as the influent ammonia mass per day divided by the MABR surface area. An ammonia loading of 2.7 g-N/m^2-day based on the influent ammonia loading for the high COD/TN case was determined to provide good performance, and a packing density of 150 m^2/m^3 was used to size the MABR zone in the model. The ammonia loading to the MABR is within the range of nitrification rates currently used to design commercial hybrid systems (1.5-3.0 g-N/m^2-day) (Côté et al., 2015; T. Kunetz et al., 2016). The ammonia loading under the low COD/TN condition pushed just beyond this to 3.1 g-N/m^2-day. Oxygen input to the MABR units was adjusted to minimize effluent TN and the bleed through of oxygen out of the biofilm and into the suspended growth. It should be noted that MABR systems transfer oxygen through diffusion caused by a differential gradient; the pressurized air in the inner lumen diffuses into the biofilm based on nitrification kinetics (Downing & Nerenberg, 2008b; Gilmore et al., 2009). However, the model in SUMO requires a hard input mass flow rate. The biofilm thickness was set at 175 μm, with the biofilm specific mass of 10 g TSS/m^2. The biofilm was divided into 3 layers, and the mass transfer boundary layer thickness (40 μm) was maintained. Water displaced by membrane and

ratio of reactor volume filled by a membrane were 0.25 and 1.0, respectively. All simulations were conducted at a temperature of 20°C.

Several nitrogen removal scenarios were run in SUMO 2020 including: simultaneous nitrification and denitrification at high and low COD/TN ratios, and with or without primary treatment. An anaerobic digester with a standard hydraulic residence time (HRT) of 20 days was used to track the extent of carbon oxidation in the secondary treatment process, and any remaining particulate and colloidal material was simulated to convert into biogas. The same influent composition was used as described in the section above (see Table 4-1), although in this instance influent flows were not separated, as the MABR was performing the nitrification. Ultimately, we wanted to see the correlation between nitrification and denitrification capacity with a true MABR module in SUMO in more granular detail, and determine if the improvements over conventional systems predicted by previous simple model still hold. Default wastewater characteristic and biological process stoichiometry and kinetics were used for the hybrid MABR processes, except that the anoxic reduction factor (also known as an eta factor) for ordinary heterotrophic organisms (OHOs), glycogen-accumulating organisms (GAOs), and PAOs which were adjusted from 0.60, 0.66, and 0.33, respectively to 0.83. This was done because the fully anoxic suspended growth component in the operation of the hybrid process would select for a higher proportion of denitrifying organisms, instead of a mixed aerobic/anoxic population in which a portion will not adapt to the anoxic environment (Orhon et al., 1996). Thus, the default anoxic reduction factor (0.60) was maintained for the MLE configuration. All other parameters, including maximum specific growth rate and half-saturation coefficients were kept at the default values. It should be noted the hydrolysis rate for both the hybrid MABR and MLE process were kept at the default value of 2.0 day^{-1}. All simulations were run in steady state mode in SUMO20. In this mode, the

software solver looks for solutions that converge to a particular value and the system behavior does not change with run time (Dynamita Process Modeling, 2020).

4.3.3 Physical Model

The next step was to evaluate if the critical design criteria from the computer models hold up in a physical bench-scale treatment system using influent dynamic wastewater from AAWWTP. The proof-of-concept and advanced MABR model estimated how the anoxic system will perform at full-scale, but inherent generalizations were imbedded in the model that require more experimentation, specifically the characteristics of the suspended growth in the anoxic bulk liquid surrounding the nitrifying MABR biofilm. The model inputs governed the extent influent particulate and colloidal carbon was hydrolyzed to rbCOD and subsequently oxidized, which were rough estimates of a real system that needed to be validated. Although some examples of fully anoxic activated sludge systems exist, research on anoxic activated sludge is mainly confined to anoxic selectors (Gabb et al., 1991; Mangrum, 1998), and there exists a gap in side-by-side comparison of aerobic and anoxic suspended growth systems performing *in situ* treatment of raw sewage (i.e., non-synthetic and without supplied external carbon). Moreover, the implicit assumption of the model was that good settling will occur in the secondary clarifier, which research shows is not always the case for anoxic systems (Flores-Alsina et al., 2010; Ekama, 2011; Cardete et al., 2017). These parameters were tested in the physical system—a series of parallel batch suspended growth reactors treating domestic wastewater—operated over the long term for nitrogen removal capacity, settleability, and the extent of carbon metabolism of an anoxic suspended growth mixed liquor compared to a typical aerobic activated sludge process.

Bench-scale units were constructed at AAWWTP (Michigan, USA), consisting of four parallel sequencing batch reactors (SBRs) that were fed with primary effluent from the plant's

western primary clarifiers. The first pair of reactors performed carbon oxidation/denitrification while the other pair of reactors performed Bio-P removal (discussed in later sections). The table below shows the reactor identification numbers. Each reactor volume was 6.4 L, with 4.2 L of influent volume per cycle, and roughly 2.2 L of settled mixed liquor return. Operation occurred on 90 min cycles: 5 min feed, 45 min reaction, 5 min waste, 20 min settling, 5 min decant, and 30 sec idle time to reset the control system. The two reaction cycles in this study were designed to be either aerobic (Reactor 1) or anoxic (Reactor 3), however it was determined that a 10 min aerated sparge was necessary for the anoxic reactor, so this time was added to both. Aeration occurred via an attached air compressor assembly controlled by a ball valve and fine-bubble aquarium stone. Anoxic conditions were created in Reactor 3 using an external supply of sodium nitrate fed with a peristaltic pump (45 mL, concentration 15-20 g-N/L depending on influent COD). Both reactors were well-mixed with an aluminum propellor attached to a stepper motor. All unit processes (motors, ball valves, influent and decant pumps) were controlled with a cycle schedule set into a programmable logic controller with prototyping platform and base operating language Arduino (Somerville, MA, USA).

Table 4-2 Sequencing Batch Reactor Identification Numbers and Processes

Reactor ID	Process	Metabolism Description
Reactor 1 (R1)	Aerobic	• Oxidation of influent carbon ($COD + O_2 \rightarrow CO_2$) • Nitrification ($NH_4^+ + O_2 \rightarrow NO_2/NO_3$)
Reactor 2 (R2)	Anaerobic/Aerobic	• Biological phosphorus removal (bio-P)
Reactor 3 (R3)	Anoxic[1]	• Denitrification (for oxidation of carbon) ($COD + NO_3 \rightarrow CO_2 + N_2$)
Reactor 4 (R4)	Anaerobic/Anoxic[2]	• Denitrifying bio-P

[1]*Supplied with external sodium nitrate solution (10-20 g/L), bulk liquid concentration (11-22 mg-N/L)*
[2]*Supplied with external sodium nitrate solution (7.0-25 g/L), bulk liquid concentration (8.2-29 mg-N/L)*

4.3.4 Wet Chemistry Methods

Table 4-3 below shows a summary of the individual measurements and sample points taken from all reactors at AAWWTP. Samples were taken at various stages along the sequencing cycle, chiefly the reactor influent (i.e., primary effluent from AAWWTP), reactor mixed liquor, and reactor effluent. A portion of the raw samples from each point were preserved for total COD, TN, and TP by titration to pH 3 with 5.0 N sulfuric acid. Influent carbon was fractionated into total, filtered, and "floc & filtered" constituents to estimate particulate, colloidal, soluble, and readily biodegradable organic matter, respectively. Total suspended solids (TSS), volatile suspended solids (VSS), and mixed liquor suspended solids (MLSS) were simultaneously measured to calculate system SRT. The raw sample was vacuum filtered over 1.5 μm glass-fiber filter (Whatman, USA). 10 mL of filtrate was stored for COD analysis, and 40 mL was passed over a 0.45 μm mixed cellulose ester filter (HAWP, MilliporeSigma, Burlington, MA) for analysis of dissolved constituents, such as ammonia, nitrate, and nitrite. The remaining portion (roughly 100 mL) of secondary filtrate was used for flocculated & filtered (floc & filtered) COD—1 mL aluminum sulfate was added to 100 mL secondary filtrate and rapidly mixed for 2 min. After 30 min of settling, 10 mL were preserved for COD analysis (Wentzel et al., 2000). All measurements were conducted in accordance with *Standard Methods for the Examination of Water and Wastewater* (2017) and the United States Environemental Protection Agency (2010). An average of the data points taken at reactor steady state, after approximately one to two SRTs of operation, were used to calculate system mass balances on all relevant nutrients to verify the hypotheses above.

Table 4-3 List of all relevant wet chemical analyses and sampling locations

Test	Sample Description[a]	Sample Points[b]		
		Influent	Mixed Liquor	Reactor Effluent
COD				
Total	*Method 5220 D* Raw sample fixed in sulfuric acid	X	X	X
Filtered	*Method 5220 D* Filtered raw sample (1.5 um glass fiber filter)	X		X
Floc&Filtered	*Method 5220 D* Filtrate of above step, flocculated with aluminum sulfate (Wentzel et al., 2000), filtered through 0.45 um filter	X		X
Solids				
TSS	*Method 2540 D* Filtered raw sample (1.5 um glass fiber filter), dried at 105°C	X	X	X
VSS	*Method 2540 E* Above ignited at 550°C	X	X	X
SVI	*Method 2710 D*		X	
Nitrogen				
Total Nitrogen	*Method 4500-N C* Raw sample, digested with persulfate *Method 4500-NO_3^- C* Second Derivative Ultraviolet Spectrophotometric Method	X		X
Total Dissolved Nitrogen	*Method 4500-N C* Filtered raw sample (0.45 um filter), digested with persulfate *Method 4500-NO_3^- C*	X		X
Nitrate	*Method 4500-NO_3^- C* Filtered raw sample (0.45 um filter), undigested	X	X	X
Nitrite	*Method 4500-NO_2^- B* Filtered raw sample (0.45 um filter), reaction with sulfanilamide	X		X
Ammonia	*Method 4500-NH_3 F* Filtered raw sample (0.45 um filter), reaction with phenate	X		X
Phosphorus				
Total	*Method 4500-N C* Raw sample, digested with persulfate *Method 4500-P E*	X	X	X

	Ascorbic acid colorimetric method			
Ortho	*Method 4500-P E* Filtered with 0.45 um filter, undigested, ascorbic acid colorimetric method	X	X	X

4.3.5 Analysis of System Mass Balances

Nitrogen Species: Some nitrogen species are an important measurement of nitrifier and denitrifier activity, and were necessary to system analysis and nitrogen removal performance; constituents like ammonia and nitrate, total nitrogen (TN), or total inorganic nitrogen (TIN) which was used in the modeling efforts. Nitrite was of secondary concern because of the small amount of anticipated partial nitrification and denitrification in the system, but nonetheless useful in validating the accuracy of the combined nitrogen data points. Nitrogenous species can be fractionated into organic and inorganic constituents, as well as dissolved and particulate/colloidal—in a similar manner as COD. Total nitrogen was a measure of all nitrogenous constituents, whereas total dissolved nitrogen measures dissolved organic nitrogen (DON), ammonia, nitrate, and nitrite. This leaves two independent paths to measuring TN—the first through direct experimental measurement of a raw sample, and the other with estimation of inorganic parameters and estimation of organic nitrogen through volatile suspended solids (see equations below). Calculation of percent error can then give a sense of the accuracy of the sample.

(1) $TN = Org - N + TDN, or\ TN = TKN + NO_x$

(2) $TDN = DON + NH_3 + NO_3 + NO_2$

(3) $Org - N = VSS * \frac{14}{113}$

where 14 denotes the molecular weight of nitrogen (g/mol), and 113 the average molecular weight of cellular biomass (Grady Jr. et al., 2011).

Fixed Solids: This is a simple mass balance around the reactor. Fixed suspended solids are inert or inorganic constituents that do not volatilize at high temperatures (550°C). Practically, these solids in the influent should be conserved in the effluent and mixed liquor. A fixed solids mass balance was conducted as a point of validation of solids measurements in the system.

(4) $FSS = TSS - VSS$

(5) $FSS_{in} = FSS_{out} - FSS_{effluent} + FSS_{mixed\ liquor}$

SRT: The SRT was calculated based on the ratio of biomass inventory to the amount of wastage from the system through the waste activated sludge (WAS) and the secondary effluent. Because these are SBRs, the WAS suspended solids is equal to the MLSS.

(6) $SRT = (MLSS * V_{total})/(MLSS * V_{WAS} + TSS_{effluent} * V_{effluent})$

Nitrate: A mass balance was conducted on nitrate for both the aerobic and anoxic reactors. For the former, nitrate is an estimation of the small amount of nitrifier activity; this will be used as a point of comparison between future MABR systems. More importantly, nitrate is the main electron acceptor in the anoxic system, and will be reduced to nitrogen gas (N_2). The difference between the known addition in the feed and the waste and effluent streams should also equal the amount of COD destroyed in the system (also calculated, see below). The calculation is a simple mass balance.

(7) $NO_3 - N\ Reacted = NO_3 - N_{influent} + NO_3 - N_{feed} - NO_3 - N * (V_{WAS} + V_{effluent})$

where NO_3-N_{feed} represents the external sodium nitrate feed.

(8) $Balance\ NO_3 = NO_3 - N\ Reacted * 2.86\ \left(\frac{mg\ COD}{mg\ NO_3 - N}\right) * N_C$

The balance NO_3 is measured in mg-COD/day, and 2.86 is a standard conversion value (Grady Jr. et al., 2011). N_C denotes the total number of reactor cycles per day.

Oxidized COD: Per our hypothesis, the aerobic and anoxic metabolisms will exhibit different patterns of carbon oxidation as the system SRT increases. The amount of carbon destroyed in the system will depend on a variety of factors, including the hydrolysis of colloidal and particulate organic matter. Plotting these directly is an important step in comparison, as well as verifying carbon capture in the previous modelling steps. Furthermore, performing this analysis for denitrification will provide confirmation of the above nitrate balance COD equivalence, i.e., the nitrate balance should equal the amount of COD destruction.

(9) $Oxidized\ COD\ (mg\ COD) = COD_{influent} - COD_{effluent} - COD_{WAS}$

The final percentage of the influent COD that is oxidized (% of Total Oxidized) is calculated by dividing Oxidized COD by the measured Influent COD.

Soluble COD (sCOD): Both reactors should quickly consume rbCOD, a portion of the overall soluble COD in the system, which does not include non-biodegradable (inert) COD, or slowly biodegradable COD that remain unreacted. However, unlike the other measurements, the amount of sCOD oxidized was calculated factoring in bioenergetics of cell maintenance, synthesis, and death. Common values for observed growth yield ($Y_{g,h}$), cell death rate (b_h), and decay ratio (f_d) were assumed to calculate net yield (Grady Jr. et al., 2011). The total fraction minus the net yield is the amount oxidized to CO_2 (1-Y_n, or f_e = 1- f_s); this remaining fraction multiplied by the amount of soluble carbon removed is equal to the amount of COD destruction attributable to soluble oxidized substrate. The difference in the total amount of COD oxidized from the soluble matter oxidized is then the hydrolyzed material.

(10) $Destroyed\ sCOD = sCOD_{influent} - sCOD_{effluent}$

(11) $Y_n = (1 - f_d * b_h * SRT) * Y_{g,h}/(1 + b_h * SRT)$

where $Y_{g,h}$ = 0.67 mg $COD_{biomass}$/mg COD, f_d = 0.2 mg debris/mg $COD_{biomass}$, b_h = 0.23 day^{-1} are all standard values for cellular yield, death, and decay. (Grady Jr. et al., 2011).

(12) $sCOD\ oxidized = (1 - Y_n) * sCOD\ Destroyed$

(13) $COD\ hydrolyzed = tCOD\ oxidized - sCOD\ oxidized$

Other relevant COD calculations: Organic matter in the various streams can be fractionated using the measurements described earlier. Besides sCOD, there contains colloidal COD (cCOD) and particulate COD (pCOD) that all sum to the total COD (tCOD) in the sample. pCOD can be calculated by subtracting filtered COD from total COD, and cCOD by subtracting floc & filtered COD from filtered COD (Rahman et al., 2016). Floc & filtered is a true measure of sCOD in the system because particulate matter was removed via filtration, and flocculant was added to remove colloidal organic matter from the system.

4.4 Results and Conclusions

4.4.1 Computer Model Results

Proof-of-concept modeling results were encouraging, and met the criteria above with achieved reductions to system SRT (<3.0 days), effluent TIN, and oxidized particulate and colloidal organic matter during denitrification (Daigger et al., 2019). Indeed, the investigation with the surrogate MABR indicated three general trends in nitrogen removal, biogas production, and operational capacity with and without primary treatment. The effluent TN (effluent TSS = zero mg/L) for the surrogate MABR suspended growth processes decreased sharply as the suspended growth bioreactor SRT increased from the lowest value simulated of 0.50 days and reached a minimum of around 2.0 mg-N/L at an SRT of about 1.5 days. This was accompanied by a rapid decrease in the proportion of influent COD directed to biogas production from 55% to 40%, as

rbCOD was fully oxidized and hydrolysis of colloidal matter started to have an effect at slightly longer SRTs. Comparison of options with and without primary treatment indicated that the principal advantage of primary treatment is the potential for increased biogas production when suspended growth SRTs were greater than about 1.0 to 1.5 days. The impact on effluent TN of the presence or absence of primary treatment is negligible, and for these simulations reached values of approximately 2.0 mg-N/L. Differences in the proportion of influent COD diverted to biogas were modest for suspended growth SRT's less than about 1 to 1.5 days, but become significant as the suspended growth SRT increases beyond this range. These results suggest that quite low effluent TN concentrations and significant diversion of influent COD to biogas production (or other productive uses) can be achieved through processes that decouple aerobic and anoxic suspended growth process without upstream primary treatment.

The advanced model followed similar trends as the simple model simulations, but included more relevant data how a hybrid MABR system might perform in a real scenario compared to a conventional MLE treatment scheme. It should be noted that we now measured effluent total inorganic nitrogen (TIN) because it eliminated minor discrepancies with particulate organic nitrogen while still including relevant nitrogen species, such as ammonia and nitrate. The effluent TIN for the hybrid MABR process decreases sharply (Figure 4-2) as the suspended growth bioreactor SRT increases from the lowest value simulated of 0.50 days and approaches minimal values of diminishing return at SRT values in the 2.5 to 3.0-day range, rather than the 1.5-day SRT predicted in the simple model. In contrast, a much longer suspended growth SRT is required for the conventional MLE process because a sufficient aerobic suspended growth zone must be maintained to allow nitrifiers to grow, in addition to the anoxic zone needed for denitrification. An effluent TIN for the MLE process of approximately 6.0 mg-N/L is indicated, which would be

acceptable according to most current standards (Hertzler et al., 2009). However, compared to an effluent TIN concentration of 1.0 mg-N/L or less for the hybrid MABR process, these simulation results illustrate the opportunity to greatly improve upon the existing system. Likewise, effluent TIN directly comparable to that achieved with the MLE process (i.e., 6.0 mg-N/L) can be achieved with the hybrid MABR process at a suspended growth SRT of around 1 day. Figures 4-2 and 4-3 show simulation results for both a high COD/TN case (11 mg-COD/mg-N) typical of U.S.-based domestic wastewater, and a low COD/TN case (6.7 mg-COD/mg-N) typical of Chinese-based wastewater, respectively. The effect of suspended growth SRT on effluent TIN for the hybrid MABR and MLE biological nitrogen removal processes is presented in Figure 4-2 for the influent wastewater 11 mg-COD/mg-N case.

The rapid decrease in effluent TIN estimated in the hybrid MABR process (with or without primary clarification) occurs because of a predicted increase hydrolysis and metabolism of particulate and colloidal organic matter as the suspended growth SRT increased from the lowest value of 0.50 days to around 2.0 days. Evidence for this can be seen in the decreased amount of biogas production discussed below, but this prediction will be addressed in detail in the next section with the SBRs at AAWWTP. Low suspended growth SRTs can be maintained while achieving such high levels of nitrogen removal because nitrification is accomplished largely in the MABR biofilm. Furthermore, influent bioavailable carbon enters the treatment process at the most effective point, the anoxic zone undergoing denitrification supplemented with nitrate diffusing from the biofilm, driving denitrification and therefore effluent TIN to asymptotically reach concentrations lower than 1.0 mg-N/L. Effluent TIN concentrations for the MLE process simulated with and without primary treatment (>6.0 mg-N/L) imply that denitrification in the anoxic zone is limited principally by nitrate recirculation from the downstream aerobic zone by the MLR.

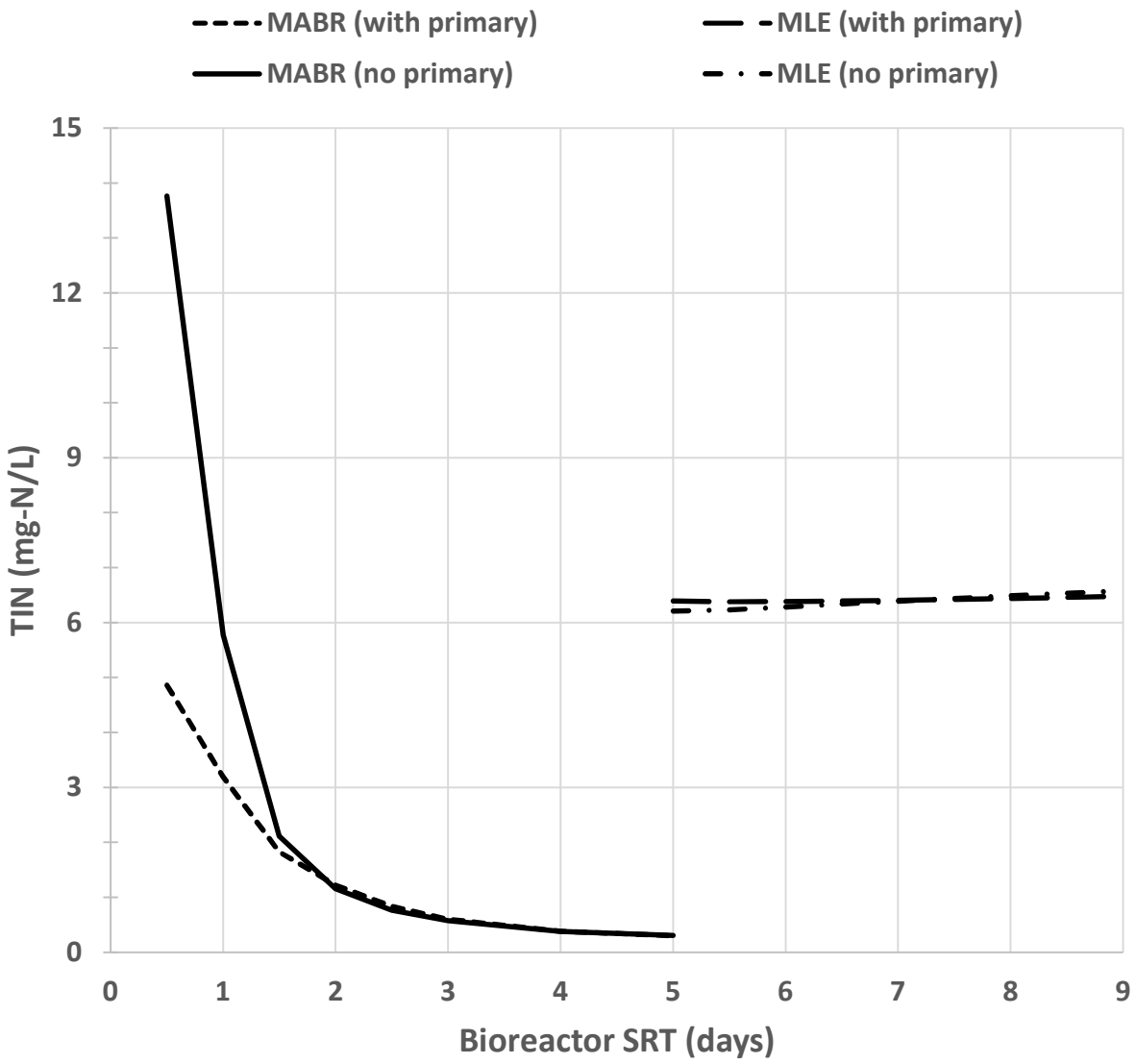

Figure 4-2 Effect of Suspended Growth Bioreactor SRT on Effluent Total Inorganic Nitrogen for Influent Wastewater COD/TN of 11.3 mg-COD/mg-N.

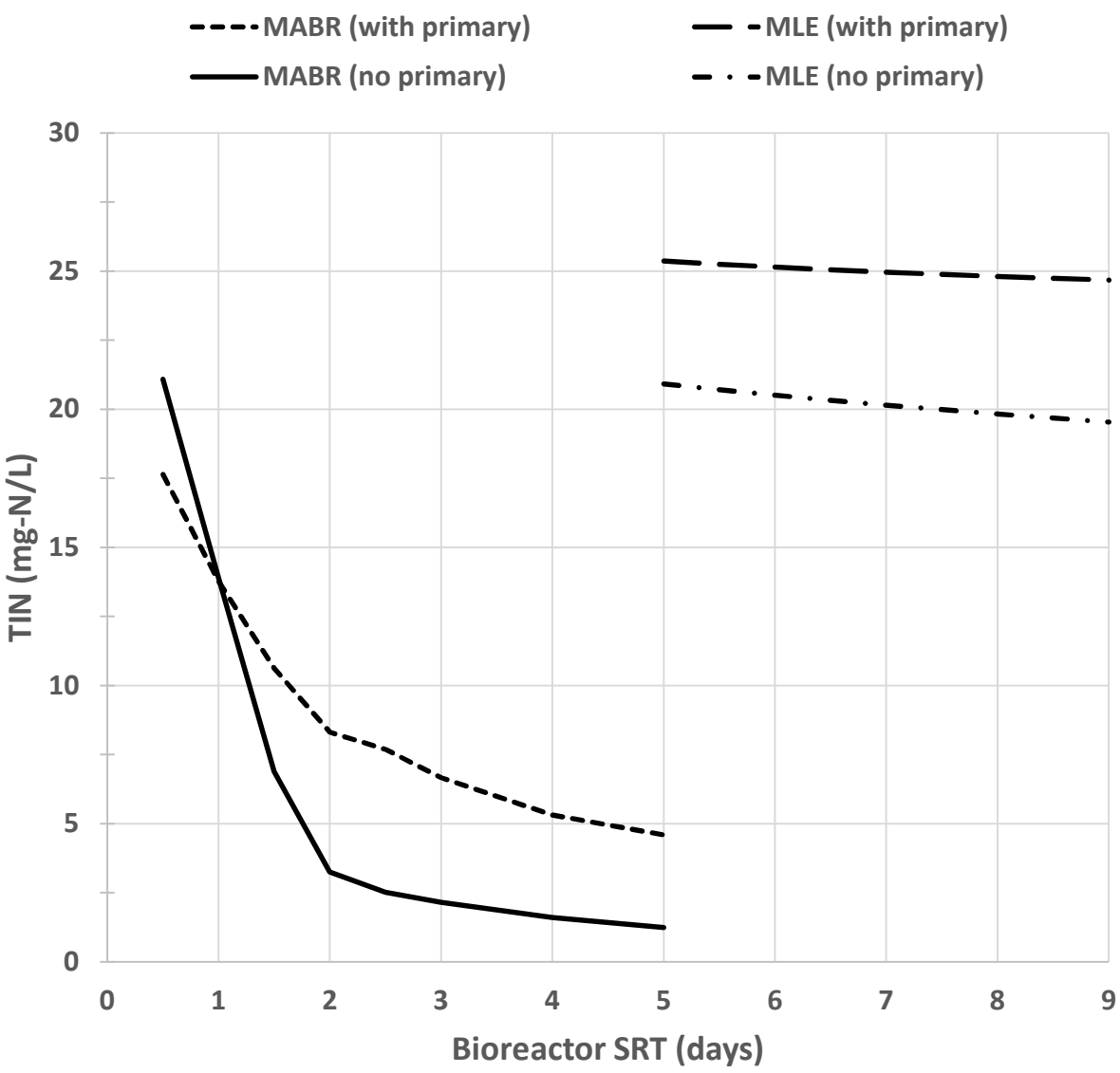

Figure 4-3 Effect of Suspended Growth Bioreactor SRT on Effluent Total Inorganic Nitrogen for Influent Wastewater COD/N of 6.7 mg-COD/mg-N.

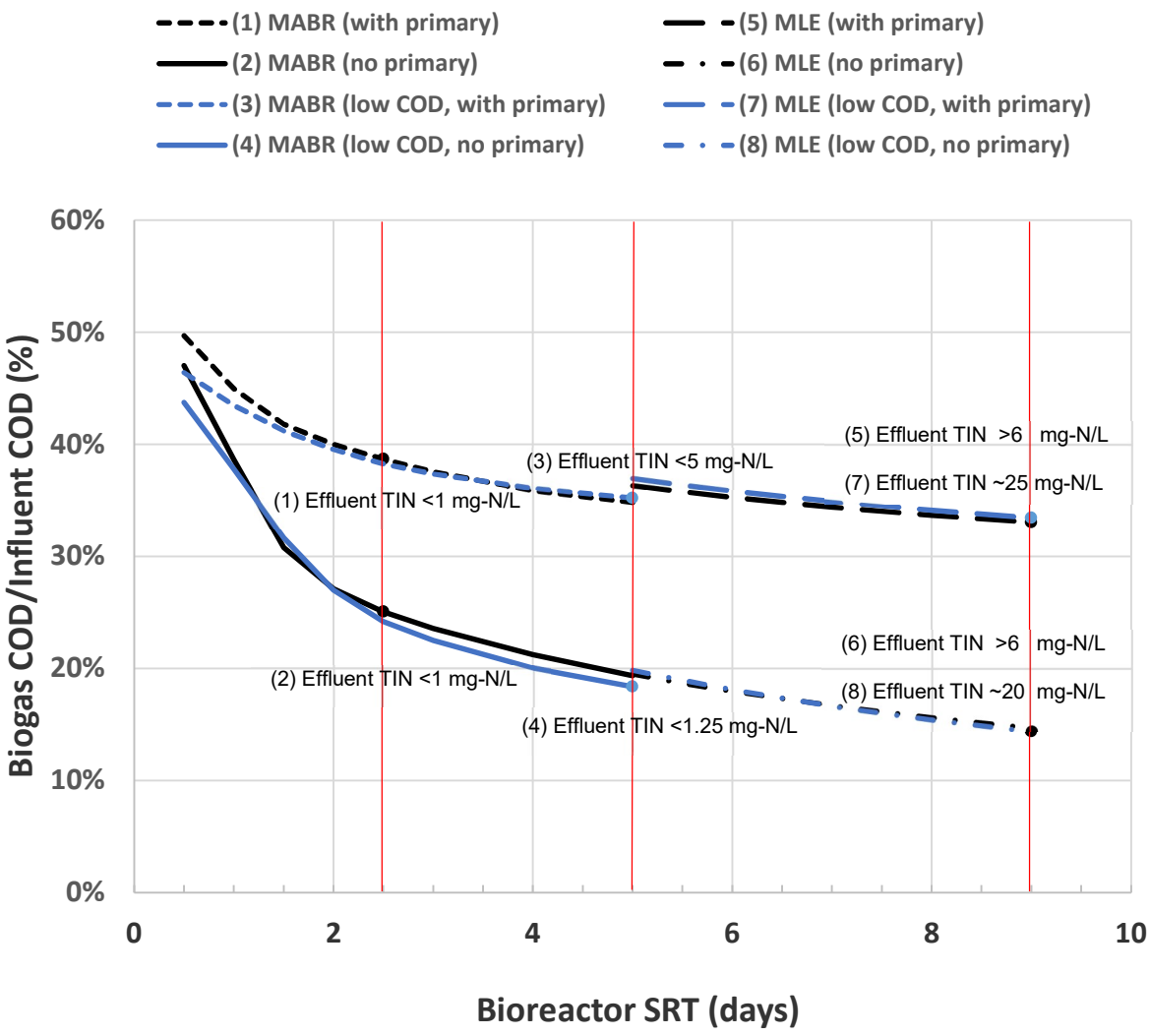

Figure 4-4 Effect of Suspended Growth Bioreactor SRT on Biogas Production as a Percent of Influent COD.

The results of simulations conducted to investigate the impacts of reduced influent wastewater COD/TN (6.3 versus 11 mg-COD/mg-N) on process performance are presented in Figure 4-3. Notice the change in the vertical scale from Figure 4-2. Effluent quality for the conventional MLE process is adversely impacted by the reduction in influent wastewater COD/TN, and effluent TIN is higher with primary treatment than without (approximately 25 mg-N/L and 20 mg-N/L, respectively) at SRT of 5.0 days. This suggests that denitrification is now carbon-limited in the anoxic zone. Effluent TIN concentrations are also elevated for the hybrid

MABR process, again regardless of primary treatment, but are much lower than for the conventional MLE process (<5.0 mg-N/L). However, higher effluent TIN can be mitigated at unfavorable influent conditions, and similar concentrations can achieved as at the higher influent wastewater COD/TN ratio discussed previously, by removing primary treatment from the hybrid MABR process and increasing the suspended growth SRT to around 5.0 days (solid line, Figure 4-3). Regardless, the hybrid MABR process can achieve better effluent TIN concentrations than the MLE process starting at a suspended growth SRT of around 1.0 day. The results presented in Figures 4-2 and 4-3 indicate that the hybrid MABR process provides increased flexibility using influent carbon for denitrification, regardless of influent carbon composition.

The results presented in Figure 4-4 provide further insight into the metabolism of carbon in the biological nitrogen removal process options. The effect of bioreactor suspended growth SRT on the fraction of plant influent COD that is converted into biogas (expressed as a percentage) in an anaerobic digester operating at a 20-day SRT in this figure is indirectly related to the process operating conditions previously depicted in Figures 4-2 and 4-3. This parameter provides one metric of the capture of useful carbon for the treatment process over the range of influent wastewater options evaluated. The flow of carbon directed to the digester includes primary sludge, during simulations where primary clarifiers were provided, and pumped WAS from secondary treatment. Increased suspended growth SRT results in less biodegradable organic matter available to direct to the anaerobic digester (i.e., a lower fraction of plant influent COD converted to biogas), suggesting that more plant influent biodegradable organic matter is oxidized in the hybrid MABR or MLE processes. The benefit of primary treatment, along with the negative impact of increased suspended growth SRT, on the capture of usable carbon are clearly illustrated in Figure 4-4 when the slopes diverge around the 1-day SRT mark. Remember, the benefits provided by the hybrid

MABR process were a lower suspended growth SRT requirement to produce a high-quality effluent with low effluent TIN, which now also translates into enhanced carbon redirection to biogas. Interestingly, the fraction of influent COD captured as biogas is essentially the same irrespective of the COD/TN ratio of the influent wastewater. However, the reason for this becomes clear when viewing the results with Figures 4-2 and 4-3: denitrification is hindered with lower influent COD/TN and low suspended growth SRTs leading to a higher effluent TIN concentration, and therefore, a higher suspended growth SRT is required to achieve similar effluent quality, which results in less influent COD captured as biogas, as indicated in Figure 4-4. In short, a higher fraction of the influent biodegradable organic matter must be used for denitrification to achieve the same effluent TIN with the hybrid MABR process when the COD/TN of the influent wastewater is lower and less favorable.

Comparison of Figures 4-2, 4-3, and 4-4 highlights the trade-offs that exist between effluent TIN and carbon capture for the hybrid MABR process. Reduced suspended growth SRT can result in increased hybrid MABR effluent TIN, but concentrations are generally less than what can be achieved by the MLE process under equivalent conditions (Figures 4-2 and 4-3), and increased carbon capture as quantified by the fraction of influent COD as biogas (Figure 4-4). Biogas conversion potential is one metric of the capture of useful carbon over the range of influent wastewater options evaluated. As seen in the figures, increased suspended growth SRT results in less biodegradable organic matter available to direct to the anaerobic digester (i.e., a lower fraction of plant influent COD converted to biogas), suggesting that more plant influent biodegradable organic matter is hydrolyzed in both the MLE and hybrid MABR processes. Hybrid MABR operation at an SRT of 2.5 days with higher strength influent wastewater (11 mg-COD/mg-N) allows effluent TIN reductions to less than 1.0 mg-N/L; however, carbon capture is higher with

the addition of primary treatment (roughly 40% versus 25% without primary treatment, Figure 4-4 points 1 and 2). When influent carbon is diminished, i.e., COD/TN is decreased to 6.7 mg-COD/mg-N, a higher hybrid MABR effluent quality (1.3 mg-N/L) but less effective carbon capture (18%) is the result of the system at a 5-day SRT without primary treatment (point 4). Therefore, in this scenario, a higher suspended growth SRT is required to achieve similar effluent quality as compared to the more favorable influent condition, resulting in less influent COD captured as biogas. Conversely, a slightly higher effluent TIN (5.0 mg-N/L) but more carbon capture is achieved at the same operation while including primary treatment (point 3). In general, when influent COD/TN is lower and less favorable, a higher fraction of the influent biodegradable organic matter must be used for denitrification to achieve the same effluent TIN with the hybrid MABR process. Figure 4-4 shows this as a decision point—forego primary treatment and reduce effluent TIN, but sacrifice available carbon for biogas conversion. Carbon capture for the conventional MLE process can be improved by including primary treatment at both high and low COD/TN ratios (points 5-8, Figure 4-4), but effluent TIN concentrations suffer in the low COD/TN scenario as a result.

The above results further indicate significant performance and economic advantages for hybrid MABR process options relative to conventional biological nitrogen removal process such as MLE. Table 4-3 summarizes a series of comparisons intended to illustrate these differences. The SRT selected for the hybrid MABR process for influent wastewater with a COD/TN ratio of 11 mg-COD/mg-N is the minimum value which achieves an effluent TIN less than 1 mg-N/L, rounded the nearest 0.5-day SRT, while the SRT selected for the hybrid MABR process for influent wastewater with a COD/TN ratio of 6.7 mg-COD/mg-N is the highest value considered. The suspended growth SRT required for the hybrid MABR process treating the influent wastewater

with a COD/TN of 11 mg-COD/mg-N is half that for the conventional MLE process while achieving a much lower effluent TIN concentration. This results in a much smaller suspended growth bioreactor for the hybrid MABR process, a reduction of roughly 40% the MLE volume. The same suspended growth SRT values are used for all options for the influent wastewater with a COD/TN of 6.7 mg-COD/mg-N, which translates to similar bioreactor sizes but a dramatically lower effluent TIN concentration (approximately 20 mg-N/L less) for the hybrid MABR process compared to the MLE design. In all case, there is a clearly illustrated benefit of reduced bioreactor volume when primary treatment is provided; however, the relationship to effluent TIN is also dependent on influent COD/TN conditions.

Examination of Table 4-3 for system process energy inputs and outputs, the hybrid MABR process displays significantly reduced energy requirement versus the MLE system. Ancillary reductions are found in the form of the required mass of oxygen, as a substantial proportion is transferred by the much more energy efficient MABR units. Estimates of OTE for hybrid MABRs in the field range from 25 to 75 percent, depending on the application, compared to 15 percent or less in conventional systems (Tchobanoglous et al., 2003; He et al., 2021) . Direct reductions, such as elimination of mixed liquor recirculation that is not needed for the hybrid MABR process, cuts energy inputs even further. Energy for necessary items such as zone mixing were not considered in this assessment, but research has shown any potential increases to energy demand for MABR system mixing over AS mixing requirements are modest, and are estimated at roughly 15 kW/m^3 (Aybar et al., 2012). Evaluation of the results with unfavorable low COD/TN influent conditions provides opportunities to save some energy without sacrificing effluent quality; for instance, the mass of oxygen required per unit of influent COD is higher in all cases for the lower influent COD/TN wastewater, but influent COD can be captured as biogas to a greater extent when primary

treatment is provided. Carbon capture is also higher for the hybrid MABR than the MLE process without primary treatment. The fraction of influent COD captured as biogas is similarly independent of the influent wastewater COD/TN ratio, thus enabling decision-making as to the extent of desired carbon capture to revolve around treatment goals and available infrastructure. Overall, a reduced suspended growth SRT can be selected for the hybrid MABR process, leading to increased effluent TIN but increased carbon capture, lower energy requirements, and reduced bioreactor volume. Note that these simulations were conducted at a wastewater temperature of 20°C. Advantages for the hybrid MABR process would increase at lower temperatures because of the greater impact of temperature on nitrifier than heterotroph growth kinetics in AS systems (Grady Jr. et al., 2011). The main observation we made during the modeling phase was the need to develop more sophisticated control strategies to maximize nitrifier growth in the biofilm and minimize heterotroph infiltration in the deep layers. This is improved with a rapidly growing, highly selected anoxic suspended growth that removes sCOD from the mixed liquor in an upfront zone. The next phase investigates the feasibility of this type of anoxic suspended growth biomass in a physical treatment systems with complex wastewater substrates.

Table 4-4 Performance Comparison for Nitrogen Removal Process Options

Item	Hybrid MABR		Conventional MLE	
	With Primary	**Without Primary**	**With Primary**	**Without Primary**
COD/TN = 11.3 mg-COD/mg-N				
Suspended Growth SRT (Days)	2.5	2.5	5.0	5.0
Effluent TIN (mg-N/L)	0.8	0.8	6.4	6.2
MLR (%)	N/A[1]	N/A	400	400
AOR/COD (mg O_2/mg Influent COD)				
MABR	0.18	0.19	N/A	N/A
Conventional	0.10	0.21	0.42	0.57
Total	0.28	0.40	0.42	0.57
Mixed Liquor Recirculation (%)	N/A	N/A	400	400
Bioreactor Volume (m^3)[2]	4,520	7,620	7,150	12,700
Biogas % (mg Biogas COD/mg Influent COD)	38.7	25.1	36.3	19.4
COD/TN = 6.7 mg-COD/mg-N				
Suspended Growth SRT (Days)	5	5	5	5
Effluent TIN (mg-N/L)	1.2	5.3	25.4	20.9
MLR (%)	N/A	N/A	400	400
AOR/COD (mg O_2/mg Influent COD)				
MABR	0.30	0.33	N/A	N/A
Conventional	0.09	0.21	0.67	0.80
Total	0.39	0.54	0.67	0.80
Bioreactor Volume (m^3)[2]	4,600	8,000	4,340	7,540
Biogas (mg Biogas COD/mg Influent COD, %)	38.3	24.2	37.0	19.8

[1] Not Applicable
[2] 3,000 mg/L MLSS

4.4.2 Anoxic Suspended Growth Physical Results

Operational and experimental results show nitrifier and heterotrophic growth in both the aerated and nitrate-fed reactors operating at SRTs less than three days, and indicate that their nitrogen removal performance aligns with theory. The AAWWTP wastewater across this time

period had an average tCOD of 210 mg-COD/L and average TN of 31 mg-N/L (COD/TN ratio of 6.8, similar to the low COD/TN model scenario), with 19 mg-N/L as ammonia-nitrogen (see Appendix Table C-1 for complete influent data set). As the control, nitrification was expected to occur in Reactor 1 as SRT increased across the discrete sampling periods from 0.75 to 3.0 days. The system influent (AAWWTP plant primary effluent) and reactor effluent had roughly the same ammonia concentration at the lowest SRTs in the study, approximately 0.5 to 1.0 days, and modest nitrate concentrations were seen in Reactor 1 effluent, implying minimal nitrification due to nitrifier washout. Variable amounts of nitrification with concurrent rise in Reactor 1 effluent nitrate can be seen between the 1.3 and 1.6-day SRT, and extensively at the 2.2-day and 3.0-day SRT (Table 4-5), which conforms to the SRT limitations dictated by traditional nitrification patterns at temperature 16-18°C (Grady Jr. et al., 2011). Thus, the control reactor was completing nitrification as expected. Reactor 3 on the other hand, had a modest baseline percentage of ammonia removal at the 1.3-day SRT mark onward possibly because, although the process was designed for denitrification, there was a small amount of aeration added at the end of the cycle. More importantly, Reactor 3 showed considerable reduction of the externally supplied nitrate concentration, as calculated by the mass differential of dissolved inorganic nitrogen (ΔNO_x) between the inputs and outputs to the system. At 3-days SRT, this delta in Reactor 3 was stable at 140 mg-N, and was variable at lower SRTs around 50-70 mg-N (Figure 4-5). These values do not factor in influent concentrations of sCOD and cCOD, which were dynamic during the entire study, but give us a good indication of the level of denitrification stability in the anoxic reactor. When the mass balance of nitrate on the system was converted to a COD-basis, it was in near total agreement with the mass balance of total COD oxidation in the system (error less than ±10%)

across the entire study period (see reduced nitrate column in Table 4-7 below, and mass balance examples in Section C-3 of the appendix).

Table 4-5 Nitrogen removal conditions for Reactors 1 and 3

PE			R1				R3				Ammonia Removal %	
Avg TN (mg-N/L)	Avg NH_3 (mg-N/L)	Avg NO_3 (mg-N/L)	SRT (days)	Avg TN (mg-N/L)	Avg NH_3 (mg-N/L)	Avg NO_3 (mg-N/L)	SRT (days)	Avg TN (mg-N/L)	Avg NH_3 (mg-N/L)	Avg NO_3 (mg-N/L)	AER R1	ANX R3
-*	30.3	0.89	0.47	-	30.0	0.89	0.66	ND	30.6	9.0	1.0	-2.3
27	18	0.88	0.75	30	18	0.54	0.45	46	17	20	0.2	2.1
-	25.3	1.07	0.96	-	24.2	0.67	0.97	ND	25.0	5.0	4.3	1.2
36	17	0.82	1.0	29	18	0.50	1.0	40	16	13	-3.4	4.8
44	24	3.9	1.3	37	23	2.6	1.3	53	20	20	4.0	15
34	25	0.92	1.6	33	22	0.90	1.5	49	22	16	12	12
21	15	0.91	2.2	16	8.2	4.2	1.8	29	15	11	46	3.6
38	20	0.99	3.0	40	14	7.1	3.0	36	17	0.61	31	14

*No data available for this measurement

Table 4-6 Carbon removal conditions for Reactors 1 and 3

PE				R1				R3			cCOD Removal %		sCOD Removal %	
Avg tCOD (mg/L)	Avg cCOD (mg/L)	Avg sCOD (mg/L)	SRT (days)	Avg tCOD (mg/L)	Avg cCOD (mg/L)	Avg sCOD (mg/L)	SRT (days)	Avg tCOD (mg/L)	Avg cCOD (mg/L)	Avg sCOD (mg/L)	AER R1	ANX R3	AER R1	ANX R3
150*	51*	53*	0.50**	71	15	46	0.50**	81	23	33	71	55	13	38
220	21	90	0.75	74	8.0	41	0.66	90	23	53	63	-9.1	54	41
190*	42*	85*	1.0**	68	23	42	1.0**	84	29	40	45	31	51	53
180	39	51	1.0	77	18	18	1.0	94	43	16	53	-9.2	64	68
190	54	68	1.3	61	20	31	1.3	98	41	27	62	24	54	60
210	48	76	1.6	83	38	16	1.5	101	40	24	20	16	78	69
150	27	61	2.2	42	9.1	17	1.8	62	15	21	66	44	72	66
270	55	58	3.0	110	38	22	3.0	79	33	20	31	40	62	66

*Samples taken in August 2022 after a change was required in the operation location. The primary effluent was from AAWWTP East train instead of West train, previously.

** Duplicate samples for total oxidation calculations taken after discovery there were wasting problems with WAS effecting the overall carbon balance

Note: each row indicates the average value for individual measurements over a select period of operation at a given reactor SRT. See Appendix Tables C-1, C-2, and C-3 for complete raw data tables with dates and steady state values.

Figure 4-5 Combined Nitrogen and Carbon Removal for Reactors 1 and 3

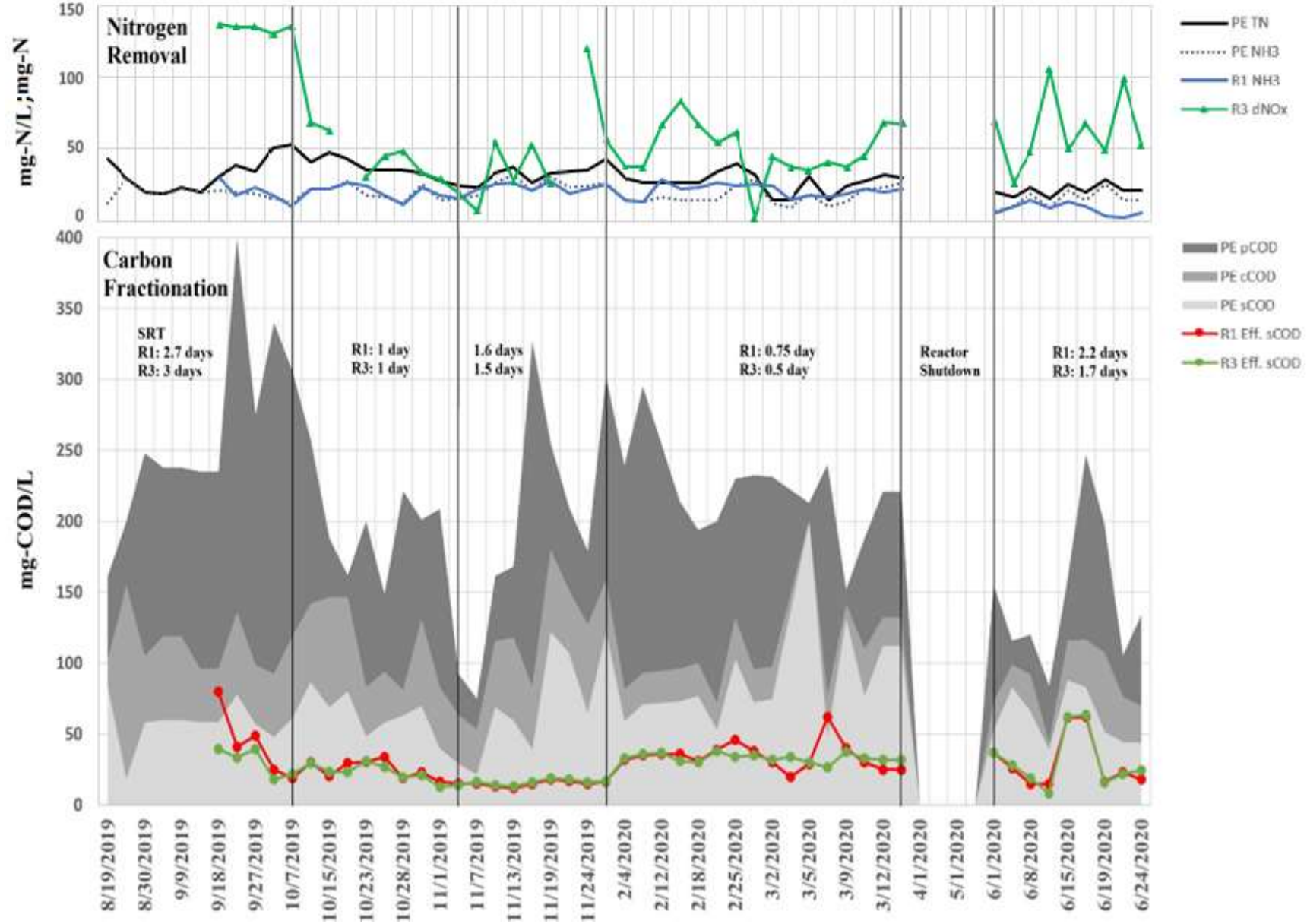

The total effect of denitrification in Reactor 3 is an achieved effluent sCOD concentrations similar to AAWWTP's finished water (also regarded as the non-biodegradable or inert carbon fraction, Figure 4-5). Not surprisingly, the aerobic and anoxic OHOs were driving carbon removal in the system, and effluent concentrations largely mirrored each other over the entire study period (Table 4-6, dotted lines in Figure 4-5). These simple observations showed that both the control reactor and anoxic suspended growth reactor in practice were performing in line with theory (Jimenez et al., 2015), and more examination of the total carbon oxidation was needed to compare to computer modeling results.

If the results from the advanced model were to hold, the extent of hydrolysis should be relatively similar between aerobic and anoxic systems operating at the same SRT. In the MLE configuration, for example, the sole driver for hydrolysis was the increased system SRT because the hydrolysis rate was set at the same default value as the anoxic hybrid MABR. The anoxic reduction factor modestly inhibited the anoxic system process rate, but the captured difference in hydrolysis of organic matter was shown in Figure 4-4, and was a function of SRT differences in the two configurations to accommodate the aerobic zone. In the SUMO model, which utilizes ASM methodology, pCOD and cCOD are hydrolyzed to smaller metabolizable material (i.e., sCOD) (Morgenroth et al., 2002). The hydrolysis rate at longer SRTs would then directly influence the amount of biodegradable matter available to the microbial community for oxidation, and thus decreased downstream biogas conversion in the anaerobic digester.

To test the model assumptions, we used direct and indirect measures for the extent of hydrolysis between the aerobic and anoxic SBRs, including the reactors used for aerobic and anoxic biological phosphorus removal (bio-P) at longer SRTs, since the fundamental differences should hold. The most direct method was to subtract filtered COD and flocculated & filtered COD

fractionations to find cCOD. As shown in Table 4-6 and Appendix Figure C-2, the anoxic Reactor 3 has elevated effluent cCOD concentrations compared to the aerobic reactor despite increasing operational SRTs, and cCOD removal percentages plateauing around 60% for the anoxic reactor, as opposed to 80-90% for the aerobic reactor, marking approximately 10-15 mg-COD/L difference. Effluent sCOD followed a relatively similar pattern between both reactors, as clearly shown in Figure C-3. Incomplete bioflocculation of colloidal organic matter is common at lower SRTs, but then at increasing SRTs the hydrolysis rate within the mixed liquor flocs would drive the amount of colloidal matter being converted to sCOD and subsequently oxidized (Jimenez et al., 2005; Hauduc et al., 2019). Colloidal flocculation is dictated by factors including the system SRT, the bulk liquid DO concentration, and amount of extracellular polymeric substance (EPS) production (Hauduc et al., 2019). One study found optimal conditions for high-rate colloidal bioflocculation similar to our modeling results at a 1.5-day SRT threshold and 0.5 mgO_2/L, while sCOD had much less reliance on either system SRT or DO (Jimenez et al., 2015).

The more indirect measure of hydrolysis was estimated through the difference in oxidized sCOD and tCOD in the system. Oxidized sCOD was similar for both Reactors 1 and 3 and bio-P Reactors 2 and 4 (dotted markers in Figure 4-5), which are the drivers for the theoretical high-rate anoxic suspended growth treatment. As the SRT increased from 0.50 days to 8.0 days in both reactors, the slopes of sCOD oxidation increased modestly until it reached a plateau around 25%. This would indicate the exhaustion of rbCOD from the influent (any remaining sCOD would be inert), and the similar effluent sCOD concentrations from aerobic and anoxic reactors would seem to confirm this assumption. However, the percentage total COD oxidation differs greatly between the two reactors, as shown by the solid-colored markers in Figure 4-5 (blue aerobic, green anoxic). Combining the observations of increasing colloidal removal in the aerobic reactor, the widening

between estimates of sCOD and tCOD oxidation represents the extent of hydrolysis. Therefore, as the amount of soluble material in both reactors is consumed for energy and cell maintenance in a similar manner, total COD oxidation increases in the aerobic system, and the amount of carbon that could be effectively captured by the treatment system diminishes. The difference between the aerobic and anoxic high-rate systems is substantial; roughly 50% of the carbon fed to Reactor 1 is oxidized to CO_2 after 3.0 days SRT, compared to 36% in Reactor 3. At even longer SRTs during later periods designed for combined nitrogen and phosphorus, anoxic oxidation sharply increased as SRT increased between 2.5-6.0 days. The oxidized tCOD in Reactor 4 increased from 30 to 50% across those systems SRTs, and was measured again at 50% with the longest SRT in the study of 12.5 days, versus aerobic oxidation between 40 to 65% (see solid-colored square markers in Figure 4-6). Slight discrepancies between the nitrogen removal reactors (R1 and R3) and biological phosphorus removal reactors (R2 and R4) at the overlapping period around 2.0-4.0 days SRT (circular versus square markers) were likely due to differences in influent characteristics. The primary effluent had higher concentrations of pCOD and cCOD that could have contributed to slight changes in oxidation. The biological phosphorus removal performance will be addressed in Chapter 5. A rapidly growing anoxic biomass is viable at these operating conditions, and the differences in high-rate treatment performance between aerobic and anoxic systems are negligible. The energetics (specifically, free energy transfer efficiency) and anoxic hydrolysis rate of organic nitrogen are lower than aerobic, so this seems like a logical outcome (Henze & Mladenovski, 1991; Orhon et al., 1996).

Table 4-7 Summary COD and nitrate mass balance agreement, and COD oxidation calculations based on yield

Reactor 1 Aerobic								
SRT (days)	tCOD Oxidized (mgCOD/day)	Influent tCOD (mgCOD/day)	COD Oxidized/ Influent COD	sCOD removed (mgCOD/day)	Y_n	(1-Y)	sCOD Destroyed (mgCOD/day)	sCOD Oxidized/ Influent COD
0.47[2]	2,770	10,100	0.28	1,030	0.62	0.38	394	0.04
0.75[1]	7,960	14,800	0.54	3,110	0.59	0.41	1,270	0.09
0.96[2]	3,810	12,700	0.30	2,890	0.57	0.43	1,230	0.10
1.0[1]	5,650	12,500	0.50	2,450	0.57	0.43	1,060	0.08
1.6	6,730	14,100	0.48	3,980	0.53	0.47	1,890	0.13
2.2	4,810	9,840	0.49	2,460	0.49	0.51	1,250	0.13
2.9	8,460	15,800	0.54	2,630	0.46	0.54	1,430	0.09

Reactor 3 Anoxic									
SRT (days)	tCOD Oxidized (mgCOD/day)	NO_3 Reduced (mgCOD/day)	Influent tCOD (mgCOD/day)	COD Oxidized/ Influent COD	sCOD removed (mgCOD/day)	Y_n	(1-Y)	sCOD Destroyed (mgCOD/day)	sCOD Oxidized/ Influent COD
0.45[1]	8,690	2,350	15,140	0.16	3,910	0.61	0.39	1,510	0.10
0.66[2]	2,690	2,550	10,100	0.25	1,430	0.60	0.40	580	0.06
1.0[2]	4,310	4,340	12,700	0.34	2,990	0.57	0.43	1,290	0.10
1.0[1]	4,540	2,620	12,900	0.20	3,000	0.57	0.43	1,300	0.10
1.5	4,330	4,530	14,400	0.31	3,570	0.53	0.47	1,680	0.12
1.8	3,250	3,040	10,100	0.30	2,790	0.51	0.49	1,360	0.14
3.0	5,550	5,620	15,800	0.36	2,760	0.45	0.55	1,520	0.10

[1]Samples were not included in the final analysis due to problems with wasting. See large imbalance between COD and nitrate mass balance
[2]Samples replaced [1] were ran in August 2022 using primary effluent from AAWWTP East treatment train instead of west train, previously.

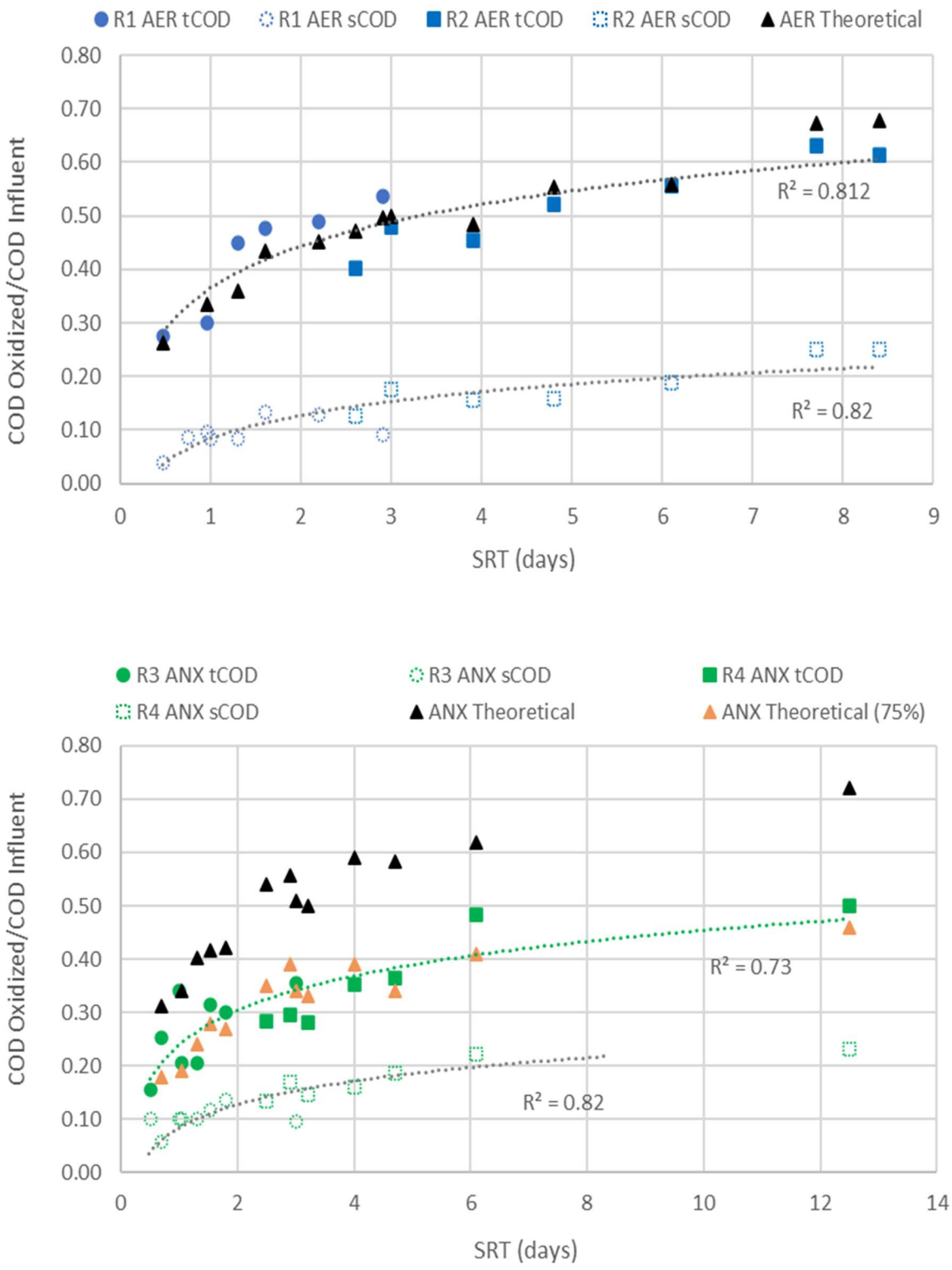

Figure 4-6 SRT effect on percent COD oxidized of total influent COD provided to aerobic (top) or anoxic (bottom) systems

Note: AER and ANX theoretical (black triangles) based on assumption of 100% hydrolysable particulate and colloidal organic matter. ANX theoretical (pink triangles) based on 75% hydrolysable material.

Furthermore, if the amount of theoretical COD oxidized is calculated using the observed yield by the amount of hydrolysable material (i.e., the difference in the influent tCOD versus the effluent sCOD, including all pCOD and cCOD in the system), the system differences become much clearer (see Equation 14 below). Embedded in this calculation is the assumption that all pCOD and cCOD in the influent was readily biodegradable through the hydrolytic processes. The aerobic reactors COD mass balance, the difference in measured COD in the influent and effluent streams, follow nearly identically to this theoretical calculation, as witnessed in Figure 4-6 (blue circles versus black triangles, respectively). The anoxic reactors, however, had much higher theoretical oxidation based on its observed yield and the hydrolysable organic matter based on the aerobic reactor. In fact, the theoretical oxidation curve tracked much closer to the measured anoxic COD mass balance when it was assumed only 75% of the material was biodegradable through hydrolysis (pink triangles, Figure 4-6). This parameter fit gives us a qualitative sense of the different behavior that can occur degrading organic particulate and colloidal material between aerobic and anoxic systems. A quantifiable anoxic correction factor for hydrolysis is important for multiple reasons. First of all, our work aligns with observations of reduced anoxic hydrolysis rate constant of Henze & Mladenovski (1991), although our work is not kinetically derived. Instead, what we conclude from these results is that anoxic hydrolysis exhibits a different behavior than aerobic systems, specifically that particular types of particulate and colloidal organic matter can be hydrolyzed under aerobic conditions and not under anoxic conditions. This is the case with or without the addition of an initial anaerobic zone in the design configuration.

$$(1 - Y_n) * \left(tCOD_{in} - sCOD_{eff}\right) = Oxidation\ of\ Hydrolysable\ Material \quad (14)$$

Other significant differences in settling characteristics were apparent between the aerobic and anoxic system. As with the hybrid MABR computer model results, the anoxic reactor required a short aeration phase at the end of the cycle due to the "rising sludge" phenomena. Rising sludge is observed when nitrogen gas (N_2) bubbles are formed after denitrification inside the mixed liquor flocs causing them to float to the surface of the water instead of settling (Ekama et al., 1997). A short pulse of aeration, roughly five min, easily counteracted this and stripped the N_2 bubbles preventing loss of biomass during the settling phase. It is likely that this modest aeration was sufficient to allow growth of low DO filaments (Chudoba, 1985; Gabb et al., 1991). Filamentous organisms are critical to the bioflocculation process, providing the backbone which bridges floc-forming colonies, polymers, proteins, and cations together (Jenkins et al., 2004). Filaments are thought to prefer aerobic environments to anoxic, although there is some evidence suggesting a denitrifying ability (Wang et al., 2016). A detailed analysis on floc size and structure, floc community composition, and diversity in anoxic mixed liquor samples was done in parallel research (He et al., 2022). Results showed a lower filamentous index for anoxic flocs, implying a strategic disadvantage in bioflocculation and preventing floc shear. However, the reduced number of filaments may have also led to a decreased physiochemical repulsion between the flocs, leading to better settled sludge. Reactor 3 effluent suspended solids was consistently higher than its aerobic counterpart (Appendix Table C-4). However, when comparing anoxic Reactor 3 that had a small aerobic polishing step at the end of the cycle, Reactor 1 had SVIs in the "Moderate" range (roughly 100 mL/g) across all the most of the lower SRTs in the study, whereas Reactor 3 had settled sludge SVIs that would qualify as near "Excellent" (80 mL/g) after the 2.5-day SRT periods studied (Grady Jr. et al., 2011). The highest-rate sample periods in both reactors had a "Moderate" rating prior to the 2-day SRT threshold (80 to 100 mL/g, Appendix Table C-4). These results appear to

mirror the correlations between SVI and SRT described in Carley (2003), and Maharajh (2010), as well as the observed historic benefit to sludge settling with addition of anoxic selectors (Parker et al., 2004). Observationally, both reactors appeared to have healthy settling biomass (minor operation adjustments notwithstanding) when including the SVIs at SRTs above 3.0 days considered during Reactor 2 and 4 operation. Evidence would suggest the anoxic mixed liquor could adapt into the secondary clarifier of a proposed hybrid MABR design model.

Final comparison of the physical system with SUMO models shows support for the denitrification capacity and carbon capture potential proposed in the hybrid MABR treatment system. With nitrification decoupled from suspended growth, high-rate anoxic suspended growth in the presence of nitrate appears able to metabolize influent rbCOD without expending as much additional colloidal organic resources as a traditional aerated system (i.e., a low extent of hydrolytic carbon oxidation), as predicted by the advanced model. Quantitative analysis estimates approximately 75% of the particulate and colloidal (hydrolysable) organic matter was hydrolyzed in the anoxic system compared to the aerobic system. The anoxic conditions did not prevent floc bridging from occurring, rather, when a minor aerated "stripping" cycle was added to prepare the flocs for settling phase, a viable flocculating biomass was measured.

4.5 Summary and Conclusions

Simulation of a hybrid MABR/anoxic suspended growth system and operation of an anoxic suspended growth system treating domestic wastewater demonstrate competitive advantages to process nitrogen removal and carbon capture compared to traditional aerated designs. the results provide further proof of concept for the envisioned hybrid MABR process. It is well demonstrated elsewhere that incorporation of an appropriately sized MABR in a non-aerated suspended growth zone can provide a nitrifying biofilm to produce the nitrate-nitrogen required for denitrification in

that zone. Sizing the MABR to accomplish a substantial proportion of the total required nitrification allows the aerated zone required within a conventional suspended growth biological nitrogen removal process to be significantly reduced in size, or eliminated, and allows the suspended growth SRT to be reduced significantly. Conversion of ammonia to nitrate in the initial portion of the suspended growth bioreactor also eliminates the need to recirculate nitrate from a downstream aerobic zone to the anoxic zone, allowing more complete denitrification to occur. Evidence of a viable high-rate anoxic suspended growth system appears throughout the advanced model, but was corroborated using a physical batch system at the AAWWTP treating domestic wastewater. Measured cCOD removal and tCOD oxidation estimates align with model carbon capture estimates, which lends support to the hypothesis that a hybrid MABR/anoxic suspended growth system utilizes biodegradable organic matter influent to the biological reactor more efficiently for denitrification (little or no oxidation in a downstream aerobic zone). The interesting observation is that a portion, roughly 25%, of the biodegradable particulate and organic matter oxidized in the aerobic system was found not to be hydrolysable under anoxic conditions. This was discovered through comparison of a theoretical oxidation calculation via observed yield versus the system carbon mass balance. Regardless of mechanisms, reduction in anoxic biodegradation of influent organic matter enables a higher fraction of influent organic carbon to be used for other purposes, e.g., biogas generation from anaerobic digesters. Reduced metabolism of biodegradable organic matter reduces the process oxygen requirement, and this, coupled with the higher OTE for MABRs compared to conventional oxygen transfer systems and elimination of the need for mixed liquor recirculation, results in further reduction of process energy requirements for the hybrid MABR process compared to conventional biological nitrogen removal systems.

The hybrid MABR model demonstrated operational tradeoffs; in a given scenario, one could maximize carbon capture by minimizing process energy requirements while also achieving significant but incomplete nitrogen removal by operating at lower suspended growth SRT. In the physical system, this is manifested as a lower overall tCOD oxidation at lower SRTs, coinciding with worse denitrification and lower mass removal of nitrate and nitrite (ΔNOx). However, the hybrid MABR process can also accommodate an influent wastewater with reduced COD/TN by increasing the suspended growth SRT to allow increased metabolism of influent biodegradable organic matter, as needed, to accomplish the desired effluent TIN concentration.

Future research will advance this idea with more aspects of BNR to include biological phosphorus removal (Chapter 5). With the successful high-rate anoxic suspended growth demonstrated in this chapter, it is envisioned that this process can also be incorporated into the hybrid MABR process by addition of an anaerobic zone upstream of the anoxic zone containing MABR units. Additional projects are underway to include MABR cassettes at both the bench-scale (Ann Arbor, MI, USA) and pilot-scale (Nanjing, China). Detailed investigation of biofilm and anoxic suspended growth population dynamics and operational symbiosis will continue to build off this body of research.

4.6 References

Aybar, M., Pizarro, G., Martin, K., Boltz, J., Downing, L., & Nerenberg, R. (2012). The air-based membrane biofilm reactor (MBfR) for energy efficient wastewater treatment. *Proceedings of the Water Environment Federation*, *2012*(10), 5458–5485.

Cardete, M. A., Mata-Álvarez, J., Dosta, J., & Nieto-Sánchez, R. (2017). Sludge settling enhancement in a pilot scale activated sludge process treating petrochemical wastewater by implementing aerobic or anoxic selectors. *Journal of Environmental Chemical Engineering*, *5*(4), 3472–3482. https://doi.org/https://doi.org/10.1016/j.jece.2017.06.021

Carley, J. M. (2003). *The Effects of Temperature and Solids Retention Time on Activated Sludge Treatment Performance*. University of Tennessee.

Chudoba, J. (1985). *Control of Activated Sludge Filamentous Bulking-VI. Formulation of basic principles*. *19*(8), 1017–1022.

Côté, P., Peeters, J., Adams, N., Hong, Y., Long, Z., & Ireland, J. (2015). *A New Membrane-Aerated Biofilm Reactor for Low Energy Wastewater Treatment: Pilot Results*.

Daigger, G. T., Carlson, A. L., Chen, X., & Johnson, B. (2019). Coupled Anoxic Supended Growth and Membraner Aerated Biofilm Reactor Process Options. *Proceedings of the Water Environment Federation*, 1312–1323.

Downing, L. S., & Nerenberg, R. (2008a). Effect of bulk liquid BOD concentration on activity and microbial community structure of a nitrifying, membrane-aerated biofilm. *Applied Microbiology Biotechnology*, *81*, 153–162. https://doi.org/10.1007/s00253-008-1705-x

Downing, L. S., & Nerenberg, R. (2008b). Effect of oxygen gradients on the activity and microbial community structure of a nitrifying, membrane-aerated biofilm. *Biotechnology and Bioengineering*, *101*(6), 1193–1204.

Downing, & Nerenberg, R. (2008c). Total nitrogen removal in a hybrid, membrane-aerated activated sludge process. *Water Research*, *42*(14), 3697–3708. https://doi.org/10.1016/j.watres.2008.06.006

Dynamita Process Modeling. (2020). *SUMO User Manual* (No. 20). Dynamita.

Ekama, G. A. (2011). Biological Nutrient Removal. In *Treatise on Water Science* (pp. 409–526). https://doi.org/10.1016/B978-0-444-53199-5.00094-4

Ekama, G. A., Barnard, J. L., Günthert, F. W., Krebs, P., McCorquodale, J. A., Parker, D. S., & Wahlberg, E. J. (1997). *Secondary Settling Tanks: Theorgy, Modelling, Design and Operation*.

Flores-Alsina, X., Comas, J., & Rodriguez-Roda, I. (2010). Analysis of rising sludge risk in Activated Sludge Systems: from operation strategies to clarifier design. *International Congress on Environmental Modelling and Software*.

Gabb, D. M. D., Still, D. A., Ekama, G. A., Jenkins, D., & Marais v., G. R. (1991). The selector effect on filamentous bulking in long sludge age activated sludge systems. *Water Science and Technology*, *23*(4–6), 867–877. https://doi.org/10.2166/wst.1991.0538

Gilmore, K. R., Little, J. C., Smets, B. F., & Love, N. G. (2009). Oxygen transfer model for a flow-through hollow-fiber membrane biofilm reactor. *Journal of Environmental Engineering*, *135*(9), 806–814.

Grady Jr., L., Daigger, G. T., Love, N. G., & Filipe, C. D. M. (2011). *Biological Wastewater Treatment* (Third). CRC Press.

Guglielmi, G., Coutts, D., Houweling, D., & Peeters, J. (2020). Full-scale Application of MABR Technology for Upgrading and Retrofitting an Existing WWTP: Performances and Process Modelling. *Environmental Engineering & Management Journal (EEMJ)*, *19*(10).

Hauduc, H., Wadhawan, T., Takacs, I., Al-Omari, A., De Clippeleir, H., Wett, B., Jimenez, J., & Rahman, A. (2019). Colloids, flocculation and carbon capture - A comprehensive plant-wide model. *Water Science and Technology*, *79*(1), 15–25. https://doi.org/10.2166/wst.2018.454

He, H., Carlson, A. L., Nielsen, P. H., Zhou, J., & Daigger, G. T. (2022). Comparative analysis of floc characteristics and microbial communities in anoxic and aerobic suspended growth processes. *Water Environment Research*. https://doi.org/doi.org/10.1002/wer.10822

He, H., Wagner, B. M., Carlson, A. L., Yang, C., & Daigger, G. T. (2021). Recent progress using membrane aerated biofilm reactors for wastewater treatment. *Water Science and Technology*, *84*(9), 2131–2157. https://doi.org/10.2166/wst.2021.443

Henze, M, & Mladenovski, C. (1991). Hydrolysis of particulate substrate by activated sludge under aerobic, anoxic and anaerobic conditions. *Water Research*, *25*(1), 61–64. https://doi.org/https://doi.org/10.1016/0043-1354(91)90099-C

Henze, Mogens, Gujer, W., Mino, T., & van Loosdrecht, M. C. M. (2000). Activated Sludge Models ASM1, ASM2, ASM2d and ASM3. *IWA Publishing*, 121. https://doi.org/10.1007/s13398-014-0173-7.2

Hertzler, P., Dufresne, L., Randall, C., Barnard, J., Stensel, D., Brown, J., & Moore, G. T. (2009). *Nutrient control design manual: state of technology review report.* (Issue January).

Houweling, D., & Daigger, G. T. (2019). *Intensification of the Activated Sludge Process Using Media Supported Biofilms*. IWA Publishing.

Houweling, D., Peeters, J., Cote, P., Long, Z., & Adams, N. (2017). Proving Membrane Aerated Biofilm Reactor (MABR) Performance and Reliability: Results from Four Pilots and a Full-Scale Plant. *Proceedings of the Water Environment Federation*, *2017*(16), 272–284. https://doi.org/10.2175/193864717822155786

Jenkins, D., Richard, M. G., & Daigger, G. T. (2004). *Manual of the Causes and Cotrol of Activated Sludge Bulking, Foaming, and Other Solids Separation Problems* (3rd edn). CRC Press.

Jimenez, J. A., La Motta, E. J., & Parker, D. S. (2005). Kinetics of Removal of Particulate Chemical Oxygen Demand in the Activated-Sludge Process. *Water Environment Research*, *77*(5), 437–446. https://doi.org/10.2175/106143005x67340

Jimenez, J., Miller, M., Bott, C., Murthy, S., De Clippeleir, H., & Wett, B. (2015). High-rate activated sludge system for carbon management - Evaluation of crucial process mechanisms and design parameters. *Water Research*, *87*, 476–482. https://doi.org/10.1016/j.watres.2015.07.032

Kunetz, T. E., Oskouie, A., Poonsapaya, A., Peeters, J., Adams, N., Long, Z., & Côté, P. (2016). Innovative membrane-aerated biofilm reactor pilot test to achieve low-energy nutrient removal at the Chicago MWRD. *WEFTEC 2016 - 89th Water Environment Federation Annual Technical Exhibition and Conference*, *1*, 2973–2987. https://doi.org/10.2175/193864716819713006

Kunetz, T., Oskouie, A., Poonsapaya, A., Peeters, J., Adams, N., Long, Z., & Côté, P. (2016). *Innovative Membrane-Aerated Biofilm Reactor Pilot Test to Achieve Low- energy Nutrient Removal at the Chicago MWRD Innovative Membrane-Aerated Biofilm Reactor Pilot Test to Achieve Low-energy Nutrient Removal at the Chicago MWRD*. https://doi.org/10.2175/193864716819713006

Li, Q. (2018). *Pilot-scale Plant Applicatio of Membrane Aerated Biofilm Reactor (MABR) Technology in Wastewater Treatment*. KTH Royal Institute of Technology.

Li, T., Liu, J., & Bai, R. (2008). Membrane Aerated Biofilm Reactors: A Brief Current Review. *Recent Patent on Biotechnology*, *2*(February 2008), 88–93. https://doi.org/10.2174/187220808784619739

Lu, D., Bai, H., Kong, F., Liss, S. N., & Liao, B. (2021). Recent advances in membrane aerated biofilm reactors. *Critical Reviews in Environmental Science and Technology*, *51*(7), 649–703. https://doi.org/10.1080/10643389.2020.1734432

Maharajh, N. (2010). *Effect of Feed Rate and Solid Retention Time (SRT) on Effluent Quality and Sludge Characteristics in Activated Sludge Systems using Sequencing Batch Reactors*. Virginia Polytechnic Institute.

Management, O. of W. (2010). *NPDES Permit Writers' Manual*. https://www.epa.gov/npdes/npdes-permit-writers-manual

Mangrum, C. (1998). *The effect of anoxic selectors on the control of activated sludge bulking and foaming*. Virginia Polytechnic Institute and State University.

Morgenroth, E., Kommedal, R., & Harremoës, P. (2002). Processes and modeling of hydrolysis of particulate organic matter in aerobic wastewater treatment – a review. *Water Science and Technology*, *45*(6), 25–40. https://doi.org/10.2166/wst.2002.0091

Orhon, D., Sözen, S., & Artan, N. (1996). The effect of heterotrophic yield on the assessment of the correction factor for anoxic growth. *Water Science and Technology*, *34*(5–6), 67–74. https://doi.org/10.1016/0273-1223(96)00630-0

Parker, D., Appleton, R., Bratby, J., & Melcer, H. (2004). North American performance experience with anoxic and anaerobic selectors for activated sludge bulking control. *Water Science and Technology*, *50*(7), 221–228. https://doi.org/10.2166/wst.2004.0463

Rahman, A., Meerburg, F. A., Ravadagundhi, S., Wett, B., Jimenez, J., Bott, C., Al-Omari, A., Riffat, R., Murthy, S., & De Clippeleir, H. (2016). Bioflocculation management through high-rate contact-stabilization: A promising technology to recover organic carbon from low-strength wastewater. *Water Research*, *104*, 485–496. https://doi.org/https://doi.org/10.1016/j.watres.2016.08.047

Sathyamoorthy, S., Tse, Y., Gordon, K., Houwelling, D., & Coutts, D. (2019). BNR Process Intensification using Membrane Aerated Biofilm Reactors. *WEF Nutrient Removal and Recovery Symposium*, 527–535.

Standard Methods for the Examination of Water and Wastewater (3rd ed.). (2017). American Public Health Association/American Water works Association/WAter Environment Federation.

Tchobanoglous, G., Burton, F. L., & Stensel, D. H. (2003). *Wastewater Engineering: Treatment and Reuse* (4th Editio). Metcalf & Eddy, Inc.

Uri-Carreño, N., Nielsen, P. H., Gernaey, K. V, & Flores-Alsina, X. (2021). Long-term operation assessment of a full-scale membrane-aerated biofilm reactor under Nordic conditions. *Science of The Total Environment*, *779*, 146366. https://doi.org/https://doi.org/10.1016/j.scitotenv.2021.146366

Wang, B., Peng, D., Zhang, X., & Wang, X. (2016). Structure and formation of anoxic granular sludge—A string-bag hypothesis. *Frontiers of Environmental Science & Engineering*, *10*(2), 311–318. https://doi.org/10.1007/s11783-014-0748-8

Water Environment Federation. (2020). *Design of Water Resource Recovery Facilities, Manual of Practice No. 8* (Sixth). WEF Press.

Wentzel, M. C., Mbewe, A., Lakay, M. T., & Ekama, G. A. (2000). Evaluation of a Modified Flocculation Filtration Method To Determine Wastewater Readily Biodegradable COD. *WISA 2000 Biennial Conference*, *June*.

Chapter 5 Analysis of fully anoxic suspended growth treatment of domestic wastewater performing biological nitrogen and phosphorus removal

5.1 Abstract

Hybrid membrane aerated biofilm reactor (MABR)/anoxic suspended growth treatment systems require better understanding of denitrifying phosphate-accumulating organism (DPAO) metabolisms in domestic wastewater environments. First, computer simulation was used to model a hybrid system versus a conventional anaerobic/anoxic/aerobic configuration. The results predicted effluent orthophosphate concentrations as low as 0.20 mg-P/L at a system solids retention time of 4.0 days versus an effluent concentration of 0.30 mg-P/L at 6.8 days, respectively. To evaluate the simulation output, anaerobic/anoxic and anaerobic/aerobic sequencing batch reactors were operated side-by-side as pilot-scale systems and fed domestic wastewater to evaluate the metabolic capacity of DPAOs compared to aerobic PAOs. A chemical water quality evaluation found reduced orthophosphate release, uptake, and ultimately removal in the anoxic zone versus its aerobic counterpart. A stoichiometric evaluation suggested that the anoxic zone had a lower P/O ratio (0.90) than the aerobic zone (1.7) that was caused by less efficient oxidation of anaerobically-stored polyhydroxybutyrate (PHB). Genomic analysis for the PAO genera *Candidatus* Accumulibacter and *Dechloromonas* sp. were assembled from shotgun metagenomic sequencing of mixed liquor samples. Both genomes contained respiratory (*nar*) and periplasmic (*nap*) nitrate reductase-encoding genes; however, the efficiency of *nap* is thermodynamically unfavorable compared to *nar* under most anoxic conditions. This reality likely influenced the

amount of ATP produced on intracellular PHB leading to a lower P/O ratio, and consequently lower biological P removal efficiency, in the anoxic/aerobic bioreactor. These results suggest that DPAO metabolic efficiency is reduced under anoxic conditions, and should be considered during MABR design and modeling efforts.

5.2 Introduction

5.2.1 Biological Phosphorus Removal Potential in MABR Treatment Systems

Research is in its infancy regarding biological phosphorus (bio-P) removal pathways in membrane aerated biofilm reactor (MABR) treatment systems, mainly because of the level of symbiosis needed to control diffusion of substrates between biofilm and suspended microbial growth. A handful of systems implementing the membrane technology have witnessed bio-P removal, but have been unable to attribute the growth to any particular microbial group in either attached or suspended environments—in other words, the system was a "black box" (Underwood et al., 2018; Kunetz et al., 2016). Others have demonstrated growth of phosphorus accumulating organisms (PAOs) in various layers of the MABR biofilm, but this requires sophisticated aeration control strategies that have not been platformed at a field scale (Sathyamoorthy et al., 2019). The objective of this research chapter is to investigate the feasibility of a hybrid MABR/anoxic suspended growth treatment design to complete bio-P removal with nitrate produced from a nitrifying MABR biofilm. However, the primary issue we wish to understand better is how a full-scale anoxic suspended growth system performs bio-P removal using only domestic wastewater. Alternative biological nutrient removal (BNR) configurations, such as a hybrid MABR treatment system, have the potential to reduce resources and energy requirements on a cost per gallon basis if the system can demonstrate robust bio-P removal with denitrifying phosphorous accumulating organisms (DPAOs). The proposed system must have comparable performance to the traditional

anaerobic/aerobic design with highly-adapted phosphorus accumulating organisms (PAOs). Further complicating our research pursuit, few full-scale anoxic BNR wastewater treatment design examples exist beyond small sub-sections of conventional activated sludge (AS) systems, such as selectors, or A/B processes (Almasi & Pescod, 1996; Parker et al., 2004; Liu et al., 2019). Consequently, elucidating the function and performance of anoxic BNR in a MABR treatment system under the dynamic conditions of a domestic wastewater plant need to be developed.

It is well-known that multiple simultaneous processes occur amongst diverse microbial populations in an attached growth MABR coupled with a mixed liquor suspended growth treatment system. The MABR is an ideal environment to select for DPAOs because nitrate formation is achievable through nitrification in the biofilm while strict anoxic redox conditions are retained in the mixed liquor bulk liquid where DPAOs can exist (Sathyamoorthy et al., 2019; Downing & Nerenberg, 2008; Houweling & Daigger, 2019). Furthermore, a hybrid MABR system is easily modified with the addition of an anaerobic zone to promote fermentation of organic material by facultative ordinary heterotrophic organisms (OHOs). The organic material present in both the influent wastewater as particulate, colloidal, and soluble organic matter is vital for OHO fermentation to volatile fatty acids (VFAs). We know from Chapter 4 that anoxic hydrolysis of particulate and colloidal organic matter was reduced, which is hypothesized to affect the availability of fermented substrates available to DPAOs. The bio-P removal process proposed in this chapter will couple these necessary fermented substrates from an initial anaerobic zone with nitrate from a large anoxic zone of hybrid MABR design to promote DPAO metabolism of phosphorus via the denitrifying phosphorylation pathway. Consequently, the anoxic selection of both OHOs and PAOs in suspension is critical for adequate performance of anoxic suspended growth Bio-P removal system.

In this chapter, we are focused on translating these complex interactions between fermenting OHOs and DPAOs into a model framework that incorporates mechanistic bioprocess modeling, supplemented with deep information from microbial community metagenomic analysis. The modeling portion was used to assess the feasibility of a hybrid MABR system for bio-P removal. Specifically, we evaluated the value of the anoxic growth (eta, η) factor to accurately simulate the growth of denitrifying heterotrophs in a fully anoxic hybrid MABR system versus a mixed culture system. The value of this parameter is influenced by both the redox potential of the electron donor and acceptor pair (Orhon et al., 1996), and stochastic (random) or deterministic (niche-related) anoxic selective pressures in the suspended growth zone (Zhou et al., 2013; Xu et al., 2022). It is not known whether a similar eta factor used in computer models will hold in a more complex system with alternate anaerobic/anoxic cycling designed for combined nitrogen and bio-P removal. Consequently, experiments are needed to evaluate this.

5.2.2 Biological Phosphorus Removal Mechanism with Denitrifying PAOs

The bio-P removal process occurs when phosphorus accumulating organisms metabolize inorganic orthophosphate (ortho-P) from influent wastewater to produce intracellular polyphosphate (poly-P). However, their broader metabolism occurs with an alternating "feast/famine" cycle, shown in the Mino PAO model (Mino et al., 1985). Reductive power in the form of nicotinamide adenine dinucleotide (NADH) is produced during the anaerobic metabolism of VFA and stored glycogen, and is transferred to the electron transport chain to the final acceptor (oxygen, or nitrate) through oxidative phosphorylation process. ATP synthesis subsequently occurs via the creation of the proton motive force. A detailed description of a typical cycle, and the stoichiometric equations behind the alternating anaerobic and aerobic/anoxic environments, can be found in the Appendix Section D-1 (Smolders et al., 1994b; Kuba et al., 1996). Finally, the

enzyme polyphosphate kinase (*ppk*) is responsible for the reformation of poly-P inside the cell (Ahn & Kornberg, 1990). The net differential in energy between anaerobic/aerobic or anaerobic/anoxic phase leads to increased storage of external orthophosphate as intracellular polyphosphate, and system wasting permanently removes the inorganic phosphorus from the system in solid form.

Historical knowledge of anoxic bio-P removal utilizing denitrifying PAOs (DPAOs, or referenced in the literature as denitrifying phosphorous-removing bacteria, DPB) goes back almost 30 years—early cultures showed the ability of DPAOs or DPB to metabolize the same organic material (VFAs, PHB, and glycogen) through similar processes as its aerobic counterpart (Kuba et al., 1994; Smolders et al., 1994b, 1995; Kuba et al., 1996). The first metabolic model of anoxic bio-P, then called "denitrifying dephosphatation", established a nearly identical stoichiometric equation as the aerobic process; the obvious lone exception being nitrate-nitrogen as the source of reduction power instead of oxygen in the electron transport chain, as described below in Equations 1 and 2 (Kuba et al., 1996).

$$NADH_2 + 0.5\,O_2 \rightarrow \delta ATP + H_2O \quad (1)$$

$$NADH_2 + 0.4\,NO_3 \rightarrow \delta ATP + 0.2N_2 + 1.2\,H_2O \quad (2)$$

Smolders et al. (1994b) utilized a critical biological parameter for comparing anoxic and aerobic bio-P metabolisms, designated the P/O ratio (δ), understood to be the ratio of ATP synthesized during oxidative phosphorylation per NADH oxidative unit supplied. Alternatively, this can be thought of as the metabolic efficiency to produce necessary energy for cell maintenance and growth during the aerobic "famine" cycle from the anaerobically stored organic substrates of the "feast" cycle. Aerobic bio-P removal was calculated to have a higher P/O ratio (δ = 1.85) than anoxic removal (δ = 1.0) (Smolders et al., 1994b; Kuba et al., 1996), which implies the DPAOs

are less efficient, and therefore at a competitive disadvantage relative to its aerobic counterpart. This conclusion is mirrored in the results of Filipe & Daigger (1999), which demonstrated that the inherent lowered thermodynamic efficiency causes washout of PAOs that can utilize either oxygen or nitrate in EBPR systems when competing with purely aerobic PAOs. These results help answer why anoxic DPAOs are not usually seen in, or have a major impact on, bio-P removal in traditional EBPR systems with an aerobic zone. Felipe & Daigger (1999) suggests however, that a designed system which decouples nitrification from suspended growth, such as the proposed hybrid MABR/anoxic suspended growth treatment system, could allow for DPAO growth, albeit in a less efficient manner.

Overall, anoxic phosphorus removal is thought to have a similar metabolic pathway as the anaerobic/aerobic metabolism employed in conventional EBPR activated sludge designs, but it is not known how a fully anoxic DPAO system would perform compared to a traditional configuration. It is also not well-understood how the anoxic environment would select DPAO characteristics, in terms of genomic capabilities. In fact, DPAOs are in many cases a subset of known PAO genera, including those commonly mentioned in the literature: *Candidatus* Accumulibacter and *Tetrasphaera* spp. (Flowers et al., 2009; Kristiansen et al., 2013; Gao, 2018). There is also a host of putative PAO classes, such as *Dechloromonas* and *Halomonas*, but so far little information is known about their role in bio-P removal (Nguyen et al., 2012; Petriglieri et al., 2021). Individual organisms in the PAO and DPAO populations have distinct genetic sequences, and some of these can be categorized into species-level sub-groups, also known as clades. Categorization into clades indicates that the individual strains of *Ca*. Accumulibacter phosphatis can be traced back to a common ancestor with a unique set of metabolic genes. For instance, the known phylogeny of the PAO species *Ca*. Accumulibacter phosphatis resolves into two distinct

sub-groups containing many different clades after sequencing both 16s rRNA and *ppk1* (S. He et al., 2007; Gao, 2018). For instance, Type I *Ca*. Accumulibacter phosphatis, containing five different clades [A-E], and Type II, containing nine [A-H] (Gao, 2018), are both DPAO sub-groups of the larger PAO species population. These two types have shown a different preference for nitrogenous electron acceptors in past experimentation. Flowers et al. (2009) conducted batch experiments with bioreactors enriched with two *Ca.* Accumulibacter phosphatis groups, Type IA and Type IIA. The reactor containing predominantly Type IA showed clear nitrate uptake coupled with ortho-P removal, whereas the parallel reactor enriched with Type IIA Accumulibacter showed nitrite uptake (Flowers et al., 2009). This would seem to indicate a clear divergence in metabolic capacity of PAO species sub-groups towards specific alternative reduction enzymes. However, a later comparative genomics study showed that periplasmic nitrate reductase gene sequences were present in both Type IA and Type IIA (Flowers et al., 2013), which illustrates the diversity of DPAO metabolic capabilities.

DPAOs may have facultative or strict ability to reduce nitrate-nitrogen instead of oxygen as their electron acceptor in the electron transport chain through nitrate, nitrite, and nitrous oxide reductase enzymes critical to the denitrification process, encoded by *nar*, *nir*, and *nor*/*nos* genes, respectively (Vaccaro et al., 2016). Research is limited as to what type, facultative or strict, of DPAO will manifest in a fully anoxic treatment system, and what encoded genes are available for bio-P metabolism. Nitrate reductase and polyphosphate kinase (*ppk*) were two genes specifically targeted during metagenomic analysis, although other genes important for bio-P were investigated, including: polyhydroxybutyrate synthase (*phaCE*) for modifying co-products of acetic acid and the acetyl-coA cycle to form PHB; and glycogen synthase (*glgAB*) for the reformation of stored

glycogen (S. He et al., 2010; Wang et al., 2014). Polyhydroxybutyrate and glycogen depolymerases (*phaZ*) and (*glgPX*) were also analyzed.

In a scenario with two divergent environments, i.e., a traditional anaerobic/aerobic bio-P configuration and anaerobic/anoxic configuration at small scale (prior to adoption in a proposed full-scale hybrid MABR system), it is not clear what genetic differences in the DPAO population would manifest under selective pressures in the anoxic system, and how this would affect overall bio-P removal performance compared to the aerobic setup. Primary metabolic models derived from an anoxic system with phosphorus limitations that the P/O ratio was lower than an aerobic system (Kuba et al., 1996). It is not known if these results will hold under fully anoxic system treating dynamic wastewater instead of highly-formulated synthetic wastewater, or if an anoxic environment will select for more efficient nitrate-respiring DPAO population. Furthermore, the range of genomic capabilities that will be accessible to the DPAOs in a fully anoxic system is not known—i.e., is the population limited to only those organisms with nitrate reductase for denitrifying phosphorylation, or those with a mixed genetic capability? Understanding what populations are growing in the system and their metabolic capabilities is especially important in a dynamic system treating domestic wastewater instead of synthetic lab-curated influent. It is also unclear what type of nitrate reductase would appear in the genome of anoxic treatment systems receiving domestic wastewater. Nitrate reductase can be assimilatory (i.e., incorporation of nitrate into the biomass, Nas), or dissimilatory (for purposes of energy generation) in the form of periplasmic (Nap) or respiratory (Nar) enzyme (González et al., 2006; Sparacino-Watkins et al., 2014). Elucidating where these forms of nitrate reductase proliferate is important to understanding DPAO how the denitrifying phosphorylation pathway generates energy and intracellular poly-P.

5.2.3 Study Approach and Goals

For this study, computer simulation was used to evaluate bio-P configurations: a hybrid MABR/anoxic suspended growth design versus a traditional anaerobic/anoxic/aerobic (A2/O) suspended growth design. These simulations were followed with performance and investigation of the DPAO population using side-by-side anaerobic/aerobic (A/O) and anaerobic/anoxic (A/An) pilot-scale systems treating domestic wastewater at the Ann Arbor Wastewater Treatment Plant (AAWWTP). Because of the number of dynamic variables, multiple involved microbial populations, and changing environments in a full hybrid MABR design, we narrowed our focus to anaerobic/anoxic treatment performance and its DPAO population without an MABR module. We used both chemical and biomolecular analyses with the pilot-scale system to investigate the PAO and DPAO microbial structure across both systems, as well as the presence or absence of functional genes relevant to these populations. From this, we collected evidence of differences between a comparable aerobic setup running on the same influent. We offer our experimental results and modeling data in this study to address research gaps in classic modeling approaches and remaining questions surrounding previous hybrid MABR systems in the field.

5.3 Materials and Methods

5.3.1 Modeling of Proposed Hybrid MABR System for Anoxic Bio-P

Computer simulation software (SUMO, Dynamita) was used to model combined nitrogen and phosphorus removal in a hybrid MABR configuration (modified from previous exercises) using fundamental mass balance, mass transfer, and kinetic equations. The difference between this model and the biological nitrogen removal model described in Section 4.2.2 is the addition of an initial anaerobic zone (ANA) as the first zone in the treatment train. The process flow diagram for

the proposed hybrid MABR treatment process is shown in Figure 5-1; the first zone is anaerobic for the production of VFAs through fermentation, nitrification occurs in the MABR zone, and is preceded by a large anoxic suspended growth (ANX) zone and a small aerated (AER) zone. The control design used to compare results was a traditional anaerobic/anoxic/aerobic (A^2/O) configuration. Primary treatment was included in both treatment trains because, similar to previous discussion, longer SRTs correlate to increased metabolism of biodegradable organic matter leading to low effluent TIN. Thus, primary treatment was included to reduce the size of the bioreactor and to provide increased carbon capture. The volumes for the anaerobic, MABR, anoxic, and aerobic bioreactor zones for the hybrid MABR bioreactor were 12%/12%/74%/2%, respectively, and the relative volumes of the A^2/O configuration ANA, ANX, and AER zones are 13%/36%/51%, respectively. The following model parameters were used, as described in Carlson et al. (2021). A packing density of 150 m^2/m^3 was used to size the MABR zone in the model. Oxygen mass flow rate input to the MABR units was adjusted to minimize the bleed through of oxygen out of the biofilm and into the suspended growth. The biofilm thickness was 175 μm, and the biofilm specific mass of 10 g TSS/m^2. The biofilm was divided into three layers, and the mass transfer boundary layer thickness (40 μm) was maintained. Water displaced by membrane and ratio of reactor volume filled by a membrane were 0.25 and 1.0, respectively. All simulations were conducted at a temperature of 20°C. The total volume was adjusted to maintain a MLSS concentration at 3,000 mg/L for both processes. Default wastewater characteristic and biological process stoichiometry and kinetics were used, except that the anoxic growth factor for ordinary heterotrophic organisms (OHOs), glycogen-accumulating organisms (GAOs), and PAOs were adjusted from 0.6, 0.66, and 0.33, respectively to 0.83 for the hybrid MABR processes to capture anoxic selective forces. This was done because anoxic operation of the suspended growth component of the hybrid process

would select for a higher proportion of denitrifying organisms. Default anoxic growth factors were maintained for the conventional A^2/O phosphorus removal process.

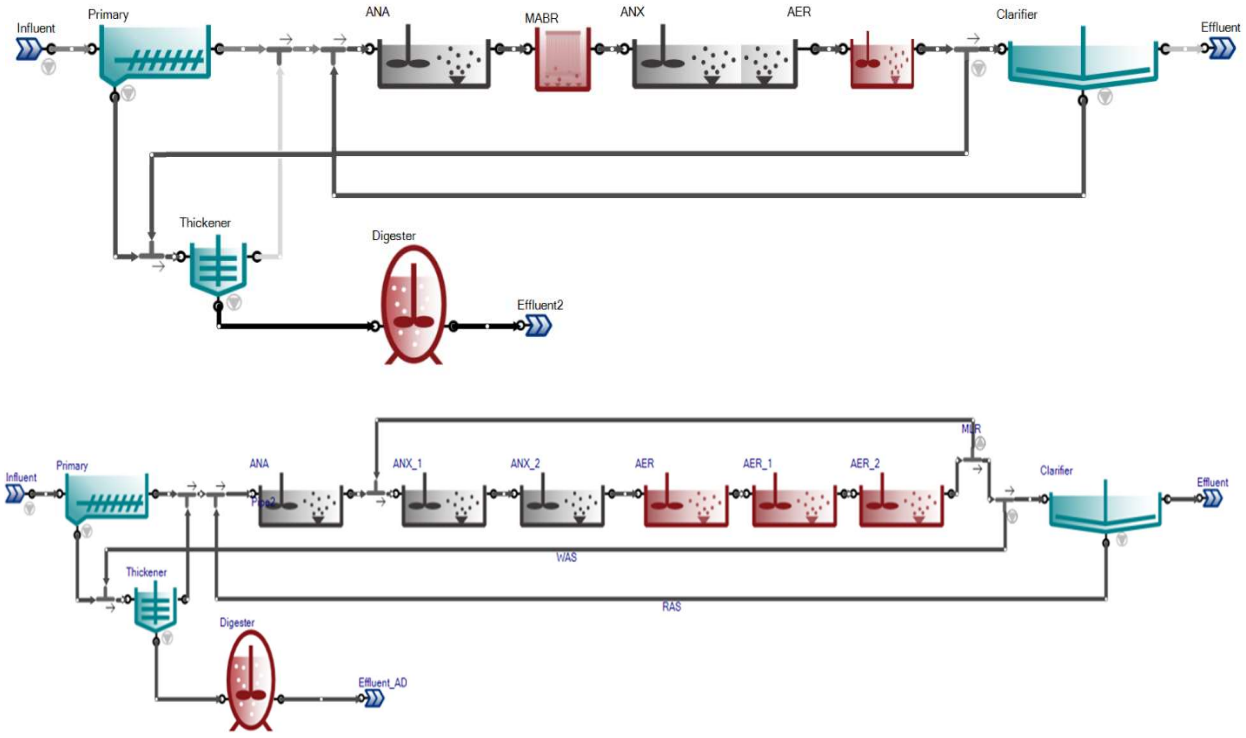

Figure 5-1 Schematic of SUMO20 process flow diagrams.
Top: Hybrid MABR/anoxic suspended growth system. Bottom: Conventional A^2O Combined nitrogen and phosphorus removal process.

5.3.2 Bioreactor Operation for Comparison of Aerobic/Anoxic Bio-P Processes

The reactor design configurations were anaerobic/aerobic (A/O) and anaerobic/anoxic (A/An) to simplify some of the variables influencing model bio-P removal predictions. The A/O Reactor 2 was the control for purposes of comparison, while A/An Reactor 4 was supplied with external nitrate. The MABR cassette was not used at this phase of experimentation for generation

of nitrate because the attached growth biofilm adds a layer of uncertainty in providing the necessary anoxic environment for DPAOs. Therefore, the suspended growth was evaluated as an idealized environment of the bulk liquid surrounding a nitrifying MABR biofilm.

The anaerobic cycle time was initially set at 25 min, and the aerobic or anoxic cycle time was 90 min. During the anaerobic cycle, the reactors were filled with 4.2 L of influent (i.e., primary effluent from AAWWTP) and were well-mixed for the entire duration of the cycle. Total filled reactor volume was 6.3 L. After the completion of the anaerobic cycle, air was supplied to Reactor 2 via an air compressor (previously closed by a ball valve), and 42 mL of sodium nitrate solution was fed to Reactor 4 via a peristaltic pump, similar to the operation description in Chapter 4. The sodium nitrate concentration varied between 15-20 g-N/L (reactor concentration 17-25 mg-N/L), based on regularly-measured dynamic wastewater chemical oxygen demand (COD).

The solids retention time (SRT) was regularly adjusted by manipulation of the waste volume. Reactor 2 was tested at SRTs between 2.6-8.4 days, and Reactor 4 was tested at SRTs between 1.7-12.5 days. Both reactors were held at a single SRT for each sampling period spanning multiple system SRTs (typically between 1.5 and 3.0 weeks) until the PAO/DPAO population reached a sufficient steady-state. Testing with conventional aerobic and anoxic bio-P reactors convened over a span of nine months between November 2020 and July 2021.

System Mass Balance Chemical Measurements: During initial testing, samples were taken from the reactor influent (stored AAWWTP primary effluent), mixed liquor waste, and secondary effluent from each reactor for subsequent chemical analysis. Mass balances on COD and nitrate, total phosphorus (TP), and orthophosphorus (ortho-P or OP) were completed. The mass balance was calculated using the experimentally measured concentration of the influent stream multiplied by the influent volume, subtracted by the concentrations of the effluent streams (secondary effluent

and waste) multiplied by their respective volumes. Removal percentages were also calculated from the difference in the mass of orthophosphorus into and out of the system divided by the influent mass. See Appendix Section C-3 for example reactor mass balance calculations.

Individual Cycle Chemical Profiles: Subsequent to mass balance calculations, chemical assessments were completed to generate VFA, nitrate, and ortho-P concentration profile curves across the entirety of a single cycle (anaerobic and aerobic or anoxic) for the two reactors. A profile consisted of mixed liquor grab samples taken at regular intervals, beginning during the anaerobic cycle through the end of the aerobic or anoxic cycle, and concentrations were plotted versus time. Each mixed liquor was glass-fiber filtered on-site immediately to separate the biology from dissolved components. Solid and liquid samples were then preserved for downstream chemical analysis (see Section 5.3.3 below). The operation schedule of the batch reactors was permanently modified in this phase to increase the anerobic cycle from 25 to 30 min, as well as to lengthen the aerobic/anoxic reaction cycle time from 90 to 140 min. Because of the extra time needed, this necessitated decreasing the number of batch cycles from 10 to 6.0 per day. The objective of profile testing was to operate the reactors at optimal SRT conditions for PAO and DPAO growth to evaluate the stoichiometry of a well-developed population.

Process calculations included ortho-P anaerobic release rate and aerobic/anoxic uptake rate (mg-P/g-VSS/hr), uptake of VFA (acetic acid) from the influent wastewater, and PHB storage/consumption rates. The release and uptake rates (mg-P/L/min) were found by dividing the slope of the ortho-P concentration plot over time by the measured VSS of the mixed liquor. It was ultimately determined that the influent wastewater concentrations of VFA were too low to support a robust DPAO population, and fermentation of soluble organic matter could not make up the difference. Thus, a modest concentration of acetic acid (15-20 mg/L) was added to the influent

wastewater during the filling phase of each cycle. Profile samples from the reactors were taken again, and the same process calculations were used. System SRT was held constant at this point based on the optimal SRT found when acetic acid was limited—5.0 days and 8.5 days for Reactor 2 and Reactor 4, respectively.

5.3.3 Chemical Analysis

The chemical analysis procedure used the same standard methods and protocols as those for nitrogen removal in Chapter 4 (see Table 4-3), but with particular focus on phosphorus constituents (TP and ortho-P). Carbon for the reactor influent and effluent was fractionated into particulate COD (pCOD), colloidal (cCOD), and soluble (sCOD) using multiple rounds of filtering. COD was measured via Method 5220 D of Standard Methods. A portion of the raw sample was preserved for COD and TP analysis, a portion was vacuum filtered over 1.5 μm glass-fiber filter (Whatman, USA). 10 mL of filtrate was stored for COD analysis, and 40 mL was passed over a 0.45 μm mixed cellulose ester filter (HAWP, MilliporeSigma, Burlington, MA) for analysis of dissolved constituents: nitrate (Method 4500-NO_3^- C), and orthophosphate (Method 4500-P E). The remaining portion (roughly 100 mL) of secondary filtrate was used for flocculated & filtered (floc & filtered) COD—1 mL aluminum sulfate was added to 100 mL secondary filtrate and rapidly mixed for 2 min. After 30 min of settling, 10 mL were preserved for COD analysis (M. C. Wentzel et al., 2000).

Phosphorus was fractioned between total phosphorus and dissolved phosphorus, as described by the filtering protocol above. To measure TP, raw samples from the influent, effluent, and mixed liquor were subjected to digestion with potassium persulfate and measured using Method 4500-P-J and E of Standard Methods (*Standard Methods for the Examination of Water and Wastewater*, 2017). Total phosphorus was validated using a fixed suspended solids (FSS) mass

balance on WAS collected at the time of wasting. Ortho-P was also measured with Standard Method 4500-P E after filtering samples with 0.45 μm cellulose filter (HAWP, Millipore-Sigma) and without the alkaline digestion.

Three milliliters of the filtrate were used for VFA determination via ion chromatography (Dionex, U.S.A) with a Dionex DX 100 conductivity detector (Smith et al., 2013). The VFA consumption curve in the liquid filtrate from anaerobic profile samples were completed on samples with and without the supplemental acetic acid. PHB accumulation in the mixed liquor was captured via gas chromatography of digested solids collected on the glass-fiber filter. To measure PHB content, mixed liquor biomass samples from individual profile points were stored on the glass-fiber filters, and freeze-dried at -20°C for preservation until analysis. At the time of analysis, filters were thawed at room temperature, biomass was removed from the filter and weighed, and then digested via a modified propanolysis with 3:1 methanol:HCl solution at 100°C for 18 hours (Riis & Mai, 1988; Furrer et al., 2007; Werker et al., 2008). Prior to digestion, the mixture was spiked with 200 μL of 10 mg/L benzoic acid internal standard. The organic phase was eluted with 100% v/v hexane, and one microliter was submitted to a HP 6890 gas chromatograph (Hewlitt Packard, USA) with flame ionized detection (GC-FID). The gas chromatograph was equipped with an HP-5 column (Hewlitt Packard, USA) and was run with the following conditions: 1 μL injection volume, 250°C injection temperature, nitrogen carrier gas 55 mL/min, 30:1 split ratio. The oven was programmed as such: 5 min hold at 70°C, delta 10°C to 290°C, 10 min hold. The polyhydroxybutyrate peak was determined from digestion of pure standards: pure poly[(R)-3-hydroxybutyric acid] of natural origin, poly(3-hydroxybutyric acid-co-3-hydroxyvaleric acid) of natural origin with 8 mol% polyhydroxyvalerate (PHV) (Millipore-Sigma, USA). The digestion method was validated through digestion of polyhydroxybutyrate (PHB) biopolymer granule, 5 mm

nominal size (Millipore-Sigma, USA). The concentration of intracellular PHB was calculated by dividing the area under the curve for peaks at retention time 6.7 min by the benzoic acid curve at retention time 12.9 min.

A portion of the biomass from two profile samples were also checked for intracellular glycogen. A glycogen assay kit was obtained (Cayman Chemical, USA), and a portion of the preserved biomass for PHB analysis was hydrolyzed by amyloglucosidase. The formed β-glucose hydrolysis product reacted with kit-supplied horseradish peroxidase and 10-acetyl-3,7-dihydroxyphenoxazine (ADHP) to produce a fluorescent resorufin. Absorbance of the assay mixture was then measured spectrophotometrically at 570 nm.

5.3.4 Microscopic Analysis

Mixed liquor samples from the bioreactors were collected at various points along the anaerobic/aerobic and anaerobic/anoxic cycles from March 2021 to August 2022. Detailed analysis on floc characteristics were performed in parallel research (H. He et al., 2022). For the purposes of this investigation, mixed liquor samples were subjected to PHA and Neisser staining, following proper sample handling and staining methods to visually inspect the inverse relationship between accumulation and degradation of stored intracellular constituents (Jenkins et al., 2004; Hennessy, 2020). Photographic observations of Reactor 2 and Reactor 4 mixed liquor flocs were made using light microscopy under direct illumination (Zeiss Axioplan EL-Einsatz, White Plains, NY, USA) to inspect whether glycogen accumulating organisms (GAOs) were proliferating in the A/O and anaerobic/anoxic reactors.

5.3.5 Biomolecular Methods and Metagenomic Analysis of Annotated Bio-P Genes

DNA Extraction and Sequencing: A total of 52 mixed liquor samples were taken for biomolecular analysis between February 2021 and August 2022. Parallel research was conducted on 42 samples using 16s rRNA Illumina sequencing, when the reactors were VFA-limited (driven by fermentation of influent wastewater only), to identify taxonomy and microbial community dynamics (H. He et al., 2022). Chemical analyses were also conducted on these mixed liquor samples (see Section 5.3.3 for details). Five mixed liquor samples from each reactor were taken alongside profiling samples while the reactors were operating at steady state and supplemented with acetic acid (April to August 2022). These samples were stored at -80°C prior to analysis. DNA extraction was conducted according to Pinto et al. (2012) using a Maxwell 16 LEV Blood/DNA kit (Promega Corporation, WI, USA). Lysis buffer was added to mixed liquor samples during three rounds of bead-beating and 1 mL of the aqueous phase was collected. Viable DNA concentrations were estimated using Qubit (Invitrogen, Waltham, MA, USA). Extracted DNA was submitted to the University of Michigan Advanced Sequencing Core for shotgun sequencing, and sequences were generated on an Illumina NovaSeq S4 300 cycle (Illumina Inc., San Diego, CA, USA) in paired-end 150 bp reads.

Bioinformatic quality control, assembly, and annotation: Analysis was completed on the University of Michigan Great Lakes High-Performance computing cluster and following a standard metagenomic workflow (see Appendix Figure D-1) to generate contiguous sequences (contigs) and eventually metagenomic-assembled genomes (MAGs) for known and putative PAO and DPAO bins. Quality control was completed using bbduk, the Joint Genome Institute's (JGI) BBTools package (Bushnell, 2014), to initially assess the short reads, as well as filter and remove Illumina adapters, index sequences, and PhiX genome used in sample processing or as internal

standards by the Sequencing Core. After eliminating low-quality or erroneous reads, the five sequence sets from each respective reactor were co-assembled into contigs using MEGAHIT, kmer lengths 21 to 255 and a step size of 8 (D. Li et al., 2015). Short reads were then mapped to the contigs using bowtie2 (Langmead & Salzberg, 2012). A consolidated file with all gene calls and annotated contigs from each reactor was imported into an Anvi'o v.7.1 collection (Eren et al., 2021).

Gene annotation and categorization: The KEGG GhostKOALA online database (Kanehisa et al., 2016) was used for taxonomic annotation. Initial categorization of annotated contigs into genus-level categories was done using GhostKoala data. However, because downstream analysis relied on the ability to separate PAO/DPAO groups from closely-related relatives in the larger bacterial community, e.g., *Ca*. Accumulibacter phosphatis versus other non-PAO species within the larger *Ca*. Accumulibacter genera, the Anvi'o bins were updated with species-level taxonomic classification using an add-on classifier package called Kaiju (Menzel et al., 2016). The final Anvi'o collection for each reactor contained multiple manually-created bins categorized by genus- and species- level taxonomy with split contigs and fully annotated gene calls.

Typical binning methods utilize differential coverage or nucleotide composition (e.g., GC gene content, tetranucleotide frequency) to fingerprint individual community members (Dick, 2019). As a means of validating our annotated gene calls contained in the Anvi'o collection, the assembled contig sequences (prior to annotation) were merged into a single fasta file with reference genomes of known and putative PAO and DPAO species from the JGI database (see Appendix Table D-1). Together, this combined file with reactor sample contigs and known genomes were binned using a tetra-nucleotide emergent self-organizing map (tetra-ESOM) (Ultsch & Mörchen, 2005) and Vizbin (Laczny et al., 2015) using 8kb contig fragments. Fragments that visually

clustered in the two programs were assumed to belong to an individual species of organisms, and those that clustered with the reference PAO/DPAO genome sequences were assumed to be closely-related. Since our gene set of interest was manageable, individual gene calls for a particular species and their associated contigs were separated from each Anvi'o bin and manually checked to ensure they also belonged to both VizBin, and tetra-ESOM bins, respectively. Finally, gene taxonomy was manually verified again through submission of nucleotide sequence to NCBI Basic Alignment Search Tool (BLAST) v.2.11.0 (Sayers et al., 2020) before final statistical analysis. The rationale for using multiple binning strategies in this way was to ensure that individual genes, such as *ppk1*, had consensus from multiple binning and annotation programs as being associated with a particular PAO/DPAO.

Metabolic Visualization of Gene Coverage and Statistical Analysis: The Anvi'o bins were examined to identify the presence or absence of critical genes for each PAO/DPAO taxonomic group. We looked for specific genes encoding for bio-P metabolic enzymes, including *ppk1*, *glgAB*, *glgPX*, *phaCE*, *phaZ*, *narGHI* and *napAB* (S. He et al., 2007; Kristiansen et al., 2013; Wang et al., 2014; Petriglieri et al., 2021; Klein et al., 2022). Relative abundance was determined by multiplying the mean coverage of the entire bin by the length of the bin, to determine the total sequences in the bin, then dividing this value by the length of reads Illumina produces per sequence (150 bp), and then again by the total number of sequences in the sample calculated during the initial quality assessment. The average relative abundance was then calculated for five samples from both reactors.

$$Relative\ Abundance\ (\%) = \frac{Mean\ Coverage * Leng\quad of\ bin\ (bp)}{150\ bp * Sequences\ in\ Sample} \qquad (3)$$

The gene calls from each bin were submitted back to KEGG's Reconstruct Tool (Kanehisa & Sato, 2020; Kanehisa et al., 2022) to visually map metabolic pathways using their original set of Kegg orthology (KO) identifiers. Only pathways designated with 100% completion were considered as part of the taxonomic evaluation. Finally, a phylogenetic tree was generated with MEGA11 using the Maximum Likelihood method (K Tamura & Nei, 1993; Koichiro Tamura et al., 2021) and a bootstrap consensus of 500 replicates to visualize the distance between *ppk1* genes within each generated bin and species from the list of references.

5.4 Results and Discussion

The resulting data from modeling, wet chemistry chemical analysis, and biomolecular methods are consolidated below. Computer model simulation conducted in SUMO was conducted to provide theoretical conditions for a hybrid MABR combined with a nitrogen and bio-P removal system. The performance of the simplified experimental system that was fed domestic wastewater and contained either anaerobic/anoxic or anaerobic/aerobic zones for BPR was characterized using chemical analyses. Furthermore, a metagenomic analysis was conducted to evaluate the DPAO population and selected relevant functions.

5.4.1 Modeling Estimates of Ortho-P Removal

One of the major unknowns in hybrid MABR technology is how to optimize the design specifically for bio-P removal. Although early evidence suggests enhanced biological phosphorus removal (EBPR) is possible at larger scale treatment facilities (Kunetz et al., 2016; Q. Li, 2018; Bicudo et al., 2019), there is little research currently projecting how and why an integrated MABR system treating domestic wastewater would decrease effluent phosphorus. Incorporating bio-P removal into the hybrid MABR process necessitates use of a somewhat longer suspended growth

SRT to accommodate the slower growing PAOs, compared to typical denitrifying heterotrophs (Grady *et al.* 2011; Sun *et al.* 2015;). Using a total SRT of 4 days, and a typical domestic influent COD/TN composition (11 mg-COD/mg-N), the hybrid MABR process achieved optimal performance with an effluent ortho-P concentration of 0.17 mg-P/L and TIN concentration of 0.50 mg-N/L. The conventional A^2/O system achieved optimal performance at an SRT of 6.8 days. Even though good effluent ortho-P concentrations can be achieved in either case, the hybrid MABR process can achieve significantly lower effluent TIN at lower SRTs. Effluent TIN was already quite low for the hybrid MABR process as total SRT was increased to 4.0 days, while adverse effects on phosphorus removal was experienced by the conventional system at longer SRTs. Deteriorated phosphorus removal performance in the A^2/O system at longer SRTs are due to 1) nitrification in the aerobic zone resulting in nitrate-nitrogen recycle into the anaerobic tank; 2) less PAO biomass is wasted at longer SRTs, which directly decreases phosphorus-rich biomass wastage from the system (Grady *et al.* 2011). A summary of operation and performance characteristics of the hybrid MABR biological nitrogen and phosphorus removal process, compared to the conventional A^2/O biological nitrogen and phosphorus removal process, are presented in Table 5-1. The model results for effluent concentration and SRT are the most important for understanding DPAO function within the conceptual treatment system, and were used as a benchmark going forward with our pilot-scale bioreactors, covered in detail in the next sections.

Process oxygen requirements are lower for the hybrid MABR process compared to the conventional A^2/O process, while the capture of influent COD as biogas is similar. Approximately two-thirds of the total oxygen required for the hybrid MABR process would be transferred using the more efficient MABR units, and the need for mixed liquor circulation would be eliminated,

leading to a significant reduction in energy requirements compared to a conventional biological nitrogen and phosphorus removal process, similar to previous discussions above. The lower suspended growth SRT required for the hybrid MABR process results in a smaller bioreactor (35 percent smaller). These results highlight important advantages of the hybrid MABR biological nitrogen and phosphorus removal process compared to conventional configurations, particularly the ability to achieve lower effluent TIN. The principal impact of incorporating biological phosphorus removal into the hybrid MABR process is a larger bioreactor than designs for nitrogen removal only. The anoxic suspended growth treatment system will further evaluate the process options outlined here, specifically investigating what factors influence PAO growth and how bio-P removal could work in a fully anoxic suspended growth system fed with domestic wastewater. The modeling results herein provide a framework for designing such experiments.

Table 5-1 Comparison of Hybrid MABR with Conventional Biological Nitrogen and Phosphorus removal process with primary treatment

Item	Hybrid MABR	Conventional A²/O
Zone SRT (Days)		
Anaerobic	0.55	0.85
Anoxic	3.4	2.5
Aerobic	0.10	3.5
Total	4.0	6.8
MLR (%)	N/A[1]	400
Effluent TP (mg-P/L)	0.17	0.30
Effluent TIN (mg-N/L)	0.50	6.8
Biogas (mg Biogas COD/mg Influent COD, %)	37	36
Bioreactor Volume (m^3)[2]	6,300	9,800

[1]Not Applicable
[2]Mixed liquor conc. 3,000 mg/L MLSS

5.4.2 Reactor Bio-P Removal Performance

Water Quality Performance: The physical system did not experience the level of anoxic bio-P removal predicted by the modeling simulations, despite evidence of DPAO activity, under VFA-limited conditions. Orthophosphate concentrations in Reactor 4 effluent were measurably lower than the influent, and show a relatively stable pattern of anoxic phosphorus removal as a function of SRT after an inflection point of 3.0-4.0 days (solid green line, Figure 5-2) to a maximum of 60% removal at a 12.5-day SRT. The traditional aerobic phosphorus removal (Reactor 2) was appreciably higher with an average ortho-P removal of 81% (solid blue line, Figure 5-2). The raw data and calculated removal percentages can be found Appendix Section D-3. The model predicted roughly 97-98% of the influent ortho-P in a hybrid MABR system would be removed. The gap between model outcomes and reality brings to mind the anoxic hydrolysis outcomes described in Chapter 4. We demonstrated in the previous chapter that the extent of anoxic

hydrolysis was reduced over longer SRTs compared to aerobic systems, which includes data from this phase of bio-P investigation (Chapter 4, Figure 4-6). Furthermore, a portion of the particulate and colloidal organic matter was found to be non-biodegradable by the anoxic biomass and not the aerobic biomass. From classical literature, Henze & Mladenovski (1991), the hierarchy of hydrolysis rate constants was established as aerobic > anaerobic > anoxic. With this logic, we deduce that some of the poor performance is attributed to reduced anoxic hydrolysis on particulate and colloidal organic matter to produce sufficient VFA for DPAO uptake. This can be investigated from multiple perspectives, including COD oxidation balances described previously.

All indications were that the reactors were operating at steady-state, and followed the same patterns of total and soluble COD oxidation from Chapter 4 previous. The reactors were housed indoors, and temperature was maintained between 16-18°C. After an SRT threshold of 4.5 days, the aerobic reactor was shown to have oxidized between 60-65% of the total influent COD. The anoxic reactor on the other hand, only oxidized 50% of the influent carbon at the longest SRT studied of 12.5 days. Both reactors had a gradually rising level of sCOD oxidation over the SRTs studied, reaching roughly 22-25% of the overall influent tCOD. This indicates that hydrolysis of particulate and colloidal matter was demonstrably lower in the anoxic reactors than the aerobic ones. producing useable fermented products to power the bio-P removal and was not a limiting factor in overall process design. Indeed, colloidal COD removal averaged 81% and 50% across all operating SRTs in Reactor 2 and Reactor 4, respectively (see Appendix Table D-3). These results also mirror the conclusion that overall carbon capture will be lower for bio-P treatment processes because more oxidative energy is necessary to power PAO metabolisms at longer SRTs.

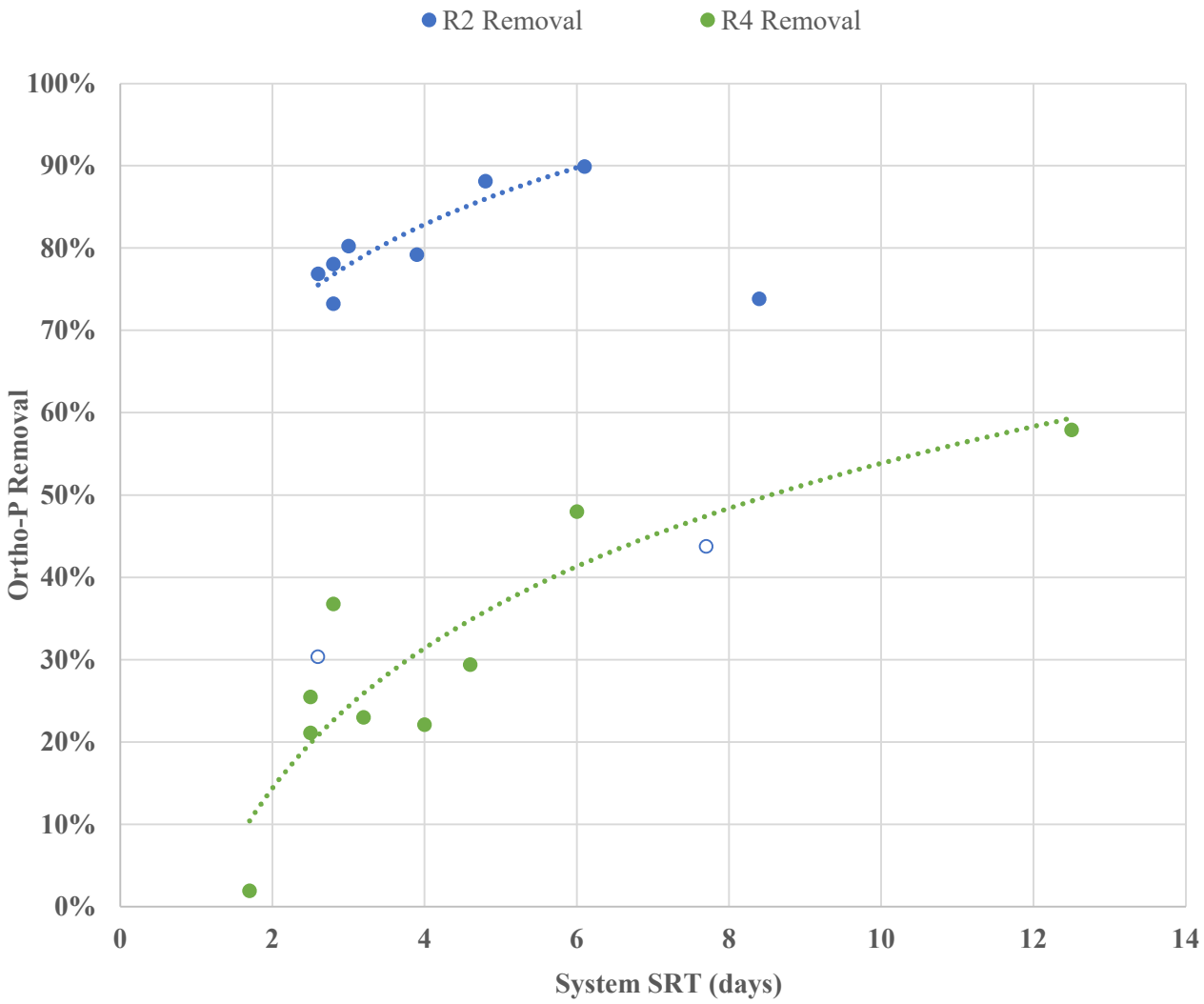

Figure 5-2 Reactor 2 & 4 Ortho-P removal under normal and cold-water conditions
Note: non-filled circles for Reactor indicate samples taken at washout (left), or during period of nitrate interference (right)

Individual Profile Assessment: It was clear from the bio-P profiles that both Reactors 2 and 4 were able to establish a population of PAOs and DPAOs, respectively, based on the amount of ortho-P reduction over the baseline influent concentration, and distinguishable ortho-P release and uptake patterns across each reactor's anaerobic cycles and aerobic/anoxic cycles (see Figure 5-3 below for example profile curve for each reactor). Key anaerobic processes were occurring as expected in Reactor 2, as seen from the evident release of orthophosphate and VFA uptake in Figure 5-3. Reactor 4 VFA uptake was comparable to that seen in Reactor 2 (average 44 mg-COD/g-VSS/hr versus 51 mg-COD/g-VSS/hr), however, the effects of VFA limitations can be seen in Figure 5-3, as initial influent acetic acid concentrations were less than 10 mg-COD/L. As a rule of thumb, 7.5 mg VFA is required for 1 mg phosphorus removal, and roughly 25 mg/L of VFAs are needed for robust bio-P (Mulkerrins et al., 2004; Randall et al., 2010). Insufficient fermentation caused by reduced anoxic hydrolysis products was likely a factor, as the average anoxic ortho-P release was modest and occurred at roughly half the rate of ortho-P release in Reactor 2 (28 mg-P/g-VSS/hr versus 14 mg-P/g-VSS/hr, see Appendix Table D-4).

The contrast in aerobic and anoxic processes for this time period is even starker. Reactor 2 average ortho-P uptake rate was nearly two and half times that of Reactor 4 (14 versus 5.5 mg-P/g-VSS/hr), which correlated in demonstrably lower overall removal performance. Furthermore, total phosphorus concentrations were also noticeably higher in Reactor 2 mixed liquor—ranging from 50 to 150 mg-P/L—than Reactor 4 mixed liquor—40 to 70 mg-P/L.

Temperature and SRT: Temperature and SRT likely contributed to the difficulty in producing stable bio-P removal, and this interaction is well-understood (Mamais & Jenkins, 1992).The control anaerobic/aerobic Reactor 2 saw removal of influent ortho-P modestly increase from 80 to 90% as SRT increased 3.9 to 6.1 days. Conversely, Reactor 4 was operated with SRTs

between 3.2 to 12.5 days in order to test the limits of the anoxic bio-P removal, and had ortho-P removal from 23% to 58% (Figure 5-2). It was determined that bio-P removal patterns could be mostly attributed to this SRT increases, because in this study period the system was contained indoors in a heated clearwell of AAWWTP. Average water temperature during this period was fairly constant between 15-18°C. Temperature effects PAO growth to a lesser extent than nitrifiers; the minimum aerobic SRT required for PAO growth at those temperatures is 1.8-2.0 days (Mamais & Jenkins, 1992). Moreover, temperature and SRT increases promote nitrification, and nitrate concentrations in the effluent and settled mixed liquor can recycle to the preceding fill cycle, interfering with anaerobic processes. According to Barker & Dold (1996), this puts PAOs in direct competition with heterotrophs, causing decreased bio-P capacity.

While testing under VFA-limited conditions, in November 2021, the building that housed the reactor units had a heating malfunction that drove system temperatures lower than 6°C, which is an inhospitable growth environment for PAOs and DPAOs (Mamais & Jenkins, 1992). This had a major effect on the biology in both reactors (compare normal and cold-water temperature averages in Appendix Tables D-2 & D-4), as ortho-P release and uptake rate decreased two- to three- fold under profiles taken at stable temperatures. The system was heavily monitored, and eventually both systems returned to pre-disruption performance. Increasing the anoxic system SRT and providing supplemental VFA were vital to culture a viable PAO-enriched biomass for stoichiometric evaluation.

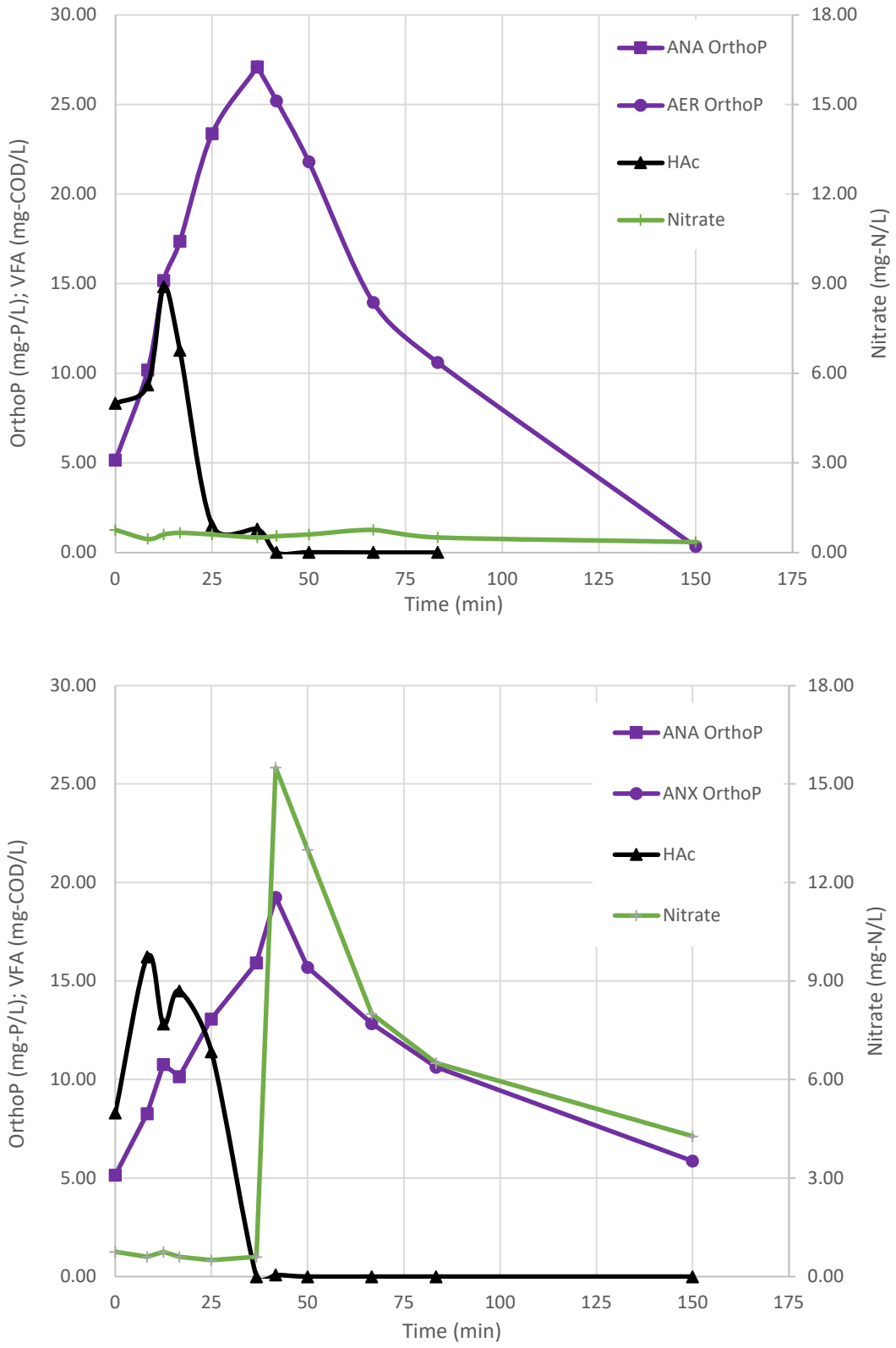

Figure 5-3 Anaerobic and Aerobic/Anoxic Profile Sample for Reactor 2 (top) and Reactor 4 (bottom)
Note: Profile sample taken March 2021 under VFA-limited conditions

Overall, the anoxic suspended growth biomass was difficult to control, and produce consistent and repeatable quality effluent despite raising SRTs over those predicted in modeling results. This was curious considering there were indications that fermentation was occurring in the anaerobic cycle, and the appearance of characteristic ortho-P release, but comparatively less release and uptake than the aerobic control. Even at an optimal conditions, much longer than would be theoretically necessary to prevent washout (SRT of 12.5 days and 18°C temperatures), Reactor 4 achieved 58% ortho-P reduction between influent and effluent. The results from profiling samples suggest that reduced anoxic hydrolysis, known to hydrolyze only a fraction of the particulate and colloidal organic matter as aerobic hydrolysis, was limiting the fermentation of soluble substrates. Side-by-side comparison of the A/O and aerobic/anoxic reactor fed with the same influent show variable patterns of fermentation and acetic acid uptake, as well as a considerably lower ortho-P release pattern.

Alternatively, the extent to which bio-P performance was successful in Reactor 4 might also be dependent on metabolic processing of stored levels of carbon, i.e., PHA and glycogen. DPAO inefficiency in converting VFA to intracellular carbon and then into usable energy for oxidative phosphorylation could certainly hamper the population in a dynamic system and challenging environmental conditions. We supplemented the VFA-limited influent wastewater to the reactors with modest amounts of acetic acid solution during filling cycles, and repeated the profiling exercises.

5.4.3 Bioreactor Stoichiometry with VFA Supplementation

System temperatures were restored (18-25°C) in March through August 2022. Two profile sample were taken in April, three in May, and one sample was taken from each reactor in August 2022 when supplemental acetic acid was utilized to promote stability in the DPAO population.

The reactors were operated at SRTs that would promote a healthy PAO/DPAO population (5.0 days for Reactor, 8.0 days for Reactor 4), and results reflect this change in operation positively facilitated growth compared to VFA-limited conditions. For instance, Reactor 4 orthophosphate removal with supplemental VFA reached 80% despite a somewhat conservative SRT of 8.0 days, and effluent concentrations dropped to 0.3 mg-P/L. However, ortho-P release and uptake rates were still demonstrably lower in Reactor 4 than Reactor 2 by roughly half (see Appendix Table D-5). It was necessary at this point to consider how inefficiency in the anoxic mixed liquor biomass was effecting the processing of carbon through the calculation of stoichiometric ratios between the key constituents in the anaerobic and aerobic/anoxic cycles.

Some of the key stoichiometric ratios to consider are divided between the anaerobic and aerobic/anoxic cycle—including P/HAc, which represents the anaerobic efficiency in released ortho-P per amount of acetic acid consumed; PHB/HAc, the amount of intracellular carbon stored from acetic acid; and P/PHB, which describes the amount of ortho-P taken up per amount of PHB oxidized for energy (Smolders et al., 1994a). In the anoxic cycle of Reactor 4, we specifically looked at the ratio of oxidized PHB to the amount of supplied nitrate consumed, PHB/NO_3-N. All of these values, when converted to molar equivalents, reflect certain elements of the chemical stoichiometry. Table D-5 shows the comparison of these values for the profile samples taken when VFA was supplemented to the reactor. In terms of anaerobic processing of HAc, Reactor 2 appears to slightly exceed the expected stoichiometric value for the amount of ortho-P released—0.45 mol-P for 1.0 mol-C of acetic acid compared to the expected value of 0.37 mol-P/mol-C in the metabolic model (Smolders et al., 1994a). Reactor 4 had a P/HAc ratio slightly below the stoichiometric value, 0.31 mol-P/mol-C. Both of these values, however, were within the measured ratios found in the phosphorus-limited measurement by Smolders et al. (1994a) and closest to those

found in the measurements of Wentzel et al. (1988)Wentzel 1988 under acetic acid limitations. Smolders indicated there can be a large range in this particular measured ratio, and is highly dependent on pH due to the energetics required for transport of acetate across the cell membrane (Smolders et al., 1994a). Furthermore, anaerobic maintenance also results in more ortho-P release at higher SRTs, but the value for mATP in our study was slight and was factored out of the overall ortho-P release concentrations (average 0.03 mg-P/L/min). Lower P/HAc ratios in Reactor 4 could be attributed to the presence of glycogen accumulating organisms (GAOs) causing VFA uptake without ortho-P release due to lack of stored polyphosphate. Microscopic evaluation did not indicate any of the standard signs of GAO prevalence, i.e., tetrad formation with glycogen accumulation.

In the anaerobic metabolic model research, Smolders mentions two alternative possibilities for the production of NADH as acetic acid is converted into stored PHB: the anaerobic TCA cycle, and the Embden-Meyerhof pathway (Smolders et al., 1994a). The former assumes some acetate is oxidized as it is converted to PHB, but comes at the expense of polyphosphate which must be degraded in order to produce ATP. The latter hypothesized that the degradation of stored glycogen was instrumental in lowering energy costs for anaerobic processes, and is widely accepted in bio-P models today. Utilization of glycogen storage has implications on the amount of PHA that is produced versus a purely TCA-cycle driven metabolism, and this shows itself in the stoichiometric equations. Smolders (1994) estimates a value of 0.89 for the TCA model, and 1.33 for the glycogen model. Our results show an exact reproducibility of the PHB/HAc found for the glycogen model (1.3 mol-C/mol-C) using the same aerobic design in Reactor 2, which indicates that the gas chromatography methods used were valid. Reactor 4 acetic acid storage was less in line with theory; the PHB/HAc ratio was over double that of the theoretical values (2.9 mol-C/mol-C)

implying that an unknown source of carbon was being metabolized by DPAOs to generate stored PHB product. Initially, we considered excess glycogen as a possible source, but results were inconclusive. See Appendix Section D-5 for more discussion on intracellular glycogen concentrations. It was likely that GAOs were contributing to VFA uptake and stored PHB concentrations in the biomass, without providing ortho-P uptake via oxidative phosphorylation. However, this interference was small and did not impact the DPAO population in Reactor 4, considering microscopic evaluation of mixed liquor flocs were negative for GAO tetrad formation. The average PHB/NO_3-N ratio for all profiles taken in Reactor 4 was 3.5 mol-C/mol-N, whereas the stoichiometric ratio was 2.0 mol-C/mol-N. This difference implies carbon oxidation was not being utilized efficiently during the critical reaction of the bio-P metabolism, and was perhaps instead being shunted into regeneration of EPS, cell maintenance, or cell growth. Finally, the inherent system inefficiency is also reflected in the P/PHB ratio, a direct measure that ties together bio-P and PHB oxidation. Reactor 2 had an average P/PHB ratio of 0.21 mol-P/mol-C, which was lower than the stoichiometric value of 0.27 mol-P/mol-C for the aerobic bio-P metabolism. However, Reactor 4 averaged a value of 0.04 mol-P/mol-C over profile samples, well short of the stoichiometric value for anoxic bio-P of 0.23 mol-P/mol-C.

The critical final measure to evaluate major differences in the aerobic and anoxic Bio-P reactors is the P/O ratio. Using measured constituents from the profile samples in Phase 3, the mass of polyphosphate accumulation was measured (M_{pp}), and the mass of electron acceptor was estimated (M_O), allowing for substitution into Equation 3 from Smolders et al. (1994b). Smolders et al. also considered in their analysis the mass of oxygen consumed without phosphorus (M_O^{-P}) but this was ultimately found to be negligible. The values for α3 and ε were assumed to be 1.0 and 7.0, respectively, as described by Smolders et al. (1994b). The former (α3) corresponds to the

amount of ATP consumed to synthesize 1.0 mol of polyphosphate, often directly related to the addition of a phosphate group. The latter (ε) is a variable estimation of the thermodynamic efficiency to transport ortho-P into the cell, based on Gibbs free energy. An average value of 7.0 was considered acceptable for this analysis.

$$\frac{M_O^{+P}}{M_{PP}} = 1.125\left[\frac{\frac{\delta}{\varepsilon} + \alpha_3}{2.25\delta + 0.5}\right] \qquad (3)$$

It is noted in Smolders et al., 1994, that this formula is the same between aerobic and anoxic conditions with a 5/4 adjustment to aerobic coefficients because of the ratio of available electrons between nitrate (5) and oxygen (4). For simplicity, this was adjusted in our analysis by converting the mass of nitrate-N consumption to COD equivalents. The final values mirrored the results of Smolders et al., with δ = 1.7 for the aerobic reactor and 0.90 for anoxic, which speaks to the inherent inefficiency of the anoxic metabolism in terms of processing energy and storing polyphosphate.

Anoxic inefficiency or lower functional use of resources was seen at almost every stage of the alternating metabolic processes. However, there was no way to distinguish PAO and DPAO metabolic capacity via these chemical analyses alone, thus metagenomic methods were employed to examine differences in the aerobic and anoxic systems from a different perspective.

5.4.4 Metagenomic Evaluation of Aerobic PAO/Anoxic DPAO Population

Biomolecular analysis from collected biomass samples with VFA supplementation was anticipated to reveal insights about the genetic capacity of the two stable bio-P removal systems. Together with the stoichiometric approach in Section 5.5.5, we desired to show mechanistic differences of PAO and DPAO populations in their respective environments with the same influent, formerly a “black box”, in order to understand what differences might exist with an

anerobic/anoxic configuration performing bio-P removal with a developed DPAO population versus an anerobic/aerobic configuration and traditional aerobic PAO population.

On average, Reactor 2 produced $4.2x10^7$ and Reactor 4 produced $3.8x10^7$ total short sequence reads across five mixed liquor samples each. The assembled and annotated contigs, categorized with species-level taxonomy using kaiju, resolved into near-100% complete bins for *Ca*. Accumulibacter and *Dechloromonas*. The former contains known PAO species *Ca*. Accumulibacter phosphatis, whereas *Dechloromonas* sp. are considered putative PAOs (Chandran et al., 2017; Stokholm-Bjerregaard et al., 2017). It should be noted, many of the *Dechloromonas* species-level taxonomic annotations appeared as an unidentified "sp." classification instead of an actual result (e.g., *Ca*. Accumulibacter phosphatis). This was expected due to incomplete annotation databases, a common problem in metagenomic methods (Dick, 2019). It was also the rationale for using alternative binning strategies (tetra-ESOM and Vizbin) to cluster our contig sequences with putative DPAO groups. Reactor 2 *Dechloromonas* contigs clustered most closely with *Dechloromonas* phosphoritropha, while Reactor 4 *ppk1* contigs did not highly cluster with either putative DPAO reference genomes, but did appear to be related to *Dechloromonas* sp. from EBPRs found in Northern European studies (see Appendix Figures D-3 and D-4 for examples).

Each bin considered contained between 530 and 910 contigs. The final bin length for *Ca*. Accumulibacter phosphatis was $8.0x10^6$ bp for Reactor 2, and $7.7x10^6$ bp for Reactor 4; the *Dechloromonas* bin was $8.5x10^6$ bp for Reactor 2, and $6.8x10^6$ bp for Reactor 4. The average relative abundance was calculated using these values for the entire *Ca*. Accumulibacter genus bin (2.8% for Reactor 2, 3.2% for Reactor 4), which further broke down as species *Ca*. Accumulibacter phosphatis. The known PAO *Ca*. Accumulibacter phosphatis population was lower in anaerobic/aerobic Reactor 2 than anaerobic/anoxic Reactor 4 (1.5% and 2.0%, respectively). The

relative abundance of the putative PAO genus *Dechloromonas* followed the same trend with 1.8% for Reactor 2 and 2.8% for Reactor 4, although specific species could not be identified as mentioned above (Appendix Table D-6). Common GAO relative abundances were also included in the table. The calculated relative abundance of known GAO species *Ca*. Contendobacter and Propionivibrio were modestly elevated in Reactor 4 (0.80%, 0.40%) over Reactor 2 (0.2%, 0.0%), although these were lower than the mentioned DPAO species. It should be noted that outlier samples (Sample 1, and Sample 10) were separated from these averages.

A phylogenetic tree was constructed using the maximum likelihood method on *ppk1* sequences found in the reactor *Ca*. Accumulibacter and *Dechloromonas* bins, and annotated reference genomes of past EBPR research (Figure 5-4, Appendix Table D-1 for reference genomes). This particular enzyme-encoding gene was used for comparison because He et al. (2007) found ppk1 genes resolved species-level differentiation more accurately than the highly conserved 16s rRNA sequences. Figure 5-4 shows Ca. Accumulibacter *ppk1* genes from Reactor 4 were highly related to the known nitrate reducer *Ca*. Accumulibacter phosphatis Type IA (Flowers et al., 2009), and Ca. Accumulibacter regalis [BA-92 and BA-93] (Petriglieri et al., 2022). Meanwhile, the reactor's *Dechloromonas* ppk1 genes were more variable, and a clear distinction can be seen between them and the more novel putative PAOs *Dechloromonas* phosphoritropha or *Dechloromonas* phosphorivorans. These were the organisms that clustered with the larger contig assembly, but it appears from analysis of their ppk1 genes had closer phylogenetic proximity to *Dechloromonas* species common in other EBPR systems. With the wide genetic variation between species, it is plausible that both the *Ca*. Accumulibacter and *Dechloromonas* species seen here are facultative aerobes with the ability to denitrify, and are commonly found in traditional EBPR systems.

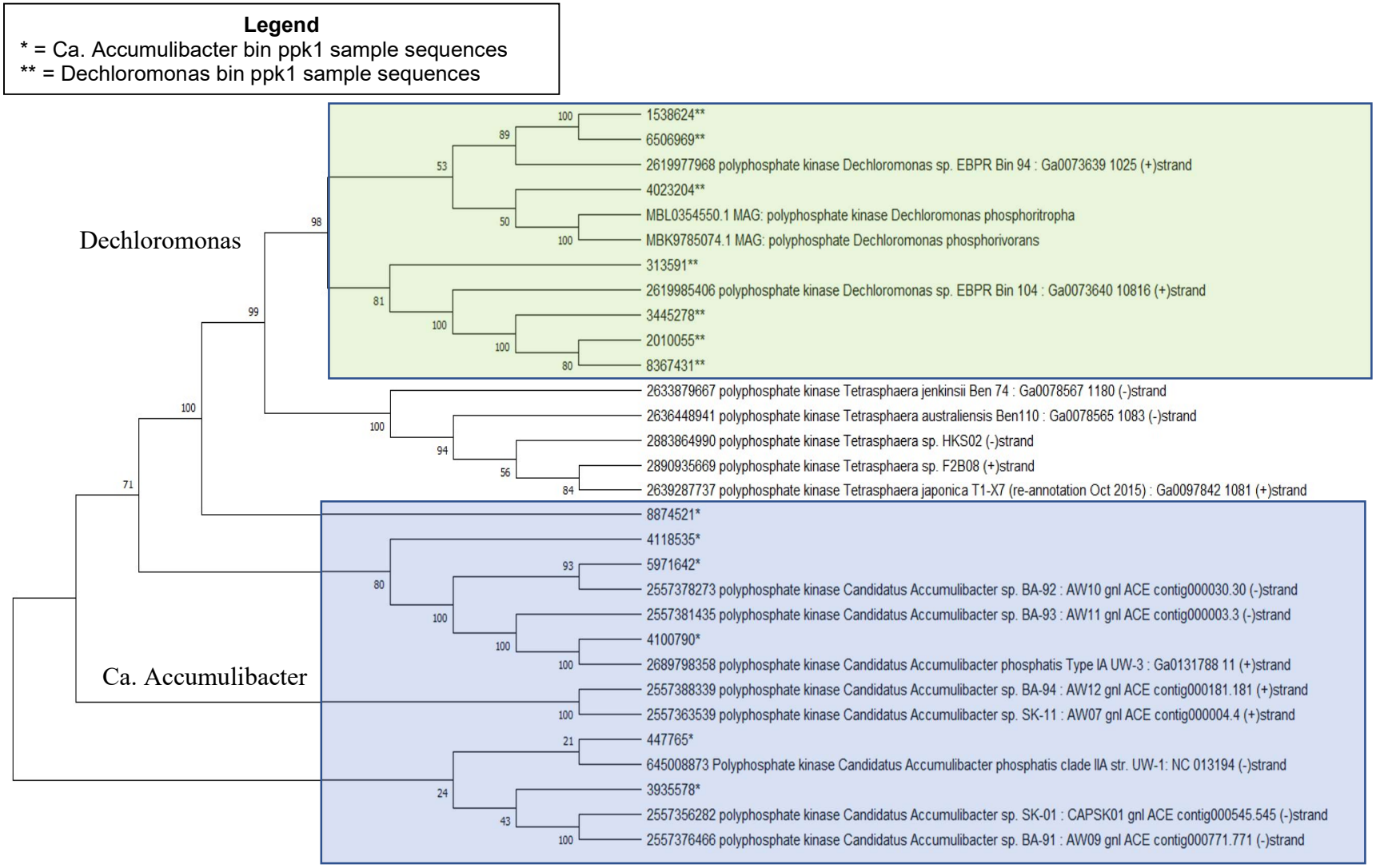

Figure 5-4 Phylogenetic tree for Reactor 4 ppk1 genes with JGI references

Note: Tree estimated using Maximum Likelihood method. Bootstrap consensus tree inferred from 500 replicates. Percentage of replicate tree with associated tax clustered together in the bootstrap test are shown next to the branches.

The final step was to further investigate the bins to reconstruct the complete set of genes mapping to key bio-P metabolic functions for each genus: oxidative phosphorylation (KEGG pathway: 00100); butanoate metabolism, which includes poly-β-hydroxybutyrate (PHB) generation (KEGG pathway: 00650); glycolysis/gluconeogenesis (KEGG pathway: 00010); and nitrogen metabolism, specifically denitrification (KEGG pathway: 00910, module: M00529). As expected, the *Ca*. Accumulibacter phosphatis species inside its larger bin contained genes encoding enzymes for electron transport (e.g., succinate dehydrogenase, fumarate reductase, and cytochrome complexes) stemming from the stoichiometric reducing agent NADH, ATP synthase via proton motive force (F-type, *atp*), inorganic pyrophosphatse (*ppa*), and finally polyphosphate kinase (*ppk1* or *ppk2*) to produce intracellular polyphosphate (Figure 5-5). No major differences were observed in the KEGG mapper reconstruction for oxidative phosphorylation and polyphosphate generation from ATP for either reactor samples, i.e., all genes necessary for oxidative phosphorylation, and polyphosphate generation from ATP were recovered from *Ca*. Accumulibacter and *Dechloromonas* bins in Reactor 2 and 4 (see green shaded enzymes Figure 5-5). This is evidence that both *Ca*. Accumulibacter and *Dechloromonas* species had the genes encoding denitrifying phosphorylation, the final critical step of bio-P removal, during VFA-supplemented conditions.

Other key enzyme-encoding genes, such as glycogen synthase (*glgA*, *glgB*), 3-polyhydroxybutyrate synthase (*phaC*, *phaE*), and periplasmic nitrate reductase (*nap*), were all present in *Ca*. Accumulibacter and *Dechloromonas* bins for both reactors. The gene encoding poly(3-hydroxybutyrate) depolymerase (*phaZ*) was only apparent in *Dechloromonas* bins for both reactors, although it is possible an alternative pathway could be utilized for PHB degradation during aerobic/anoxic phase. The periplasmic nitrate reductase gene (*nap*) was ubiquitous in the

both the aerobic and anoxic PAO/DPAO populations. The enzyme-encoding gene included three of the common major complexes (*napABD*) that are required to convert nitrate to nitrite. Moreover, the rest of the denitrification gene pathway (*nir*, *nor*, *nos*) was complete. It should be noted that genes for respiratory nitrate reductase pathway (*narGHI*) was not found in either reactors' *Dechloromonas* bin, and more importantly was not found in the Reactor 2 *Ca*. Accumulibacter bin, whereas it was found in the Reactor 4 *Ca*. Accumulibacter bin. The presence of respiratory nitrate reductase in the Reactor 4 *Ca*. Accumulibacter bin represented a major diversion from Reactor 2 samples. The presence of *nar* suggests that the anoxic environment selected for a small number of species capable of substituting nitrate for oxygen in the phosphorylation pathway, instead of forcing facultative aerobes to grow anoxically. However, the average gene coverage for *narGHI* was three-fold lower than *napAB* for *Ca*. Accumulibacter phosphatis (see Appendix Figure D-5 for full gene coverage results), so it is unclear the magnitude of this effect on the bio-P performance results. Periplasmic nitrate reductase genes (*napAB*) appeared to predominate in the *Ca*. Accumulibacter and *Dechloromonas* genera bins.

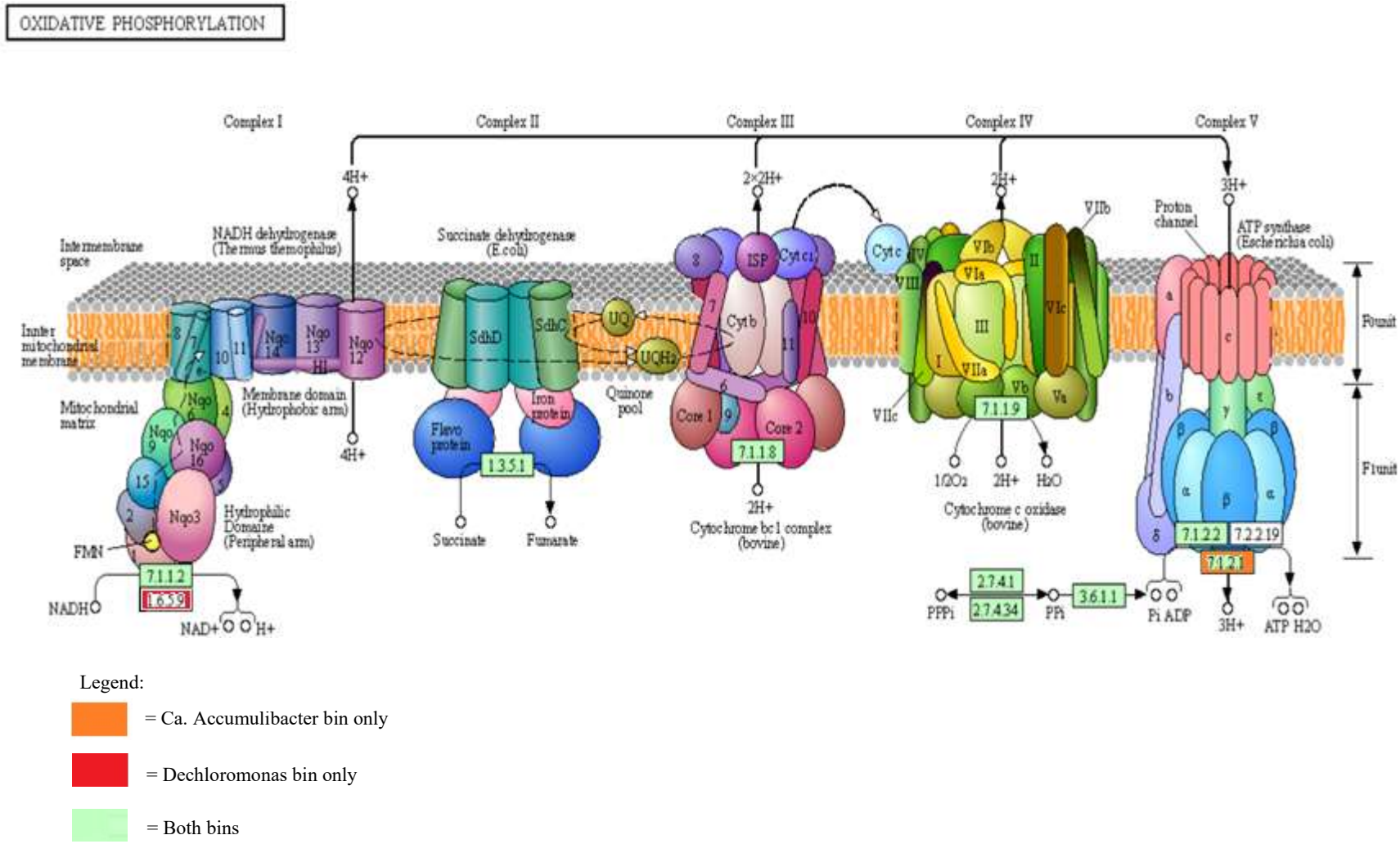

Legend:

= Ca. Accumulibacter bin only

= Dechloromonas bin only

= Both bins

Figure 5-5 Reactor 2/Reactor 4 KEGG pathway for oxidative phosphorylation

Final overall comparison of bio-P samples seems to point towards anoxic selection of nitrate-reducing species of known PAOs (specifically *Ca*. Accumulibacter phosphatis) and putative DPAOs in Reactor 4. The various clades of *Ca*. Accumulibacter phosphatis are known from past research to have denitrifying phosphorylation capability coupled specifically with nitrate reduction (Flowers et al., 2009, 2013), whereas *Dechloromonas* species are speculated to have denitrifying phosphorylation capacity (Petriglieri et al., 2021). Both genera contain complete sets of genes encoding for oxidative phosphorylation, and other enzymes that are critical to the overall alternating "feast/famine" bio-P metabolism. The gene coverage on these enzyme-encoding genes appear to correlate with each other, another sign they are working in concert to achieve an overall biological pathway. We conclude here, based on observations of nitrate reductase in the two genera annotated bins, that the lower functional inefficiency in the anaerobic/anoxic bio-P removal performance implicates respiratory (Nar) and periplasmic (Nap) nitrate reductase enzymes in the electron transport chain. In general, nitrate reduction results in two hydrogen (H^+) ions to generate a proton gradient across the cellular membrane for energy creation (as described in the introduction), and is considered about 40% as efficient at ATP generation as traditional oxidative phosphorylation involving the reduction of oxygen to water (Kuba et al., 1996; Oehmen et al., 2007). The NapABC complex, that was observed more frequently in this metagenomic analysis, resides in the periplasm and oxidizes ubiquinol, which releases two electron and two hydrogen (H^+) ions (Kern & Simon, 2009; Sparacino-Watkins et al., 2014). Nitrate is then reduced to nitrite via the transfer of those electrons in the NapAB portion of the complex. The respiratory enzyme Nar also produces a proton gradient via reduction of nitrate on the inside of the cytoplasm (González et al., 2006). However, it has been suggested that thermodynamic inefficiencies exist in the NapABC transport complex due to its reliance on formate oxidation and lower redox potential,

leading to less ATP generated per mol of reduction equivalent than Nar alone (Jepson et al., 2007; Gates et al., 2007; Sparacino-Watkins et al., 2014). Other research has suggested that Nap may counter some of the thermodynamic impediments with higher affinity to nitrate in the periplasm, or with various other sub-complexes (e.g., NapGH) to produce more translocated protons (Potter et al., 2001; Sparacino-Watkins et al., 2014), which could be the reason for observed bio-P removal, albeit in a less efficient manner. More research is required to deduce the specific roles of periplasmic and respiratory nitrate reductase have on bio-P removal. Our metagenomic evaluation was conducted to complement the stoichiometric analysis, but further analysis on the expression and activation of these enzymes in real-time (e.g., qPCR methods for quantifying transcription during anoxic periods, transcriptomics, or proteomics) would provide valuable knowledge as to which nitrate reducing enzymes are influencing bio-P performance in anoxic wastewater environments.

5.5 Summary and Conclusions

In this chapter, we provided evidence to further advance knowledge of fully anoxic bio-P removal in wastewater treatment systems through the use of advanced computer modeling, chemical analysis, and biomolecular techniques. This chapter served to expand on the nitrogen removal results of Chapter 4, in which practical research has been ongoing with full-scale systems. The mechanisms of combined nitrogen and phosphorus removal with an enriched DPAO biomass in a fully anoxic environment, however, has been an understudied topic. The results from reactor treatment over a long time-scale in dynamic conditions strongly correlate to past metabolic models, but highlight what differences exist between side-by-side anaerobic/anoxic and anaerobic/aerobic configurations, and use chemical and biological perspectives to explain why those differences manifest themselves.

Continued computer simulation of a hybrid MABR/anoxic suspended growth, using similar parameters as Chapter 4, predicted a viable bio-P removal operation through the addition of an anaerobic zone upstream of the MABR anoxic zones. Model results over various SRTs predicted ortho-P concentrations below 0.20 mg-P/L (98% overall removal), TIN concentrations below a conventional A^2/O system (0.50 versus 6.8 mg-N/L), at roughly two-thirds the needed treatment volume. Carbon capture was predicted by the model to be modestly lower due to longer system SRT and the combined nitrogen and phosphorus process needs, which also resulted in moderate increases to process oxygen requirements. However, considering the demonstrated advantages over the conventional AS options, including lower effluent TIN and footprint reduction, there lacked apparent downsides to implementing bio-P with a hybrid MABR for nitrification and phosphorus removal using nitrate in the anoxic suspended growth.

The application of anoxic suspended growth in the field treating dynamic sewage from a treatment plant proved more difficult and worse performance than the computer model would show. Mass balances on an anerobic/anoxic SBR during Phase 1 sampling estimated optimal ortho-P removal at 58% under a 12.5-days system SRT, compared to over 90% removal at a 6-day SRT for the anaerobic/aerobic reactor. The gap in performance was even wider during low temperature conditions. In terms of carbon capture, effluent cCOD concentrations were consistently elevated across the SRTs studied in Chapter 5 and Chapter 4, although these values did appear to stabilize at longer SRTs. The reduced hydrolysis of particulate and colloidal organic matter observed in Chapter 4 appeared to play a significant role in the amount of fermentation available to the anaerobic/anoxic system. VFA limitations severely impacted performance compared to the anaerobic/aerobic system that was shown to have near complete hydrolysis of this organic matter. Profiling the constituents across individual cycles gave us more insight about the

differences in anaerobic and aerobic/anoxic processing rates of PAOs in the mixed liquor. Acetic acid (the most prevalent VFA in wastewater) was measured relative to the distinguishable ortho-P release during the anaerobic cycle, and subsequent aerobic ortho-P uptake. The anoxic reactor process rates were shown to be approximately half of its aerobic counterpart. With this knowledge, a potential solution would be to allow for sufficient fermentation, such as side-stream fermentation configurations, to direct more resources to the anoxic suspended growth that may struggle to convert anaerobically-stored products to energy using nitrate reductase. Overall, the anoxic suspended growth portion of the proposed hybrid MABR system shows potential, because in a full-scale treatment system, increased fermentation of organic material to produce VFAs would result in less sCOD diffusing into the biofilm for oxidation by heterotrophs. Competition between nitrifiers and heterotrophs for oxygen is a common issue in MABR treatment systems, thereby leaving more resources for the nitrifying population to generate nitrate. Integrated research of fermentation and bio-P removal with MABR biofilm and anoxic suspended growth at larger scale will obviously be needed to assess this theory. More research on this topic is being conducted at the pilot-scale plant in Nanjing, China, studying nitrogen and phosphorus removal.

Historical research has shown inefficiency in DPAO metabolism could also explain reduced ortho-P removal in Reactor 4 measured performance. The known P/O ratio of DPAOs was calculated to be 1.0 versus 1.85 for aerobic PAOs. At the beginning of study, we were unsure what effect selective forces might play in DPAO adaption in a fully anoxic wastewater environment, considering there were examples of phosphorus removal coupled with nitrate uptake in small-scale lab studies (Flowers et al., 2009, 2013), as well as at larger scale in MABR systems (Underwood et al., 2018; Kunetz et al., 2016; Q. Li, 2018). However, we reported an anoxic P/O ratio in this study of 0.90, which aligned well with past fundamental research. Our experiments with

supplemented acetic acid showed better ortho-P removal than on VFA-limited wastewater alone, but our overall difficulty in anoxic bio-P removal seemed to rebut the process models that suggest fully decoupling nitrate generation would result in better performance than a traditional A^2/O configuration. Process modelers attempting to simulate hybrid MABR systems should modify their parameters to accurately reflect the lower efficiency of DPAOs than PAOs to utilize intracellular products in the denitrifying phosphorylation pathway.

In this study, we used metagenomic techniques to examine this issue from a different perspective by sequencing the genetic capacity of PAOs/DPAOs in their respective systems. Genomic bins were created to sort the various PAO/DPAO populations in samples taken from anaerobic/aerobic and anaerobic/anoxic reactors fed with the same influent wastewater. From this evaluation, a known PAO (*Ca*. Accumulibacter phosphatis) and a putative PAO (*Dechloromonas* sp.) were shown to have complete bins and high relative abundance in both reactors. Mapping the genes contained in these bins showed a full suite of enzymes necessary for phosphorus accumulation, including the important polyphosphate kinase (*ppk*) gene for intracellular poly-P production. However, apparent differences in nitrate reduction—including the presence of respiratory complex (*narGHI*) in the *Ca*. Accumulibacter phosphatis bin—were observed between Reactor 2 and 4 samples. The presence of respiratory nitrate reductase was overshadowed by a higher prevalence of periplasmic nitrate reductase complexes (*napABC*), which were observed in both *Ca*. Accumulibacter and *Dechloromonas* bins. Past research has concluded the Nap may not be as energetically favorable to produce hydrogen ions in the proton motive force for energy generation. This could translate to a less efficient bio-P removal metabolism, as our chemical results would imply, although future research should focus on quantifying the expression of various nitrate reductases to better understand this dynamic.

5.6 References

Ahn, K., & Kornberg, A. (1990). Polyphosphate kinase from Escherichia coli. Purification and demonstration of a phosphoenzyme intermediate. *Journal of Biological Chemistry*, *265*(20), 11734–11739. https://doi.org/https://doi.org/10.1016/S0021-9258(19)38459-5

Almasi, A., & Pescod, M. B. (1996). Wastewater treatment mechanisms in anoxic stabilization ponds. *Water Science and Technology*, *33*(7), 125–132. https://doi.org/https://doi.org/10.1016/0273-1223(96)00347-2

Barker, P. S., & Dold, P. L. (1996). Denitrification behaviour in biological excess phosphorus removal activated sludge systems. *Water Research*, *30*(4), 769–780. https://doi.org/https://doi.org/10.1016/0043-1354(95)00217-0

Bicudo, J., Heffernan, B., Klassen, A., Rao, M., McConomy, J., Syron, E., & McDermott, L. (2019). A one year demonstration of nutrient removal with Membrane Aerated Biofilm Reactor (MABR). *Nutrient Removal and Recovery Symposium 2019*.

Bushnell, B. (2014). *BBMap: Short read aligner, and other bioinformatic tools*. Joint Genome Institute. https://sourceforge.net/projects/bbmap/

Carlson, A. L., He, H., Yang, C., & Daigger, G. T. (2021). Comparison of hybrid membrane aerated biofilm reactor (MABR)/suspended growth and conventional biological nutrient removal processes. *Water Science and Technology*, *83*(6), 1418–1428. https://doi.org/10.2166/wst.2021.062

Chandran, K., Smith, C. J., Bruno-Barcena, J. M., Stokholm-Bjerregaard, M., Mcilroy, S. J., Nierychlo, M., Karst, S. M., Albertsen, M., & Nielsen, P. H. (2017). *A Critical Assessment of the Microorganisms Proposed to be Important to Enhanced Biological Phosphorus Removal in Full-Scale Wastewater Treatment Systems*. https://doi.org/10.3389/fmicb.2017.00718

Dick, G. (2019). *Genomic Approaches in Earth and Environmental Sciences* (First). Wiley Blackwell.

Downing, & Nerenberg, R. (2008). Total nitrogen removal in a hybrid, membrane-aerated activated sludge process. *Water Research*, *42*(14), 3697–3708. https://doi.org/10.1016/j.watres.2008.06.006

Eren, A. M., Kiefl, E., Shaiber, A., Veseli, I., Miller, S. E., Schechter, M. S., Fink, I., Pan, J. N., Yousef, M., Fogarty, E. C., Trigodet, F., Watson, A. R., Esen, Ö. C., Moore, R. M., Clayssen, Q., Lee, M. D., Kivenson, V., Graham, E. D., Merrill, B. D., … Willis, A. D. (2021). Community-led, integrated, reproducible multi-omics with anvi'o. *Nature Microbiology*, *6*(1), 3–6. https://doi.org/10.1038/s41564-020-00834-3

Filipe, C. D. M., & Daigger, G. T. (1999). Evaluation of the Capacity of Phosphorus-Accumulating Organisms To Use Nitrate and Oxygen as Final Electron Acceptors: A Theoretical Study on Population Dynamics. *Water Environment Research*, *71*(6), 1140–1150. https://doi.org/10.2175/106143097x122103

Flowers, J. J., He, S., Malfatti, S., Glavina Del Rio, T., Tringe, S. G., Hugenholtz, P., & Mcmahon, K. D. (2013). Comparative genomics of two ‘Candidatus Accumulibacter’ clades performing biological phosphorus removal. *The ISME Journal*, *7*, 2301–2314. https://doi.org/10.1038/ismej.2013.117

Flowers, J. J., He, S., Yilmaz, S., Noguera, D. R., & McMahon, K. D. (2009). Denitrification capabilities of two biological phosphorus removal sludges dominated by different Candidatus Accumulibacter clades. *Environmental Microbiology Reports*, *1*(6), 583–588. https://doi.org/10.1111/j.1758-2229.2009.00090.x

Furrer, P., Hany, R., Rentsch, D., Grubelnik, A., Ruth, K., Panke, S., & Zinn, M. (2007). Quantitative analysis of bacterial medium-chain-length poly([R]-3-hydroxyalkanoates) by gas chromatography. *Journal of Chromatography A*, *1143*(1), 199–206. https://doi.org/https://doi.org/10.1016/j.chroma.2007.01.002

Gao, H. (2018). *Nitrogen and Phosphorus Removal and Energy Production via Microbial Nitrous Oxide Generation from Wastewater*. Northwestern University.

Gates, A. J., Richardson, D. J., & Butt, J. N. (2007). Voltammetric characterization of the aerobic energy-dissipating nitrate reductase of Paracoccus pantotrophus: exploring the activity of a redox-balancing enzyme as a function of electrochemical potential. *Biochemical Journal*, *409*(1), 159–168. https://doi.org/10.1042/BJ20071088

González, P. J., Correia, C., Moura, I., Brondino, C. D., & Moura, J. J. G. (2006). Bacterial nitrate reductases: Molecular and biological aspects of nitrate reduction. *Journal of Inorganic Biochemistry*, *100*(5), 1015–1023. https://doi.org/https://doi.org/10.1016/j.jinorgbio.2005.11.024

Grady Jr., L., Daigger, G. T., Love, N. G., & Filipe, C. D. M. (2011). *Biological Wastewater Treatment* (Third). CRC Press.

He, H., Carlson, A. L., Nielsen, P. H., Zhou, J., & Daigger, G. T. (2022). Comparative analysis of floc characteristics and microbial communities in anoxic and aerobic suspended growth processes. *Water Environment Research*. https://doi.org/doi.org/10.1002/wer.10822

He, S., Gall, D. L., & McMahon, K. D. (2007). "Candidatus accumulibacter" population structure in enhanced biological phosphorus removal sludges as revealed by polyphosphate kinase genes. *Applied and Environmental Microbiology*, *73*(18), 5865–5874. https://doi.org/10.1128/AEM.01207-07

He, S., Kunin, V., Haynes, M., Martin, H. G., Ivanova, N., Rohwer, F., Hugenholtz, P., & McMahon, K. D. (2010). Metatranscriptomic array analysis of 'Candidatus Accumulibacter phosphatis'-enriched enhanced biological phosphorus removal sludge. *Environmental Microbiology*, *12*(5), 1205–1217. https://doi.org/10.1111/j.1462-2920.2010.02163.x

Hennessy, R. (2020). *Updated Handbook for Wastewater Microscopy Applications and Filamentous Morphotype ID: Methods Knowledging recent Genetic Findings*.

Houweling, D., & Daigger, G. T. (2019). *Intensification of the Activated Sludge Process Using Media Supported Biofilms*. IWA Publishing.

Jenkins, D., Richard, M. G., & Daigger, G. T. (2004). *Manual of the Causes and Cotrol of Activated Sludge Bulking, Foaming, and Other Solids Separation Problems* (3rd edn). CRC Press.

Jepson, B. J. N., Mohan, S., Clarke, T. A., Gates, A. J., Cole, J. A., Butler, C. S., Butt, J. N., Hemmings, A. M., & Richardson, D. J. (2007). Spectropotentiometric and Structural Analysis of the Periplasmic Nitrate Reductase from Escherichia coli*. *Journal of Biological Chemistry*, *282*(9), 6425–6437. https://doi.org/https://doi.org/10.1074/jbc.M607353200

Kanehisa, M., & Sato, Y. (2020). KEGG Mapper for inferring cellular functions from protein sequences. *Protein Science*, *29*(1), 28–35. https://doi.org/https://doi.org/10.1002/pro.3711

Kanehisa, M., Sato, Y., & Kawashima, M. (2022). KEGG mapping tools for uncovering hidden features in biological data. *Protein Science*, *31*(1), 47–53. https://doi.org/https://doi.org/10.1002/pro.4172

Kanehisa, M., Sato, Y., & Morishima, K. (2016). BlastKOALA and GhostKOALA: KEGG Tools for Functional Characterization of Genome and Metagenome Sequences. *Journal of Molecular Biology*, *428*(4), 726–731. https://doi.org/https://doi.org/10.1016/j.jmb.2015.11.006

Kern, M., & Simon, J. (2009). Electron transport chains and bioenergetics of respiratory nitrogen metabolism in Wolinella succinogenes and other Epsilonproteobacteria. *Biochimica et Biophysica Acta (BBA) - Bioenergetics*, *1787*(6), 646–656. https://doi.org/https://doi.org/10.1016/j.bbabio.2008.12.010

Klein, E., Weiler, J., Wagner, M., Čelikić, M., Niemeyer, C. M., Horn, H., & Gescher, J. (2022). Enrichment of phosphate-accumulating organisms (PAOs) in a microfluidic model biofilm system by mimicking a typical aerobic granular sludge feast/famine regime. *Applied Microbiology and Biotechnology*, *106*(3), 1313–1324. https://doi.org/10.1007/s00253-022-11759-8

Kristiansen, R., Nguyen, H. T. T., Saunders, A. M., Nielsen, J. L., Wimmer, R., Le, V. Q., McIlroy, S. J., Petrovski, S., Seviour, R. J., Calteau, A., Nielsen, K. L., & Nielsen, P. H. (2013). A metabolic model for members of the genus Tetrasphaera involved in enhanced biological phosphorus removal. *ISME Journal*, *7*(3), 543–554. https://doi.org/10.1038/ismej.2012.136

Kuba, T., Murnleitner, E., Van Loosdrecht, M. C. M., & Heijnen, J. J. (1996). A metabolic model for biological phosphorus removal by denitrifying organisms. *Biotechnology and Bioengineering*, *52*(6), 685–695. https://doi.org/10.1002/(SICI)1097-0290(19961220)52:6<685::AID-BIT6>3.3.CO;2-M

Kuba, T., Wachtmeister, A., van Loosdrecht, M. C. M., & Heijnen, J. J. (1994). Effect of Nitrate on Phosphorus Release in Biological Phosphorus Removal Systems. *Water Sci*, *30*(6), 263–269.

Kunetz, T. E., Oskouie, A., Poonsapaya, A., Peeters, J., Adams, N., Long, Z., & Côté, P. (2016). Innovative membrane-aerated biofilm reactor pilot test to achieve low-energy nutrient removal at the Chicago MWRD. *WEFTEC 2016 - 89th Water Environment Federation Annual Technical Exhibition and Conference*, *1*, 2973–2987. https://doi.org/10.2175/193864716819713006

Laczny, C. C., Sternal, T., Plugaru, V., Gawron, P., Atashpendar, A., Margossian, H. H., Coronado, S., der Maaten, L. van, Vlassis, N., & Wilmes, P. (2015). VizBin - an application for reference-independent visualization and human-augmented binning of metagenomic data. *Microbiome*, *3*(1), 1. https://doi.org/10.1186/s40168-014-0066-1

Langmead, B., & Salzberg, S. L. (2012). Fast gapped-read alignment with Bowtie 2. *Nature Methods*, *9*(4), 357–359. https://doi.org/10.1038/nmeth.1923

Li, D., Liu, C.-M., Luo, R., Sadakane, K., & Lam, T.-W. (2015). MEGAHIT: an ultra-fast single-node solution for large and complex metagenomics assembly via succinct de Bruijn graph. *Bioinformatics*, *31*(10), 1674–1676. https://doi.org/10.1093/bioinformatics/btv033

Li, Q. (2018). *Pilot-scale Plant Applicatio of Membrane Aerated Biofilm Reactor (MABR) Technology in Wastewater Treatment*. KTH Royal Institute of Technology.

Liu, Y., Gu, J., & Zhang, M. (2019). *A-B Processes: Towards Energy Self-Sufficient Municipal Wastewater Treatment*. IWA Publishing.

Mamais, D., & Jenkins, D. (1992). The Effects of MCRT and Temperature on Enhanced Biological Phosphorus Removal. *Water Science and Technology*, *26*(5–6), 955–965. https://doi.org/10.2166/wst.1992.0537

Menzel, P., Ng, K. L., & Krogh, A. (2016). Fast and sensitive taxonomic classification for metagenomics with Kaiju. *Nature Communications*, *7*(1), 11257. https://doi.org/10.1038/ncomms11257

Mino, T., Kawakami, T., & Matsuo, T. (1985). Behaviour of intracellular polyphosphate in the biological phosphate removal process. *Water Science and Technology*, *17*(11–12), 11–21. https://doi.org/10.2166/wst.1985.0218

Mulkerrins, D., Dobson, A. D. W., & Colleran, E. (2004). Parameters affecting biological phosphate removal from wastewaters. *Environment International*, *30*(2), 249–259. https://doi.org/https://doi.org/10.1016/S0160-4120(03)00177-6

Nguyen, H. T. T., Nielsen, J. L., & Nielsen, P. H. (2012). "Candidatus Halomonas phosphatis", a novel polyphosphate-accumulating organism in full-scale enhanced biological phosphorus removal plants. *Environmental Microbiology*, *14*(10), 2826–2837. https://doi.org/10.1111/j.1462-2920.2012.02826.x

Oehmen, A., Lemos, P. C., Carvalho, G., Yuan, Z., Keller, J., Blackall, L. L., & Reis, M. A. M. (2007). Advances in enhanced biological phosphorus removal: From micro to macro scale. *Water Research*, *41*(11), 2271–2300. https://doi.org/https://doi.org/10.1016/j.watres.2007.02.030

Orhon, D., Sözen, S., & Artan, N. (1996). The effect of heterotrophic yield on the assessment of the correction factor for anoxic growth. *Water Science and Technology*, *34*(5–6), 67–74. https://doi.org/10.1016/0273-1223(96)00630-0

Parker, D., Appleton, R., Bratby, J., & Melcer, H. (2004). North American performance experience with anoxic and anaerobic selectors for activated sludge bulking control. *Water Science and Technology*, *50*(7), 221–228. https://doi.org/10.2166/wst.2004.0463

Petriglieri, F., Singleton, C. M., Kondrotaite, Z., Dueholm, M. K. D., McDaniel, E. A., McMahon, K. D., & Nielsen, P. H. (2022). Reevaluation of the Phylogenetic Diversity and Global Distribution of the Genus " Candidatus Accumulibacter" . *MSystems*, *7*(3). https://doi.org/10.1128/msystems.00016-22

Petriglieri, F., Singleton, C., Peces, M., Petersen, J. F., Nierychlo, M., & Nielsen, P. H. (2021). "Candidatus Dechloromonas phosphoritropha" and "Ca. D. phosphorivorans", novel polyphosphate accumulating organisms abundant in wastewater treatment systems. *ISME Journal*, *15*(12), 3605–3614. https://doi.org/10.1038/s41396-021-01029-2

Pinto, A. J., Xi, C., & Raskin, L. (2012). Bacterial Community Structure in the Drinking Water Microbiome Is Governed by Filtration Processes. *Environmental Science & Technology*, *46*(16), 8851–8859. https://doi.org/10.1021/es302042t

Potter, L., Angove, H., Richardson, D., & Cole, J. B. T.-A. in M. P. (2001). *Nitrate reduction in the periplasm of gram-negative bacteria* (Vol. 45, pp. 51–112). Academic Press. https://doi.org/https://doi.org/10.1016/S0065-2911(01)45002-8

Randall, C., James, B., Stensel, H. D., & Defresne, L. (2010). *Nutrient Control Design Manual*. www.epa.gov/nrmrl

Riis, V., & Mai, W. (1988). Gas chromatographic determination of poly-B-hydroxybutyric acid in microbial biomass after hydrochloric acid propanolysis. *Notes*, *445*, 285–289.

Sathyamoorthy, S., Tse, Y., Gordon, K., Houwelling, D., & Coutts, D. (2019). BNR Process Intensification using Membrane Aerated Biofilm Reactors. *WEF Nutrient Removal and Recovery Symposium*, 527–535.

Sayers, E. W., Beck, J., Brister, J. R., Bolton, E. E., Canese, K., Comeau, D. C., Funk, K., Ketter, A., Kim, S., Kimchi, A., Kitts, P. A., Kuznetsov, A., Lathrop, S., Lu, Z., McGarvey, K., Madden, T. L., Murphy, T. D., O'Leary, N., Phan, L., … Ostell, J. (2020). Database resources of the National Center for Biotechnology Information. *Nucleic Acids Research*, *48*(D1), D9–D16. https://doi.org/10.1093/nar/gkz899

Smith, A. L., Skerlos, S. J., & Raskin, L. (2013). Psychrophilic anaerobic membrane bioreactor treatment of domestic wastewater. *Water Research*, *47*(4), 1655–1665. https://doi.org/10.1016/j.watres.2012.12.028

Smolders, G. J. F., Klop, J. M., van Loosdrecht, M. C. M., & Heijnen, J. J. (1995). A metabolic model of the biological phosphorus removal process: I. Effect of the sludge retention time. *Biotechnology and Bioengineering*, *48*(3), 222–233. https://doi.org/10.1002/bit.260480309

Smolders, G. J. F., van der Meij, J., van Loosdrecht, M. C. M., & Heijnen, J. J. (1994a). Model of the anaerobic metabolism of the biological phosphorus removal process: Stoichiometry and pH influence. *Biotechnology and Bioengineering*, *43*(6), 461–470. https://doi.org/10.1002/bit.260430605

Smolders, G. J. F., van der Meij, J., van Loosdrecht, M. C. M., & Heijnen, J. J. (1994b). Stoichiometric model of the aerobic metabolism of the biological phosphorus removal process. *Biotechnology and Bioengineering*, *44*(7), 837–848. https://doi.org/10.1002/bit.260440709

Sparacino-Watkins, C., Stolz, J. F., & Basu, P. (2014). Nitrate and periplasmic nitrate reductases. *Chemical Society Reviews*, *43*(2), 676–706. https://doi.org/10.1039/c3cs60249d.Nitrate

Standard Methods for the Examination of Water and Wastewater (3rd ed.). (2017). American Public Health Association/American Water works Association/WAter Environment Federation.

Stokholm-Bjerregaard, M., McIlroy, S. J., Nierychlo, M., Karst, S. M., Albertsen, M., & Nielsen, P. H. (2017). A critical assessment of the microorganisms proposed to be important to enhanced biological phosphorus removal in full-scale wastewater treatment systems. *Frontiers in Microbiology*, *8*(APR), 1–18. https://doi.org/10.3389/fmicb.2017.00718

Sun, L., Wang, Z., Wei, X., Li, P., & Zhang, H. (2015). Enhanced biological nitrogen and phosphorus removal using sequencing batch membrane-aerated bio fi lm reactor. *Chemical Engineering Science*, *135*, 559–565. https://doi.org/10.1016/j.ces.2015.07.033

Tamura, K, & Nei, M. (1993). Estimation of the number of nucleotide substitutions in the control region of mitochondrial DNA in humans and chimpanzees. *Molecular Biology and Evolution*, *10*(3), 512–526. https://doi.org/10.1093/oxfordjournals.molbev.a040023

Tamura, Koichiro, Stecher, G., & Kumar, S. (2021). MEGA11: Molecular Evolutionary Genetics Analysis Version 11. *Molecular Biology and Evolution*, *38*(7), 3022–3027. https://doi.org/10.1093/molbev/msab120

Ultsch, A., & Mörchen, F. (2005). *ESOM-Maps : tools for clustering , visualization , and classification with Emergent SOM*.

Underwood, A., McMains, C., Coutts, D., Peeters, J., Ireland, J., & Houweling, D. (2018). Design and startup of the first full-scale membrane aerated biofilm reactor in the United States. *Proceedings of the Water Environment Federation*, 1282–1296.

Vaccaro, B. J., Thorgersen, M. P., Lancaster, W. A., Price, M. N., Wetmore, K. M., Poole, F. L., Deutschbauer, A., Arkin, A. P., & Adams, M. W. W. (2016). Determining roles of accessory genes in denitrification by mutant fitness analyses. *Applied and Environmental Microbiology*, *82*(1), 51–61. https://doi.org/10.1128/AEM.02602-15

Wang, Z., Guo, F., Mao, Y., Xia, Y., & Zhang, T. (2014). Metabolic Characteristics of a Glycogen-Accumulating Organism in Defluviicoccus Cluster II Revealed by Comparative Genomics. *Microbial Ecology*, *68*(4), 716–728. https://doi.org/10.1007/s00248-014-0440-3

Wentzel, M. C., Mbewe, A., Lakay, M. T., & Ekama, G. A. (2000). Evaluation of a Modified Flocculation Filtration Method To Determine Wastewater Readily Biodegradable COD. *WISA 2000 Biennial Conference*, *June*.

Wentzel, M., Loewenthal, R., Ekama, G., & Marais, G. (1988). Enhanced polyphosphate organism cultures in activated sludge systems - Part 1: Enhanced culture development. *Water SA*, *14*(2), 81–92.

Werker, A., Lind, P., Bengtsson, S., & Nordström, F. (2008). Chlorinated-solvent-free gas chromatographic analysis of biomass containing polyhydroxyalkanoates. *Water Research*, *42*(10), 2517–2526. https://doi.org/https://doi.org/10.1016/j.watres.2008.02.011

Xu, R., Fu, Y., Xu, Y., Zheng, X., Huang, Y.-X., & Meng, F. (2022). Comparing biotransformation of extracellular polymeric substances (EPS) under aerobic and anoxic conditions: Reactivities, components, and bacterial responses. *Chemosphere*, *296*, 133996. https://doi.org/https://doi.org/10.1016/j.chemosphere.2022.133996

Zhou, J., Liu, W., Deng, Y., Jiang, Y. H., Xue, K., He, Z., Van Nostrand, J. D., Wu, L., Yang, Y., & Wang, A. (2013). Stochastic assembly leads to alternative communities with distinct functions in a bioreactor microbial community. *MBio*, *4*(2), 1–8. https://doi.org/10.1128/mBio.00584-12

Chapter 6 Conclusions, Significance, and Future Research

6.1 Overview

Conventional activated sludge (AS) configurations for biological nutrient removal (BNR) have been a significant contributor to the health of natural water bodies for the last 40 years. Nitrogen and phosphorus removal strategies are now regarded not only as preventative measures to harmful algal blooms, or mitigation for downstream drinking water sources, but as generators of economic products. Investment in and optimization of BNR technologies opens up opportunities for sustainable regeneration of non-renewables, such as fertilizers (nitrogen and phosphorus) or energy (in the form of methane biogas). Membrane technologies have the unique capacity to fit into developed solutions, while providing strategic advantages in plant footprint, energy demand, and operational performance. Our research objectives in this dissertation are ultimately an expansion on the traditional approaches used in practice when applied to two emerging BNR membrane technologies in practice, membrane bioreactors (MBRs) and membrane aerated biofilm reactors (MABRs). Advanced methods were utilized, including chemical, microscopic, and biomolecular techniques, beyond what is typically employed at a wastewater plant. The results informed us of the physiochemical environment of suspended growth interaction in different modes of application: the fouling environment negatively impacting performance of an MBR, and the positive interactions facilitating optimum removal of pollutants in a MABR. The investigation of MBR fouling at Traverse City in Chapter 3 had real and immediate impact on day-to-day operation. In Chapters 4 and 5, the results served to provide practical knowledge on hybrid MABR systems to advance the capacity for fully anoxic nitrogen processing in the bulk liquid, but also provide metrics in terms of hydrolysis of organic matter and capture carbon. Furthermore, Chapter 5 provided critical insight into fully anoxic phosphorus removal; the chapter described the

inefficiencies inherent to denitrifying phosphorus accumulating organism (DPAO) metabolic functions, but revealed more mechanistic information as to how specific populations and species would grow under anoxic wastewater conditions. Throughout this dissertation, advanced methods were utilized: experimentation on systems in practice were conducted to investigate the pillars driving success or failure, computer modeling was used to validate conceptual premises, and physical BNR processes were deployed to understand *in situ* microbial community metabolisms.

6.2 Fouling Mitigation in MBR Treatment Systems

Wastewater is a complex medium, especially full-scale domestic systems where dynamic shifts in composition can cause significant changes in plant chemical environment and biological community. Influent characteristics are often determined by external factors: demographics, industrial or agricultural operations, or even the quality of drinking water provided in the service area. MBR plant operation can be affected by the confluence of different components in the wastewater, but also by microbial by-products that are generated as a response to the environment created in the plant through the influent.

Chapter 3 investigated what drivers were contributing to poor performance (mainly, loss of permeability and high transmembrane pressure) in a full-scale MBR plant located in Traverse City, MI. At the onset of this rapid performance issues, plant personnel used operational data and the standard methods available to provide a hypothesis as to the biological driver—a dispersed gram-positive bacteria that was apparent in the plant's mixed liquor. These organisms were found to be in the genus *Staphylococcus*, and were a useful visual link to conditions causing plant permeability upsets. However, upon investigation, they were also found in similar abundance under healthier mixed liquor conditions where the plant was performing optimally. Chemical analysis was conducted on mixed liquor to estimate concentrations of micronutrients, and was

found to have statistical differences in monovalent and divalent cations between periods of permeability decline and normal operation, as well as another municipal MBR wastewater plant in the area. Mixed liquor tests with dosed cation confirmed a response difference under physical filtration.

Consolidation of all the data and observations suggested a polymer bridging fouling mechanism was occurring. High positively-charge calcium concentrations can bridge with negatively-charged organic compounds in the plant's influent wastewater to form a gel layer over the membrane surface. This was consistent with plant data and personnel observations over the course of several years. The recommendations made to plant staff at the conclusion of this study were to provide additional monitoring tools, such as a conductance probe at the headworks, as a warning to changes in mixed liquor quality. A special sampling campaign was also initiated in the plant's distribution area and industrial customers to characterize the organic substances flowing into the plant exacerbating fouling issues.

6.3 Hybrid MABR Concept

Throughout Chapters 4 and 5, we discussed the idea of a hybrid MABR/suspended growth design configuration. This builds upon the already existing MABR equipment for use in a suspended growth AS system for purposes of BNR. The fundamental idea is not new, and some example treatment systems are becoming commercialized that operate in this exact manner. Past experience with these systems has shown capability for simultaneous nitrification and denitrification (SND). However, what we proposed is that the MABR become the feature process of the treatment train, which allows decoupling of nitrification from the suspended growth. This would allow for significant downsizing, or even elimination, of the aerated portions of the suspended growth zones, while retaining a large anoxic zone for denitrification. High-rate

denitrification, i.e., solids retention times (SRTs), of less than three days was also a key feature of this proposed system. Utilizing the well-demonstrated beneficial aspects of MABR technology, high oxygen transfer efficiency (OTE) and high oxygen transfer rate (OTR), and a high-rate anoxic suspended growth configuration, we estimated from computer process simulation a substantial reduction in energy demand (both in process oxygen requirements and carbon regeneration potential), reduced mixed liquor recycle, while retaining high level of total nitrogen (TN) removal. These results were mirrored in experimentation with a high-rate physical anoxic suspended growth treatment system treating domestic wastewater compared to a side-by-side aerobic system at the Ann Arbor Wastewater Plant (AAWWTP).

A wide range of scenarios were tested with the process model and physical treatment system to understand more completely how a hybrid MABR would behave under desirable (higher COD/TN) or undesirable (low COD/TN) influent conditions. Process tradeoffs exist in the desired level of TN removal versus amount of carbon capture. The highest level of nitrogen removal activity was shown between the 2.5 to 3-day SRT in our model, and at the 3-day SRT mark for the bioreactor. The amount of total COD oxidation that occurred in the anoxic suspended growth was directly correlated to SRT, which obviously reduced that matter to be used in downstream biogas generation. However, depending on the influent C:N ratio and influent wastewater conditions, this could prove to be the only option for treatment plant personnel needing to achieve certain effluent concentrations to meet their permit requirements. Chapter 4 provides advanced methods to help clarify how operation decisions could affect overall performance of a hybrid MABR under various scenarios.

The mass balance of organic material on the bioreactors at AAWWTP showed that anoxic hydrolysis of particulate and colloidal matter was reduced compared to the aerobic systems.

Measured particulate and colloidal matter removal coupled with the observed yield of the system was compared to tCOD oxidation from the system mass balance. It was observed that a portion, roughly 75%, of the particulate and organic matter was oxidized compared to the theoretical estimates. In other words, a fraction of the organic matter was not hydrolyzed under anoxic conditions. Reduced metabolism of biodegradable organic matter reduces the process oxygen requirement, and this, coupled with the higher OTE for MABRs compared to conventional oxygen transfer systems and elimination of the need for mixed liquor recirculation, results in further reduction of process energy requirements for the hybrid MABR process compared to conventional biological nitrogen removal systems. However, reduced anoxic hydrolysis also prevents soluble organic matter to be generated for downstream fermentation to volatile fatty acids (VFA) in the biological phosphorus removal pathway.

6.4 Fully Anoxic Biological Phosphorus Removal

The detailed mechanisms of anoxic biological phosphorus removal (bio-P) in hybrid MABR systems continue to confound practitioners in the field. As is the case with conventional EBPR configuration, bio-P removal can occur with addition of an upstream anaerobic zone to generate fermented products that power PAO metabolism. However, the underlying answers as to what organisms (PAOs or DPAOs) and where they were growing (in the bulk liquid or in a special redox zone created in the biofilm) could not be answered with standard chemical analysis of inputs and outputs. In Chapter 5, we showed through process modeling with domestic wastewater a simulated outcome that indicated combined nitrogen and phosphorus removal could occur (effluent concentrations less than 0.2 mg-P/L, 0.5 mg-N/L) at longer SRTs than the nitrogen removal hybrid systems in Chapter 4. This system process rate was lower than a conventional EBPR configuration by a third, and with two-thirds the required bioreactor volume. The tradeoff

in those scenarios was increased process oxygen requirements and reduced carbon capture, as was the case for hybrid MABR systems in the previous chapter. Longer SRTs increase biomass inventory which is demonstrated in both chapters to correlate with total COD oxidation.

The lynchpin in Chapter 5 was demonstrating sustained bio-P activity in a fully anoxic biomass treating domestic wastewater supplemented with external nitrate. Classic research in the 1990's revealed the ability of some PAOs to denitrify, and research since then has resolved these metabolisms even further into nitrite- and nitrate-reducing. For instance, phylogeny of known PAO species *Ca*. Accumulibacter phosphatis broke into two distinct sub-groups: Type I and Type II. Type I was found to perform nitrate reduction in an anoxic environment, whereas Type II is known to reduce nitrite. Connecting the chemical performance across a period of high bio-P to the bioreactor DPAO community through sophisticated biomolecular methods was key to understanding mechanistically how an anoxic suspended growth would function in a hybrid MABR system generating nitrate. We wished to address the major knowledge gap of key species involved in anoxic biological phosphorus removal, and connect DPAO genomic capacity to measured chemical treatment in a functioning bio-P reactor.

Generating the conditions for a successfully functioning anoxic bio-P reactor proved to be more difficult than modeling results would suggest. Several phases of experimentation over the course of two years were required at SRTs longer than 5 days and with supplemental VFA. Results showed a general reluctance in the anoxic reactor; ortho-P removal was roughly 55% compared to 95% in a side-by-side anaerobic/aerobic (AO) reactor at optimal conditions. We had hypothesized the anoxic process would place selective forces on the DPAO population, resulting in nitrate reductase genes for oxidative phosphorylation, but in so doing also accentuates any anoxic metabolic inefficiencies processing the available resources from the wastewater. Lower anoxic

hydrolysis prevented fermentation of VFA using organic matter from the wastewater. This inefficiency was measured in profile sampling in Chapter 5; lower HAc/P and higher PHA/HAc ratios in the anaerobic zone, followed by lower PHA/P ratios in the anoxic reactor versus the aerobic. Ultimately in Chapter 5, the P/O ratio was calculated for both aerobic and anoxic reactors, and the results (1.7 and 0.90, respectively) mirrored that of historical research. Anoxic bio-P removal will face headwinds due to internal metabolic inefficiency when nitrate reduction drives oxidative phosphorylation.

Finally, DNA sequencing and analysis of mixed liquor samples revealed the identity and relative abundance of key groups within the DPAO population, the presence of genomic sequences in denitrification and oxidative phosphorylation process, and the gene coverage patterns correlating to phosphorus metabolic pathways. *Ca*. Accumulibacter and *Dechloromonas* were two genera with the highest relative abundance and most complete genomic bins. Both appear in the aerobic and anoxic reactors to a consistent degree across sampling periods, but anoxic selection forces appear to influence certain types of genomic machinery. Gene coverage of periplasmic nitrate reductase (gene *napAB*) was found most common in the bins, although low coverage of respiratory nitrate reductase complexes (*narGHI*) was seen in the *Ca*. Accumulibacter bin only for the anoxic reactor. Periplasmic nitrate reductase is considered less thermodynamically efficient, i.e., producing less energy per reduction equivalent, which could explain certain aspects of the lower P/O ratio. Because of the immense amount of data contained within metagenomic sequences, and the inability to predict expression of proteins during operation, more research is needed in this particular area.

6.5 Future Research Needs

Experimentation at both TCRWWTP and AAWWTP is ongoing. With the recommendation provided in Chapter 3, TCRWWTP personnel continue to monitor for critical changes in their distribution system. Regular measurement of carbohydrates and cationic micronutrients at industrial customer outfalls was implemented. The capacity of treatment plants to quickly analyze permeability disruptions, characterize potential foulants, and identify drivers of their membrane fouling problems, however, remains an area to address for the future of MBR technology. The topic of fouling in a wastewater treatment scenario is considerably complex; many different mechanisms, chemical components, or combinations of components exist that can create fouling conditions for a membrane. The consensus is that more research is needed to characterize biomolecular components, e.g., extracellular polymeric substances (EPS), soluble microbial products (SMP), and biopolymers, to better understand the composition of the microbial environment interfering with the membrane surface. Because of the interplay between the mixed liquor community and the production of these compounds, advanced chemical and biomolecular methods could be used in these assessments.

Lastly, the operation of aerobic and anoxic reactors is ongoing, with upgrades that integrated a functioning MABR with the anoxic suspended growth. More research is needed to validate the results with its attached growth supplying diffuse nitrate instead of external supplies. The addition of biomolecular techniques, such as qPCR, could determine the level of real-time activity of organisms *in situ*. Ultimately, the hybrid MABR process described here needs to be tested at larger scale. A hybrid MABR pilot-scale project commenced in Nanjing, China, in 2021 prompted by the modeling results of Chapter 4. This continued research will provide valuable knowledge on the operation of combined nitrogen and phosphorus removal in hybrid MABR

treatment systems with influent domestic wastewater. In both cases, a comprehensive chemical and biomolecular analysis regiment was established. The next goal will be to develop clearer information on nitrifier, OHO, and DPAO interactions in these practical applications.

Appendices

Appendix A Supplementary Information for Chapter 2

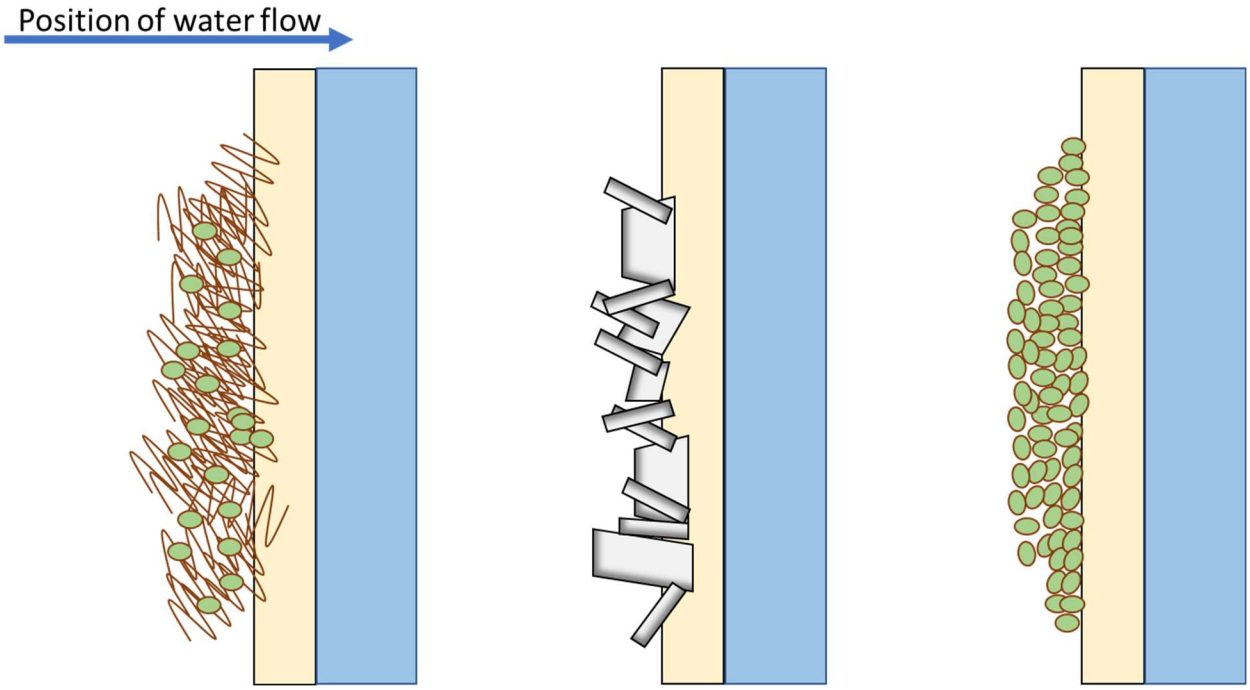

Figure A-1 Diagram of various types of fouling mechanisms

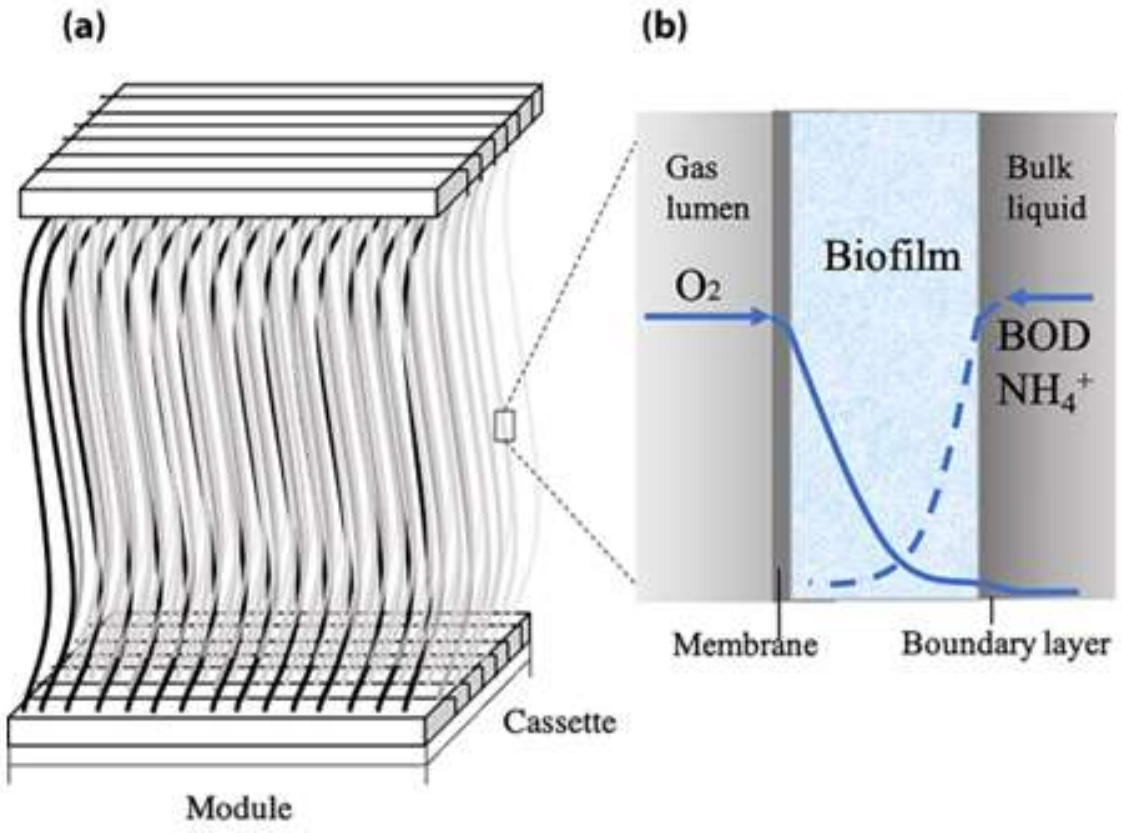

Figure A-2 Visual representation of MABR cassette and attached biofilm

Appendix B Supplementary Information for Chapter 3

Appendix B-1 TCRWWTP MBR Initial Permeability Upset Data

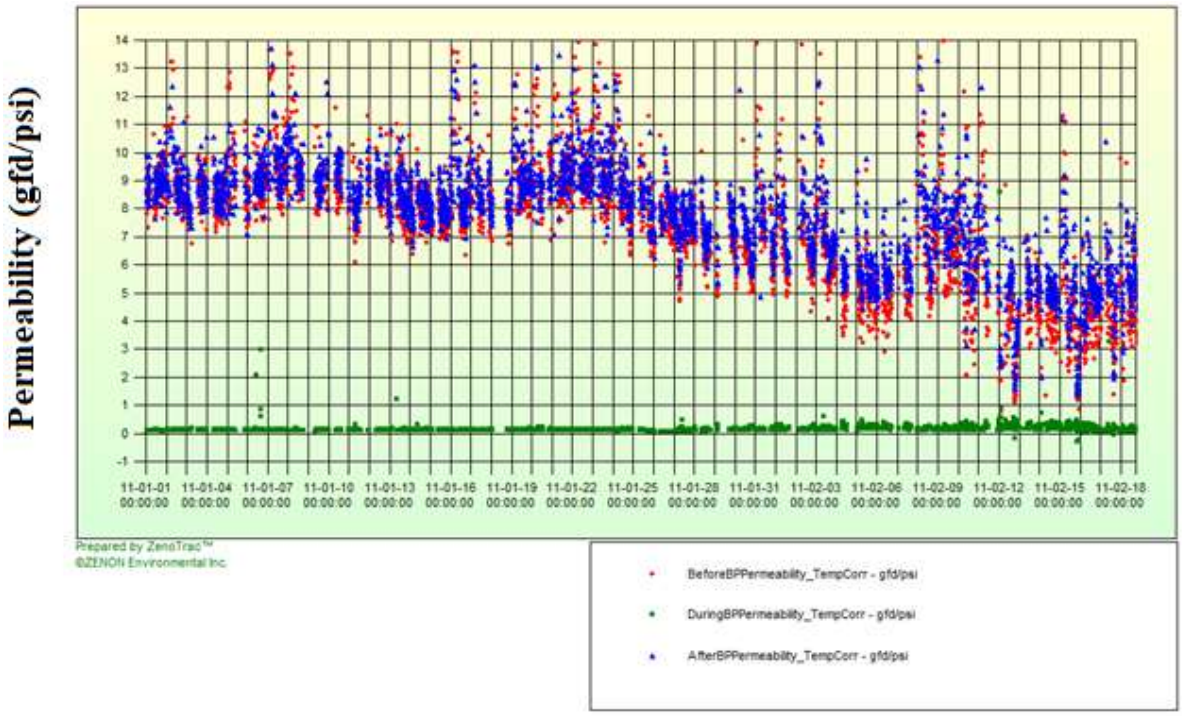

Figure B-1 Permeability Graph

Source: (Blair, 2012)

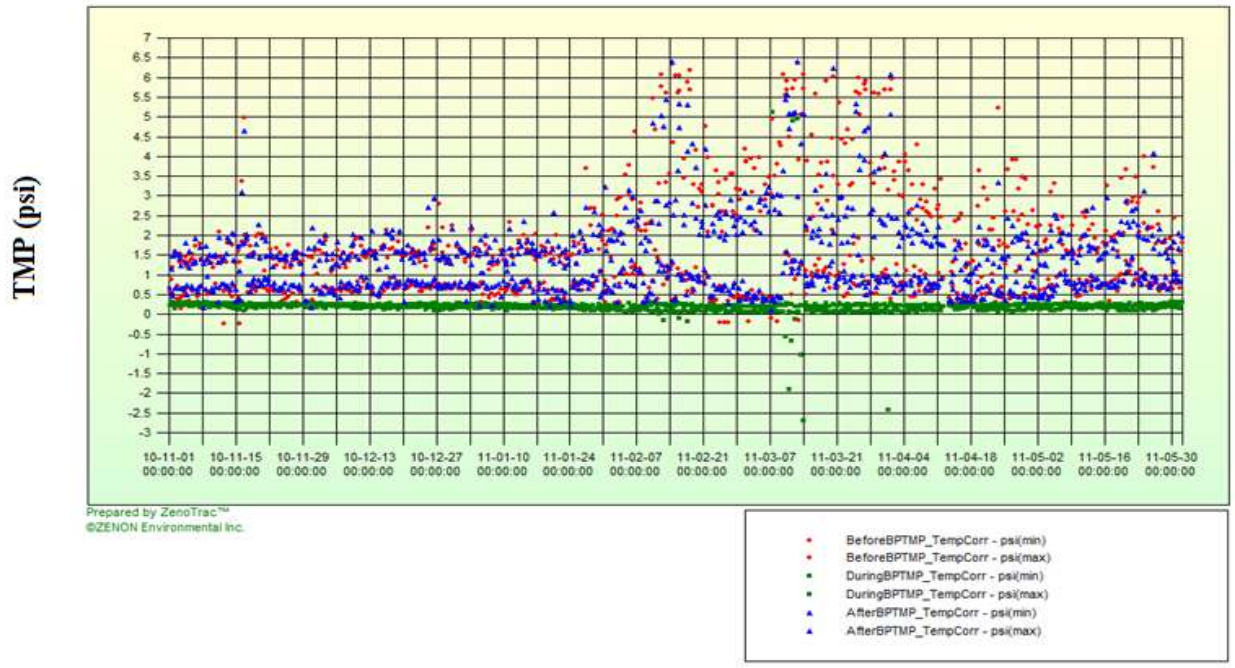

Figure B-2 Transmembrane Pressure Graph

Source: (Blair, 2012)

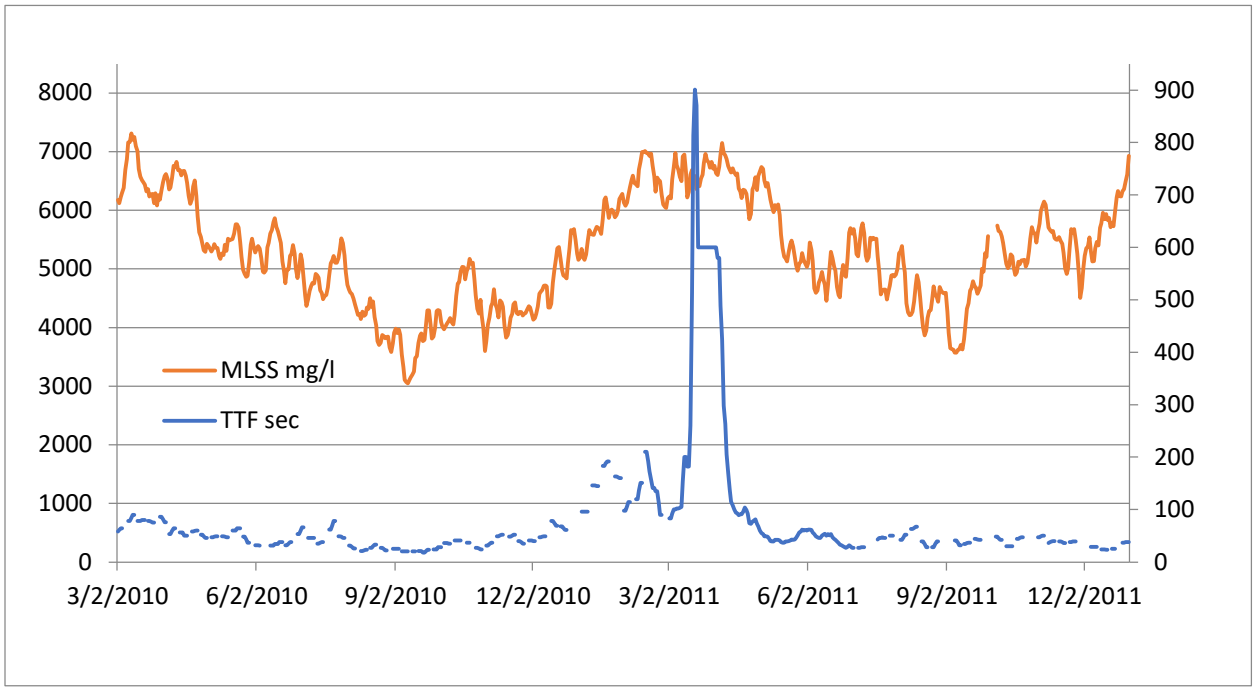

Figure B-3 Time-to-filter Graph

Source: (Blair, 2012)

Appendix B-2 TCRWWTP Plant Personnel Observations

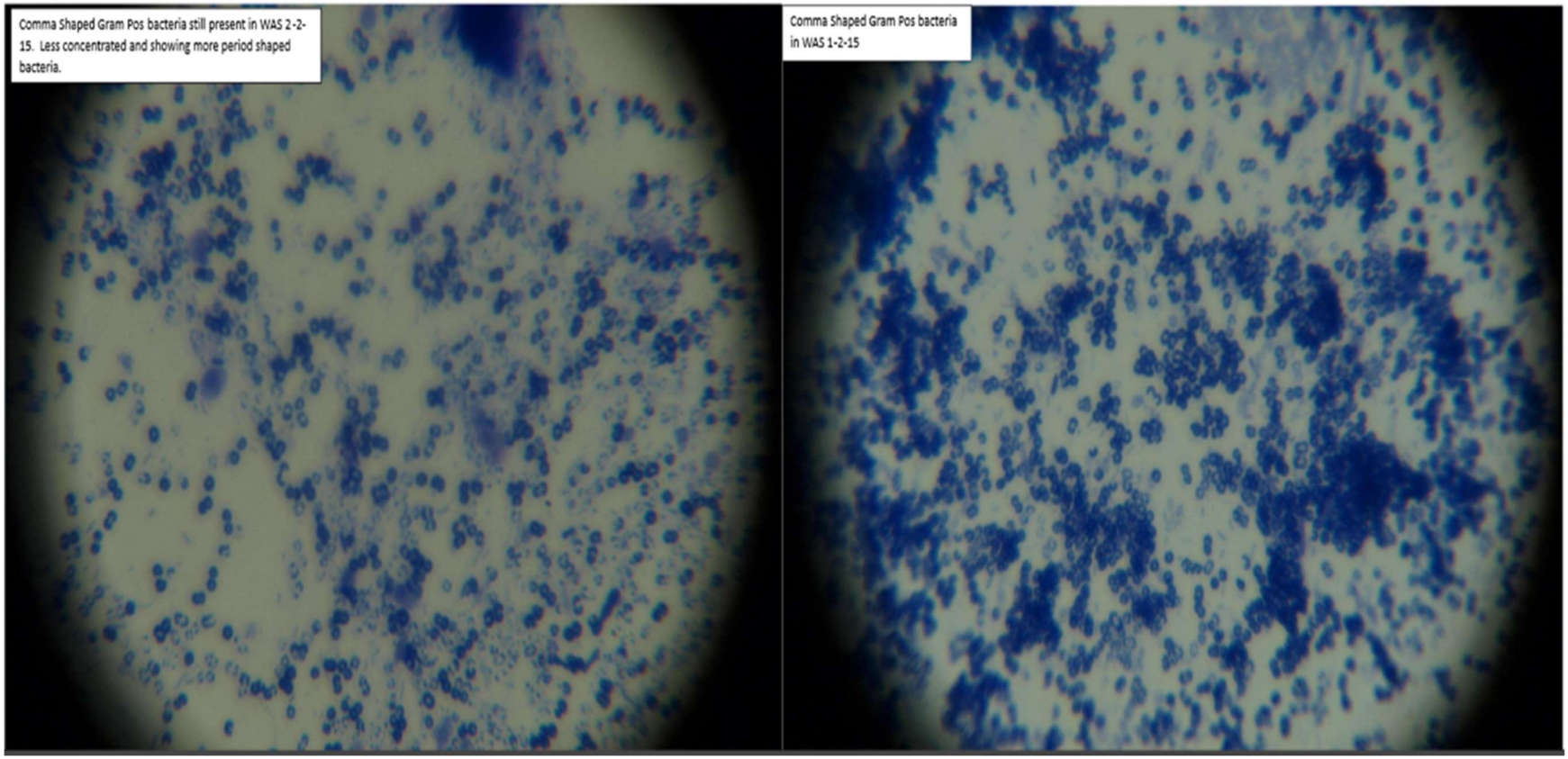

Figure B-4 Comma Shaped Gram-Positive Bacteria in RAS samples

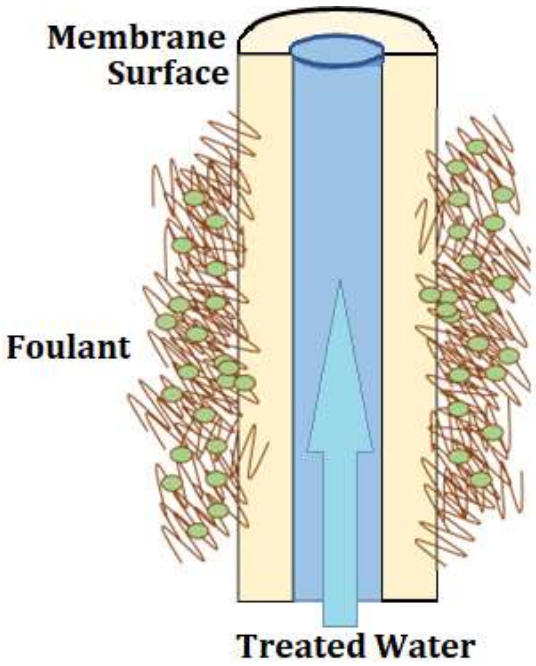

Figure B-5 Visual representation of TCRWWTP MBR permeability resistance

Appendix B-3 Chapter 3 Supplemental Method Information

Table B-1 Summary of sampling events across all periods of permeability upsets and normal operation with accompanying sample identifying codes, and completed experimentation

Sample ID[a,b,c]	Date	Purpose
RP-Initial	1/15/2011	Historical Data Review (no samples) **Reduced Permeability Periods**
RP-1	6/1/2012	
RP-2	9/9/2012	
RP-3	12/17/2012	
RP-4	2/1/2013	
RP-5	12/24/2014	
RP-6	9/2/2015	
RP-7	3/16/2017	
RP-TC-ML 1	3/22/2017	Settled Biomass Culture, Sanger Sequencing, **Reduced Permeability Period**
RP-TC-ML 2		
RP-TC-ML 3		
RP-TC-ML 4		
RP-TC-ML 5		
RP-TC-ML E1	3/22/2017	Dispersed Culture, Sanger Sequencing, Enriched with Problem Bacteria, **Reduced Permeability Period**
RP-TC-ML E2		
RP-TC-ML E3		
RP-TC-ML E4		
RP-TC-ML E5		
RP-TC-ML Week 1	3/22/2017	Carbohydrate/Protein Analysis, Micronutrients Analysis, Illumina Sequencing, **Reduced Permeability Period**
RP-TC-ML Week 2	3/29/2017	
RP-TC-ML Week 3	4/5/2017	
RP-TC-ML Week 4	4/12/2017	
C-TC-ML Week 5	8/15/2017	Carbohydrate/Protein Analysis, Micronutrients Analysis, Illumina Sequencing, **Normal Operation**
C-TC-ML Week 6	8/23/2017	
C-TC-ML Week 7	9/7/2017	
C-TC-ML Week 8	9/14/2017	
C-TC-ML-FISH 1	10/5/2017	FISH[d] (centrifuged biomass), **Normal Operation**
C-TC-ML-FISH 2		FISH (gravity settled biomass), **Normal Operation**
RP-TC-ML-FISH 3	12/12/2017	FISH (centrifuged biomass), **Reduced Permeability Period**
RP-TC-ML-FISH 4		FISH (gravity settled biomass), **Reduced Permeability Period**
RP-TC-ML-FISH 5	12/19/2017	FISH (centrifuged biomass), **Reduced Permeability Period**
RP-TC-ML-FISH 6	12/27/2017	FISH (gravity settled biomass), **Reduced Permeability Period**
RP-TC-ML Week 9	1/12/2018	Carbohydrate/Protein Analysis, Micronutrients Analysis, Illumina Sequencing, **Reduced Permeability Period**
RP-TC-ML Week 10	1/18/2018	
RP-TC-PE Week 11	2/26/2018	Micronutrients Analysis, **Reduced Permeability Period**
RP-TC-PE Week 11	2/28/2018	
RP-TC-PE Week 12	3/2/2018	
RP-TC-PE Week 13	3/5/2018	Micronutrients Analysis, **Reduced Permeability Period**
RP-TC-ML Week 13		
C-TC-PE Week 13	6/18/2018	Micronutrients Analysis, **Normal Operation**

C-TC-ML Week 13		
C-TC-INF Week 14	7/13/2018	Carbohydrate/COD[e] Analysis, **Normal Operation**
C-TC-INF Week 15	7/25/2018	
C-TC-INF Week 16	7/31/2018	
C-TC-INF Week 17	8/7/2018	
C-TC-INF Week 18	8/14/2018	
SRF-TC-PE 1	8/27/2018	Specific Resistance to Filtration, **Normal Operation**
SRF-TC-PE 2	8/28/2018	
SRF-TC-ML 1		
SRF-TC-ML 2	8/29/2018	
SRF-TC-PE 3		
SRF-TC-ML 3	8/30/2018	
C-TC-INF Week 19	9/26/2018	Carbohydrate/COD Analysis, **Normal Operation**
C-TC-INF Week 20	9/28/2018	
C-TC-INF Week 21	10/1/2018	
SRF-TC-PE 4	10/24/2018	Specific Resistance to Filtration, **Normal Operation**
SRF-TC-ML 4		
SRF-TC-PE 5	10/29/2018	Specific Resistance to Filtration, **Normal Operation**
SRF-TC-ML 5		
SRF-DUN-ML 1	11/25/2018	Specific Resistance to Filtration (Na^+ and Ca^{2+} spiked additions), Dundee Wastewater Treatment Plant, **Normal Operation**
SRF-DUN-ML 2		
SRF-TC-ML 6	11/29/2018	Specific Resistance to Filtration (Na^+ and Ca^{2+} spiked additions), **Normal Operation**
SRF-TC-ML 7	11/30/2018	
SRF-TC-ML 8	12/1/2018	
C-TC-INF Week 22	4/1/2019	Carbohydrate/COD Analysis, **Normal Operation**
C-TC-INF Week 22	4/2/2019	
C-SIU-EFF Week 22		
C-TC-INF Week 22	4/4/2019	
C-SIU-EFF Week 22		
C-TC-INF Week 22	4/9/2019	
C-SIU-EFF Week 22		
C-TC-INF Week 23	4/15/2019	
C-SIU-EFF Week 23	4/16/2019	

Table Notes:

a. RP- indicates a sample taken during a period of reduced permeability or permeability decline
E- indicates a sample enriched for problem bacteria
C- indicates a control sample from a period of normal operation, without reduced or declining permeability
SRF- indicates a sample taken for the purposes of running a specific resistance to filtration experiment, which included addition of carbohydrates and cations to invoke the symptoms of reduced permeability

b. -TC- indicates a sample taken at Traverse City Regional Wastewater Treatment Plant (Traverse City, MI)
-DUN- indicates a sample taken at Dundee Wastewater Treatment Plant (Dundee, MI)
-SIU- indicates a sample taken at one of TCRWWTP's Significant Industrial Users, or businesses that contribute to the distribution system

c. -ML indicates a mixed liquor sample
-PE indicates a primary effluent sample, or a sample after the primary clarifier
-INF indicates a plant influent sample
-EFF indicates an effluent or outfall sample

d. FISH indicates a sample washed in 1X phosphate buffer solution and fixed in 100% ethanol. Because centrifugation was originally thought to pose a risk of altering the spatial relationship of the problem

organisms with the rest of the flocculated healthy biomass causing negative effects to visualization during the microscopy phase, a gravity settled sample was simultaneously taken. It was found from visualization samples C-TC-ML-FISH 1-2 and RP-TC-ML-FISH 3-4 that no detectable difference existed—i.e. the FISH probes appeared to work with the same efficacy at fluorescing target organisms.

e. Total carbohydrate and filtered carbohydrates (1.5 µm glass fiber, Whatman 934-AH. At this point in analysis, influent protein concentration was assumed low.

Table B-2 DECIPHER FISH probe sequences for identified relevant gram-positive genera

Probe Sequence	Target Sequence	Mismatches	Genus Specificity
5'-CCC ACC CTT TCG CTC CT -3'	5'-AGG AGC GAA AGG GTG GG-3'	0	*Microbacterium*
5'-CCC AAA GGG GAA ACC GTA TCT CTA CG -3'	5'-CGT AGA GAT ACG GTT TCC CCT TTG GG-3'	0	*Micrococcus*
5'- TCG CAC ATC AGC GTC AGT T -3'	5'-AAC TGA CGC TGA TGT GCG A-3'	0	*Staphylococcus*

Appendix B-4 Chapter 3 Historical Data Review

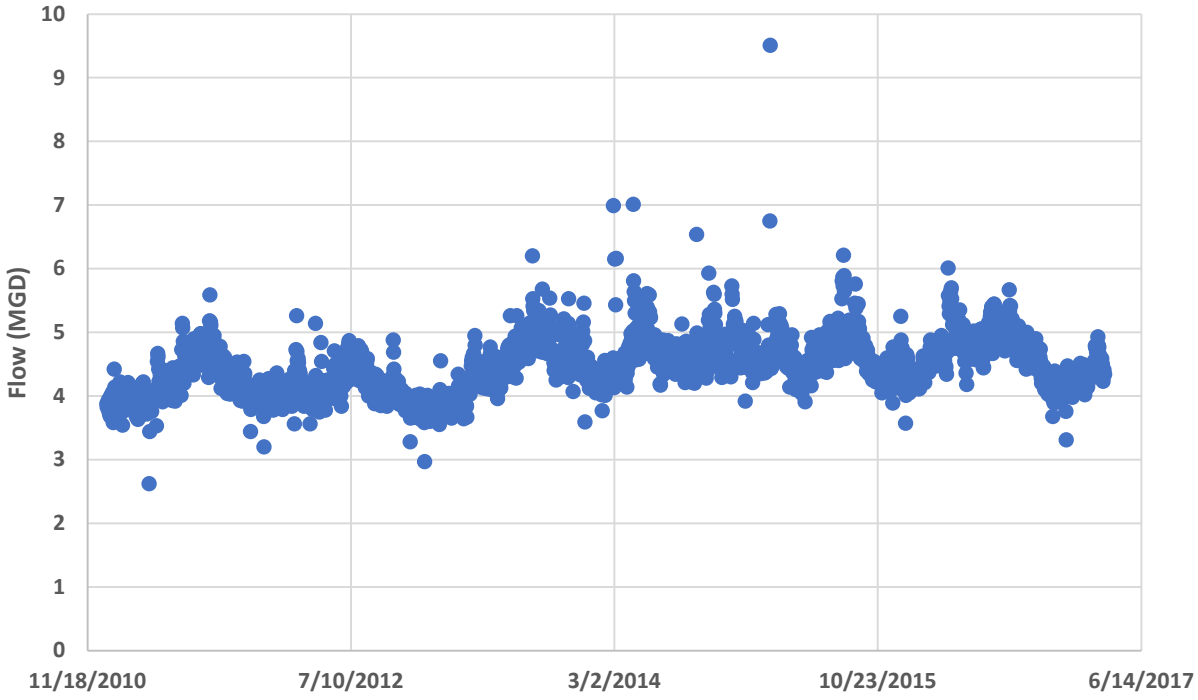

Figure B-6 Influent Raw Water Flow January 2011-March 2017

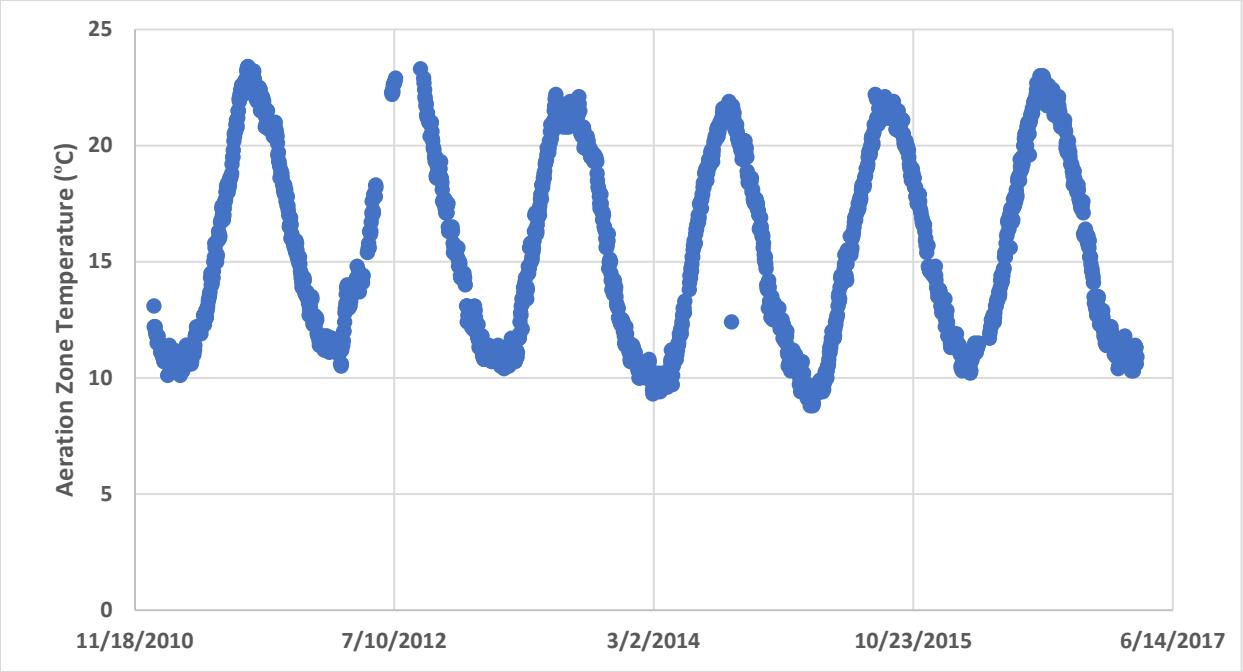

Figure B-7 Aeration Basin Water Temperature January 2011-October 2016

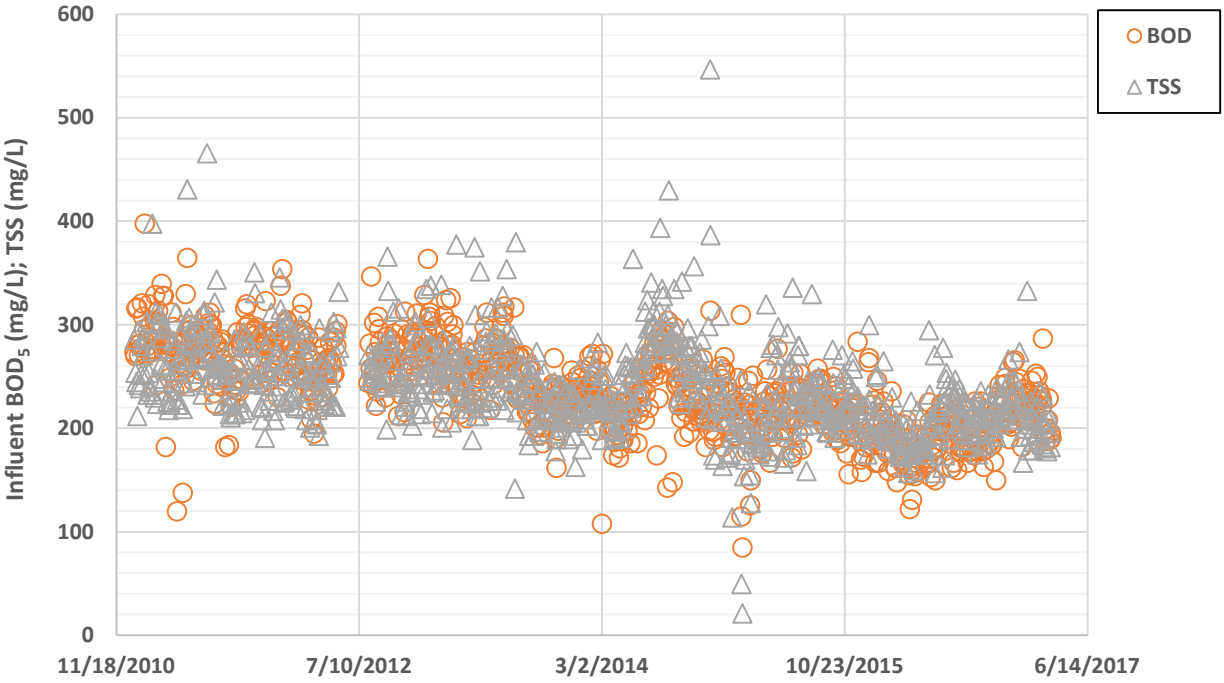

Figure B-8 Influent BOD_5 and TSS Concentrations January 2011-March 2017

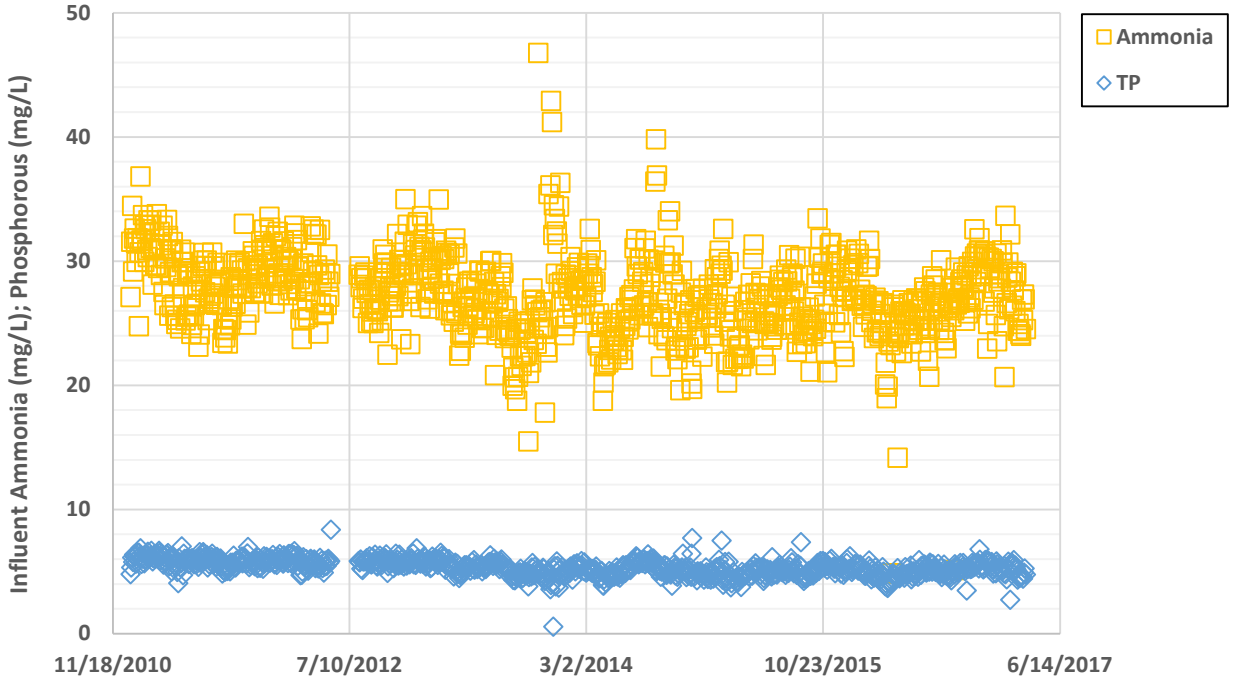

Figure B-9 Influent Ammonia and TP Concentrations January 2011-March 2017

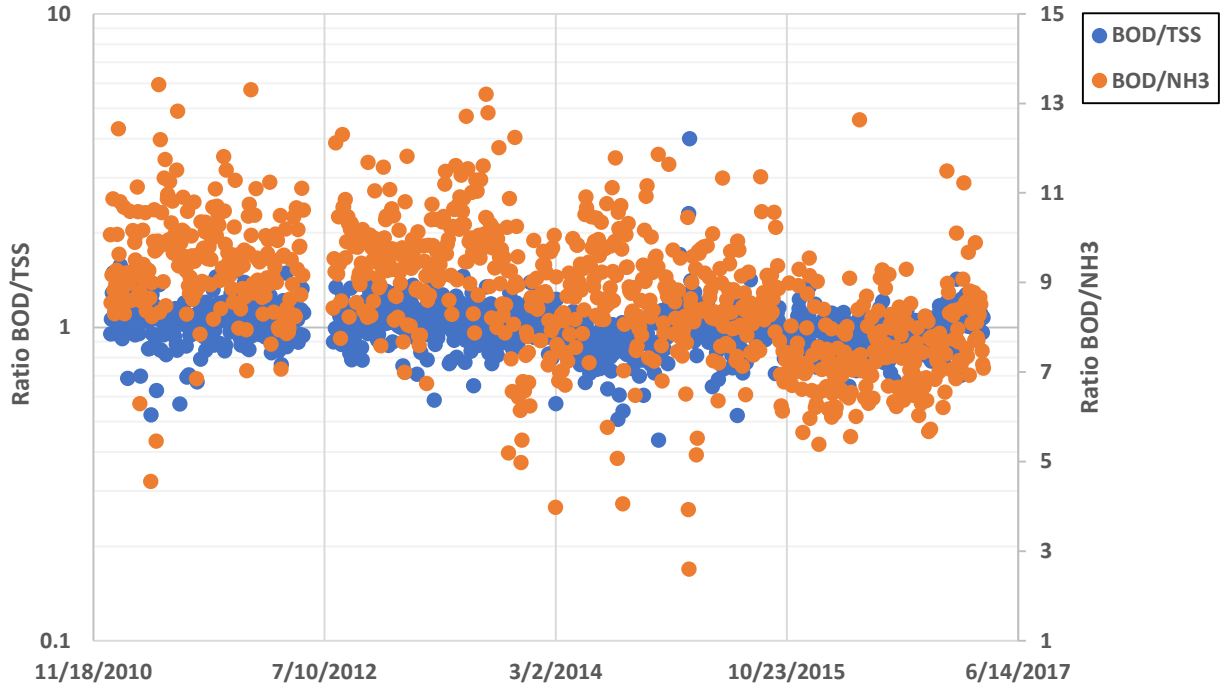

Figure B-10 Influent BOD_5 to TSS and BOD_5 to Ammonia Ratios 2011-2017

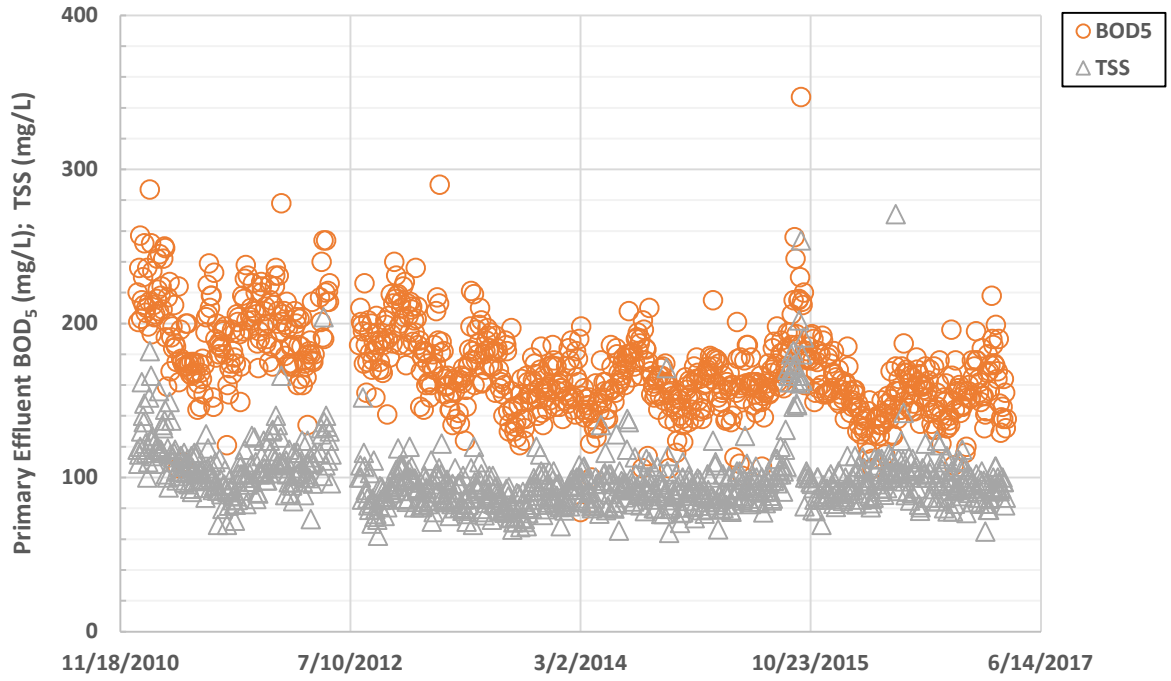

Figure B-11 Primary Effluent BOD_5 and TSS Concentrations 2011-2017

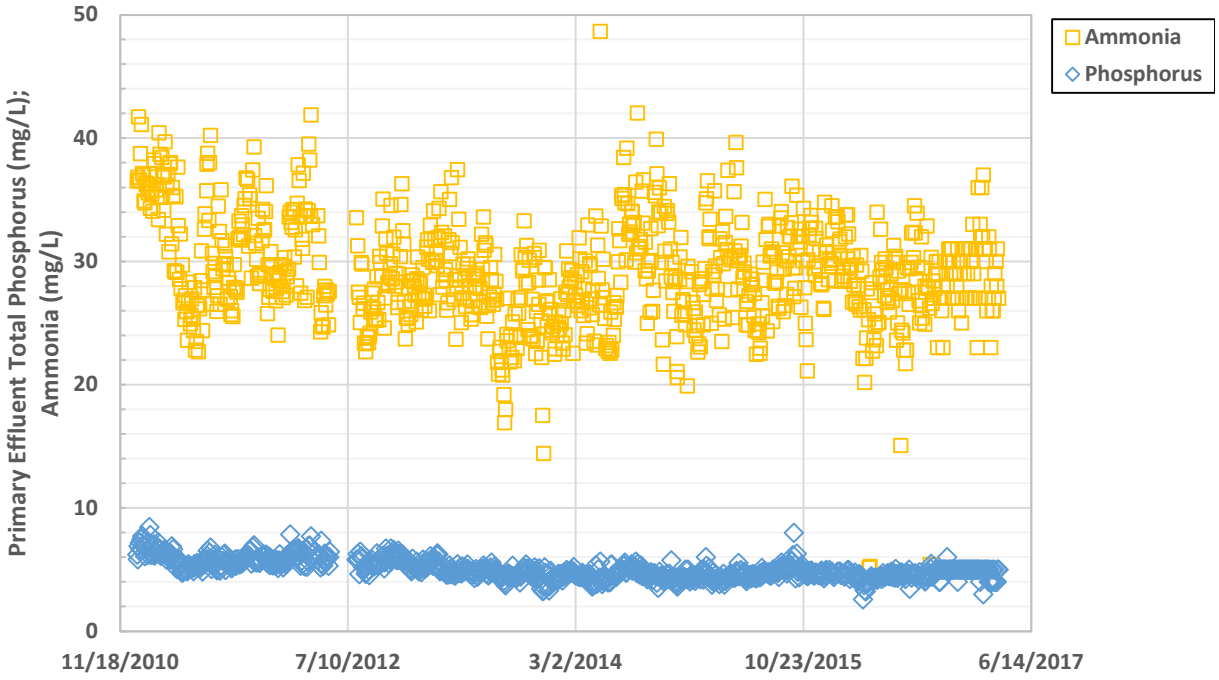

Figure B-12 Primary Effluent Ammonia and TP Concentrations 2011-2017

Table B-3 Year to Year Average Mass Loading and System Water Quality

Year	Avg. Flow (MGD)	MCRT (days)		Influent			Primary Effluent			
			BOD_5 (lbs/day)	TSS (lbs/day)	NH_3 (lbs/day)	TP (lbs/day)	BOD_5 (lbs/day)	TSS (lbs/day)	NH_3 (lbs/day)	TP (lbs/day)
2011	4.22	12.9	9,730	9,300	1,020	207	6,920	3,820	1,120	207
2012	4.13	13.9	9,310	8,820	983	200	6,750	3,520	1,010	201
2013	4.45	12.2	9,270	9,100	1,010	194	6,190	3,290	1,020	179
2014	4.70	12.1	9,070	10,050	1,040	202	6,200	3,640	1,140	178
2015	4.66	9.1	8,300	8,390	1,030	196	6,600	4,020	1,140	182
2016	4.69	10.6	7,800	8,370	1,040	203	5,830	3,900	1,090	179
2017[1]	4.36	14.2	8,020	7,490	990	183	5,880	3,340	1,080	171

[1]Note: Values through March 2017 only

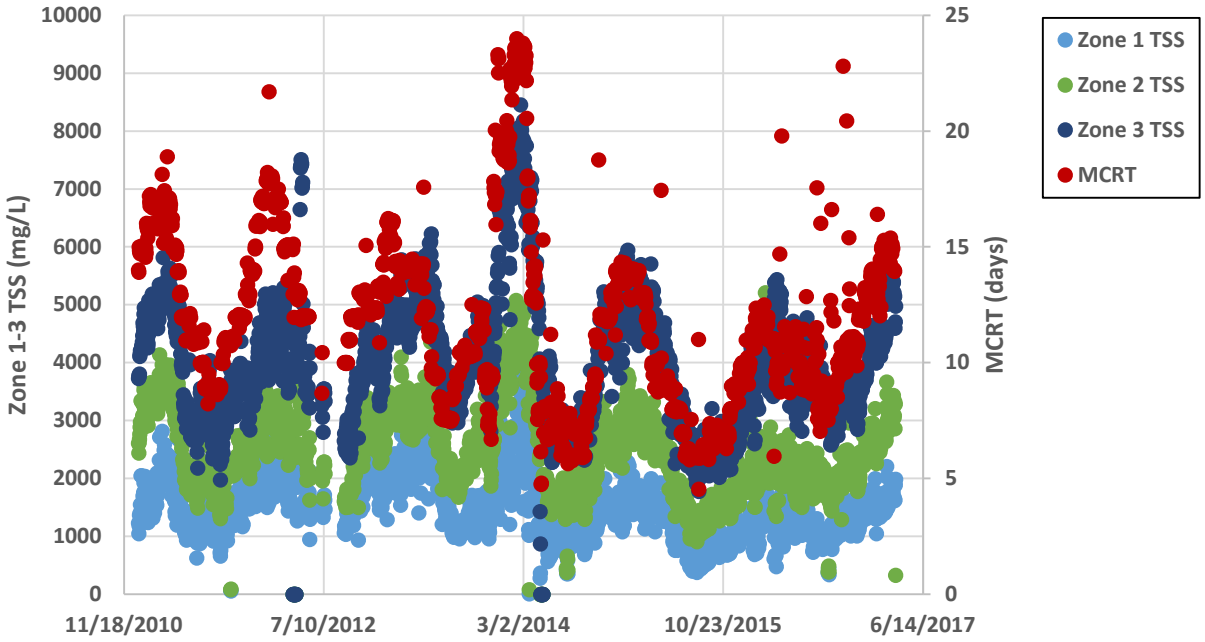

Figure B-13 Seasonal Changes in MLSS as a function of MCRT in North Aeration Basin

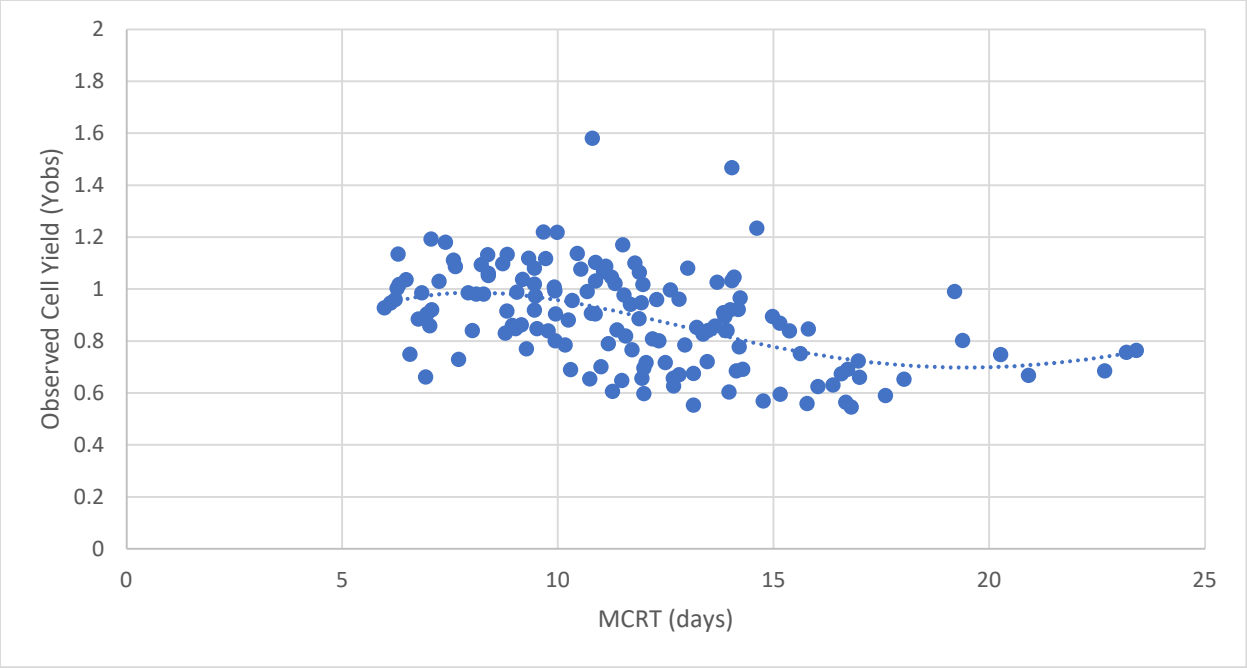

Figure B-14 Cell Yield as a function of MCRT[1]

[1]*Note: MCRT was taken as a 14-day average*

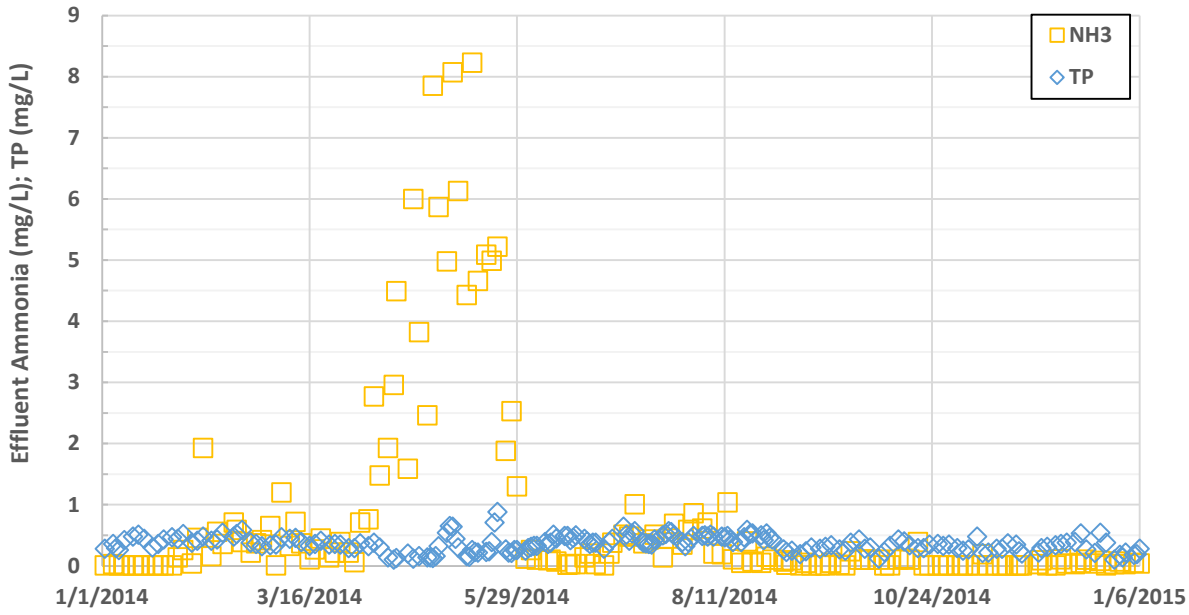

Figure B-15 Effluent Ammonia and Phosphorous Concentrations

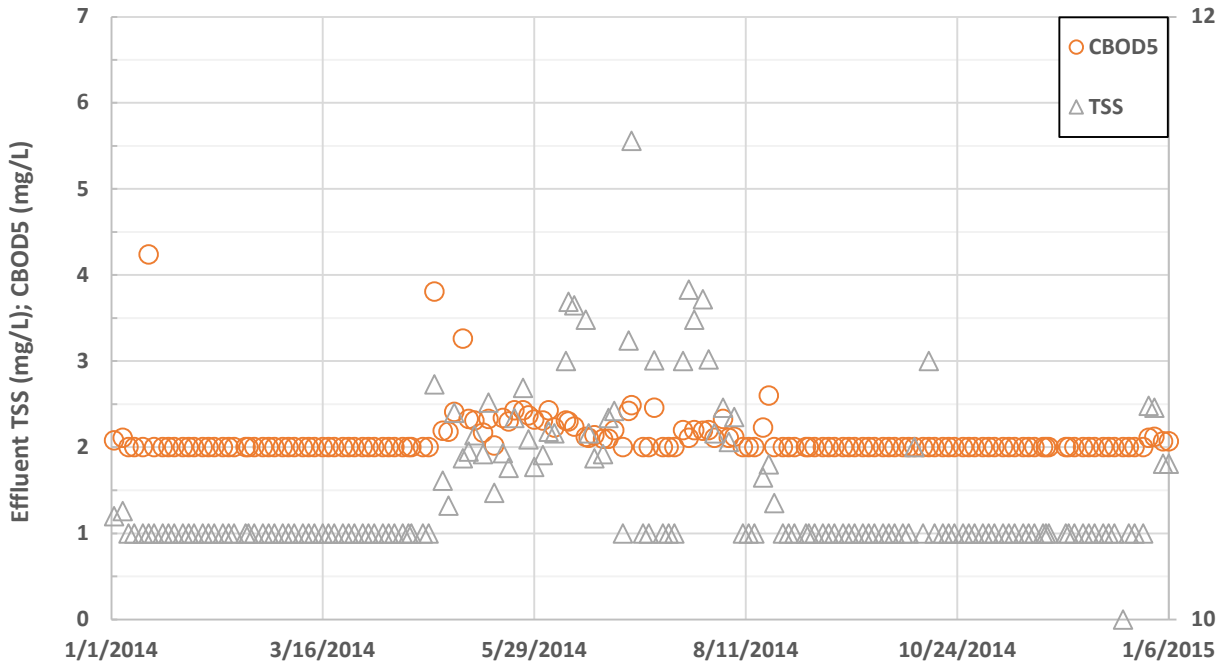

Figure B-16 Effluent $cBOD_5$ and TSS Concentrations

5′-
TACGTAGGTGGCAAGCGTTATCCGGAATTATTGGGCGTAAAGCGCGCGTAGGCGGT
TTTTTAAGTCTGATGTGAAAGCCCACGGCTCAACCGTGGAGGGTCATTGGAAACTGG
AAAACTTGAGTGCAGAAGAGGAAAGTGGAATTCCATGTGTAGCGGTGAAATGCGCA
GAGATATGGAGGAACACCAGTGGCGAAGGCGACTTTCTGGTCTGTAACTGACGCTG
ATGTGCGAAAGCGTGGGG ATCAAACAGG -3′

Figure B-17 OTU 0910 Sequence

Table B-4 Relative Abundance of Staphylococcus (verified with OTU 0910) during plant upsets (March/April 2017, January 2018) and period of normal operation (August 2017).

Sample ID	Relative Abundance (OTU count/Total OTU counts)	Plant Status
RP-TC-ML Week 1	4.08×10^{-05}	Reduced Permeability
RP-TC-ML Week 2	0.00×10^{00}	Reduced Permeability
RP-TC-ML Week 3	3.66×10^{-05}	Reduced Permeability
RP-TC-ML Week 4	7.06×10^{-05}	Reduced Permeability
C-TC-ML Week 5	1.18×10^{-04}	Normal
C-TC-ML Week 6	4.04×10^{-05}	Normal
C-TC-ML Week 7	4.68×10^{-05}	Normal
C-TC-ML Week 8	3.01×10^{-05}	Normal
RP-TC-ML Week 9	6.13×10^{-05}	Reduced Permeability
RP-TC-ML Week 10	6.36×10^{-06}	Reduced Permeability

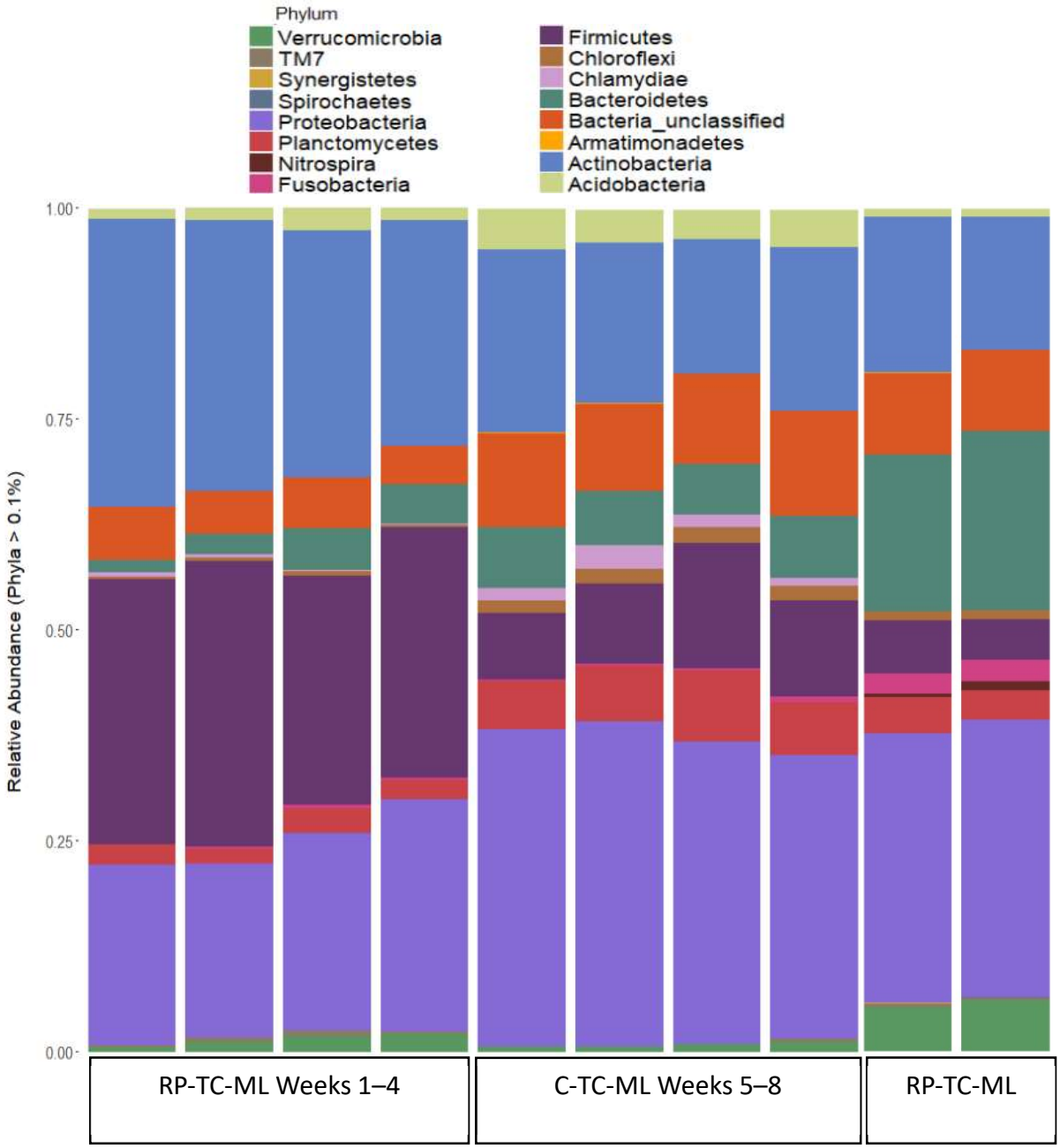

Figure B-18 Relative abundance of phylum-level OTUs for mixed liquor samples periods March/April 2017 (RP-TC-ML Weeks 1–4), August/September 2017 (C-TC-ML Weeks 5–8), and January 2018 (RP-TC-ML Weeks 9–10)
Note: a minimum cut off of 0.1% was used for illustrative purposes.

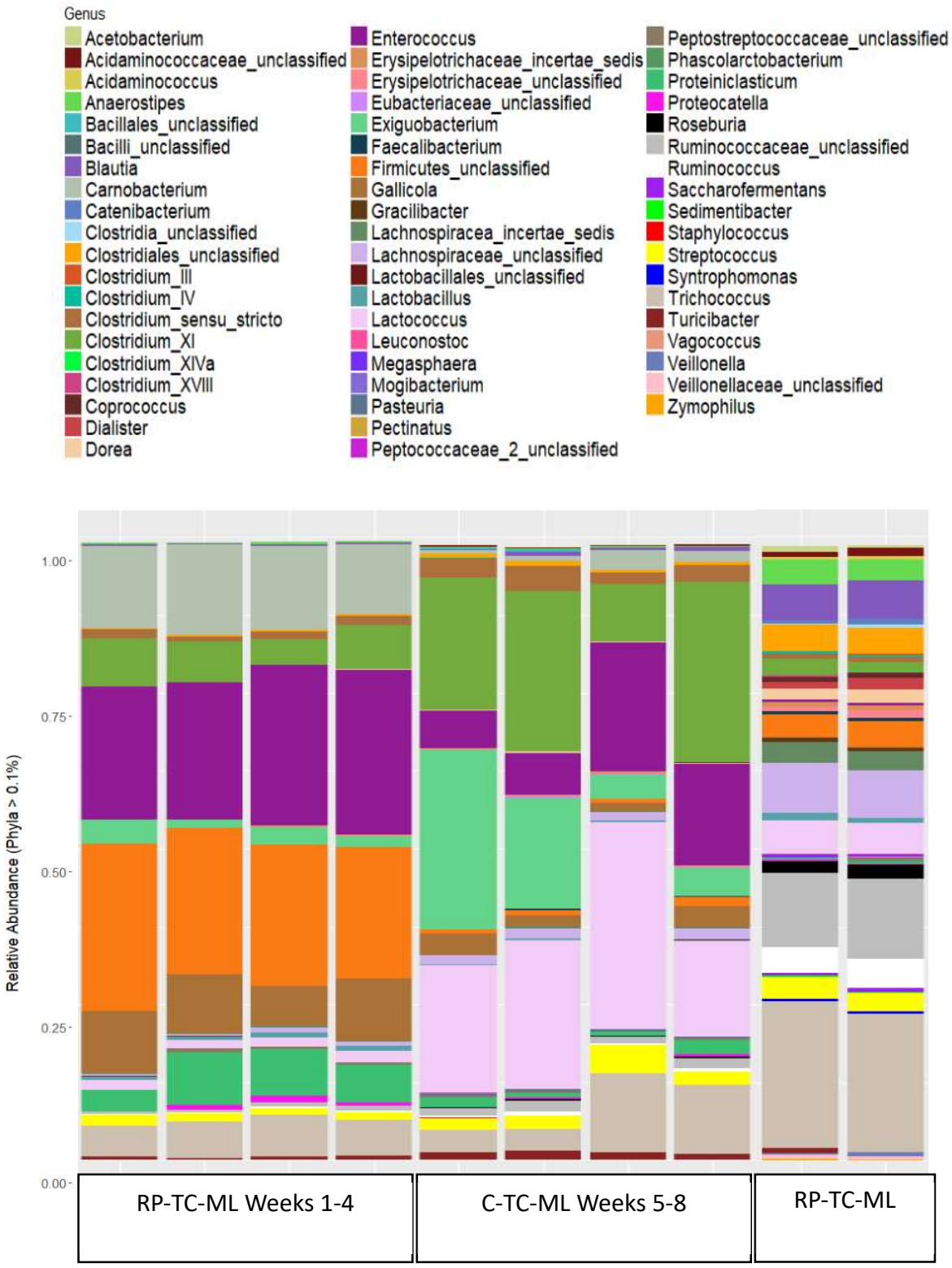

Figure B-19 Relative abundance of genus OTUs for members within the phylum Firmicutes for March/April 2017 (RP-TC-ML Weeks 1–4), August/September 2017 (C-TC-ML Weeks 5–8), and January 2018 (RP-TC-ML Weeks 9–10). Note: a minimum cut off of 0.1% was used for illustrative purposes.

Appendix B-6 Chapter 3 Mixed Liquor Chemical Characterization

Table B-5 Complete Nutrient Analysis for Mixed Liquor Samples 2017-2018

Sample Date	K^+ (mg/L)	Na^+ (mg/L)	Ca^{2+} (mg/L)	Mg^{2+} (mg/L)	Monovalent (mEq/L)	Divalent (mEq/L)	Mono/ Div[a]	BOD_5/NH_3-N PE mass ratio[b]	BOD_5/TSS PE mass ratio[b]
March	65.1	103	**278**	52.8	8.2	18.3	0.45	5.47	1.64
2017	79.4	109	**175**	43.1	9.0	12.4	0.72	5.17	1.66
April	57.5	50.1	**175**	33.0	5.8	11.5	0.51	4.63	1.42
2017	85.6	88.0	**200.**	40.1	8.3	13.3	0.62	4.55	1.40
August	53.0	111	127	29.8	8.1	8.8	0.92	5.50	1.59
2017	51.7	104	130.	36.6	7.7	9.6	0.81	6.26	1.72
September	55.1	98.4	127	36.3	7.5	9.4	0.80	5.68	1.74
2017	55.5	97.8	118	32.5	7.5	8.6	0.87	5.38	1.62
January	**69.4**	**106**	**138**	**39.5**	**8.2**	**10.2**	**0.81**	**6.68**	**1.09**
2018	**68.5**	**132**	**132**	**35.9**	**9.4**	**9.6**	**0.97**	**6.14**	**1.04**
March 2018	55.3	105	114.5	31.8	7.9	8.4	0.94	**6.81**	1.43
June	53.1	107	126.2	35.8	7.8	9.3	0.84	5.57	1.34
2018	59.0	104	119.0	35.0	7.8	8.9	0.88	5.69	1.40
August 2018	32.7	112	137.9	47.6	7.2	10.9	0.67	8.49	1.36
October 2018	35.8	111	143.1	27.1	7.6	9.4	0.80	6.25	1.86
November 2018	22.7	112	101.3	42.9	7.3	8.6	0.84	6.26	2.13

Note:

a. Monovalent/Divalent cation mass ratio
b. PE denotes that the constituents were measured in the primary effluent to TCRWWTP's aeration basin (mg BOD_5/mg NH_3-N) or (mg BOD_5/mg TSS), respectively

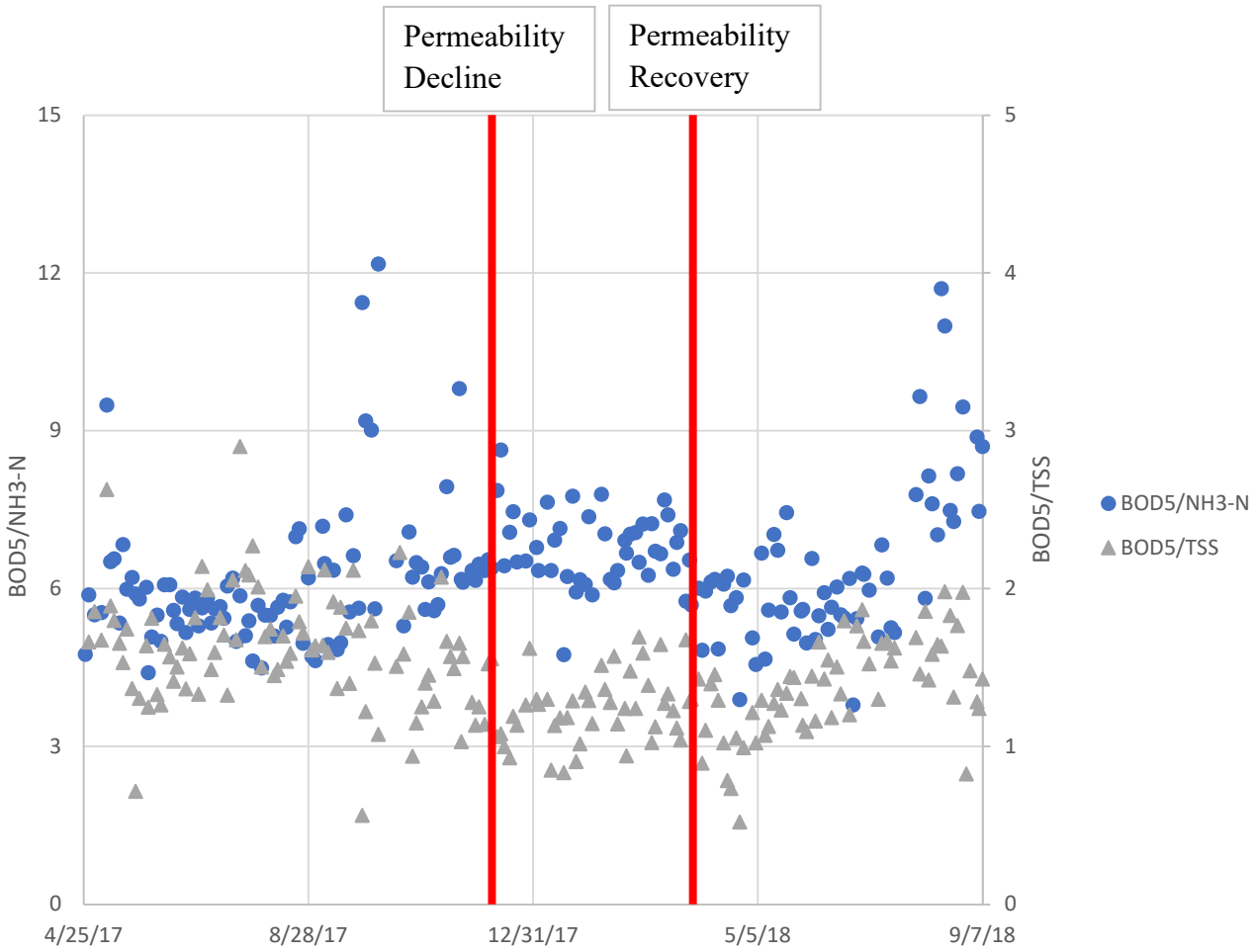

Figure B-20 Biological oxygen demand (BOD_5) to Total Suspended Solids (TSS) and BOD_5 to ammonia (NH_3-N) mass ratios from TCRWWTP's primary effluent.

An uncharacteristic pattern emerged correlating to reduced permeability event in January 2018. Red line denotes the events start and end date.

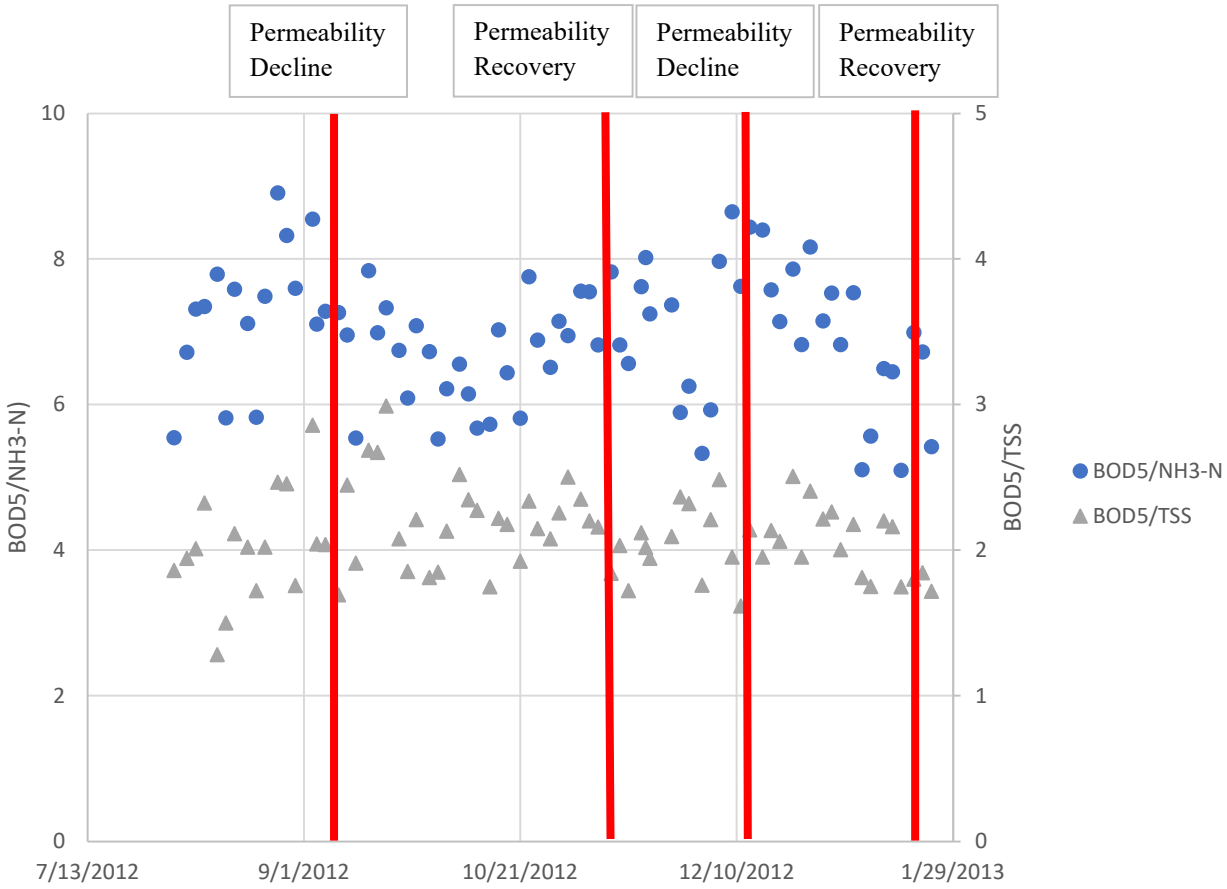

Figure B-21 Biological oxygen demand (BOD_5) to Total Suspended Solids (TSS) and BOD_5 to ammonia (NH_3-N) mass ratios from TCRWWTP's primary effluent.

A pattern emerged relating elevated BOD_5 to NH_3-N mass ratio to a series of reduced permeability events in 2012 and 2013. Red line denotes the events start and end date.

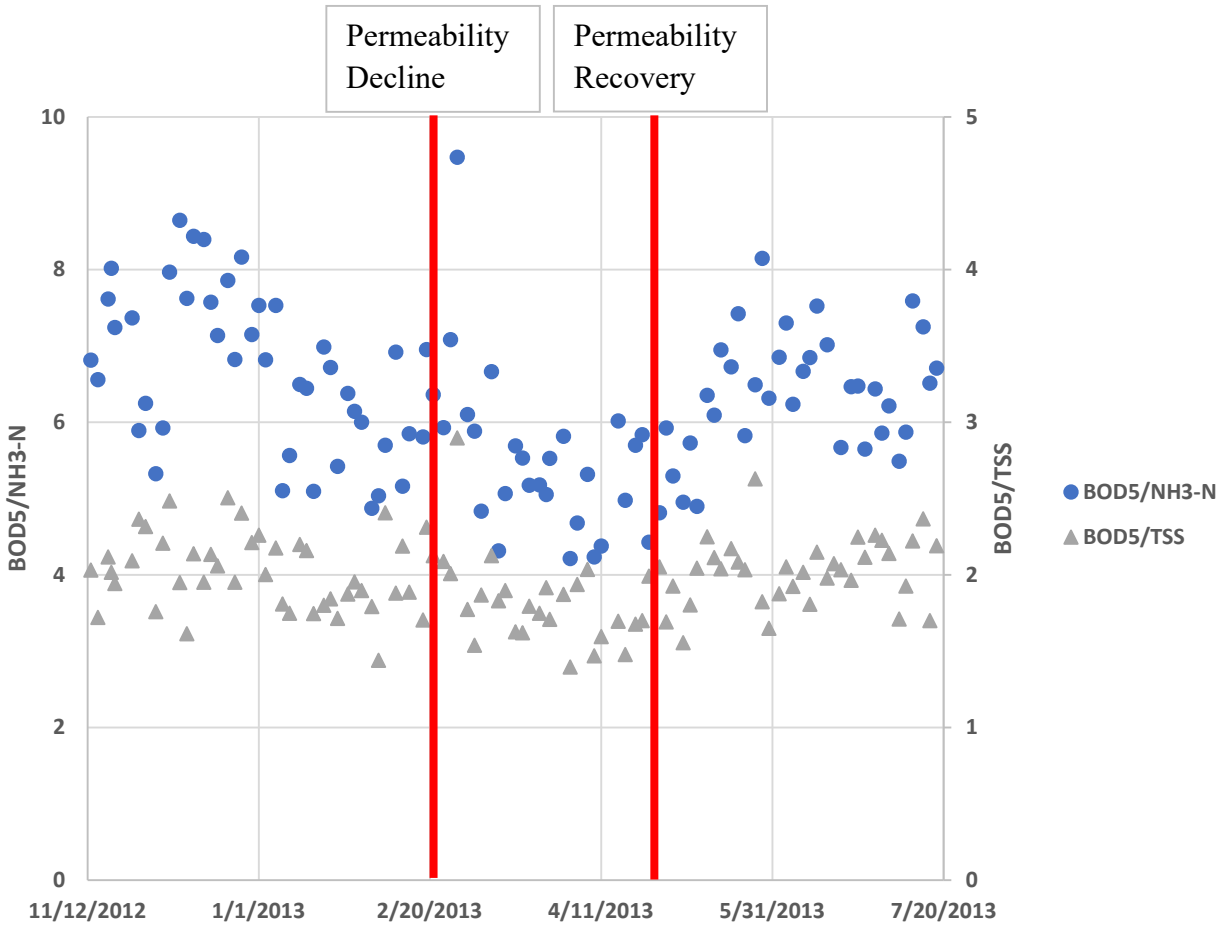

Figure B-22 Biological oxygen demand (BOD_5) to Total Suspended Solids (TSS) and BOD_5 to ammonia (NH_3-N) mass ratios from TCRWWTP's primary effluent.

A different pattern than previous years emerged demonstrating decreased BOD_5 to NH_3-N mass ratio to a reduced permeability events in 2013. Red line denotes the events start and end date.

Appendix B-7 Chapter 3 Physical SRF tests

The SRF experiments provide a plausible explanation for the brief period of permeability decline in 2017 at TCRWWTP, where nearly 7 mM calcium concentration was observed in the mixed liquor the first week after the upset began. However, this logic proves insufficient in describing what occurred in January 2018, where no such inorganic concentration spike was seen. Because the solids retention time is around 14 days at TCRWWTP, EPS material could be accumulating in the MBR from a shock load of organics according to the biological processes in the aeration basin. A simple time-dependent SRF experiment was developed to validate the possibility of an organic loading event that would produce EPS and bridge with cations to decrease permeability. One part primary effluent from TCRWWTP (full of dissolved organic carbon) was added to three parts of a sample of the plant's mixed liquor to simulate the fraction of pure influent and return mixed witnessed coming into the aeration basin. From there, a 5 mM dose of calcium was added to the solution. SRF values substantially increased, a resistance over 10X that of a fresh mixed liquor sample or the combined primary effluent-mixed liquor solution. This also marked a considerable increase over the calcium spiked addition values discussed above. More work is still needed to characterize what happened between hours 15 and 18. A prior experiment (data not shown) with mixed liquor tested 24 hours apart showed a change in SRF of about threefold in which no other substrate was provided to the mixed liquor. This experimental design, on the other hand, was intended to provide excess carbon to simulate a shock load event. It is unclear exactly what contribution calcium played in the context of the resistance seen in this experiment, but previous examples seem to suggest that binding occurred as EPS was excreted from the cells into suspension around hour 15, which likely caused the jump in resistance at hour 18.

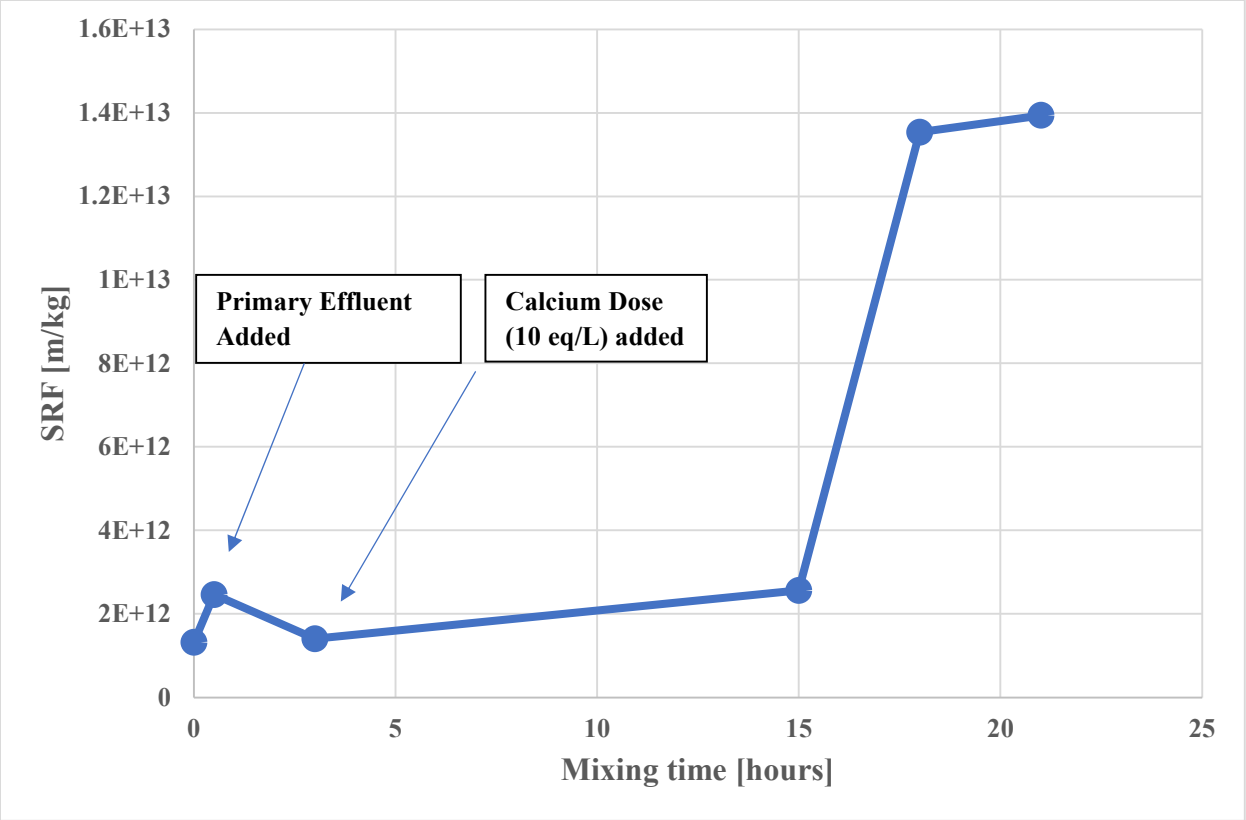

Figure B-23 Time-dependent SRF changes with shock loads of organic (primary effluent) addition and inorganic (5 mM calcium).

Appendix C Supplementary Information for Chapter 4

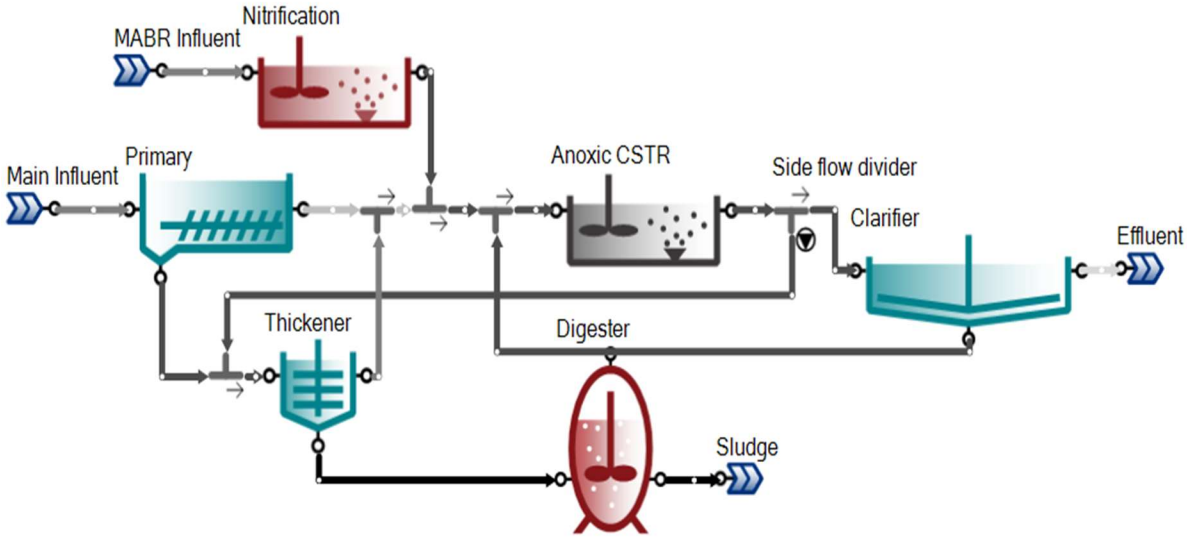

Figure C-1 Surrogate MABR Process for simplified proof-of-concept hybrid MABR model

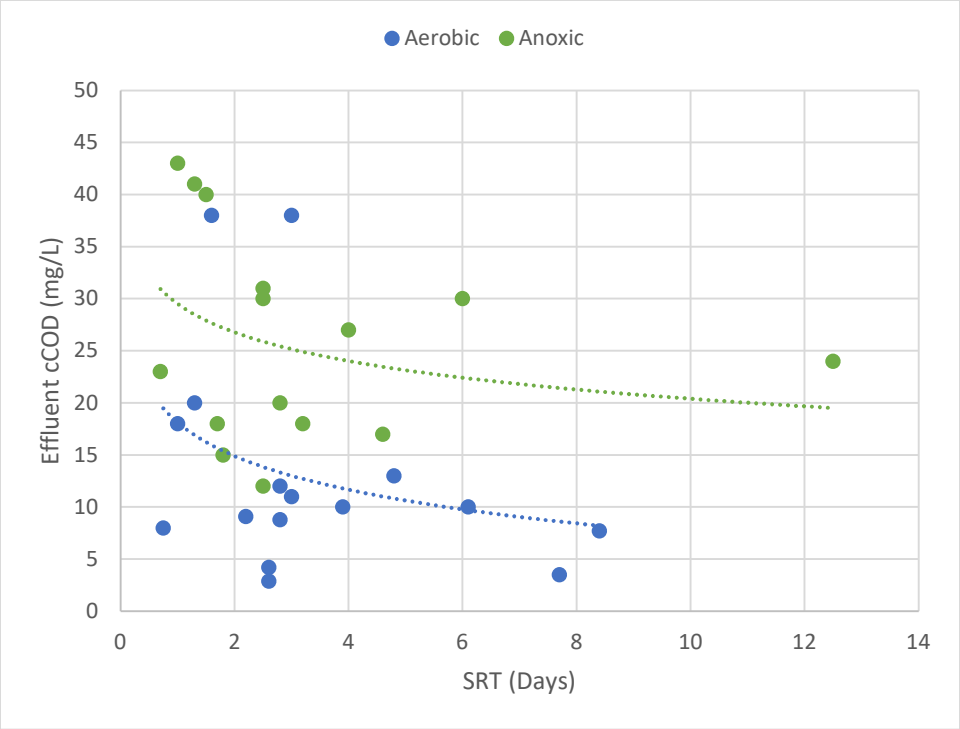

Figure C-2 Comparison of the colloidal COD removal performance between the aerobic and anoxic bioreactors

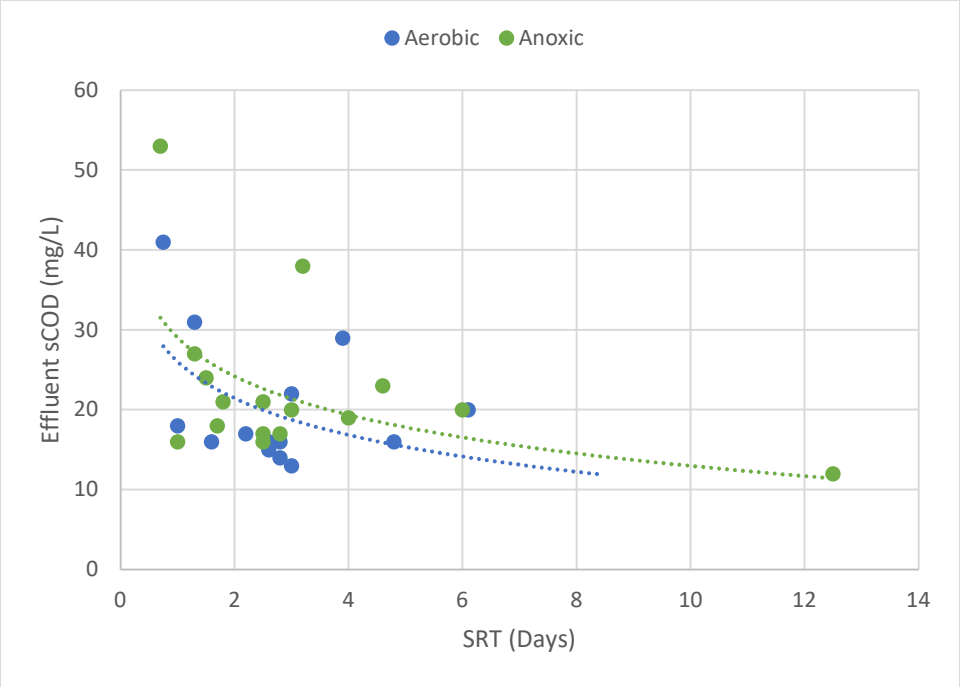

Figure C-3 Comparison of the soluble COD removal performance between the aerobic and anoxic bioreactors

Appendix C-1 Chapter 4 Supplementary Physical Model Results

Table C-1 AAWWTP Primary Effluent Average Wastewater Characteristics for nitrogen removal sample periods

Sample No.	Sample Date	TSS (mg/L)	VSS (mg/L)	VSS/TSS %	Total COD (mg/L)	Filtered COD (mg/L)	Floc&Filt COD (mg/L)	TN (mgN/L)	TDN (mgN/L)	NH_3 (mgN/L)	NO_3^- (mgN/L)	NO_2^- (mgN/L)
081919PE	8/19/2019	50.7	43.3	84.3	161	102	84.0	43.7	35.3	12.5	0.90	0.0
082619PE	8/26/2019	41.5	38.0	91.6	200	155	18.5	1.4	29.4	29.6	2.1	0.0
083019PE	8/30/2019	133	111	83.3	248	105	58.0	14.4	50.0	19.9	0.70	0.0
090319PE	9/3/2019	102	88.5	87.2	238	119	60.0	13.5	26.5	18.6	0.60	0.0
090919PE	9/9/2019	96.5	83.5	86.5	-	-	-	17.9	29.4	22.3	0.90	0.0
091119PE	9/11/2019	206	173	84.2	-	-	-	8.90	26.7	19.7	1.30	0.0
091819PE	9/18/2019	121	106	87.6	235	96.0	58.5	30.7	27.3	21.0	1.90	1.4
092019PE	9/20/2019	231	200	86.5	400	136	78.0	39.0	36.3	20.5	0.80	0.0
092719PE	9/27/2019	129	117	90.8	275	98.5	57.0	34.3	27.0	19.4	1.00	0.0
093019PE	9/30/2019	217	191	88.0	340	92.5	48.0	51.0	42.0	16.0	1.00	0.0
100719PE	10/7/2019	115	105	91.3	306	119	61.5	53.0	31.3	13.3	0.70	0.0
AVERAGE		**131**	**114**	**87.4**	**267**	**114**	**58.2**	**28.0**	**32.8**	**19.3**	**1.10**	**0.1**
100919PE	10/9/2019	60.8	49.2	81.6	258	142	86.5	40.7	32.3	22.8	1.1	0.0
101519PE	10/15/2019	52.3	51.5	98.6	188	147	69.0	48.0	35.6	22.0	5.30	0.1
101719PE	10/17/2019	43.1	37.7	87.6	162	147	80.0	43.7	35.6	27.3	5.30	0.0
102319PE	10/23/2019	93.1	87.7	94.3	200	83.0	48.5	35.6	28.9	17.3	0.60	0.0
102519PE	10/25/2019	41.5	36.9	89.9	149	94.0	58.0	35.6	31.1	16.6	0.80	0.1
AVERAGE		**58.2**	**52.6**	**90.4**	**191**	**122**	**68.4**	**40.7**	**32.7**	**21.2**	**2.60**	**0.0**
102819PE	10/28/2019	89.2	83.0	89.4	221	81.0	63.0	0.0	17.8	11.8	0.70	0.0
103019PE	10/30/2019	35.4	33.9	95.6	201	131	70.0	0.0	29.6	25.9	1.20	0.0
110119PE	11/1/2019	109	96.2	88.7	209	83.0	40.0	0.0	16.5	14.1	0.80	0.30
110519PE	11/5/2019	27.4	25.9	94.6	92.5	63.5	29.0	-	-	-	-	-

AVERAGE		65.1	59.8	92.1	181	89.6	50.5	0.0	21.3	17.3	0.90	0.10
110719PE	11/7/2019	31.4	27.1	86.4	75.0	53.5	21.5	23.0	23.0	17.8	0.60	0.2
111119PE	11/11/2019	40.8	34.5	85.3	161	116	69.0	33.8	27.9	26.1	0.90	0.2
111319PE	11/13/2019	54.3	46.7	86.5	168	118	59.5	38.2	32.4	32.0	0.90	0.2
111519PE	11/15/2019	36.1	34.5	95.5	327	83.5	39.0	26.5	23.7	20.8	0.70	0.1
111919PE	11/19/2019	56.3	47.5	84.0	255	180	122	33.3	32.9	31.2	1.20	0.1
112119PE	11/21/2019	43.1	38.5	89.5	210	152	107	34.7	31.6	23.3	1.1	0.1
112419PE	11/24/2019	36.9	35.4	95.8	179	127	65.0	35.5	42.1	24.5	0.8	0.0
112619PE	11/26/2019	88.8	85.0	96.1	302	159	123	43.4	34.2	26.5	1.3	0.2
AVERAGE		48.5	43.7	89.9	210	124	75.7	33.6	31.0	25.3	0.90	0.10
020420PE	2/4/2020	137	120	87.4	239	81.5	59.0	29.8	22.7	15.0	0.90	0.10
020620PE	2/6/2020	182	151	83.1	295	93.0	71.0	27.2	21.3	13.5	0.80	0.20
021220PE	2/12/2020	247	207	83.9	-	-	-	-	-	17.0	0.80	0.0
021420PE	2/14/2020	106	96.0	90.6	214	96.0	73.0	26.8	20.0	14.3	-	0.4
021820PE	2/18/2020	91.0	78.0	85.7	194	100	77.0	26.3	18.2	15.0	1.00	0.30
022020PE	2/20/2020	291	256	87.8	-	72.0	53.0	34.3	18.5	14.3	1.30	0.0
022520PE	2/25/2020	79.5	72.5	91.4	230	132	103	39.6	32.2	25.9	1.40	0.0
022820PE	2/28/2020	47.7	44.5	93.2	234	95.8	72.7	32.4	26.5	28.8	0.80	0.0
030220PE	3/2/2020	126	111	88.1	-	-	-	14.7	16.2	12.5	0.70	0.0
030320PE	3/3/2020	78.0	69.0	88.5	-	-	-	25.0	22.1	9.5	0.50	0.20
030320PE	3/3/2020	47.0	44.5	94.8	-	-	-	14.7	17.7	19.7	0.50	0.0
030520PE	3/5/2020	48.0	44.0	92.6	213	200	200	30.9	29.4	19.0	0.70	0.0
030720PE	3/7/2020	155	135	87.1	240	48.5	77.0	14.7	22.1	10.1	0.30	0.0
030920PE	3/9/2020	57.0	52.0	91.3	152	142	132	24.3	13.8	13.9	0.50	0.0
031020PE	3/10/2020	46.0	42.2	91.6	188	110	77.0	28.3	30.9	22.5	0.70	0.0
031220PE	3/12/2020	42.5	38.5	90.6	221	132	112	32.2	27.0	23.0	1.70	0.0
031320PE	3/13/2020	21.0	20.5	97.8	-	-	-	29.6	24.3	26.3	1.70	0.0
AVERAGE		106	93.0	89.7	220	109	92.2	26.9	22.7	17.7	0.90	0.10
060120PE	6/1/2020	69.0	63.0	91.3	155	73.0	53.0	19.8	13.9	7.00	2.00	0.50
060420PE	6/4/2020	41.0	33.0	80.4	116	99.0	83.0	16.5	17.2	10.3	0.60	0.0

060820PE	6/8/2020	45.0	38.0	84.8	120	92.0	66.0	23.8	22.4	19.3	0.60	0.0
061120PE	6/11/2020	31.0	28.0	91.7	84.0	43.5	39.0	15.4	15.4	8.9	1.30	0.0
061520PE	6/15/2020	26.0	25.0	96.2	159	116.0	88.0	25.1	22.4	21.2	0.40	0.0
061720PE	6/17/2020	79.0	67.0	84.8	247	117	83.0	19.9	13.6	14.6	0.70	0.0
061920PE	6/19/2020	74.0	68.0	92.0	197	107	51.7	28.6	23.6	25.4	1.50	0.0
062220PE	6/22/2020	42.0	31.0	73.8	105	76.3	44.3	21.1	19.9	14.9	0.60	0.0
062420PE	6/24/2020	59.0	48.0	81.3	134	70.0	44.0	21.0	18.9	14.9	0.50	0.0
AVERAGE		**49.3**	**47.0**	**97.7**	**146**	**88.2**	**61.3**	**21.2**	**18.6**	**15.2**	**0.9**	**0.10**
070820PE	7/8/2020	41.3	34.7	83.6	125	70.7	36.3	16.5	14.4	12.1	0.60	0.0
071020PE	7/10/2020	40.7	36.7	90.1	84.0	54.0	29.0	23.5	20.0	18.1	0.60	0.40
071320PE	7/13/2020	30.0	30.0	100	78.0	49.3	29.3	17.2	14.4	16.0	0.50	0.0
071520PE	7/15/2020	45.3	40.7	89.7	123	78.3	43.0	22.0	19.1	16.0	0.50	0.0
071720PE	7/17/2020	26.7	22.7	82.7	100	59.7	29.7	19.1	17.6	11.4	0.50	0.0
072020PE	7/20/2020	24.7	23.3	94.3	92.0	66.7	39.0	23.5	19.1	14.1	0.50	0.0
072220PE	7/22/2020	18.0	16.7	92.3	66.0	48.7	27.7	18.6	14.4	11.5	0.40	0.0
072420PE	7/24/2020	18.0	16.7	92.3	89.3	66.7	36.3	21.4	15.8	13.9	0.50	0.0
072720PE	7/27/2020	30.7	26.0	85.0	111	78.7	40.3	24.2	25.6	17.3	1.10	0.0
072920PE	7/29/2020	20.7	20.7	100	-	-	-	20.1	17.4	14.5	0.50	0.0
073120PE	7/31/2020	21.3	20.7	97.1	138	73.0	40.3	18.8	17.4	16.2	0.50	0.0
080320PE	8/3/2020	36.0	34.7	96.4	144	102	57.0	25.7	27.1	18.4	0.60	0.0
080420PE	8/4/2020	34.0	30.7	90.2	117	76.0	43.3	18.8	14.6	10.6	0.50	0.10
AVERAGE		**29.7**	**27.4**	**92.8**	**106**	**68.6**	**37.6**	**21.1**	**18.8**	**14.2**	**0.6**	**0.0**
Final Avg		**85.9**	**75.7**	**89.2**	**206**	**109**	**70.3**	**30.5**	**26.1**	**19.2**	**1.09**	**0.09**
Min		**21.0**	**20.5**	**73.8**	**75.0**	**43.5**	**18.5**	**14.7**	**13.6**	**6.97**	**0.27**	**0.00**
Max		**291**	**256**	**99**	**400**	**200**	**200**	**53.0**	**50.0**	**32.0**	**5.30**	**1.39**
Standard Dev.		**61.7**	**52.9**	**4.78**	**68.0**	**32.2**	**31.3**	**9.56**	**7.80**	**5.99**	**0.93**	**0.22**

Table C-2 Reactor 1 Effluent Average Wastewater Characteristics for nitrogen removal sample periods

Sample No.	Sample Date	TSS (mg/L)	VSS (mg/L)	VSS/TSS %	Total COD (mg/L)	Filtered COD (mg/L)	FlocFilt COD (mg/L)	TN (mgN/L)	TDN (mgN/L)	NH_3 (mgN/L)	NO_3 (mgN/L)	NO_2 (mgN/L)	SRT (days)
081519R1	8/15/2019	52.0	43.0	82.9	-	-	-	-	-	12.2	6.75	2.96	3.08
091819R1	9/18/2019	84.5	77.5	91.7	250	127	80	44.0	43.0	29.6	8.36	1.14	
092019R1	9/20/2019	76.5	68	88.9	159	74	41	27.0	26.3	17.7	0.6	0.43	
092719R1	9/27/2019	23	19	100	108	86.5	49	46.0	39.7	23.7	0.83	0.06	
093019R1	9/30/2019	**20**	**17**	**93.8**	**65**	**42**	**25**	**40.3**	**32.0**	**17.6**	**7.33**	**0.03**	
100719R1	10/7/2019	**32**	**23**	**90.6**	**55**	**38**	**19**	**38.7**	**34.3**	**10.1**	**6.81**	**1.41**	
AVERAGE		**26.0**	**20.0**	**92.2**	**60.0**	**40.0**	**22.0**	**39.5**	**33.2**	**13.9**	**7.1**	**0.7**	
100919R1	10/9/2019	32.5	31	95.4	105	67.5	30	44.7	41.0	22.4	3.1	4.1	1.30
101119R1	10/11/2019	54	53	98.2	116	65	40	46.3	35.3	22.2	1.01	0.03	
101519R1	10/15/2019	40	37.5	93.8	100	73	20.5	35.3	33.3	22.4	5.4	0.02	
101719R1	10/17/2019	**26.5**	**24**	**90.6**	**56**	**54**	**29.5**	**34.0**	**33.3**	**27.0**	**6.5**	**0.01**	
102319R1	10/23/2019	**23.9**	**22.6**	**94.7**	**67**	**51**	**30.5**	**40**	**35.56**	**24.4**	**0.38**	**0.03**	
102519R1	10/25/2019	**20**	**18.5**	**92.3**	**61**	**50**	**34**	**35.56**	**28.89**	**17.9**	**0.82**	**0.06**	
AVERAGE		**23.5**	**21.7**	**92.5**	**61.3**	**51.7**	**31.3**	**36.5**	**32.6**	**23.1**	**2.6**	**0.0**	
102819R1	10/28/2019	22.3	22.3	100	75	58	19.1	32.4	29.61	11.67	0.54	0.03	0.97
103019R1	10/30/2019	32.3	28.5	88.2	109	77.5	23	31.8	28.29	23.9	0.43	0.04	
110119R1	11/1/2019	**29.2**	**29.2**	**100**	**85.5**	**71.5**	**16.3**	**24.0**	**20.39**	**17.62**	**0.54**	**0.09**	
110519R1	11/5/2019	**27.7**	**24.6**	**88.9**	**67.5**	**33.5**	**15.3**	-	-	-	-	-	
AVERAGE		**28.5**	**26.9**	**94.5**	**76.5**	**52.5**	**15.8**	**24.0**	**20.4**	**17.6**	**0.5**	**0.1**	
110719R1	11/7/2019	15	11.4	76.4	48.5	38.5	15.3	20.9	20.2	21.8	0.53	0.05	1.63
111119R1	11/11/2019	16.2	14.6	90.5	62.5	43.0	20.0	30.0	27.9	25.7	0.77	0.01	
111319R1	11/13/2019	18.5	15.4	83.3	51.0	57.5	16.3	31.4	28.6	27.0	0.70	0.02	
111519R1	11/15/2019	12.3	10.0	81.3	58.0	43.0	18.5	22.3	21.6	20.9	0.60	0.01	
111919R1	11/19/2019	**28.5**	**24.6**	**87.1**	**38.5**	**70.5**	**12.0**	**26.4**	**29.0**	**27.5**	**1.15**	**0.70**	
112119R1	11/21/2019	**20.7**	**18.6**	**89.5**	**71**	**70**	**-**	**27.8**	**35.5**	**18.6**	**1.01**	**0.67**	

112419R1	11/24/2019	**25.0**	**22.1**	**88.6**	**92.5**	**53.5**	**-**	**34.2**	**27.6**	**22.17**	**0.91**	**0.55**	
112619R1	11/26/2019	**33.8**	**30.8**	**91.1**	**98.0**	**68.5**	**-**	**36.8**	**34.2**	**25.92**	**0.77**	**0.08**	
AVERAGE		**27.0**	**24.0**	**89.1**	**75.0**	**65.6**	**12.0**	**31.3**	**31.6**	**23.5**	**1.0**	**0.5**	
020420R1	2/4/2020	-	-	-	-	-	-	-	-	-	-	-	
020620R1	2/6/2020	-	-	-	-	-	-	-	-	-	-	-	
021220R1	2/12/2020	15	15	100	-	-	-	-	-	28.6	0.53	0.01	
021420R1	2/14/2020	18.3	17.3	88.2	56	41	36	29.2	27.8	21.9	-	0.04	
021820R1	2/18/2020	**57.5**	**48.8**	**88.6**	**90**	**43**	**31.0**	**32.9**	**28.9**	**23.7**	**0.48**	**0.01**	
022020R1	2/20/2020	**16**	**15**	**93.8**	**67**	**47.5**	**39.0**	**32.1**	**30.3**	**26.2**	**1.00**	**0.01**	
022520R1	2/25/2020	**44.5**	**39**	**87.7**	**102**	**61**	**46.0**	**35.2**	**30.7**	**24.8**	**1.18**	**0**	0.75
022820R1	2/28/2020	**16**	**14.5**	**90.8**	**78.8**	**48.1**	**38.0**	**26.5**	**38.2**	**26.0**	**0.77**	**0**	
030220R1	3/2/2020	**24**	**24**	**100**	**-**	**-**	**-**	**22.06**	**23.5**	**24.2**	**0.34**	**0**	
030320R1	3/3/2020	**14**	**14**	**100**	**-**	**-**	**-**	**47.06**	**20.6**	**14.7**	**0.34**	**0**	
030520R1	3/5/2020	**34**	**28**	**88.8**	**68.0**	**-**	**-**	**25**	**19.1**	**17.44**	**0.73**	**0.04**	
030720R1	3/7/2020	**16**	**16**	**100**	**61.0**	**47.5**	**29.0**	**23.53**	**19.1**	**16.3**	**0.45**	**0**	
030920R1	3/9/2020	**14**	**13**	**92.9**	**63.0**	**62.0**	**78.5**	**23.03**	**16.5**	**19.1**	**0.36**	**0.01**	
031220R1	3/12/2020	**22**	**22**	**100**	**63.5**	**35.0**	**25.0**	**30.92**	**27.0**	**20.6**	**0.82**	**0.04**	
AVERAGE		**25.8**	**23.4**	**94.2**	**74.2**	**49.2**	**40.9**	**29.8**	**25.4**	**21.3**	**0.6**	**0.01**	
060120R1	6/1/2020	17	17	100	63	56	37	15.8	13.9	5.52	1.19	0.65	
060420R1	6/4/2020	30	21	70.1	74.5	48	-	14.5	15.8	9.85	3.36	0.16	
060820R1	6/8/2020	10	9	91.7	26	19	15	18.2	19.6	14.21	2.56	1.11	
061120R1	6/11/2020	**15.2**	**12.1**	**80.4**	**29**	**25**	**15**	**14.03**	**15.4**	**8.6**	**8.13**	**0.87**	
061520R1	6/15/2020	**19**	**17**	**88.7**	**78**	**73**	**61.5**	**19.6**	**19.56**	**13.3**	**1.92**	**1.14**	2.18
061720R1	6/17/2020	29	24	82.8	105	71.5	62	16.13	14.9	9.6	2.06	1.93	
061920R1	6/19/2020	**15**	**14**	**93.7**	**37.0**	**24.7**	**16.3**	**12.4**	**12.38**	**3.5**	**4.02**	**3.1**	
062220R1	6/22/2020	**18**	**17.8**	**135**	**41.7**	**34.0**	**23.0**	**16.13**	**14.9**	**2.13**	**6.9**	**4.61**	
062420R1	6/24/2020	**14**	**13.8**	**186.7**	**39.0**	**30.0**	**18.0**	**15.42**	**15.4**	**5.91**	**4.09**	**3.23**	
AVERAGE		**15.2**	**14.0**	**92.0**	**41.8**	**34.3**	**24.8**	**16.0**	**16.2**	**7.9**	**4.6**	**2.3**	

Table C-3 Reactor 3 Effluent Average Wastewater Characteristics for nitrogen removal sample periods

Sample No.	Sample Date	TSS (mg/L)	VSS (mg/L)	VSS/TSS %	Total COD (mg/L)	Filtered COD (mg/L)	FlocFilt COD (mg/L)	TN (mgN/L)	TDN (mgN/L)	NH3 (mgN/L)	NO3 (mgN/L)	NO2 (mgN/L)	SRT (days)
081519R3	8/15/2019	95.5	81.0	84.9	-	-	-	-	-	8.43	1.75	0.555	
091819R3	9/18/2019	73	65	89.0	200	98.5	39.5	34.7	32.0	28.6	0.84	0.66	
092019R3	9/20/2019	114.5	105.5	92.1	250	84.5	33.5	33.0	33.0	16.5	0.56	0.13	2.96
092719R3	9/27/2019	40.5	40	98.7	127.5	65	39.5	45.0	42.0	24.5	0.79	0.06	
093019R3	9/30/2019	**36**	**30**	**83.4**	**91**	**54.5**	**18**	**34.7**	**28.0**	**17.5**	**0.77**	**1.17**	
100719R3	10/7/2019	**21.5**	**20.5**	**95.3**	**66**	**51.5**	**22**	**36.7**	**26.0**	**16.76**	**0.44**	**0.1**	
AVERAGE		**28.8**	**25.3**	**89.4**	**78.5**	**53.0**	**20.0**	**35.7**	**27.0**	**17.1**	**0.6**	**0.6**	
100919R3	10/9/2019	22.5	21	93.4	90	62	29.5	42.3	34.0	22.83	0.82	0.1	
101119R3	10/11/2019	41.5	41	98.8	102	60.5	42.5	49.0	22.4	21.35	1.01	0.04	
101519R3	10/15/2019	79	68.5	86.6	137	81	23.5	67.3	48.9	23.19	25.83	2.66	
101719R3	10/17/2019	**42**	**37**	**88.1**	**113**	**78**	**23.5**	**44.0**	**42.2**	**24.18**	**40**	**0.66**	1.30
102319R3	10/23/2019	**30**	**27.7**	**92.4**	**89.5**	**63.5**	**31**	**51.11**	**44.44**	**21.32**	**8.04**	**0.68**	
102519R3	10/25/2019	**32.3**	**44.6**	**104.3**	**90.5**	**62.5**	**27**	**48.89**	**35.56**	**13.08**	**4.43**	**1.4**	
AVERAGE		**34.8**	**36.4**	**94.9**	**97.7**	**68.0**	**27.2**	**48.0**	**40.7**	**19.5**	**17.5**	**0.9**	
102819R3	10/28/2019	20.8	19.2	92.6	71	59.5	19.6	33.3	30.9	12.7	10.6	1.77	
103019R3	10/30/2019	**33.8**	**30**	**89**	**123.5**	**63.5**	**21**	**47.8**	**44.1**	**22.6**	**12.9**	**3.31**	
110119R3	11/1/2019	**29.2**	**28.6**	**97.6**	**90**	**74.5**	**12.9**	**38.4**	**34.9**	**13.8**	**14.8**	**2.06**	1.03
110519R3	11/5/2019	**20.8**	**20.8**	**100**	**68**	**38**	**13.9**	-	-	-	-	-	
AVERAGE		**27.9**	**26.5**	**95.5**	**93.8**	**58.7**	**15.9**	**43.1**	**39.5**	**18.2**	**13.9**	**2.7**	
110719R3	11/7/2019	22.1	17.1	77.3	51.5	27	16.3	43.85	41.76	19.2	20.1	1.48	
111119R3	11/11/2019	26.9	25.4	94.3	81	55.5	26	44.54	40.38	25.91	9.62	1.48	
111319R3	11/13/2019	30.8	28.5	92.5	92.5	61.5	28	50.79	45.93	32.72	12.71	4.58	1.51
111519R3	11/15/2019	23.1	20.8	90.3	80	57	25	45.24	40.38	23.91	16.52	2.47	
111919R3	11/19/2019	45.4	40.8	89.98	140	90.5	-	59.72	55.26	27.6	22.48	2.89	

112119R3	11/21/2019	38.6	31.3	79.7	97.5	63	-	56.94	56.58	19.18	29.14	2.45	
112419R3	11/24/2019	27.1	21.4	79.4	79	56.5	-	34.21	32.89	22.65	2.95	1.25	
112619R3	11/26/2019	50	47.7	95.4	127	73	-	56.58	56.58	25.13	14.86	3.83	
AVERAGE		**38.6**	**33.5**	**84.8**	**101.2**	**64.2**	**23.8**	**49.2**	**48.7**	**22.3**	**15.7**	**2.5**	
020420R3	2/4/2020	-	-	-	-	-	-	-	-	-	-	-	
020620R3	2/6/2020	-	-	-	-	-	-	-	-	-	-	-	
021220R3	2/12/2020	37.3	37.3	100	98	57	37	-	-	27.6	0.87	0.03	
021420R3	2/14/2020	43.1	39.4	91.1	71	45	31	42.8	36.4	23.9	-	1.41	
021820R3	2/18/2020	36.2	31.2	86.2	71	48	30	40.3	36.7	24.6	8.1	0.59	
022020R3	2/20/2020	20.5	19	92.5	115	64	38	46.0	39.4	24.2	10.95	0.72	
022520R3	2/25/2020	64	56	87.4	88.75	53.5	34	35.1	30.7	22.6	0.94	0.04	0.45
022820R3	2/28/2020	28	25.5	91.1	-	-	-	61.7	52.9	24.9	29.09	1.33	
030220R3	3/2/2020	39	38	97.5	-	-	-	48.5	47.0	17.7	20.83	-	
030320R3	3/3/2020	24	24	100	-	-	-	44.1	38.2	13.3	21.7	0.54	
030520R3	3/5/2020	44	40	91.1	105	-	-	51.4	41.1	17.9	20.83	1.98	
030720R3	3/7/2020	32	32	100	76	55	26.5	45.5	38.2	15.4	20.42	0.74	
030920R3	3/9/2020	30	26	86.7	73.5	67	37.5	46.7	49.3	17.6	21.79	0.57	
031220R3	3/12/2020	39.5	36	91.2	47	43	32	40.1	37.5	21.6	11.79	4.74	
AVERAGE		**36.4**	**33.4**	**92.3**	**80.9**	**53.6**	**32.7**	**45.7**	**40.7**	**20.4**	**16.6**	**1.3**	
060120R3	6/1/2020	16	13	81.7	57	44	37	21.1	21.1	5.88	2.02	1.02	
060420R3	6/4/2020	20.4	15.3	77.1	54	31	-	22.42	21.54	8.95	9.17	0.61	
060820R3	6/8/2020	24	20	83.3	70	30	19	25.14	25.5	18.15	4.48	0.34	
061120R3	6/11/2020	17	15	88.2	34	25	8	32.08	33.4	11.34	28.65	0.37	
061520R3	6/15/2020	23	23	100	87.5	71.5	62	39.03	34.9	18.2	11.5	0.24	1.75
061720R3	6/17/2020	22	21	95.8	102.5	82.5	63.5	24.9	23.6	16.7	7.68	0.34	
061920R3	6/19/2020	33	29	88.9	61.0	34.3	15.7	28.6	26.1	9.33	12.32	0.78	
062220R3	6/22/2020	27	39	92.5	65.7	39.7	22.0	19.9	18.6	15.01	0.49	0.61	
062420R3	6/24/2020	30	36	90	58.0	33.0	24.5	30	29.3	13.61	10.09	1.19	
AVERAGE		**30.0**	**34.7**	**90.5**	**61.6**	**35.7**	**20.7**	**26.2**	**24.7**	**12.7**	**7.6**	**0.9**	

Appendix C-2 Chapter 4 Sludge Settling Characteristics

Table C-4 Aerobic and Anoxic Sludge Volume Index (SVI) and Effluent Suspended Solids (SS)

Aerobic Reactors			
Reactor ID	**SRT (days)**	**SVI (mL/g)**	**Effluent TSS (mg/L)**
R1	0.75	128	25.8
	1.0	134	23.5
	1.6	114	27.0
	2.2	109	18.6
	3.0	95.0	25.0
R2	2.6	90.0	7.00
	2.6	103	8.05
	2.8	108	8.30
	3.0	96.0	14.4
	3.9	106	9.50
	4.8	99.0	10.0
	6.1	85.0	10.6
	7.7	72.0	10.2
	8.4	84.0	8.10

Anoxic Reactors			
Reactor ID	**SRT (days)**	**SVI (mL/g)**	**Effluent TSS (mg/L)**
R3	0.50	24.0	36.4
	1.0	110	34.8
	1.5	102	38.6
	1.8	106	28.0
	2.9	87.5	28.8
R4	1.6	98.0	35.7
	1.7	90.0	27.9
	2.5	95.6	42.6
	2.8	79.0	19.9
	3.2	85.0	16.5
	4.0	72.0	17.5
	4.5	71.0	19.1
	6.0	83.0	20.2
	12.5	68.0	18.7

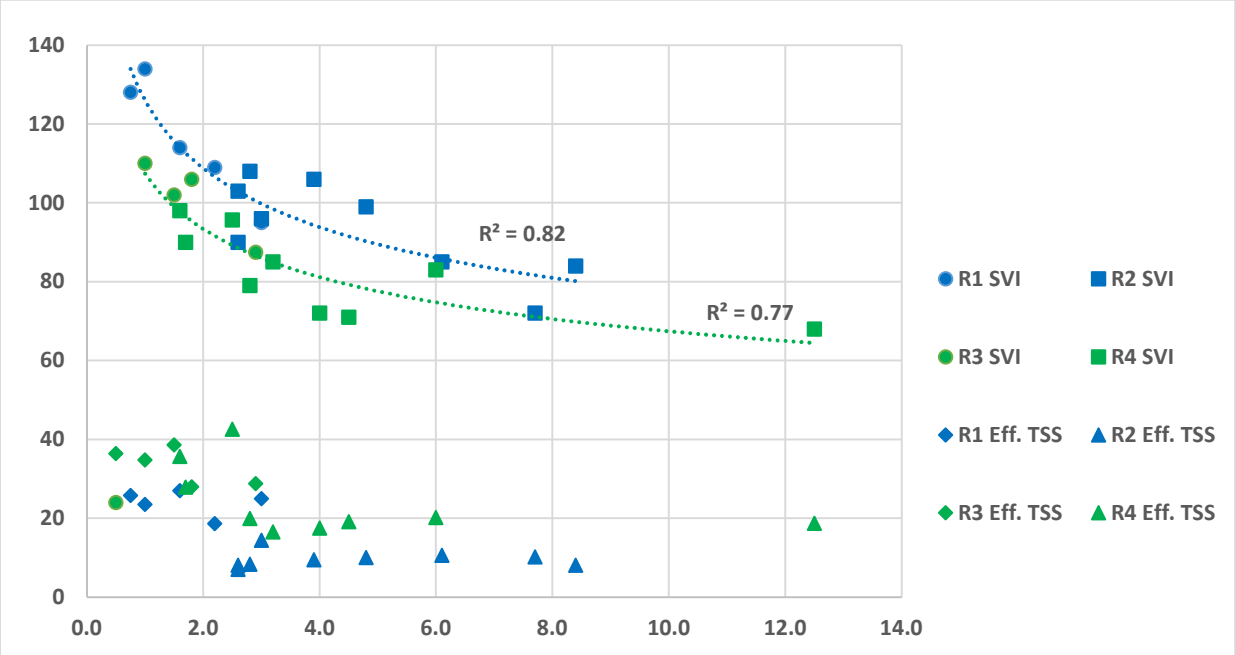

Figure C-4 Aerobic and Anoxic Sludge Volume Index (SVI) and Effluent Suspended Solids (SS)

Reactor 1 Aerobic Mass Balance Example

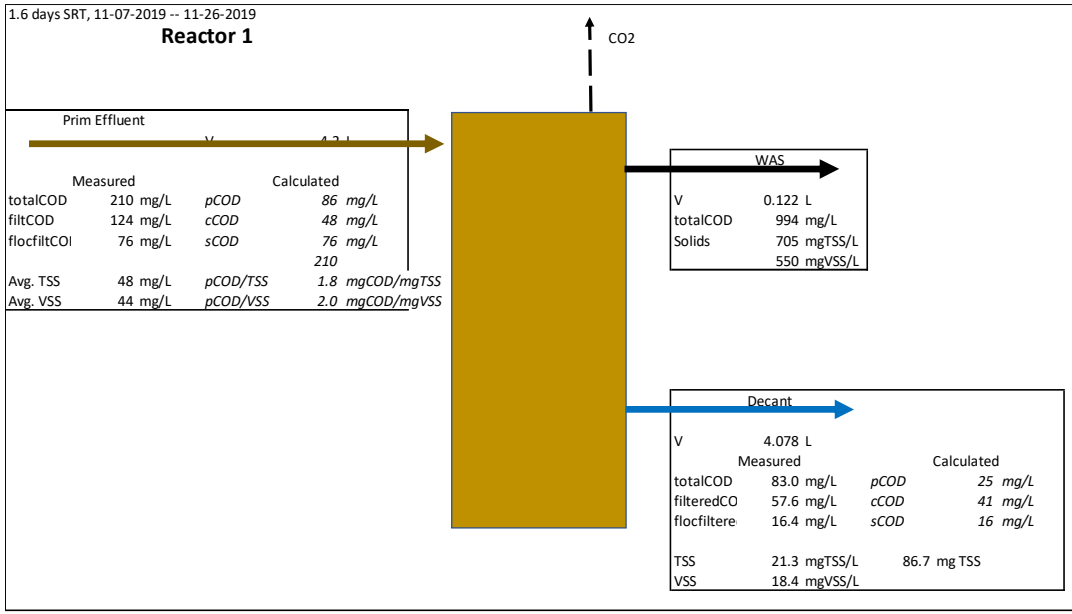

Inert Solids Balance		
FSSin	323.40	*mg FSS/day*
FSSout	314.03	*mg FSS/day*
Balance	0.97	
Sanity Check ML COD		
Theoretical COD/TSS	*1.2*	*mg COD/mg TSS*
Theoretical COD/VSS	*1.42*	*mg COD/mg TSS*
Theoretical ML COD	846	mgCOD/L
Theoretical/Measured	0.85	

COD Balance		
CODwas	1,940	mgCOD/day
CODeff	5,416	mgCOD/day
CODinf	14,089	mgCOD/day
Balance COD oxidized (Ss0-Ss+Xs0-Xs)	**6,733**	mgCOD/day
Soluble CODinf (Ss0)	5,086	mgCOD/day
Soluble COD destroyed (Ss0-Ss)	3,983	mgCOD/day
COD oxidized of Influent COD	47.8	%
cCODinf	3213.0	
Colloidal COD	0.163	mgCOD/day

Mass Balance Calculations		
MLSSwas	1376	mgTSS
SSeff	1387	mgTSS
*Xm,t*V*	2763	mgTSS
SRT estimate	1.63	days
SRT calculated,designed	2	days

Note: August samples for Reactor 1 (SRT 0.45 days and 1.0 days) were replacements for samples ran previously that were discarded due to problems with wasting in the aerobic reactor. Below is the primary effluent characteristics and mass balances for this period. Oxidation reflected in Table 4-7 (see note 2) were based on these influent concentrations.

Sample No.	Sample Date	TSS (mg/L)	VSS (mg/L)	Total COD (mg/L)	Filtered COD (mg/L)	Floc&Filt COD (mg/L)	NO_3 (mg-N/L)
081322PE	8/13/2022	45	39.0	133	116	38	0.87
081522PE	8/15/2022	35.5	35.0	153	133.3	79	0.97
081822PE	8/18/2022	33.5	30.5	182	133.7	77.7	0.78
082122PE	8/21/2022	41	38.0	155	108.3	82.7	0.92
082322PE	8/23/2022	34.4	30.2	226	142	91	0.97
082422PE	8/24/2022	33.0	26.3	152	111	78	1.03
082522PE	8/25/2022	33.6	28.2	142	98	50	1.23
082622PE	8/26/2022	31	25.1	158	110	56	1.00

Reactor 3 Anoxic Mass Balance Example

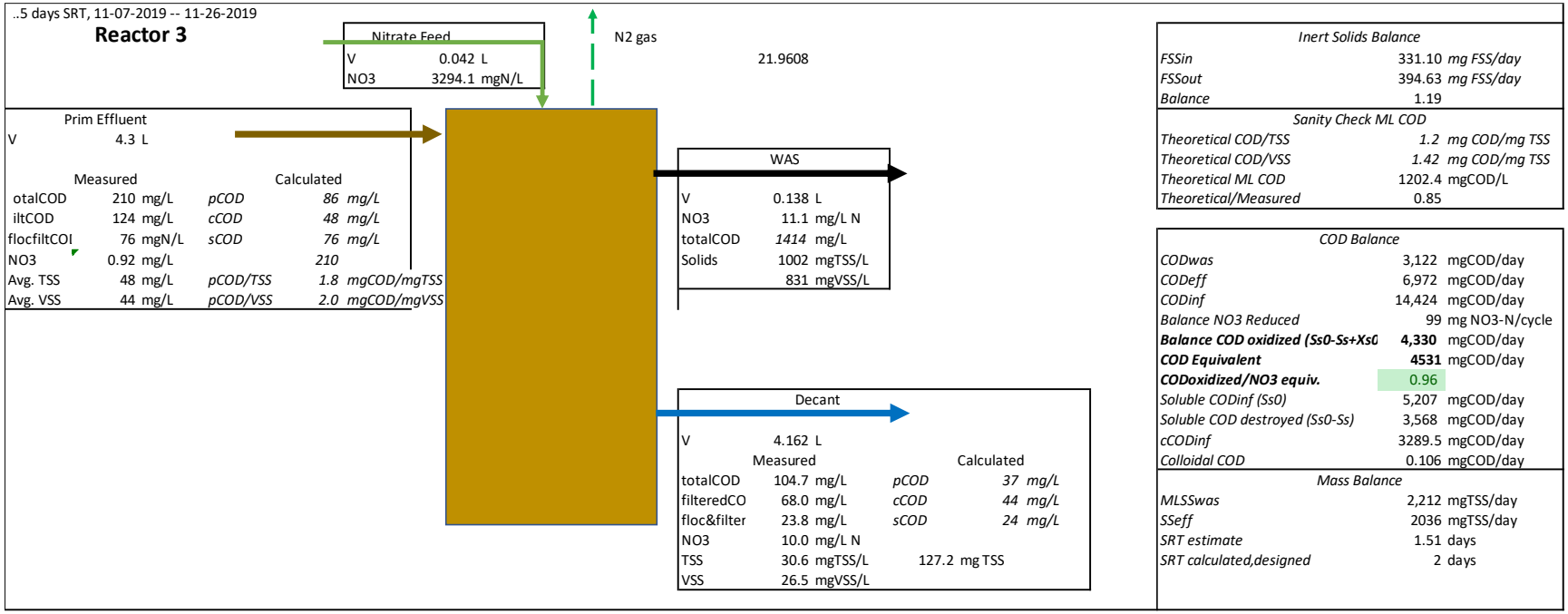

Inert Solids Balance		
FSSin	331.10	*mg FSS/day*
FSSout	394.63	*mg FSS/day*
Balance	1.19	

Sanity Check ML COD		
Theoretical COD/TSS	*1.2*	*mg COD/mg TSS*
Theoretical COD/VSS	*1.42*	*mg COD/mg TSS*
Theoretical ML COD	1202.4	mgCOD/L
Theoretical/Measured	0.85	

COD Balance		
CODwas	3,122	mgCOD/day
CODeff	6,972	mgCOD/day
CODinf	14,424	mgCOD/day
Balance NO3 Reduced	99	mg NO3-N/cycle
Balance COD oxidized (Ss0-Ss+Xs0	**4,330**	mgCOD/day
COD Equivalent	**4531**	mgCOD/day
CODoxidized/NO3 equiv.	0.96	
Soluble CODinf (Ss0)	5,207	mgCOD/day
Soluble COD destroyed (Ss0-Ss)	3,568	mgCOD/day
cCODinf	3289.5	mgCOD/day
Colloidal COD	0.106	mgCOD/day

Mass Balance		
MLSSwas	2,212	mgTSS/day
SSeff	2036	mgTSS/day
SRT estimate	1.51	days
SRT calculated,designed	2	days

Appendix D Supplementary Information for Chapter 5

Appendix D-1 Chapter 5 Biological Phosphorus Stoichiometric Equations

Biological phosphorus removal begins with the uptake of small-chain VFAs, which are primarily acetic acid (HAc) with smaller concentrations of proprionic acid, are converted into various fat reserve compounds such as, intracellular poly-hydroxyalkanoates (PHA)—or more specifically polyhydroxybutyrate (PHB)—using energy generated from the degradation of intracellular supplies of polyphosphate and glycogen. Molecular transport of 1.0 mol HAc into the cell requires an energy expenditure of approximately 0.50 mol adenosine triphosphate (ATP) to activate the acetate permease protein (ActP), and 0.50 mol ATP to convert the HAc to a useable intracellular form (acetyl-CoA) (Mino et al., 1985; Saunders et al., 2007). Glycolysis provides some of the required energy. Consumption of 1.0 C-mol of stored glycogen provides 0.50 ATP and 0.25 mol NADH that are used to convert acetyl-CoA to PHA (Smolders et al., 1994). ATP is mainly generated in the anaerobic phase through the hydrolysis of 1.0 mol poly-P to 1.0 mol ortho-P. Release of mineralized ortho-P from PAOs bound with magnesium or potassium during the anaerobic cycle creates a proton gradient, allowing for ATP generation through the proton motive force (PMF) (Oehmen et al., 2007; Saunders et al., 2007). Poly-P hydrolysis provides energy for cell maintenance during the anaerobic cycling period ($2.5x10^{-3}$ mol ATP/mol-C/hour) (Mino et al., 1985; Kuba et al., 1996). Thus, during the anaerobic "feast" cycle, the observation of HAc uptake coincides with glycogen degradation, the loss of a phosphate group from intracellular poly-P, a subsequent increase of ortho-P concentration in the bulk liquid, and intracellular PHA storage. In the subsequent aerobic "famine" phase, the PAOs oxidize their PHB fat reserve to replenish

intracellular glycogen, and uptake excess ortho-P to regenerate stored polyphosphate (Arun et al., 1988).

Aerobic Biological Phosphorus Removal (Smolders et al., 1995)

Anaerobic Processes:

Acetate Uptake:

$$-CH_2O - 0.5\,CH_{1.67}O_{0.83} - 0.37HPO_3 + 1.33CH_{1.5}O_{0.5} + 0.17CO_2 + 0.37H_3PO_4 + 0.05H_2O = 0$$

Cell Maintenance:

$$-HPO_3 - H_2O + H_3PO_4$$

Aerobic Processes:

Biomass Synthesis:

$$-1.37CH_{1.5}O_{0.5} - 0.2NH_3 - 0.015H_3PO_4 - 0.42O_2 + CH_{2.09}O_{0.54}N_{0.2}P_{0.015} + 0.37CO_2 + 0.305H_2O = 0$$

Phosphate Uptake:

$$-0.27CH_{1.5}O_{0.5} - 0.31O_2 - H_3PO_4 + HPO_3 + 0.27CO_2 + 1.2H_2O = 0$$

Glycogen Formation:

$$-1.12CH_{1.5}O_{0.5} - 0.26O_2 + CH_{1.67}O_{0.83} + 0.12CO_2 + 0.007H_2O$$

Cell Maintenance:

$$-CH_{1.5}O_{0.5} - 1.125O_2 + CO_2 + 0.75H_2O = 0$$

Denitrifying Biological Phosphorus Removal (Kuba et al., 1996)

Anaerobic Processes:

Acetate Uptake:

$$-CH_2O - 0.5\ CH_{1.67}O_{0.83} - 0.36HPO_3 + 1.33CH_{1.5}O_{0.5} + 0.17CO_2 + 0.36H_3PO_4 + 0.059H_2O = 0$$

Cell Maintenance:

$$-HPO_3 - H_2O + H_3PO_4$$

Anoxic Processes:

Biomass Synthesis:

$$-1.63CH_{1.5}O_{0.5} - 0.2NH_3 - 0.015H_3PO_4 - 0.57HNO_3 + CH_{2.09}O_{0.54}N_{0.2}P_{0.015} + 0.28N_2 + 0.63CO_2 + 0.78H_2O = 0$$

Phosphate Uptake:

$$-0.46CH_{1.5}O_{0.5} - 0.41HNO_3 - H_3PO_4 + HPO_3 + 0.21N_2 + 0.46CO_2 + 1.55H_2O = 0$$

Glycogen Formation:

$$-1.27CH_{1.5}O_{0.5} - 0.35HNO_3 + CH_{1.67}O_{0.83} + 0.17N_2 + 0.27CO_2 + 0.29H_2O$$

Maintenance:

$$-CH_{1.5}O_{0.5} - 0.9HNO_3 + 0.45N_2 + CO_2 + 1.2H_2O = 0$$

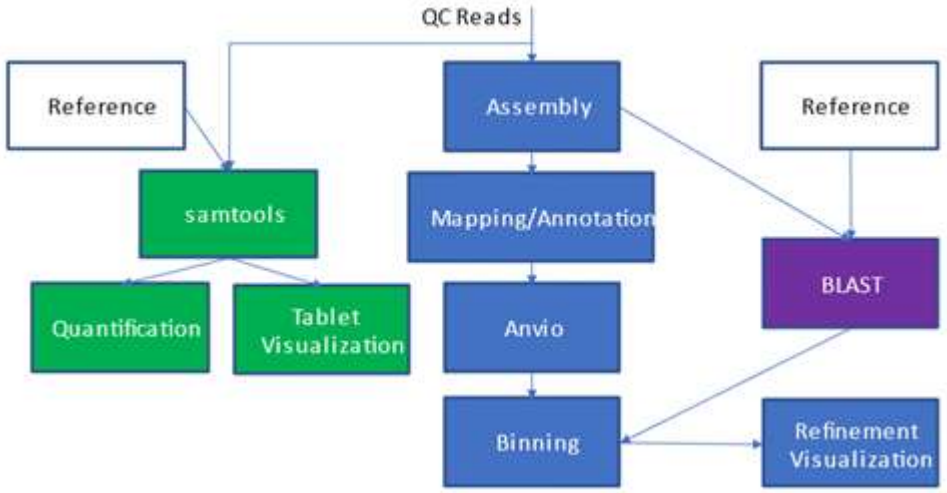

Figure D-1 Metagenomics workflow

Table D-1 JGI and NCBI known and putative PAO reference sequences

Genome Name	**IMG Gene ID**	**JGI Locus Tag**
Candidatus Accumulibacter phosphatis Type IA UW-3	2689798358	Ga0131788_11181
Candidatus Accumulibacter phosphatis clade IIA str. UW-1	645008873	Ga0131788_11181
Candidatus Accumulibacter sp. BA-91	2557376466	AW09_05024
Candidatus Accumulibacter sp. BA-92	2557378273	AW10_01760
Candidatus Accumulibacter sp. BA-93	2557381435	AW11_00288
Candidatus Accumulibacter sp. BA-94	2557388339	AW12_03015
Candidatus Accumulibacter sp. SK-01	2557356282	CAPSK01_03197
Candidatus Accumulibacter sp. SK-11	2557363539	AW07_00781
Dechloromonas sp. EBPR_Bin_94	2619977968	Ga0073639_10256
Dechloromonas sp. EBPR_Bin_104	2619985406	Ga0073640_108161
Tetrasphaera sp. HKS02	2883864990	Ga0439515_01_3044395_3046656
Tetrasphaera jenkinsii Ben 74	2633879667	Ga0078567_118018
Tetrasphaera sp. F2B08	2890935669	Ga0440813_22_37933_40194
Tetrasphaera australiensis Ben110	2636448941	Ga0078565_10839
Tetrasphaera japonica T1-X7	2639287737	Ga0097842_10815
Genome Name	**NCBI Accession**	**NCBI Project No.**
Dechloromonas phosphoritropha	MBL0354550.1	JADKGN01
Dechloromonas phosphorivorans	MBK9785074.1	JADKIP01

Appendix D-3 Chapter 5 Supplementary Reactor Chemical Results

Table D-2 Phosphorus Removal Conditions for Reactors 2 and 4 in Phase 1 and Phase 2

PE			**R2**				**R4**				**AER R2 % Removal[1]**		**ANX R4 % Removal**	
Avg TP (mgP/L)	Avg OP (mgP/L)	Avg NO3 (mgN/L)	SRT (days)	Avg TP (mgP/L)	Avg OP (mgP/L)	Avg NO3 (mgN/L)	SRT (days)	TP (mgP/L)	OP (mgP/L)	NO3 (mgN/L)	TP	OP	TP	OP
VFA-limited Conditions[2]														
3.3	2.3	0.56	2.6	3.0	1.6	11	1.7	3.8	2.3	7.3	7.9%	30%	-17%	1.9%
6.3	3.3	1.8	2.6	1.3	0.8	0.5	2.5	4.8	2.5	12	80%	77%	24%	25%
3.7	2.4	0.67	2.8	1.6	0.6	4.2	2.5	3.8	2.7	0.61	57%	73%	-3.4%	-13%
4.1	2.6	0.64	2.8	1.3	0.6	0.4	2.5	4.1	2.1	0.69	67%	78%	1.0%	21%
4.7	3.0	0.59	3.0	1.0	0.6	0.3	2.8	3.0	1.9	14	78%	80%	36%	37%
8.2	7.2	0.99	3.9	2.3	1.5	0.6	3.2	5.9	5.5	8.9	72%	79%	29%	23%
4.6	3.5	0.68	4.8	0.9	0.4	0.5	4.0	3.5	2.7	6.6	80%	88%	24%	22%
4.1	3.5	0.81	6.1	0.5	0.4	4.1	4.6	3.0	2.5	9.5	88%	90%	28%	29%
7.4	5.0	0.82	8.4	2.2	1.3	11	6.0	3.1	2.6	3.9	71%	74%	58%	48%
4.2	3.7	0.49	7.7	2.7	2.1	8.1	12.5	1.6	1.6	6.7	37%	44%	61%	58%
Cold Water Conditions[3]														
	2.8	0.90	5.6		1.6	0.55	4.3		2.4	7.54		43%		15%
	4.7	0.94	5.6		3.9	1.7	4.3		4.4	11		17%		5.0%
	8.3	0.61	7.7		4.9	0.50	7.0		7.1	6.3		45%		19%
ND	5.6	0.66	6.5	ND	4.2	0.77	11	ND	4.9	5.8	ND	25%	ND	12%
	10	0.60	6.0		6.9	0.50	6.2		10	1.3		33%		-3.0%
	12	0.80	5.0		9.2	0.80	7.1		11	2.5		24%		7.0%
	13	0.80	5.1		9.0	0.50	8.5		11	0.50		41%		25%

[1]Red font indicates there were issues during the operation of the reactors that lead to erroneous performance. Samples were omitted from averages.
[2]Not in chronological order. System SRT was varied to ensure there was no bias between sampling periods. See Figure 5-2 for chronological order of operation.
[3]Reactor building had a boiler malfunction during the Fall/Winter of 2021. Water temperatures dropped below 8°C during this time.

Table D-3 Carbon Removal conditions for Reactors 2 and 4 in Phase 1

PE			R2				R4				cCOD Removal %		sCOD Removal %	
Avg tCOD (mg/L)	Avg cCOD (mg/L)	Avg sCOD (mg/L)	SRT (days)	Avg tCOD (mg/L)	Avg cCOD (mg/L)	Avg sCOD (mg/L)	SRT (days)	Avg tCOD (mg/L)	Avg cCOD (mg/L)	Avg sCOD (mg/L)	AER R2	ANX R4	AER R2	ANX R4
106	31	38	2.6	24	4.2	16	1.7	56	18	18	87	43	58	52
135	34	47	2.6	21	2.9	15	2.5	44	12	17	92	65	69	63
121	49	33	2.8	30	8.8	16	2.5	69	30	16	82	39	52	52
130	42	56	2.8	38	12	14	2.5	78	31	21	72	27	75	63
142	40	55	3.0	35	11	13	2.8	52	20	17	74	50	76	69
172	38	77	3.9	47	10	29	3.2	67	18	38	73	52	62	51
167	65	53	4.8	38	13	16	4.0	66	27	19	80	59	69	64
154	44	68	6.1	42	10	20	4.6	59	17	23	77	61	70	65
158	46	63	8.4	10	7.7	0.0	6.0	51	30	20	83	34	100	68
153	37	58	7.7	16	3.5	0.9	12.5	52	24	12	90	36	98	79

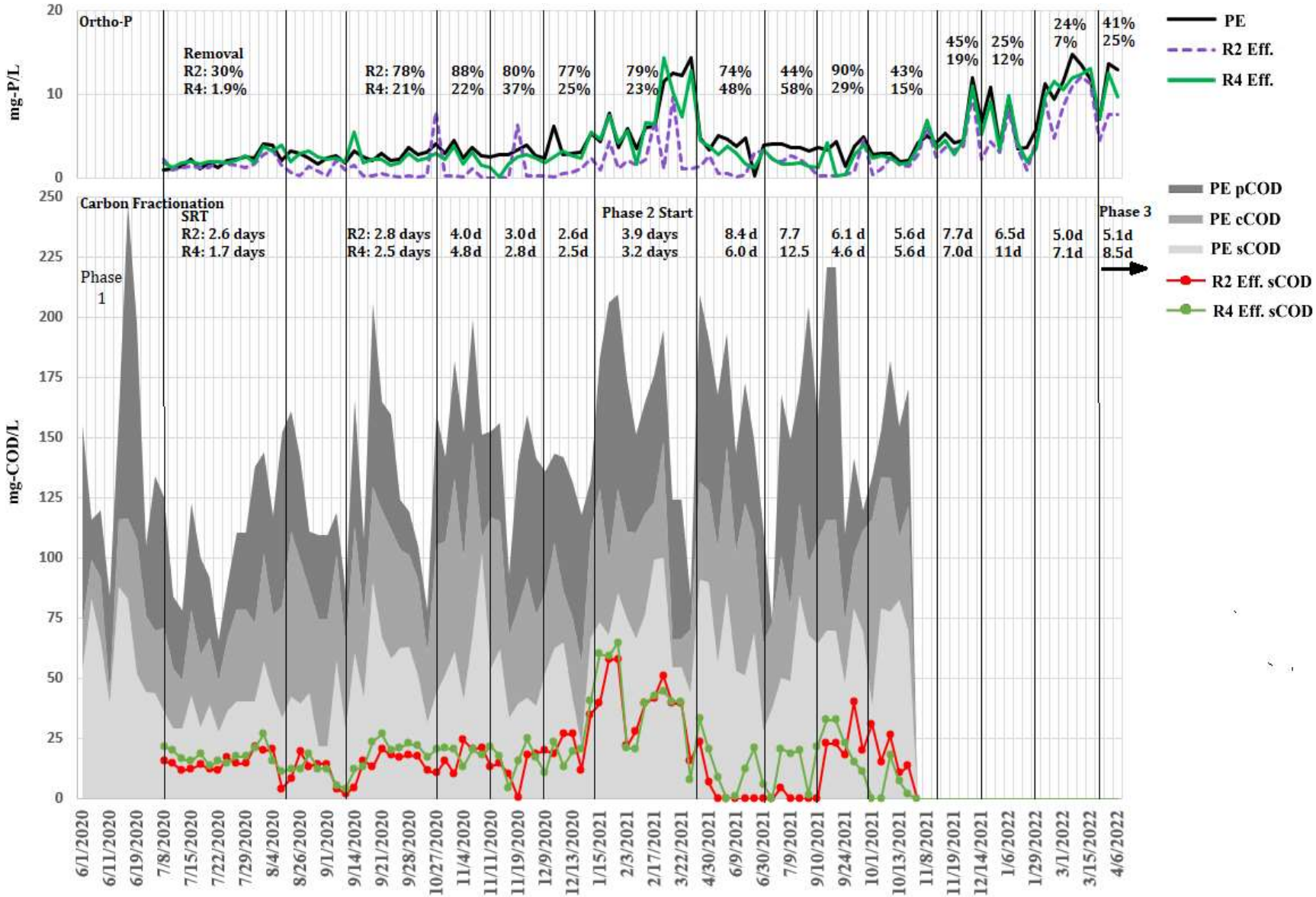

Figure D-2 Chemical Methods Chronological Timeline
Phosphorus Removal (top) and Carbon Removal (bottom)

Table D-4 Key process rates for bio-P removal in Reactors 2 and 4 during VFA-limited conditions

	Anaerobic/Aerobic (R2)				**Anaerobic/Anoxic (R4)**				
Date	SRT (days)	HAc Uptake (mgCOD/ gVSS/hr)	OP release Rate (mgP/gVSS/hr)	OP uptake Rate (mgP/gVSS/hr)	SRT (days)	HAc Uptake (mgCOD/ gVSS/hr)	OP release Rate (mgP/gVSS/hr)	OP uptake Rate (mgP/gVSS/hr)	Nitrate uptake Rate (mgN/gVSS/hr)
October-November 2020	4.8	-	26	18	4.0	-	6.5	2.2	8.7
January-March 2021	3.9	31	35	14	3.2	37	18	7.7	14
March-July 2021	7.7	46	25	11	6.0	72	19	5.5	7.1
	8.4	51	27	9.7	12.5	39	14	4.8	3.6
September 2021	6.1	48	25	17	4.6	58	14	7.2	8.5
November 2021	5.6	31	19	7.1	4.3	31	4.0	2.2	9.1
December 2021	7.5	19	17	5.1	7.0	33	6.9	1.6	8.7
January 2022	6.5	ND*	6.1	4.3	11	33	4.5	0.93	4.9
February 2022	6.0	15	12	4.5	6.2	34	4.7	1.0	5.5
March 2022	5.0	110	4.2	1.8	6.5	45	4.4	1.3	11
March 2022 *Prior to Phase 3*	5.0	41	26	11	7.1	35	8.2	3.9	18
Normal Temp. Avg		44	28	14		51	14	5.5	8.4
Cold Water Avg		22	13	5.3		33	5.0	1.4	7.1
Prior to Phase 3		75	15	6.5		40	6.3	2.6	14.4

*Acetic acid (HAc) slope was not able to be calculated, the uptake occurred too rapidly

Table D-5 Summary of important ratios for VFA-supplemented conditions

Reactor 2 (ANA/AER or A/O design)					
Sample Date	ANA P/HAc	ANA PHB/HAc	AER P/PHB	ANA OP release (mgP/gVSS/hr)	AER OP uptake (mgP/gVSS/hr)
Stoichiometric Value[1]	*0.37*	*1.33*	*0.27*	-	-
4/7/2022	0.46	1.1	0.22	17	9.5
4/9/2022	0.46	1.3	0.26	20	11
5/14/2022	0.42	ND[3]	ND[4]	29	11
5/21/2022	0.20	1.4	0.16	15	12
5/28/2022	0.55	1.3	ND[4]	19	0.0
8/21/2022[2]	0.19	1.8	0.08	7.0	9.3
Number of Samples	5	4	3	6	6
AVERAGE	**0.45**	**1.3**	**0.21**	**20**	**11**
Std Dev.	0.14	0.12	0.04	4.8	1.0
AVERAGE (including August)	**0.40**	**1.4**	**0.18**	**18**	**11**

Reactor 4 (ANA/ANX or Anoxic design)						
Sample Date	ANA P/HAc	ANA PHB/HAc	ANX P/PHB	ANX PHB/NO_3-N	ANA release (mgP/gVSS/hr)	AER uptake (mgP/gVSS/hr)
Stoichiometric Value[1]	*0.36*	*1.33*	*0.23*	*1.95*		
4/7/2022	0.20	3.3	0.02	5.4	9.3	3.7
4/9/2022	0.25	3.2	0.07	2.5	6.0	3.4
5/14/2022	0.44	2.6	0.04	2.1	15	2.8
5/21/2022	0.35	ND	ND	ND	5.5	3.2
5/28/2022	0.07	2.6	0.03	3.90	9.2	5.6
8/21/2022[2]	0.14	0.80	0.04	3.46	9.1	4.3
Number of Samples	4	4	4	5	6	6
AVERAGE (April/May samples)	**0.31**	**2.9**	**0.04**	**3.5**	8.9	3.8
Std Dev.	0.09	0.33	0.02	1.3	3.0	0.90
AVERAGE (including August)	**0.24**	**2.5**	**0.04**	**3.47**	9.0	3.8

[1]Source: Smolders et al. (1995)

[2]August samples were taken using primary effluent from different treatment train at AAWWTP than April/May samples due to a train shutdown

[3]HAc uptake too rapid to calculate slope

[4]PHB digestion incomplete

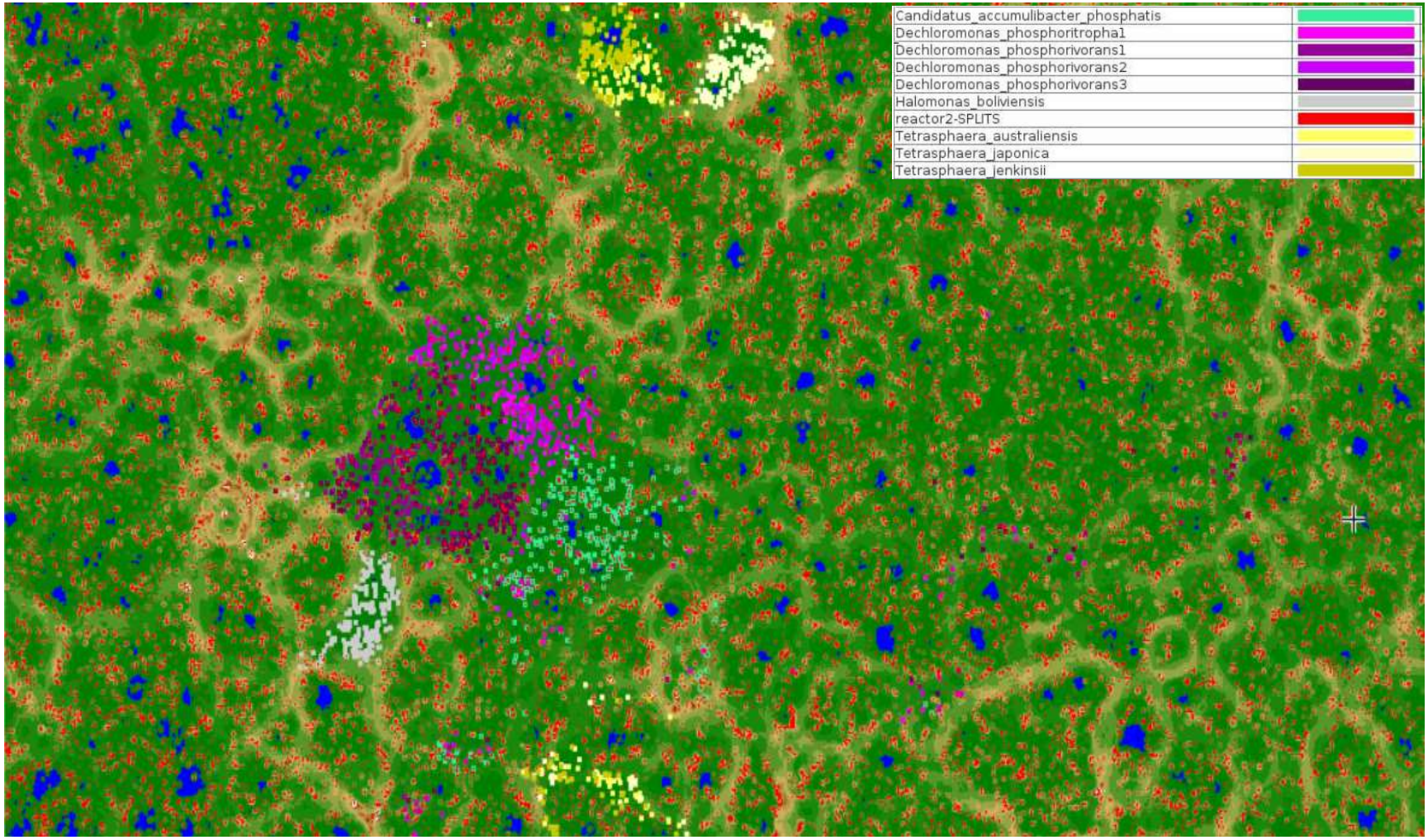

Figure D-3 Tetra-ESOM viewer of Reactor 2 split sequences and reference sequences (8-10kb)

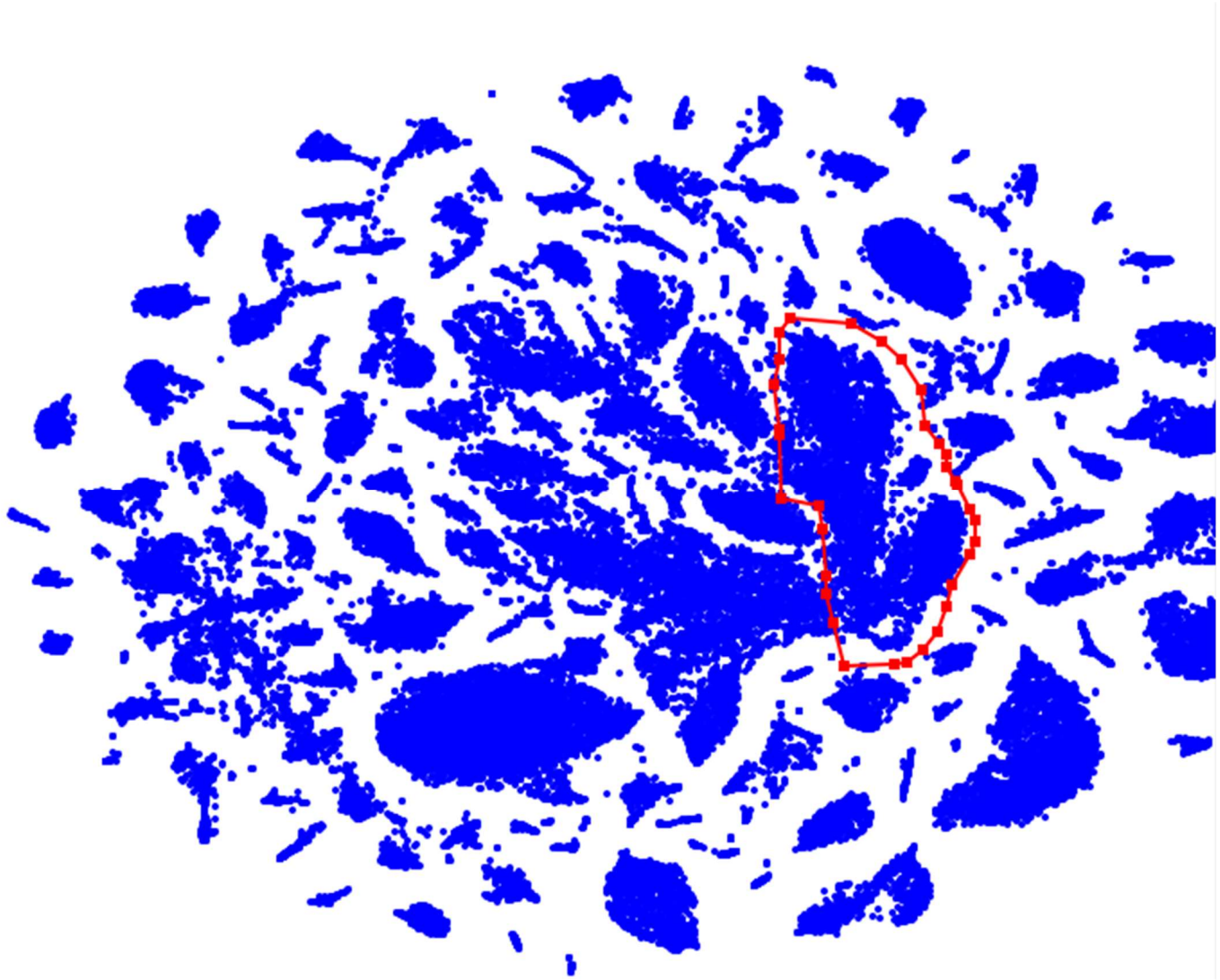

Figure D-4 VizBin Reactor 2 Ca. Accumulibacter phosphatis bin (circled) clustered with reference sequences

Table D-6 Reactor 2 Relative Abundance of Key Species and Gene Coverage of Bio-P Genes

R2 SPECIES	**AVG.**		Min	Max	Std. Dev.
Relative Abundance	Sample 1-4	Sample 1-5			
Candidatus Accumulibacter	**2.8%**	**2.4%**	0.8%	4.5%	0.01
Candidatus Accumulibacter phosphatis	1.5%	1.2%	0.1%	2.5%	0.01
Dechloromonas	1.8%	1.7%	1.1%	1.9%	0.00
Dechloromonas sp.	1.0%	0.9%	0.4%	1.2%	0.00
Unknown Competibacteraceae	0.4%	0.3%	0.2%	0.4%	0.00
Ca. Competibacter	0.0%	0.0%	0.0%	0.0%	0.00
Ca. Contendobacter	0.2%	0.2%	0.1%	0.4%	0.00
Propionivibrio	0.0%	0.0%	0.0%	0.1%	0.00
R4 SPECIES	**AVG.**		Min	Max	Std. Dev.
Relative Abundance	Sample 7-9	Sample 6-10			
Candidatus Accumulibacter	**3.2%**	**2.8%**	0.9%	4.1%	0.01
Candidatus Accumulibacter phosphatis	2.0%	1.6%	0.1%	2.6%	0.01
Dechloromonas	**2.8%**	**2.3%**	0.5%	3.6%	0.01
Dechloromonas sp.	0.9%	0.8%	0.4%	1.5%	0.00
Unknown Competibacteraceae	1.5%	1.5%	1.0%	1.7%	0.00
Ca. Competibacter	0.0%	0.1%	0.0%	0.3%	0.00
Ca. Contendobacter	0.8%	1.0%	0.4%	2.1%	0.01
Propionivibrio	0.4%	0.3%	0.1%	0.5%	0.00

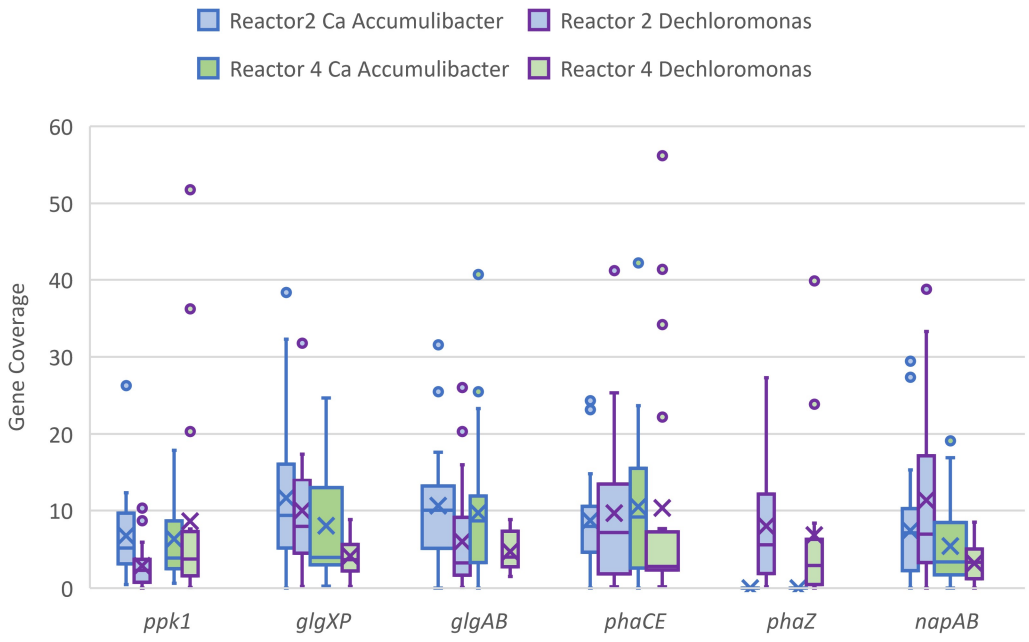

Figure D-5 Gene coverages of auxiliary bio-P metabolic genes

Our logic was that if a particular species of PAO were proliferating in a system during normal operating conditions, mean coverage of glycogen synthase should be similar to glycogen degradation (*glgP*, *glgX*) and PHB synthase, and polyphosphate kinase (*ppk1*) coverage should be similar to nitrate reductase. The average gene coverage can be seen in Figure D-5, which shows there is evidence to support this logic, in most cases. This is not always exact because genes can have multiple copies. However, gene coverages appear to have correlation with each other, and the outliers could likely be attributed to different members within a particular population growing in the system.

The average gene coverage across Samples 1-4 in Reactor 2 for *Ca*. Accumulibacter phosphatis *glgAB*, *glgPX*, and *phaCE* was 12, 17, and 10, respectively, while *ppk1* and *napAB* was 8.7 and 15. On the whole, the pattern for Reactor 2 *Dechloromonas* gene coverages existed in the same manner as *Ca*. Accumulibacter mentioned previously, although at lower levels of coverage. *Dechloromonas ppk1* had a coverage of 2.8; *glgAB*, *glgPX* had a coverage of 5.4 and 9; *phaCE* and *phaZ* had a coverage 11 and 9.0. Surprisingly, in an aerobic environment controlled for limited nitrification, several different annotations of *napAB* existed in Reactor 2 for both *Ca*. Accumulibacter and *Dechloromonas* genera. For the Accumulibacter encoded *napAB* genes, this correlated into three major categories: *Ca*. Accumulibacter phosphatis, unknown/unclassified *Ca*. Accumulibacter, and other known species, such as *Ca*. Accumulibacter regalis BA-93. Variations of the annotated *napAB* gene existed in the *Dechloromonas* bin, which is known to have denitrifying species, such as *Dechloromonas* denitrificans, but appeared inconsistently compared to other bio-P marker genes. It is possible the putative PAO species in the *Dechloromonas* genera (*Ca*. Dechloromonas phosphoritropha and *Ca*. Dechloromonas phosphorivorans) are closely related to *Dechloromonas* denitrificans, or gene transfer occurred amongst highly similar species.

For the purposes of this research, we could not discern which species the napAB genes were connected to, but that they were in the Dechloromonas bin containing the other necessary genes for phosphorylation and denitrification.

In comparison, Reactor 4 had several key differences that were observed through the gene coverage methodology discussed above. Along with higher relative abundances of *Ca*. Accumlibacter (specifically *Ca*. Accumulibacter phosphatis) and *Dechloromonas*, the average levels of gene coverage for *ppk1* were increased over Reactor 2 samples by two-fold and four-fold, respectively; however, the other carbon processing genes considered from Reactor 4 (*glgAB*, *phaCE*, *phaZ*) had no statistical difference between those in Reactor 2. This was somewhat unexpected considering the complete opposite glycogen processing that occurred in Reactor 4.

Appendix D-5 Chapter 5 Supplementary Metagenomic Analysis Results

Glycogen degradation and uptake in the anaerobic and anoxic cycles did not follow the expected patterns. In fact, glycogen levels were accumulated in the anaerobic zone parallel to intracellular PHB and degraded in the anoxic zone, contrary to what the theoretical metabolic models state. Both the Reactor 4 mixed liquor samples taken in April and August 2022, under different influent conditions and temperatures, showed clear increases to mixed liquor glycogen between the beginning and end of the anaerobic cycle (5-50 min), and subsequent decrease to the end of the cycle (50-167 min). Even more interesting is the fact that the magnitude of glycogen levels is much greater in the April sample than August (1.1 versus 0.15 mol-C, respectively). Furthermore, while the April anaerobic glycogen concentrations increase fairly linearly, the August sample appears to initially decrease in the first 20 min before increasing rapidly. Because carbon is being metabolized in noticeably different ways than expected, it is hypothesized that a

number of different metabolic processes are actually being completed. The theoretical models are based on pure cultures under lab conditions, but wastewater contains a vast amount of bacterial populations with unique metabolic functions. One potential source of anaerobic glycogen storage in consort with phosphorus removal could reside with putative PAOs, such as *Dechloromonas* sp. or *Tetrasphaera*, whose anaerobic metabolisms form glycogen from exocellular glucose. Anaerobic accumulation of glycogen would not indicate considerable competition with glycogen accumulating organisms (GAOs), as they store glycogen aerobically (Wang et al., 2014). The mixed liquor profiles were taken using spiked additions of HAc following a cycle with influent wastewater. It is envisioned that extracellular polymeric substances (EPS) could be hydrolyzed to glycogen by these bacterial groups to form excess stored product to power an inefficient anoxic polyphosphate accumulation process. According to visual comparison of the glycolysis/gluconeogenesis pathway on KEGG (Figure D-6), one difference is Reactor 4 *Dechloromonas* bin contained both genes for the enzyme glyceraldehyde-3-phosphate dehydrogenase (*gapA* and *gapB*), which have been shown to be active in either catabolic or anabolic states (Fillinger et al., 2000). It is possible that the appearance of these two enzymes in the anoxic mixed liquor could explain the dual-directionality of some of the carbon processing in the anaerobic/anoxic cycle and not the anaerobic/aerobic, although more research would be required.

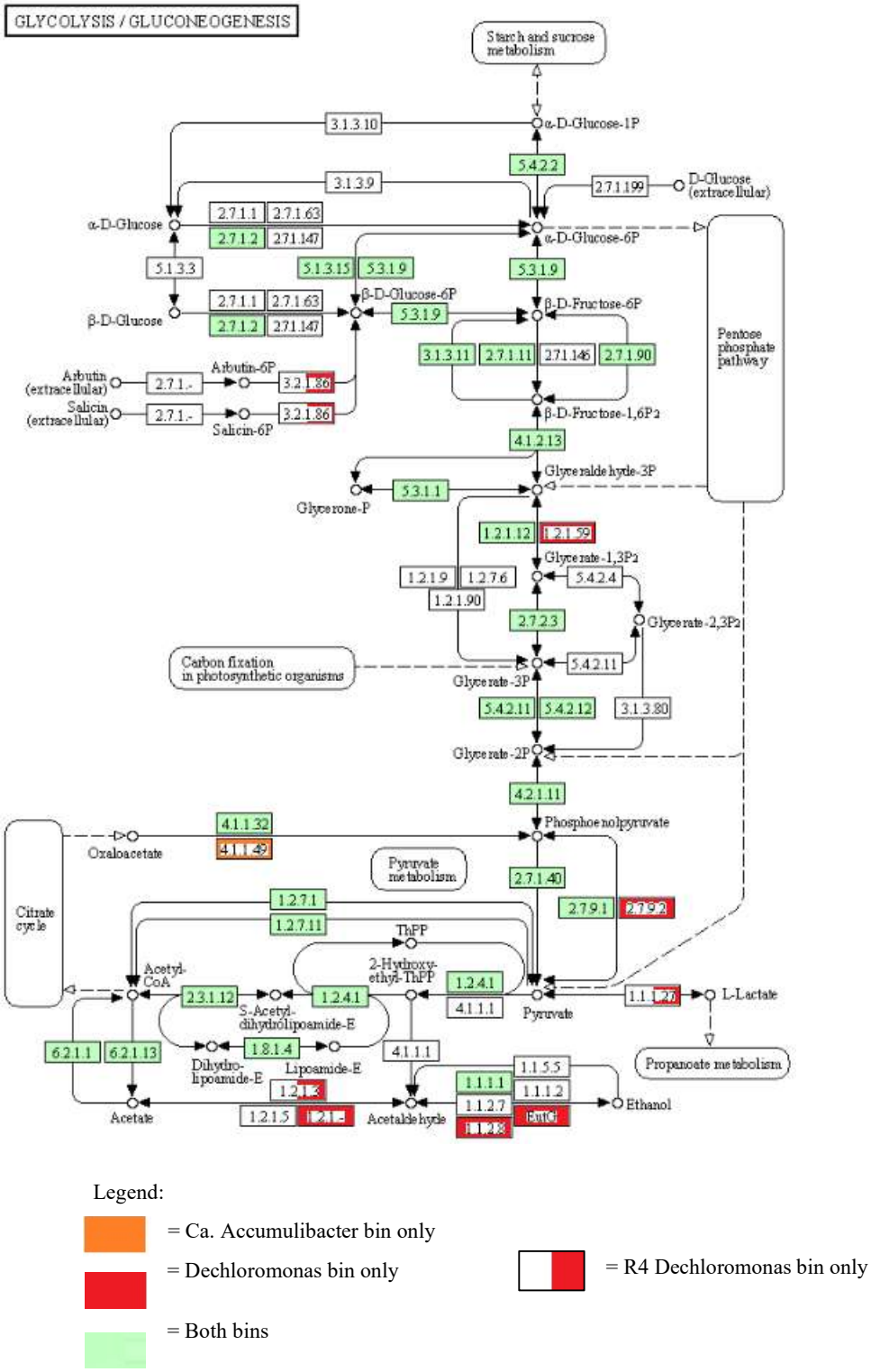

Figure D-6 Reactor 2 & Reactor 4 KEGG pathway for glycolysisis/gluconeogenesis

References

Arun, V., Mino, T., & Matsuo, T. (1988). Biological mechanism of acetate uptake mediated by carbohydrate consumption in excess phosphorus removal systems. *Water Research*, *22*(5), 565–570. https://doi.org/10.1016/0043-1354(88)90056-5

Blair, S. (2012). Investigation into causes of a permeability crisis at large membrane bioreactor. *Proceedings of the Water Environment Federation*.

Fillinger, S., Boschi-Muller, S., Azza, S., Dervyn, E., Branlant, G., & Aymerich, S. (2000). Two glyceraldehyde-3-phosphate dehydrogenases with opposite physiological roles in a nonphotosynthetic bacterium. *Journal of Biological Chemistry*, *275*(19), 14031–14037. https://doi.org/10.1074/jbc.275.19.14031

Kuba, T., Murnleitner, E., Van Loosdrecht, M. C. M., & Heijnen, J. J. (1996). A metabolic model for biological phosphorus removal by denitrifying organisms. *Biotechnology and Bioengineering*, *52*(6), 685–695. https://doi.org/10.1002/(SICI)1097-0290(19961220)52:6<685::AID-BIT6>3.3.CO;2-M

Mino, T., Kawakami, T., & Matsuo, T. (1985). Behaviour of intracellular polyphosphate in the biological phosphate removal process. *Water Science and Technology*, *17*(11–12), 11–21. https://doi.org/10.2166/wst.1985.0218

Oehmen, A., Lemos, P. C., Carvalho, G., Yuan, Z., Keller, J., Blackall, L. L., & Reis, M. A. M. (2007). Advances in enhanced biological phosphorus removal: From micro to macro scale. *Water Research*, *41*(11), 2271–2300. https://doi.org/https://doi.org/10.1016/j.watres.2007.02.030

Saunders, A. M., Mabbett, A. N., McEwan, A. G., & Blackall, L. L. (2007). Proton motive force generation from stored polymers for the uptake of acetate under anaerobic conditions. *FEMS Microbiology Letters*, *274*(2), 245–251. https://doi.org/https://doi.org/10.1111/j.1574-6968.2007.00839.x

Smolders, G. J. F., Klop, J. M., van Loosdrecht, M. C. M., & Heijnen, J. J. (1995). A metabolic model of the biological phosphorus removal process: I. Effect of the sludge retention time. *Biotechnology and Bioengineering*, *48*(3), 222–233. https://doi.org/10.1002/bit.260480309

Smolders, G. J. F., van der Meij, J., van Loosdrecht, M. C. M., & Heijnen, J. J. (1994). Model of the anaerobic metabolism of the biological phosphorus removal process: Stoichiometry and pH influence. *Biotechnology and Bioengineering*, *43*(6), 461–470. https://doi.org/10.1002/bit.260430605

Wang, Z., Guo, F., Mao, Y., Xia, Y., & Zhang, T. (2014). Metabolic Characteristics of a Glycogen-Accumulating Organism in Defluviicoccus Cluster II Revealed by Comparative Genomics. *Microbial Ecology*, *68*(4), 716–728. https://doi.org/10.1007/s00248-014-0440-3